DEVELOPMENT OF BIOTRAPS BASED ON *CLADOPHORA SP* ALGA FOR THE BIOSORPTION OF MERCURY FROM ENVIRONMENTAL WATERS

JOY GAOGAKWE MOKONE

A Thesis submitted to the Faculty of Science, University of the Witwatersrand, Johannesburg, in fulfillment of the requirements for the degree of Doctor of Philosophy

2018

DECLARATION

I declare that this thesis is my own unaided work. It is being submitted for the Degree of Doctor of Philosophy at the University of the Witwatersrand, Johannesburg. It has not been submitted before for any degree or examination at any other university.

… ……

(Signature of candidate)

ABSTRACT

Trace metal pollution of environmental waters is a serious ecological concern that causes degradation of water quality in rivers and lakes. Mercury is considered as one of the most toxic trace metals due to its propensity to bioaccumulate in food webs thus causing severe detriment to human health. Biosorption using algae as biosorbents is emerging as a technology for the remediation of trace metal-polluted waters because algae are widely abundant and have high adsorption capacities. Algae can also be immobilized on polymeric supports to enhance their performance, selectivity, and industrial applicability.

This work presents the development of novel algal-based biosorbents via the immobilization of *Cladophora sp* alga in silica gel and alginate beads for the removal of mercury from synthetic aqueous solutions under batch equilibrium and continuous flow modes. Both the modified and unaltered algae were also characterized for biosorption of mercury using several techniques including Fourier Transform Infrared Spectroscopy (FTIR), Braunner-Emmet-Taylor (BET), Scanning Electron Microscopy (SEM) and Electron Dispersive Spectroscopy (EDX). The research also describes a first attempt to elucidate the mechanism for mercury biosorption using pristine and modified forms of *Cladophora sp* alga. The best performing modified biosorbent (alga immobilized in alginate beads) was also utilized to construct biotraps where were then utilized for mercury removal from acid mine water formed by dissolving salt crusts in deionized water.

Batch equilibrium studies revealed that the optimum conditions for metal biosorption were pH 5, 10 g L^{-1} biosorbent dosage and 25˚C for the modified forms of *Cladophora sp* alga. However, the equilibrium agitation time and initial metal concentration using the biosorbents were 30 minutes and 100 mg L^{-1}, respectively. The maximum biosorption capacities were 121.3 and 183.4 mg g^{-1} for the alga immobilized in silica gel and alga immobilized in alginate beads. These biosorption capacities represented removal efficiencies of 82.75 and 86.6%, respectively. Biosorption experimental data also fitted the pseudo-second kinetic model, the Langmuir, and Dubinin-Radushkevich isotherms thus suggesting that biosorption

occurs on a homogeneous layer and was limited by chemisorptive ion exchange mechanism. Kinetic modeling using the Webber-Morris model showed that intraparticle diffusion was rate limiting only at the start of the biosorption process. Mercury adsorption using the biosorbents involved several functional groups. Chemical modification, FTIR analysis and EDX analysis showed that the amine, sulfonate and carboxyl groups were key players in the mechanism for the biosorption of mercury by the biosorbents. The biosorption process occurred via complex processes wherein ion exchange was the most dominant mechanism. This was confirmed using FTIR analysis, EDX analysis and chemical modification of functional groups on the algal surface. The biosorbents were also effective in retrieving mercury from multi-elemental synthetic aqueous solutions. However, the alga immobilized in alginate beads was more selective for mercury removal than that immobilized in silica gel.

Optimal removal under continuous flow operation occurred at 7 cm bed height, 2 mL min^{-1} flow rate and 2 mg L^{-1} inlet metal concentration. The column data was also best described by the Bed depth service time, Thomas and Yoon Nelson models. This implied that the service time of the column was proportional to the bed height and external mass transfer and internal diffusion were not the rate limiting mechanisms. Application of the biotraps to acid-impacted environmental waters also significantly reduced the total mercury concentration. The adsorption capacity and removal efficiency obtained were 6.081 mg g^{-1} and 67.81% respectively. These results demonstrated that *Cladophora sp* algal-based biotraps have potential for use in remediation technologies for mercury in environmental samples. They can be used to augment wetlands by offering protective screens that will reduce the direct impact of wastewaters flowing through them thus enhancing their longevity.

ACKNOWLEDGEMENTS

First and foremost, I would like to thank my supervisor, Prof. Ewa Cukrowska for affording me the opportunity to work with her on this project. I am thankful for the invaluable advice, encouragement, support and constructive feedback she has given me over the years. I am also grateful for the assistance and support granted to me by my co-supervisors Prof. Luke Chimuka and Prof. Hlanganani Tutu.

To my colleagues at the Environmental Analytical Chemistry Research Laboratory, thanks for making my stay at Wits a memorable one. A special mention to Xolisiwe Maputsoe (Q), Kitondo Mwelwa (Mr. K), Somandla Ncube (Bab Ngwenya) and Odwa Mbanga (Odwalicious) for being my confidantes and escorts during sampling excursions.

I am also thankful for the Botswana Government and BIUST for funding my studies through the BIUST scholarship. Thanks also to the University of the Witwatersrand for their funding through the Postgraduate Merit Award (PMA). I am also grateful to Phatshimo Matshediso at BITRI for assistance in the SEM-EDX analysis of my samples.

No amount of words can express the gratitude and indebtedness I feel towards my family. Thanks a million for your undying love and support throughout this long and trying period in my life. Mama and Papa, thanks for always supporting me and believing in me even when I was losing hope. Making you proud is still the reason I wake up every morning. Thanks, again for stepping in as parents to my 'Rori'. Maps, Chubbilele, Shimanyana and Kabzela, you guys rock. You are a true testament to the African narrative that "It takes a village to raise a child". Le kamoso Batloung.

As for my 'Australian ray of Sunshine' Rorisang Mokone, thanks for being my inspiration and understanding that Mummy is doing all of this for you. Love you to the moon and back.

Last, but, definitely not least, I would like to thank the Almighty God through whom all things are possible.

DEDICATION

To my parents, Meshack and Lydia Mokone, with love

TABLE OF CONTENTS

LIST OF FIGURES

LIST OF TABLES

LIST OF ABBREVIATIONS

ABC	Active barium calcium
AC	activated carbon
ALD	anoxic limestone drains
AMD	acid mine drainage
b	Langmuir constant
β	activity co-efficient
BAM	Bold's acidic medium
BDST	Bed depth service time
BET	Braunner-Emmet-Taylor
C_0	initial metal concentration
C_e	equilibrium metal concentration
CRM	certified reference material
DETA	diethylenetriamine
EDX	Electron dispersive X-ray spectroscopy
E_s	energy of sorption (kJ mol^{-1})
F	flow rate of packed bed column (mL min^{-1})
FTIR	Fourier transform infrared spectroscopy
ICP-OES	Inductive Plasma Optical Emission Spectroscopy
IC	Ion Chromatography
K_{AB}	Adams-Bohart model kinetic constant (L mg^{-1} min^{-1}),
K_D	distribution co-efficient
K_F	Freundlich constant
K_{TH}	Thomas model rate constant (mL min^{-1} mg^{-1})
K_{YN}	Yoon-Nelson model rate constant (min^{-1}),
k_1	rate constant for pseudo- first order kinetics (min^{-1})
k_2	rate constant for pseudo-second order kinetics (g mg^{-1} min^{-1})

k_p	intraparticle diffusion rate constant (mg g^{-1} $min^{-0.5}$)
LOD	limit of detection
LOQ	limit of quantification
MBI	2-mecarptobenzimidazole
m_{total}	total amount of Hg^{2+} ions fed into packed bed column (mg)
MeHg	methylmercury
n	adsorption intensity calculated using the Freundlich isotherm
N_o	saturation concentration (mg L^{-1}),
PC	phytochelatin
PRB	permeable reactive barrier
PTFE	polytetrafluoroethylene
q	adsorption capacity (mg g^{-1})
q_m	maximum adsorption capacity (mg g^{-1})
q_{total}	the total amount of mercury adsorbed in packed bed column (mg)
q_o	the equilibrium metal uptake, Thomas model (mg g^{-1})
r%	total percent removal of packed bed column (%)
SD_{blank}	standard deviation of the blank
SEM	scanning electron microscopy
SRB	sulfur reducing bacteria
t_b	breakthrough time of packed bed (minutes)
t_e	exhaustion time of packed bed column (minutes)
τ	symbol used in the Yoon Nelson method to represent 50% of the time required to reach breakthrough (minutes)
TETA	triethylenetetramine
TGA	Thermogravimetric analysis
US EPA	United States Environmental Protection Agency
v_b	breakthrough volume of packed bed column (mL)
v_e	exhaustion volume of packed bed column (mL)
WMAs	Waste management areas

CHAPTER 1: INTRODUCTION

In this chapter, background information on gold mining and acid mine drainage in the South African context is provided. An introduction to the research problem and the methodology utilized for its resolution are also given.

1.1 Background information

The Witwatersrand Basin in South Africa is renowned for its gold mining activities with excavations dating as far back as the mid-1800s (McCarthy, 2011; Naicker et al., 2003). Gold-bearing ore in this region is comprised primarily of quartz (70-90 %), phyllosilicates (10-30 %) and minor minerals (1-5 %). Pyrite is the most predominant minor mineral with compositions reaching up to 5% (Feather and Koen, 1975; Tutu et al., 2008). Initially, mining operations in the area utilized a mercury amalgam method which released mercury into the environment. Later, this method was abandoned in favor of the McArthur Forest cyanide method which gave greater yields at higher excavation depths. In general, these mining processes involved unearthing of gold-bearing layers and their subsequent crushing prior to gold extraction. The resultant waste rocks were then disposed of in slime or tailing dumps (McCarthy, 2011; Naicker et al., 2003).

Though, mining ceased in the 1960's, the benefit of such activities are evident in the splendor of the cosmopolitan city of Johannesburg which has become the economic hub of the entire African continent (Naicker et al., 2003). Nonetheless, the gloomy remnants of mining are the prevalence of large volumes of mining dumps in some parts of the region (Naicker et al., 2003). These dumping sites contain elevated amounts of pyrite, uraninite (UO_2) and brannerite ($UO_3Ti_2O_4$), arsenopyrite (FeAsS), cobaltite (CoAsS) and galena (PbS), pyrrhotite (FeS), gersdorffite (NiAsS) and chromite ($FeCr_2O_4$) minerals which were unaffected by gold processing (Naicker et al., 2003; Tutu et al., 2008). Some of the tailing dumps also contain mercury released by the amalgam extraction method (Lusilao-Makiese et al., 2013).

Over time, exposure of pyrite and other sulfide bearing components to oxygen and moisture leads to iron oxidation and acid formation. The resultant acidic water can percolate through the dumps and enter the groundwater regime and public waterbodies along the Witwatersrand basin (Akcil and Koldas, 2006; Naicker et al., 2003). This acidic water also contains elevated quantities of iron and other trace metals and is known as acid mine drainage (Akcil and Koldas; 2006; McCarthy, 2011; Naicker et al., 2003). The high metal load in acid mine drainage (AMD) is of great environmental concern because it leads to degradation of the quality of water in receiving water bodies. The metalliferous discharge is detrimental to human health, wildlife, plant life and aquatic ecosystems in general (Gaikwad and Gupta 2008; Kuyucak, 2002; Riefler et al., 2008; Siddiquee et al., 2015). Therefore, to safeguard environmental sustainability, it is vital to devise methods for the prevention or remediation control of acid mine drainage in the area (Kefeni et al., 2017).

Wetlands are one of the most favored technologies for the alleviation of metal pollution in AMD because they offer the advantages of longevity, cost-effectiveness and minimal production of toxic waste products (Gazea et al., 1996; Sheoran and Sheoran, 2006). As a result, they are found along streams and rivers adjacent to mines and tailings in the Witwatersrand region (Tutu et al., 2008).

1.2 Problem statement

Albeit, the successful utilization of wetlands for remediation of metal pollutants in AMD is well-documented in the literature, their main setback is that the saturated and anoxic conditions prevailing in these systems support the methylation of inorganic mercury to methylmercury (Gustin et al., 2006; King et al., 2002; Windham-Myers et al., 2014). Hence, they are major sources of methylmercury (MeHg) production and its exportation to downstream waterbodies (Branfireun et al., 1999; Creswell et al., 2017; Hall et al., 2008). In fact, wetlands are reported to have a higher rate of methylmercury formation than other aquatic systems (Hoggarth et al., 2015). Nonetheless, significant variation in Hg methylation is observed in different types of wetlands due to variations in hydrologic conditions

(seasonal versus permanent flooding) and chemical variability (Hoggarth et al., 2015).

Methylation in wetlands is facilitated by the activity of a variety of microbes including sulfur and iron reducing bacteria found in the ecosystem and also depends on the availability of inorganic mercury (Hoggarth et al., 2015; Liu et al., 2015; Windham-Myers et al., 2014). Hence, factors like electrical conductivity, pH, sulfur speciation, dissolved organic carbon (DOC) and temperature which impact the bioavailability of mercury and activity of microbes are of great significance (Creswell et al., 2017; Hall et al., 2008; Hoggarth et al., 2015; Windham-Myers et al., 2014). The transformation of inorganic mercury to MeHg is of environmental concern because MeHg is a toxic neurotoxin that bioaccumulates in food chains (Branfireun et al., 1999; Frohne et al., 2012; Gustin et al., 2006; Hall et al., 2008). It poses, therefore, a threat to humans, wildlife and other living biota in higher trophic levels (Hoggarth et al., 2015). Hence, there is an eminent need to develop remediation technologies such as biotraps to enhance the capabilities of wetlands in removing mercury from AMD before it is converted to this toxic pollutant.

Traditional methods for removal of mercury from industrial effluents are costly, ineffective at low metal concentrations and produce toxic by-products. On the other hand, biosorption using algae as biosorbents is an economic, eco-friendly and effective technique. Therefore, in the present study, *Cladophora sp* alga was immobilized in polymeric supports and the modified biosorbents were utilized to build biotraps whose efficiency in retrieval of mercury was tested using acid mine drainage sample. According to the author's knowledge, no previous study reports the modification of *Cladophora sp* by immobilization in silica gel and alginate beads followed by use of the best performing modified biosorbent to build biotraps for sequestering mercury from acid impacted environmental samples.

CHAPTER 2: LITERATURE REVIEW

This chapter gives a brief survey and critique of the current literature on the mitigation strategies used for the remediation of acid mine drainage paying particular attention to wetland technologies. The benefits, mode of operation and limitations of wetlands system have also been reviewed. Much focus was placed on their incapacity to effectively remove mercury from industrial effluents and their role as major sources of methylmercury into aquatic ecosystems. Current trends in the field of remediation of mercury-laden wastewaters have also been reviewed with a specific interest in biosorption which entails the use of biological materials as biosorbents for sequestration of toxic metal pollutants. Advances in the industrial application of biosorption technology are also discussed.

2.1 Acid mine drainage

Acid mine drainage (AMD) is a well-known environmental problem plaguing most mining economies globally. It is formed when iron-bearing sulfides (especially pyrite) in rocks are exposed to oxygen and water which oxidize iron and produce sulfuric acid (McCarthy, 2011; Muhammad et al., 2015; Nyquist and Greger, 2009). The resultant drainage is also infested with Al, Fe, metalloids (As) and toxic heavy metals like mercury, uranium, lead and cadmium (Akcil and Koldas, 2006; Equeenudin et al., 2010). Essentially, the high metal content in AMD is of great environmental concern because it has the potential of contaminating nearby ground and surface waters (Akcil and Koldas, 2006; McCarthy, 2011; Pozo-Antonio et al., 2014; Smith, 1997). Ultimately, this negatively impacts human health and other life-forms in aquatic ecosystems (Durand, 2012; Etale et al., 2016; Tutu et al., 2008).

2.1.1 Properties of AMD

Many research studies have focused on the characterization of AMD and they agree that the chemical composition of the acidic effluent varies significantly between sites. This is mainly due to differences in geology, mineralogy, climate, and hydrogeochemistry at different sites (McCarthy, 2011, Santa Cruz et al., 2013;

Valente et al. 2013). Another disturbing property of AMD is that it is a long-term environmental problem that persists long after mine closure (Egiebor and Oni, 2007; Smith, 1997). For instance, while most mining operations in the Witwatersrand goldfields ceased in the 1960's, the problem of AMD still persists in the region (McCarthy, 2011; Naicker et al., 2003). The persistence of AMD has a direct impact on the cost of implementation of remediation systems (Egiebor and Oni, 2007). Due to these facts, it is necessary to adopt site-specific and economic approaches that would permit long-term application at affected areas (Garland, 2011, Kalin et al., 2006).

2.1.2 Sources of AMD

AMD formation occurs naturally via a sluggish process that allows for interception through neutralization by calciferous minerals like dolomite and calcite (Akcil and Koldas, 2006; McCarthy, 2011). Mining exacerbates this problem by exposing and segregating rock materials thus increasing their surface area and acid-producing capability (McCarthy, 2011; Smith, 1997). Sources of AMD from mining processes include open pits and underground workings from active and abandoned mines (Akcil and Koldas, 2006; Egiebor and Oni, 2007; Gazea et al., 1996; Johnson and Hallberg, 2005). Abandoned mines are known to have higher AMD generating potential than their active counterparts. Therefore, the majority of AMD remediation attempts reported in the literature, particularly in developing countries, have focused on abandoned mines (Egiebor and Oni, 2007; Johnson and Hallberg, 2005).

Surface drainage from tailings and rock heaps are also important sources of AMD pollution (Akcil and Koldas, 2006; Egiebor and Oni, 2007; Johnson and Hallberg, 2005). In fact, mine tailings are a major environmental threat because AMD from these sources tends to be more concentrated and disassembled thus inflicting greater damage (Egiebor and Oni, 2007; Johnson and Hallberg, 2005). Spoil heaps, on the other hand, are less perilous because they often contain carbonate materials which assist in neutralizing some of the acid formed (Akcil and Koldas, 2006).

2.1.3 Formation of AMD

The formation of AMD at its sources occurs via a complex process incorporating many interrelated reactions in which pyrite is oxidized to form sulfuric acid and iron oxyhydroxides (Neculita et al., 2007; Johnson and Hallberg, 2005, Kuyucak, 2002). Even though the mechanism is still vaguely comprehended, the entire process can be summarized as per eqn. 2.1 (Johnson and Hallberg, 2005, Kuyucak, 2002).

$$FeS_2\ (s) + {}^{15}/_{4}\, O_2\ (g) + {}^{7}/_{2}\, H_2O\ (l) \rightarrow Fe(OH_3(s) + 2H_2SO_4(aq) \qquad (2.1)$$

According to this equation, the key requirements for the formation of AMD are moisture, dissolved oxygen and the availability of oxidizable iron sulfides such as pyrite (Neculita et al., 2007; Johnson and Hallberg, 2005, Kuyucak, 2002). Notwithstanding, bacterial activity particularly that of *Acidithiobacillus ferrooxidans* is another limiting factor because it catalyzes the process (Neculita et al., 2007). A combination of other parameters including pH, temperature, surface area of the exposed sulfides and presence of competing oxidants, buffering capacity and the availability of alkaline minerals also have an impact on the rate of AMD generation (Akcil and Koldas, 2006; Neculita et al., 2007; Kuyucak, 2002; Pozo-Antonio et al., 2014).

2.1.4 Effects of AMD formation

Once formed, AMD is detrimental to humans and other living beings in aquatic and terrestrial ecosystems (Kumari et al., 2010; Simate and Ndlovu, 2014). In humans, exposure to some of the heavy metals present in AMD leads to ailments such as bronchitis, skin irritations and renal dysfunction, pulmonary disorders, hypertension and gastrointestinal tract disorders, fatigue, irritability and mental retardation in young children (Simate and Ndlovu, 2014). Heavy metal poisoning in plants causes oxidative stress, cellular damage and disrupts homeostasis in plants. Growth and reproduction in fish are also negatively impacted by exposure to elevated levels of heavy metal pollutants (Kumari et al., 2010). Long-term exposure to some heavy metal pollutants can result in mortality of some biota and thus affect

the biodiversity of aquatic ecosystems (Kumari et al., 2010; Simate and Ndlovu, 2014).

2.1.5 Strategies for the remediation of AMD

Generally, the two approaches that are utilized for the remediation of AMD are source control and mitigation strategies. The source control approach involves the creation of conditions that chemically, biochemically or physically prevent the formation of AMD at the source (Egiebor and Oni, 2007; Kang et al., 2016). This is mainly achieved by eliminating either one or more of the key elements required for the formation of AMD (Egiebor and Oni, 2007; Johnson and Hallberg, 2005). On the converse, mitigation entails the treatment of AMD that has already been formed and reducing its impact on the environment (Egiebor and Oni, 2007; Johnson and Hallberg, 2005; Skousen et al., 2017). Each approach has its pros and cons which need to be considered before selecting the appropriate remediation technology (Egiebor and Oni, 2007; Johnson and Hallberg, 2005; Kalin et al., 2006; Riefler et al., 2008).

2.1.5.1 Source control strategies for AMD

Theoretically, the preclusion of AMD formation at source is best because it is more permanent and eliminates the need for further treatment after mine closure (Kang et al., 2016; Pozo-Antonio et al., 2014). Hence, several researchers have focused on developing methods targeted at preventing the formation of AMD at source (Egiebor and Oni, 2007; Kefeni et al., 2017; Kuyucak, 2002; Riefler et al., 2008; Simate and Ndlovu, 2014).

The simplest and most commonly used techniques for preventing the formation of AMD are those that physically prevent contact between AMD forming materials and oxygenated water. These methods include flooding and sealing, underwater storage, surface water diversion and soil compaction (Akcil and Koldas, 2006; Johnson and Hallberg, 2005; Pozo-Antonio et al., 2014). Flooding and sealing are used for curbing the formation of AMD at abandoned mines. In this process, abandoned mine shafts are flooded with water such that the dissolved oxygen inside

is depleted. Subsequently, the shafts are sealed to prevent the replenishment of oxygen supply (Akcil and Koldas, 2006; Pozo-Antonio et al., 2014).

Underwater storage, on the other hand, is applicable to the storage and disposal of mine tailings whereby the tailings are buried underground and sealed with shallow water covers. Subsequently, dry covers are placed on top as supplementary protection from exposure to air (Johnson and Hallberg, 2005). Nonetheless, dry covers are often made of clay material which cracks during dry seasons and reduces the efficiency of the technique (Johnson and Hallberg, 2005). As a solution, Pozo-Antonio et al., (2014) suggested the use of organic materials like polyvinyl chloride (PVC) as dry covers because they are more durable. However, PVC sheets are more expensive than clay and would, therefore, increase the overall cost of the technique.

Soil compaction can also be used to prevent the formation of AMD by mine tailings. It reduces the permeability, water flow, and oxygen influx into the tailings thus decreasing their susceptibility to generate acidic effluents (Pozo-Antonio et al., 2014). The major obstacle to large-scale adaptation of this technique is that it is not effective on its own and needs to be used in conjunction with others (Pozo-Antonio et al., 2014).

To overcome some of the challenges faced with physical methods, some researchers report the use of chemical treatment to prevent oxidation of pyrite-bearing materials (Chen et al., 2006a; Pozo-Antonio et al., 2014). Chen et al., (2006a) reported the use of triethylenetetramine (TETA) and diethylenetriamine (DETA) to hinder the production of acid by sulfide-containing mine wastes. Similarly, Chander and Zhou, (1992) deduced that treating mine wastes with reagents containing carboxyl groups bound to aromatic hydrocarbons reduced their acid mine drainage formation. Nevertheless, this technology is not fully developed and requires the use of specialized and expensive reagents. (Egiebor and Oni, 2007). The biological toxicity of the chemical reagents used has also not been fully investigated (Jiang et al., 2000).

Passivation where in precipitates are formed on the surface of the acid forming sulfides has also been recommended as a means of inhibiting AMD formation. Accordingly, Shamshuddin et al., (2004) reported the use of KH_2PO_4 and Na_2SiO_3

to form a protective precipitate barrier over AMD-forming pyrites. Jiang et al., (2000) also demonstrated that coating pyrites with a hydrophobic film of sodium oleate reduced their AMD-forming potential. However, the long-term applicability of this method and adaptability of the precipitates formed to seasonal variations has not been fully investigated.

Another approach to preventing AMD formation is the application of bactericides to curb the bacterial catalytic action of *Acidithiobacillus ferrooxidans* (Jiang et al., 2000; Pozo-Antonio et al., 2014; Skousen et al., 2017). For instance, Kleinmann and Erikson, (1982) evaluated the bactericide potential of different surfactants (sodium lauryl sulfate, alkyl benzene sulfonate and alfa olefin sulfonate) in reducing the activity of the bacterial catalyst. They found that sodium lauryl sulfate was most effective in decreasing the activity of *Acidithiobacillus ferrooxidans*. Nonetheless, they discovered that the bacteria re-appeared within two weeks thus indicating that the method is also not a long-term solution. In addition, the requirement for continuous application of bactericides is uneconomical (Pozo-Antonio et al., 2014).

Despite the extensive research performed on the source control approach to AMD remediation, preventative interventions are generally costly and do not offer long term solutions (Akcil and Koldas, 2006; Egiebor and Oni, 2007; Johnson and Hallberg, 2005). They also have technical limitations and often require to be coupled with other technologies. Consequently, till date, no technology has been universally accepted as a means for prohibiting the formation of AMD at source. It is believed that a better comprehension of the mechanism and kinetics of AMD generation would aid in development of preventative methods that can be widely accepted (Egiebor and Oni, 2007). In the interim, research attention has shifted towards mitigation control measures (Kefeni et al., 2017; Riefler et al., 2008).

2.1.5.2 Mitigation control strategies for AMD

Mitigation control strategies of AMD are commonly classified into two broad categories viz-a-viz active and passive technologies (Johnson and Hallberg, 2005). Active treatment of AMD involves the mechanical addition of alkaline chemicals to increase the effluent pH and precipitate metals from solution (Gaikwad and Gupta, 2008; Kefeni et al., 2017; Simate and Ndlovu, 2014; Zienkiewicz et al.,

1997). On the contrary, passive technologies utilize naturally occurring chemical, biological and physical processes to treat AMD with minimal resource input (Kefeni et al., 2017; Skousen et al., 2017).

- **Active technologies for AMD remediation**

The most commonly applied active mitigation method for AMD is neutralization using alkaline agents like lime, calcium carbonate and sodium hydroxide (Gazea et al., 1996; Mbonimpa et al., 2016). This reduces the acidity of the effluent and also causes metals to precipitate out of solution (Neculita et al., 2007; Mulopo, 2015; Pozo-Antonio et al., 2014). The shortcomings of this technique are that it is costly, requires continuous addition of chemicals and produces large volumes of toxic sludge (Neculita et al., 2007; Gazea et al., 1996; Johnson and Hallberg, 2005). As a result, some research workers have focused on developing processes for overcoming some of the challenges faced during chemical neutralization of AMD (Akcil and Koldas, 2006).

A 'high density sludge' method wherein the flocculation aggregates the toxic sludge which then settles was suggested as a possible solution for the issue of voluminous toxic sludge generation (Akcil and Koldas, 2006). Similarly, other researchers reported the replacement of lime by fly ash, bentonite, kaolinite and cement as neutralizing agents to reduce the cost of the process (Egiebor and Oni, 2007). Nonetheless, the costs of operation and maintenance of such treatment plants still remains exorbitantly high (Johnson and Hallberg, 2005; Skousen et al., 2017).

Kefeni et al., (2017) also reported the design and application of the 'GYP-CIX' process by the Western Area mine in South Africa. This method utilizes reusable ion exchange resins to remove calcium and sulfate ions from AMD. Widespread industrial application of the technique has not been reported due to handling difficulty and toxicity of the sludge produced. The method also only targets calcium and leaves other more toxic metal ions in solution (Akcil and Koldas, 2006; Pozo-Antonio et al., 2014).

Recently, Mulopo, (2015) also reported the application of the 'Active barium calcium' (ABC) desalination process for the treatment of AMD. The author was

able to neutralize acidity in AMD, precipitate metals and lower the concentration of sulfate ions. In addition, the process allowed for the processing and recycling of resultant sludge. However, the method is relatively expensive and has only been applied at pilot scale (Kefeni et al., 2017; Mulopo, 2015). Albeit, numerous efforts to develop and improve active control measures for AMD, the strategy still remains uneconomic, produces hazardous materials and is unsuitable for long term applications in abandoned mines (Simate and Ndlovu, 2014). Hence, cost-effective, site specific and maintenance-free passive systems are gaining much research ground (Whitehead and Prior, 2006).

- **Passive technologies for the remediation of AMD**

Passive treatment methods for AMD are favored over active ones because they are generally self-sustaining and do not require external operational resources. They rely on natural biological, chemical and physical processes for the effective and eco-friendly removal of metal pollutants from AMD resources (Neculita et al., 2006; Gazea et al., 1996; Kalin et al., 2006; Skousen et al., 2017). The passive methods that are commonly used for mitigation of acid production in mines are anoxic limestone drains (ALDs), permeable reactive barriers (PRBs) and wetlands (Skousen et al., 2017).

ALDs are comprised of beds of limestone gravel buried in impervious trenches to exclude the entry of moisture and air (Cravotta and Trahan, 1999; Johnson and Hallberg, 2005; Skousen et al., 2017). The carbon dioxide content in these drains is also kept high so as to facilitate the dissolution of limestone which in turn neutralizes AMD. At the same time, anoxic conditions are maintained so as to curb the precipitation of iron (III) onto limestone which would interfere with the neutralization process (Cravotta and Trahan, 1999). Many researchers report successful use of ALDs to treat de-aerated AMD with low metal content (Cravotta and Trahan, 1999; Cravotta, 2003; Skousen et al., 1999; Ziemkiewicz et al., 2003). The limitation of these systems is that they cannot be used for the treatment of oxygen-rich acidic water with elevated levels of iron, aluminum and manganese (Johnson and Hallberg, 2005; Skousen et al., 2017; Ziemkiewicz et al., 2003). Furthermore, the effectiveness of ALDs declines when calcite saturation is reached

(Skousen et al., 2017). ALDs also produce variable alkaline outputs and maintaining the pH of the effluent over time is very difficult. Hence, they are often used in conjunction with wetlands for enhanced performance (Skousen et al, 1997; Skousen et al., 2017).

Permeable reactive barriers (PRBs) have also gained ground over the past two decades as passive methods for acidic water treatment (Neculita et al., 2007). They are made up of reactive material zones buried in channels to treat acid-infested groundwater. Their role is to remove target metal contaminants from AMD polluted waters passing through them (Gibert et al., 2011). Earlier works in the literature reported the use of zero-valent iron as the reactive material of choice. Recently, biological materials such as sulfur reducing bacteria (SRB) are receiving attention as plausible replacements (Neculita et al., 2007; Gibert et al., 2011). SRB work by converting the sulfates in AMD to sulfides which then precipitate dissolved metals in AMD passing through them (Gilbert et al., 2011). Though not many researchers report the use of this technology to lessen the impact of AMD, it is cost-effective, highly efficient at low pH and requires minimal energy input (Neculita et al., 2007).

Gibert et al., (2011) studied the performance of SRB in treating AMD from a site in Azuacollar, Spain. They found that the system was able to effectively neutralize pH and remove metal contaminants from groundwater for 3 years. One major disadvantage of using these systems is that design flaws like the inaccurate characterization of sites and varying climatic conditions can result in incomplete desalination of AMD. In addition, the process yields limited sulfate reduction due to short residence times and poor decomposition of organic matter (Gibert et al., 2011). The reliance of SRB on the availability of additional organic carbons is another critical limiting factor of the technology. Hence, some researchers report the use of waste materials from the food and agricultural industries as additional organic carbon sources (Neculita et al., 2007). Zhang and Wang, (2014) evaluated the feasibility of using manure and sawdust as organic carbon sources for the facilitation of metabolic activity of SRB. They found that chicken manure, cow manure and sawdust could successfully be used as supplementary carbon sources thus enhancing the metal uptake capabilities of the SRB (Zhang and Wang, 2014).

Another shortcoming of using SRB is that their long term applicability has not been fully evaluated. The speciation of the metals removed and the ecotoxicology of the treated AMD are also rarely studied (Neculita et al., 2007). Hence, adaptation of the technology to wide-scale industrial use has been rather slow. Given the limitations of the above-mentioned passive AMD remediation methods, much emphasis has been placed on the use of wetlands for the removal of metal pollutants from AMD.

2.2 Wetlands as mitigation control strategies for AMD

In the past few decades, the use of wetlands as technologies for remediating AMD has intensified because they are cost-effective, efficient environmentally friendly and self-sustaining (Hafeznezami et al., 2012; Kadler and Knight, 1996; Kivaisi et al., 2001; Matagi et al., 1998; Sheoran and Sheoran, 2006; Vymazal, 2010). Wetlands are also flexible, less prone to loading and can be established at the AMD production site (Matagi et al., 1998; Yeh, 2008). Nonetheless, to take full advantage of wetlands as mitigation control strategies for AMD, it is essential to study the different types of wetlands, their characteristics and mechanisms of action.

2.2.1 Definition and classification of wetlands

Wetlands are complex ecosystems that exhibit transitional features between terrestrial and aquatic ones (Kivaisi et al., 2001; Mitsch and Gosselink, 2000; Verhoeven and Meuleman, 1999). They are characterized by shallow waters which have unique soils, vegetation and biota that are adapted to waterlogged and anoxic conditions (Kivaisi et al., 2001; Mitsch and Gosselink, 2000; Verhoeven and Meuleman, 1999; Vymazal, 2010). There are a wide variety of wetlands in the environment; therefore, they are commonly classified using different criteria (Mitsch and Gosselink, 2000; Verhoeven and Meuleman, 1999).

First, wetlands can be categorized as seasonal or perennial with respect to degree and duration of saturation. Seasonal wetlands are those that are only flooded for part of the year whereas perennial ones are saturated throughout the year. Most of the wetlands in southern Africa are seasonal because the region is semi-arid and experiences low, seasonal rainfall (De Klerk, 2013; Tutu et al., 2008). Wetlands can

also be classified as natural or constructed depending on the extent of human interference. Natural wetlands are those that have been part of nature for many years and have survived with minimal human interferences (Dean et al., 2013; Vymazal, 2010). Constructed wetlands, on the contrary, are engineered so as to emulate their natural counterparts (Mitsch and Gosselink, 2000; Qasaimeh et al., 2015; Zhi and Ji, 2012; Zhang et al., 2014).

The main advantage of constructed wetlands is that their operational conditions can be monitored, manipulated and controlled for optimum efficiency (Kivaisi et al., 2001; Sheoran and Sheoran, 2006; Zhang et al., 2014). In addition, the load rates and removal efficiencies for most metals are greater in constructed than natural wetlands (Kivaisi et al., 2001; Sheoran and Sheoran, 2006). Regulatory bodies globally also discourage the treatment of wastewaters using natural wetlands because of the rising concern regarding the negative impacts of the toxic metals on the ecosystem. Hence, most the remediation efforts reported in the literature describe the use of constructed wetlands (Chen et al., 2006b; Khan et al., 2009; Kivaisi et al., 2001; Maine et al., 2009; Zhi and Ji, 2012).

2.2.2 Benefits of wetlands

Wetlands are valuable ecosystems that offer many benefits to local, regional and global environments (Kivaisi et al., 2001; Vymazal, 2010). They provide habitats for the survival, breeding and feeding of living biota like wildlife, birds, plants, and mammals (Kivaisi et al., 2001; Mitsch and Gosselink, 2000; Zhang et al., 2014). Wetlands also aid in storm abatement, flood mitigation and protect shorelines from soil erosion (Kivaisi et al., 2001, Mitsch and Gosselink, 2000). They also offer recreational, historical and aesthetic, scientific and cultural values to humans (Mitsch and Gosselink, 2000; Vymazal, 2010).

Their most significant function is the ability to act as biogeochemical filters for metal pollutants thus aiding in the maintenance of the integrity of waterbodies (Kivaisi et al., 2001; Kosolapov et al., 2004; Mitsch and Gosselink, 2000; Vymazal, 2010). Consequently, they are considered as viable options for resolving water quality issues such as AMD (Kivaisi et al., 2001; Sheoran and Sheoran, 2006). They

depend on inhabitant plants, soils, sediments and micro-organisms to sequester metal contaminants through various mechanisms (Kivaisi et al., 2001; Matagi et al., 1998; Sheoran & Sheoran, 2006; White et al., 2011).

2.2.3 Mechanisms for metal uptake in wetlands

Heavy metal uptake in wetlands occurs via physical, biological and chemical processes in the hydrology, substratum and biota compartments of the ecosystem (Matagi et al., 1998; Sheoran and Sheoran, 2006; Qasaimeh et al., 2015; Vymazal, 2010). These processes are complex and involve the interaction of numerous mechanisms including sedimentation, flocculation and adsorption, precipitation, oxidation, plant uptake and bacterial degradation (Kivaisi et al., 2001; Matagi et al., 1998; Sheoran and Sheoran, 2006; Yeh, 2008). The extent of occurrence of each mechanism is determined by a number of factors such as plants species present, substratum properties, chemical composition of the wastewater and metal properties (Kosolapov et al., 2004; Matagi et al., 1998; Sheoran and Sheoran, 2006). Therefore, a thorough comprehension of these mechanisms allows for manipulation of the systems to improve their performance (Kosolapov et al., 2004; Sheoran and Sheoran, 2006).

2.2.3.1 Sedimentation and flocculation

Sedimentation and flocculation are the most critical mechanisms for the effective removal of metals from wastewaters as particulate matter. The former entails the gradual settling of dense particles in water to underwater sediments (Sheoran and Sheoran, 2006). The efficiency of metal removal via this mechanism depends on the rate of settling and the dimensions of the wetlands. Hence, the process is generally slow and aided by floating plants in these ecosystems which also acts as sediment traps (Matagi et al., 1998; Sheoran and Sheoran, 2006). A study by Noller et al., (1994) revealed that sedimentation in wetlands effectively removed 75-99.7% cadmium, 26% lead, 75.9% silver and 66.7% zinc from AMD.

Flocculation, on the other hand, facilitates effective removal of metals as particulate matter through the formation of ‘flocs’ which then settle faster than lighter individual particles (Matagi et al. 1998; Sheoran and Sheoran, 2006). Flocs also bind to suspended heavy metal particles and drag them to the sediments. The factors

favoring flocculation in wetlands are high pH, high concentration of suspended matter, ionic strength and high concentration of algae (Matagi et al. 1998; Sheoran and Sheoran, 2006). Through sedimentation and flocculation, heavy metal pollutants are removed from the water and transferred to sediments where they are trapped thus protecting downstream waterbodies (Matagi et al. 1998; Sheoran and Sheoran, 2006). However, these processes are often preceded by precipitation and co-precipitation which aggregate metals into large enough particles (Matagi et al., 1998; Sheoran and Sheoran, 2006).

2.2.3.2 Precipitation and co-precipitation

Precipitation plays a significant role in heavy metal removal in wetlands because it limits their bioavailability through their dissolution. It is controlled by the solubility product (K_{sp}) of metals, pH of wetland water and the availability of competing ions (Matagi et al., 1998; Sheoran and Sheoran, 2006). The prevalence of sulfates and sulfur reducing bacteria in wetlands make the precipitation of metals as sulfides highly favored (Sheoran and Sheoran, 2006). Mungur et al., (1997) reported the removal of 81.7% Cu in wetlands through sulfide precipitation while Schiffer, (1989) observed 83.3% removal of Pb in natural wetlands as sulfide precipitates.

Carbonate precipitates of metals can also be formed in wetlands if there is a high concentration of hydrogen carbonates in the water (Sheoran and Sheoran, 2006). They play a pivotal role in the initial trapping of metals even though they are not as stable as sulfides. Carbonates are reported to be effective at precipitating Pb and Ni from AMD waters (Sheoran and Sheoran, 2006). Schiffer, (1989) also reported the removal of 79% of Mg and 25% Ni in the form of carbonates from wastewater at a wetland in Central Florida, USA.

Co-precipitation is a complimentary mechanism whereby the precipitates formed through precipitation adsorb other metals dissolved in the water (Matagi et al., 1998; Sheoran and Sheoran, 2006). In such instances, metal pollutants like As, Cu, Zn and Ni co-precipitate with Fe hydroxides. The rate of adsorption of metal ions by hydroxides is affected by the concentration of iron in solution, pH and redox potential, presence of specific anions and contact time (Matagi et al., 1998; Sheoran and Sheoran, 2006). Hydroxyoxides of Fe can be negatively or positively charged

depending on the pH; therefore, they co-precipitate with varying metal ions depending on solution pH. Fe oxides are also redox sensitive and may go back into solution when redox potentials change (Matagi et al., 1998; Sheoran and Sheoran, 2006).

2.2.3.3 Adsorption

Basically adsorption of metals in wetlands involves their binding to soil particles through either cation exchange or chemisorption. Cation exchange depends on the exchange capacities of soils and involves temporary binding of metal ions onto clay or organic matter components of soil by electrostatic attraction (Matagi et al., 1998; Sheoran and Sheoran, 2006). On the converse, chemisorption results in stronger and more stable metal binding. The capacity of soil to bind metals using this process is linked to physical and chemical properties of the water, metal properties and the presence of other metals and ligands. Once bound in this manner, metal ions remain that way and do not biodegrade. However, the metal speciation can vary with changes in soil properties (Matagi et al., 1998; Sheoran and Sheoran, 2006).

Precipitates formed by the oxidation and hydrolysis of iron, aluminum and manganese can also adsorb other metals dissolved in the water. The rate of adsorption of metal ions by metal hydroxides is affected by the concentration of iron in solution, pH and redox potential, presence of specific anions and contact time (Matagi et al., 1998; Sheoran and Sheoran, 2006).

2.2.3.4 Phytoremediation

The most prevalent biological mechanism for metal retrieval in wetlands is phytoremediation or plant uptake (Matagi et al., 1998; Qasaimeh et al., 2015; Sheoran and Sheoran, 2006). Hence, their role in metal uptake is well-documented in the literature (Kivaisi et al., 2001; Qasaimeh et al., 2015; Yeh, 2008). There are a wide range of plants in wetlands inclusive of emergent, surface floating and free floating, rooted leaves, submerged macrophytes and trees which contribute to overall clean-up of heavy metal pollution in wetlands (Qasaimeh et al., 2015; Sheoran and Sheoran, 2006). Emergent and surface floating plants take up metals through their roots while submerged, floating and free floating species do so through both leaves and roots. In addition, submerged plants are capable of

extracting metals from sediments and water while those without roots only have access to metals in the water (Qasaimeh et al., 2015; Sheoran and Sheoran, 2006).

The removal rate of metals by plants is a function of plant species, plant growth, pH, sediment chemistry, temperature and concentration of heavy metals (Khan et al. 2009; Qasaimeh et al., 2015). Notwithstanding, macrophytes are reported to have the highest metal uptake capabilities and therefore play a huge role in wetland treatment systems. In fact, *Typha* and *Sphagnum* are the two most extensively used macrophytes species for heavy metal removal in wetlands because they can withstand high metal concentrations without any visible effects on their morphology (Qasaimeh et al., 2015; Sheoran and Sheoran, 2006; Yeh, 2008). Accordingly, Gomes et al., (2014) demonstrated in a pilot scale study that *Typha domingensis* plants contributed 99.6% to the removal of mercury in wetlands.

Hegazy et al., (2011) also studied the accumulation of Al(III), Fe(III), Zn(II) and Pb(II) in different parts of *Typha domingensis* plants found in a constructed wetland in El-Sadat, Egypt. They found that metal uptake by the different parts of the plants varied with seasonality and highest uptake was observed in the summertime. The accumulation of metals was also highest in the roots and rhizomes compared to the leaves for all metals studied. Bonanno, (2013) also compared the performance of *Typha domingensis, Phragmites australis* and *Arundo donax* in removing heavy metals from wastewaters in wetlands. They deduced that *T. domingensis, P. australis* had higher capacities than *A. donax* for removal of all metals. Kolbash and Romanoski, (1989) also reported removal of 50% of the Fe in AMD from a coal mine by *Typha latifolia* plants.

2.2.4 Limitations of wetlands

Even though wetlands are proven to be outstanding methods for treating AMD, they have inherent limitations that affect the performance and applicability of the systems. First, they require a lot of land to set up; this adds to the overall cost of application of the technology. The performance of wetlands is also greatly impacted by large fluctuations in water levels due to floods and droughts (Lizama et al. 2011; Neculita et al. 2007; Pozo-Antonio et al. 2014; Whitehead and Prior, 2006).

Wetlands are also not effective in rocky or steep soils and are prone to accumulation of precipitates. Problems also arise when there are elevated concentrations of sulfates. In such cases, it would be necessary to provide supplementary carbon sources for the nutritional maintenance of bacteria (Sheoran and Sheoran, 2006). The ecosystems are also subject to the effect of seasonal variations and in some cases may experience catastrophic system failures such as the Wheal Jane mine disaster of 1992 (Neculita et al. 2007; Pozo-Antonio et al. 2014; Whitehead and Prior, 2006).

Another significant limitation of wetlands is their inability to effectively remove mercury from wastewaters (Faulwetter, 2009; Hall et al., 2008). Instead, they convert the pollutant to a more potent form (MeHg) and transport it to downstream waterbodies where it can debilitate human health and entire ecosystems. Mercury in these systems is also easily lost to the atmosphere via evapotranspiration (Creswell et al., 2017; Hall et al., 2008).Therefore, it is vital to develop methods to enhance the removal of mercury from wastewaters passing through wetlands. In order to successfully develop and remediation methods for mercury, it is crucial to fully understand the properties, speciation, biogeochemical cycling and environmental impacts of the pollutant.

2.3 Mercury as a global pollutant

Over the years, mercury has been the subject of many research works due to its toxicity, persistence in the environment and ability to be transported globally over long distances (Cyr et al., 2002; Gomes et al., 2014; Nicolardi et al., 2014; Plaza et al., 2011; Sunseth et al., 2017). It also bioaccumulates in food webs thus posing threats to humans and other animals in higher trophic levels (Khoramabadi et al.; 2008; Lehnherr, 2013, Nanseu-Njiki et al., 2009; Shabudeen et al., 2013). As a result, it has been listed by the United States environmental protection agency (US EPA) as a priority pollutant. The World Health Organization (WHO) has also stipulated permissible limits for industrial discharge and drinking water at 2 and 1 $\mu g\ L^{-1}$ respectively (Lin and Pehkonen, 1999; Wang et al., 2012; Windham-Myers et al., 2014). Hence, a large number of scientific works have focused on developing ways for remediating mercury contaminated waters before they are released into

public waterbodies (Dash and Das, 2012; Driscoll et al., 2013; Hutchinson and Atwood, 2003; Shabudeen et al., 2013; Wang et al., 2012; Zhu et al., 2009).

In order, to develop new treatment methods for mercury contaminated waters or improve existing ones, it is necessary to identify and evaluate its different sources to the environment. Consequently, a number of studies in the literature are devoted to investigating the sources of mercury to the environment (Sunseth et al., 2017).

2.3.1 Sources of mercury

Though mercury exists naturally in the environment as cinnabar (HgS) which is relatively immobile and non-bioavailable to living biota, it can be released as labile species from a variety of sources (Dash and Das, 2012; Gomes et al., 2014; Pirrone et al., 2010). The sources of mercury are often categorized as natural or anthropogenic (Boening, 2000; Ebinghaus et al., 1999; Huang et al., 2016; Rafaj et al., 2013).

2.3.1.1 Natural sources of mercury

Natural sources of mercury are important contributors to the overall emission of mercury to the environment at local, regional and global scales (Pacyna et al., 2006; Pirrone et al. 2010). It is postulated that these sources emit about 5207 Mg of mercury into the environment yearly (Lehnherr, 2013; Pirrone et al., 2010; Sunseth et al., 2017). Approximately 36% of this quantity originates from oceans while the rest is released from terrestrial surfaces (Pirrone et al., 2010; Sunseth et al., 2017). Natural sources of mercury pollution are further subdivided into primary natural or re-emission sources depending on the origin of the mercury they emit (Pacyna et al., 2006; Sunseth et al., 2017).

Primary natural sources release mercury originating from geological minerals in the earth's core; they include processes such as volcanic eruption, hot springs and other geothermal activities (Boening, 2000; Ebinghaus et al., 1999; Gomes et al., 2014; Pacyna et al., 2006). On the other hand, re-emission sources remobilize mercury which has previously been emitted and deposited on plants, surface waters and wetlands (Ebinghaus et al., 1999; Pirrone et al., 2010; Sunseth et al., 2017).

2.3.1.2 Anthropogenic sources of mercury

Anthropogenic sources of mercury include industrial activities such as chlor-alkali plants, fossil fuel burning and waste incineration, small scale gold mining, metal refinery and the use of medical devices (Boening, 2000; Ebinghaus et al., 1999; La Bella & Hilliker, 2003; Lehnherr, 2013; Han et al., 2014). These processes are believed to be the major contributors to global mercury emissions; hence, the majority of research works on mercury emissions place emphasis on those emanating from anthropogenic sources and the impact they have on aquatic ecosystems (Pirrone et al., 2010; Sunseth et al., 2017; Walters et al., 2011). As a result, the methodologies for evaluating the inventory of anthropogenic sources are very advanced and robust (Sunseth et al., 2017). These technological advancements have also aided in predicting future global emissions from anthropogenic sources (Pacyna et al., 2010).

Anthropogenic sources of mercury are also categorized as primary and secondary based on whether they intentionally use mercury in their processes (Pirrone et al., 2010). Primary anthropogenic sources release mercury from geological origin as a by-product of high temperature industrial processes (Pirrone et al., 2010; Sundseth et al., 2017). The major source of mercury in this category is coal combustion which provides energy for other industrial activities. In the year 2000, it was reported that 66% of the total global anthropogenic emissions were from coal combustion (Pacyna et al., 2006). Africa and Asia were also identified as the world's major contributors to Hg emission by coal combustion (Pacyna et al., 2006).

On the converse, secondary anthropogenic sources such as small scale gold mining, chlor-alkali plants, waste incineration and crematoria intentionally use mercury in their processes (Pacyna et al., 2010; Pirrone et al., 2010). Artisanal gold mining is one of the major users of mercury in Africa, Asia and South America. However, due to the under-handedness of the entire process, emissions from this source of mercury are not well-documented (Pacyna et al., 2010). Chlor-alkali plants are the third largest mercury consuming industrial processes; but, the release of mercury by this industry has declined over the past decade. This is mainly due to the adoption of techniques for monitoring the hydrogen gas stream like mist eliminators, scrubbers and application of activated carbon to adsorb mercury at strategic points

(Pacyna et al., 2006). However, most of the control methods have only been adopted in affluent countries (Pirrone et al., 2010). Waste incineration and crematoria are also important anthropogenic sources of mercury (Dash and Das, 2012). But, knowledge on their overall contribution to global emission is still lacking. Of the little research done on these sources, most of the data is from Europe, United States, and Canada (Pacyna et al., 2006)

All the above-mentioned sources of mercury release different species of the pollutant which have varying ecotoxicological and human health effects (Munthe et al., 2001). Hence, it is important to investigate the speciation of mercury released into the environment so as to develop appropriate remediation methods for the pollutant.

2.3.2 Mercury speciation

One intriguing aspect of mercury is that it exists in aquatic systems as different species with different chemical and physical properties (Mazyck et al., 2009; Schroeder and Munthe, 1998; Wang et al., 2004). The main species of mercury found in aquatic ecosystems are elemental mercury (Hg^0), monovalent mercury (Hg^+), divalent mercury (Hg^{2+}), methylmercury (MeHg) and mercury bound to various complexing agents (Amde et al., 2016; Boening, 2000; Hutchison and Atwood, 2003; Lehnherr, 2013; Schroeder & Munthe, 1998; Wang et al., 2004). Hg^+ is very reactive species that exists as dimers which readily dissociate to Hg^0 or Hg^{2+} which are more stable (Hutchison and Atwood, 2003; Schroeder & Munthe, 1998).

Conversely, Hg^0 constitutes 10-30% of the mercury in aquatic systems (Selin, 2009; Ulrich et al., 2001). This species is only sparingly soluble in water; but, it is still an environmental threat because it easily volatilizes to the atmosphere where it persists for long periods and can be transported over long distances (Lehnmerr, 2013; Pacyna et al., 2006; Selin, 2009; Ulrich et al., 2009). Nonetheless, it is only recently that researchers have started to direct their attention towards the removal of this species from the environment (Shao et al. 2016; Wang et al., 2016a; Xu et al., 2013).

Hg^{2+} is the most abundant species of mercury in aquatic ecosystems; hence, it is the subject of many research studies (Dash and Das, 2012; Nanseu-Njiki et al., 2009;

Rocha et al., 2014; Shabudeen et al., 2013). It exists in aquatic systems as either free ions or forms complexes with organic or inorganic ligands (Amde et al., 2016; Ebinghaus et al., 1999, Hutchinson and Atwood, 2003, Pirrone et al., 2010; Wang et al., 2004). The complexed configuration is the most stable and often interferes with remediation efforts (Lehnherr, 2013; Wang et al., 2004).

Methylmercury (MeHg) is the most predominant form of organic mercury in aquatic systems (Branfireun et al., 1999; Selin, 2009). It is formed via the methylation of inorganic species, especially Hg^{2+} with the aid of sulfur reducing bacteria and is stable in natural waters (Amde et al., 2016; La Bella & Hilliker, 2003; Lehnmerr, 2013; Mazyck et al., 2009). MeHg is the most toxic form of mercury because of its lipophilicity and ability to bioaccumulate in living beings. The dominance of each species in aquatic systems depends on the redox potential (E_h), pH and concentrations of complexing agents (Branfireun et al., 1999; Lehnmerr, 2013, Ulrich et al., 2001). The different species of Hg are also interconverted, biogeochemically transformed and transported through many processes occurring in aquatic ecosystems. Hence, it is crucial to fully understand the biogeochemical cycling of the various species of mercury in aquatic systems (Ebinghaus et al., 1999; Dash and Das, 2012; Selin, 2009).

2.3.3 Biogeochemical cycling of mercury in aquatic systems

The chemistry of mercury in aquatic systems is very complex; therefore, predicting its behavior in aquatic systems is not an easy task (Ulrich et al., 2001). The aquatic mercury cycle illustrated in Fig. 2.1 summarizes the entry, release and interconversions of the different species of mercury in aquatic ecosystems. Mercury generally enters aquatic systems as Hg^0 or Hg^{2+} through direct deposition, run-off from watersheds and direct wastewater discharge (Braaten et al., 2014; Mason et al., 1994; Selin, 2009; Zillioux et al., 1993). Since Hg^0 is volatile most of it escapes to the atmosphere through volatilization (Lehnmerr, 2013; Selin, 2009; Ulrich et al., 2001).

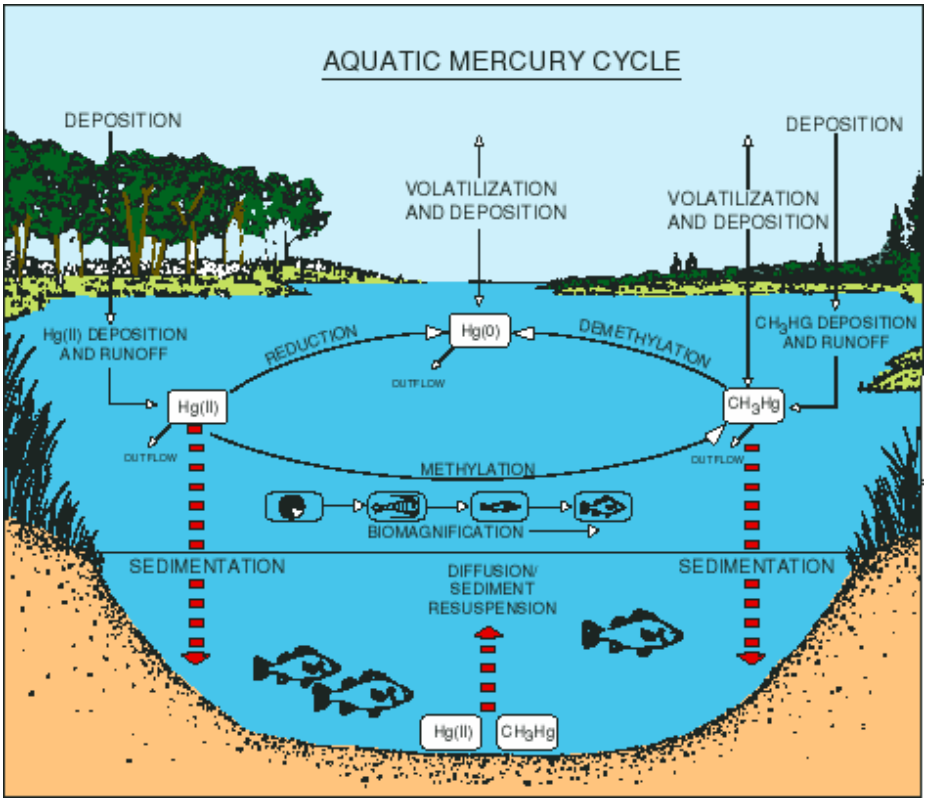

Fig. 2.1: The aquatic mercury cycle (Source: Krabbenhoft &Rickert, 1995)

A small portion of the inorganic mercury is also converted to MeHg through methylation (Lehnmerr, 2013; Selin, 2009; Ulrich et al., 2001). Methylation is a pivotal step in the cycling of mercury because it converts inorganic species to a more toxic form that severely affects human and other living biota (Lehnmerr, 2013; Ulrich et al., 2001). It is a biologically-mediated process that depends on numerous environmental conditions such as the availability of Hg^{2+}, activity of sulfur-reducing bacteria, total organic carbon and redox potential (Lehnmerr, 2013; Selin et al. 2009; Ulrich et al., 2001; Zillioux et al., 1993). The process generally occurs at the sediment-water interface in natural waters even though some degree of methylation has been observed in water columns as well (Eckley and Hintelmann, 2006; Lehnmerr, 2013; Selin, 2009).

Despite that, methylation occurring in the water column is most important because the volume is larger than that in the sediments. Demethylation also occurs as a regulatory measure wherein the carbon-mercury bond is broken with the aid of

enzyme activity to form methane and Hg^{2+} which are less toxic (Lehnmerr, 2013). Both methylation and demethylation processes occur simultaneously until equilibrium conditions are attained wherein the concentration of MeHg in the sediments remains constant at 1-1.5% of total mercury (Ulrich et al., 2001).

Mercury also has a tendency to bind to particulate matter suspended in water. Hence, suspended particular matter is another major driving force for mercury transport and transformation in aquatic systems (Ulrich et al., 2001). The particles that are normally suspended in water are organic matter, oxyhydroxides, bacteria, and algae. Organic matter plays a pivot role because it forms very stable complexes with mercury. Hence, the majority of the mercury in these systems will be present as organic matter complexes. Iron and manganese oxides also have high binding affinities for mercury; therefore, due to their large surface areas they are also able co-precipitate mercury from solution (Ulrich et al., 2001).

Organic matter and oxyhydroxides tend to bind preferentially to Hg^{2+} over MeHg. Hence, in natural aquatic systems, most of the Hg^{2+} will be bound to particular matter whilst MeHg remains in the water column (Ulrich et al., 2001). Accordingly, a study by Hudson et al., (1994) evaluated the cycling of mercury in Wisconsin lakes and found that 94-99% of the Hg^{2+} was complexed with organic matter and the degree of complexation was affected by redox potential, pH and the presence of sulfide ligands.

The settling of particulate matter is a major delivery vector for mercury to the sediments (Ulrich et al., 2001). In fact, according to Covelli et al., (1999), 25% of the mercury in aqueous systems can be released from the sediments yearly and recycled at the sediment-water boundary. The process of release and delivery of mercury to the sediments depends on several factors including the sediment-water partition co-efficients, pH, temperature, complexing agents and the availability of nutrients. For instance, anoxic conditions, low pH and high temperatures favor the release of mercury (Ulrich et al. 2001).

The uptake of mercury especially MeHg by living biota and its subsequent bioaccumulation in food chains is another critical process in the aquatic mercury cycle. Through this process, even low concentrations of MeHg can be

bioaccumulated to such high levels that they affect humans and other living biota (Ulrich et al., 2001). Albeit, only 10-30% of mercury in aquatic ecosystems is MeHg, 85-90% of the mercury in fish is MeHg. Thus, through this process, trace amounts of MeHg can be bioaccumulated to dangerous levels in higher trophic level organisms.

2.3.4 Environmental and human health impacts of mercury pollution

Mercury is known to have adverse effects on human health and other living biota in aquatic ecosystems. The main exposure routes for mercury poisoning in humans are drinking contaminated water, fish consumption and occupational exposure (Harris et al., 2006; Lehnmerr, 2013). The human groups that are most susceptible to mercury poisoning are pregnant women, developing embryos, young children and fish-eating populations residing in polluted areas (Mazyck et al., 2009). Different species of mercury are also known to have differing effects on human health.

Hg^0 and Hg^{2+} are believed to collectively cause autoimmune responses, renal failure, pulmonary malfunctioning and liver damage (Driscoll et al., 2013; Lehnmerr, 2013). In contrast, MeHg is a powerful neurotoxin that can cross the blood brain barrier thus damaging the central nervous system. Therefore, it is linked to neurodegenerative illnesses like Alzheimer and Parkinson (Lehnmerr, 2013; Wang et al., 2012). MeHg also debilitates motor sensory activity and causes emotional instability in adults. It can also cross the placental barrier and harm developing fetuses (Driscoll et al., 2013; Lehnmerr, 2013). Mercury poisoning is also believed to be carcinogenic in humans and linked to teratogenic effects such as reduction in fertility (Wang et al., 2012).

Mercury poisoning is also detrimental to the survival, reproduction and growth balance of other organisms in the aquatic ecosystem (Wang et al., 2012). It diminishes the reproductive success of some fish populations and alters the genetic structures and functional diversities of some bacterial species (Driscoll et al., 2013; Wang et al., 2012). Plant photosynthesis, growth and crop production, nutrient uptake and homeostasis are also negatively impacted by mercury poisoning (Wang et al. 2012). Mercury is also reported to inhibit growth, photosynthesis and nitrogen

fixation in algae. The chlorophyll content of some algal species is also known to be severely affected by exposure to mercury (Agrawal et al., 1992). Hence, it is important to remove mercury from wastewaters such as AMD before they are released into main water supplies.

2.3.5 Global scenario of mercury pollution

It is reported that Asian countries are the major contributors to the global mercury pool (Dash and Das, 2012; Pacyna et al., 2006; Pirrone et al., 2010). The continent contributes 54% and is followed by Africa which is responsible for 18% of the global emissions (Dash and Das, 2012). Among the Asian nations, China is known to be the greatest contributor to the global mercury budget. Countries like Japan, India and North Korea are also responsible for substantial amounts of global mercury emissions (Dash and Das, 2012). The staggering levels of mercury pollution in these regions are mainly attributed to economic development and population growth (Dash and Das, 2012; Pacyna et al., 2006). Surprisingly, the literature on mercury pollution in Asia is lagging behind that of developed regions like Europe and Northern America (Pacyna et al., 2006).

Streets et al., (2005) produced an inventory of mercury emissions from anthropogenic sources in China. They found that 536 tons of mercury were released yearly and 56% of this amount was elemental mercury, 32 % was Hg^{2+} while only 12% was reported as mercury associated to particular matter. Similarly, Chen et al., (2016) showed that of the 603 tons of mercury released annually in China in 2003, 395 tons were Hg^{0}, 30 tons were Hg^{2+} and only 70 tons were mercury associated to particular matter (Chen et al., 2016).

Mercury emissions in Europe and North America are reported to be the lowest and contribute less than 10% to the total mercury released globally (Dash and Das, 2012; Pacyna et al., 2006; Pirrone et al., 2010). This is mainly because of the widespread adaptation of new technologies aimed at reducing mercury pollution in these regions (Dash and Das, 2012; Pacyna et al., 2006). Research on the levels of mercury emission and their impact on the environment is also advanced in these parts of the world (Pacyna et al., 2006).

Pacyna et al., (2005) used source test measurements to evaluate the speciation of mercury released by coal power stations and waste incinerators in Europe. They showed that elemental and oxidized mercury were the main forms released at combustion plants. The mercury fraction bound to particulate matter was found to be low for the power stations. MeHg was also not detected in the exhaust gases emanating from these plants (Pacyna et al., 2005). But, further studies are still required at major point sources to get a clearer picture of the speciation in mercury emissions (Pacyna et al., 2005).

Dash and Das, (2012) also reported that Europe releases 145.2 Mg of mercury per annum and 52% of these emissions originated from coal combustion. Industrial processes like chloralkali plants and cement production contributed 38% while only 10% originated from waste incineration in the region (Dash and Das, 2012). A study published by Dufault et al., (2009) also showed that sources in the United States of America (USA) only contributed 3% to the global mercury emission and 60% of these emissions were from anthropogenic sources. Minnesota, Wisconsin, Little Rock Lake and Crab Lake were also identified as 'hot spots' for mercury pollution in the USA (Dash and Das, 2012; Dufault et al., 2009; Swain et al., 1992).

2.3.6 The state of mercury pollution in South Africa

Despite the numerous accounts of mercury emissions from various sources and their impact on aquatic environment in other parts of the world, there is still ambiguity in values for low-income regions like Africa (Pacyna et al., 2006; Pirrone et al., 2010). Hence, a limited number of studies report the state of mercury pollution and its impact on aquatic ecosystems in South Africa (Walters et al., 2011).

Walters et al., (2011), performed research work on mercury pollution in South Africa and its potential threat to humans and aquatic ecosystems in the country. They collected water, sediment and biota samples from 62 sites in 19 water management areas (WMAs) across the country and measured their mercury content. They revealed that the concentration of total mercury in the water samples varied from 0.02 to 26.65 ng L^{-1}. On the contrary, MeHg levels were in the range 0.02 to 2.73 ng L^{-1}. There were also variations in total and organic mercury content in samples collected from different sites. The designation of Olifants, Upper Vaal and

WMAs as mercury hotspots was also attributed to their close proximities to coal power stations and areas plagued by small scale gold mining (Walters et al., 2011). Nevertheless, long term monitoring of these sites was not performed to gain more insight on pollution in the area. The authors also did not carry out seasonality studies to fully understand mercury pollution in the representative sites.

Lusilao-Makiese et al., (2013) also assessed the effect of mercury use in gold mining in the West Rand region. They collected water, soil and sediment samples from an abandoned mine in the Randfontein area. Their findings showed that water from the mine was acidic and had high concentrations of total mercury. High metal concentrations were also found in the sediment samples. Water from a borehole in the Krugersdorp Game Reserve which is downstream from the mine also contained 223 ng L^{-1} of mercury. High concentrations of MeHg were also recorded in these waters and surface sediments. These results and those in other studies show that there is a need to develop methods for remediating mercury pollution in aquatic ecosystems in South Africa.

2.3.7 Conventional remediation technologies for mercury in wastewaters

The extreme environmental and public health threats of mercury pollution has driven researchers to focus on the inception of remediation technologies best suited for the removal of the contaminant from wastewaters (Figueira et al., 2011; Fu and Wang, 2011; Shabudeen et al., 2013; Wang et al., 2012). The selection of treatment methods is generally influenced by performance, metal speciation, and initial metal concentration, presence of interfering entities, cost-effectiveness and ease of operation (Kurniawan et al., 2006; Motsi et al., 2009). For that reason, the techniques that are traditionally used for the treatment of mercury-infested waters are chemical precipitation, membrane separation, coagulation and ion exchange (Abdel-Raof and Abdul-Raheim, 2017; Blue et al., 2008; Michalak et al., 2013; Zeraatkar et al., 2016). However, these methods are costly to maintain have drawbacks such as inefficiency at low metal concentration and production of large amounts of toxic sludge as a by-product (Abdi and Kazemi, 2015; Tsekova et al., 2010; Vijayaghavan and Balasubramanian, 2015; Vinodhini and Das, 2010). Therefore, activated carbon adsorption has gained much research and industrial

application interest (Anirudhan and Sreekumari, 2011; Mohan and Singh, 2002; González and Pliego-Cuervo, 2014).

2.3.8 Activated carbon adsorption

Adsorption basically entails the transfer of metal ions from the liquid phase to the surface of an adsorbent via chemical or physical binding to the surfaces of suitable adsorbents (Di Natale et al., 2011; Hadi et al., 2015). Though the technology allows for the use of a broad spectrum of adsorbents, activated carbon (AC) is the most commonly used because it has textural properties and functional groups which make it suitable for the removal of heavy metals from wastewaters (Hadi et al. 2015; Wang et al., 2009; Yardim et al., 2003; Zabihi et al., 2010). However, activated carbon has a low selectivity for mercury; therefore, it is often modified using halide, sulfur and nitrogen groups to enhance its performance (De et al., 2013; Hadi et al., 2015; Di Natale et al., 2011; Wang et al., 2009).

Wang et al., (2009) illustrated that impregnating sulfur on ACs improved their adsorption capacities for mercury removal from aqueous solutions. The adsorption capacity of the modified sorbents were found to be thrice those of the pristine materials. It was also shown that at low metal concentrations, metal uptake by the sulfur-impregnated sorbents was unaffected by solution pH whereas the presence of chloride ions reduced mercury sequestration at all concentrations studied (Wang et al., 2009). The major shortcoming of the study was that the speciation of the mercury adsorbed was not evaluated.

Zhu et al., (2009) also demonstrated the modification of ACs with amine groups and their subsequent use for the sorption of mercury from aqueous solutions. They revealed that the performance of the modified adsorbents was dependent on the treatment temperature and the highest mercury uptake was achieved using activated carbons treated at 70˚C. The amine functionalized adsorbents were also shown to have higher sorption capacities than native ones. In spite of this, the authors did not evaluate the effects of pH, initial metal concentration and biosorbent dosage on metal removal by the adsorbents. The efficiency of the adsorbents in treating multi-metal aqueous systems was also not assessed.

Even with all these achievements in improving the selectivity of activated AC, the use of commercial AC still remains costly and its reusability has not been fully evaluated (De et al., 2013; Di Natale et al., 2011; Hadi et al., 2015; Wang et al., 2009). Hence, much research has focused on the use of ACs derived from waste materials as sorbents for the sequestration of mercury from aqueous solutions (De et al., 2013; Hadi et al., 2015; Namasivayam and Kadirvelu, 1999; Yardim et al., 2003; Zhang et al., 2005).

Zhang et al., (2005) reported mercury uptake by various types of ACs obtained from organic sludge. They showed that chemical activation improved the performance of the activated carbons. Adsorbents activated using zinc chloride also had higher sorption capacities than those treated with phosphoric and sulfuric acids. The adsorption process was also influenced by pH, activated carbon dosage and initial mercury concentration. The optimum pH for mercury adsorption was also reported as pH 5 which implied that the adsorbents could be applicable for treatment of acidic effluents. Kinetic and adsorption isotherm modelling also revealed that the experimental data fitted Lagergen's pseudo-first-order kinetic model and the Freundlich isotherm. Metal ions could also be easily desorbed from the surfaces of the ACs using 0.1 M nitric acid (Zhang et al., 2005). The equilibrium times for the native and modified activated carbon were in the range 180 to 420 minutes which is relatively long compared to CAC and activated carbons from other sources (Di Natale et al., 2011; Namasivayam and Kadirvelu, 1999; Yardim et al., 2003).

Furthermore, Yardim et al., (2003) assessed the mercury adsorption behavior on AC derived from furfural at different contact times, metal concentrations, sorbent dosage and pH. They showed that the adsorption capacity of the adsorbent increased with pH until a maxima was reached at pH 5. Equilibrium was also attained within 1 hour and the data suited Langmuir and Freundlich isotherms. Desorption of mercury from the adsorbents using hot water also gave a very poor yield (6%) (Yardim et al., 2003).

Even though effective removal of mercury from solutions using ACs from cheaper sources has been demonstrated in the above studies, activation of the waste materials requires high energy inputs. The adsorptive characteristics of the resultant

activated carbons depends on the properties of its predecessor, treatment times, temperature and oxidizing materials (Zabihi et al., 2010). Consequently, research trends show a shift towards the utilization of low cost sorbents with comparable adsorption capacities for the sequestration of mercury from wastewaters (Babel and Kurniawan, 2003; Kurniawan et al., 2006; Meena et al., 2004).

2.3.9 Low cost adsorbents

The term 'low cost adsorbents' refers to materials that are naturally abundant or can be acquired as industrial byproducts and have been shown to have high metal binding capacities (Kurniawan et al., 2006). Many studies in the literature illustrate the use of low cost abiotic materials like zeolites, clays and fly ash for the removal of mercury from wastewaters (Chojnacki et al., 2004; Kurniawan et al., 2006; Kuncoro and Fahmi, 2013; Manohar et al., 2002; Park et al., 2010). Biological materials including chitosan, plant biomass, microbial biomass and algae have also been shown to have good sorption properties for mercury (Demirbas, 2008; Kong et al., 2016; Kurniawan et al., 2006; Ji et al., 2012; Siddiquee et al., 2015).

2.3.9.1 Zeolites as adsorbents for mercury sequestration from wastewaters

Zeolites are naturally occurring aluminosilicate minerals; they are reported to be effective in the retrieval of heavy metals from aqueous solutions (Kurniawan et al., 2006). However, they are reported to have a low selectivity towards mercury. Hence, few works illustrate their use for treatment of mercury infested waters (Chojnacki et al., 2004; Zhang et al., 2009). In those few research works, they are often treated with thiol groups to enhance their mercury removal capacities (Zhang et al., 2009).

Zhang et al., (2009) reported the improvement in the performance of zeolites after thiolation. Nonetheless, the downside of using the thiolated zeolite was that the time required to attain equilibrium using these adsorbents was long (3 hours) compared to that of natural zeolites (1 hour) (Zhang et al., 2009). The reusability of the zeolites and the effect of competing ions on the sorption of mercury were not investigated. But, these factors have an impact on the cost and industrial applicability of the treatment technology. Another major disadvantage of using this

adsorbent is that its performance is poor under acidic conditions (Zhang et al., 2009). Therefore, it would not be suitable for treating acidic solutions like AMD.

Fardmousavi and Faghihian, (2014) also utilized thiol functionalized hierarchical zeolite nanocomposites to remove mercury from aqueous solutions. The resultant nanocomposites were shown to have high selectivity for mercury and could be regenerated using nitric acid. Experimental findings also showed a good fit with the Freundlich isotherm (Fardmousavi and Faghihian, 2014). The inadequacies of this research work though, are that the authors did not optimize the adsorption process for concentration of adsorbent and pH. In addition, the thiolation process required the use of expensive reagents.

2.3.9.2 Clay as an adsorbent for mercury sequestration from wastewaters

Clay is a naturally occurring mineral component of soil which is also reported to have a good metal adsorption capacity. The above-average uptake capacity of clay is believed to be due to its high surface area and exchange capacity (Babel and Kurniawan, 2003; Kurniawan et al., 2006; Manohar et al., 2002). Therefore, Manohar et al., (2002) modified clay with 2-mercaptobenzimidazole (MBI) and used it as an adsorbent for mercury from wastewaters. Their results revealed that loading MBI onto clay improved its mercury removal capacity. The maximum time for removal was also in the range 240-360 minutes for different mercury concentrations. The optimum pH for metal uptake was also reported as 6 and increasing the sorbent dosage led to a reduction in removal capacity in the range studies (Manohar et al., 2002). Mercury uptake using this adsorbent was also unaffected by the presence of other cations indicating that it would be effective for treating multi-elemental effluents like AMD. The removal efficiency of the clay sorbent in wastewater from a chloralkali plant was found to be 99.7 % (Manohar et al., 2002). Despite these good findings, regeneration studies were not performed to evaluate the reusability of the sorbent. The treatment of clay with MBI also augmented the total cost purification system thus reducing its chances of being adopted in developing countries.

2.3.9.3 Fly ash as an adsorbent for the sequestration of mercury from wastewaters

Fly ash is a by-product of the thermal power generation industry; it is comprised of carbonyl and carboxyl functional groups which make it suitable for metal binding (Kuncoro and Fahmi, 2013; Verna and Tripathi, 2014). Kuncoro and Fahmi, (2013) revealed that the adsorption capacities of coal fly ash for mercury (0.40 mg g^{-1}) was higher than that of lead (0.30 mg g^{-1}). However, the authors did not evaluate the effects of contact time, adsorbent dosage and solution pH on the adsorption capacity of the adsorbent. They also did not investigate the performance of the adsorbent in solutions containing more than one ion. The regeneration and possible reusability of the adsorbent was also not evaluated.

Recently, Verma and Tripathi, (2014) also conducted a detailed assessment of the capability of fly ash in removing Hg^{2+} from synthetic wastewater. They determined that the optimum time for maximal removal of mercuric ions was 2 hours and the optimum pH was 10. The removal efficiency of the system also decreased with increases in metal concentrations showing that the sorbent would be best suited for treating dilute aqueous solutions (Verma and Tripathi, 2014). Still, the applicability of the adsorbent in treating multi-component metal solutions was not studies and the adsorbent was found not to be suitable for treating low pH samples.

2.3.10 Biosorption of trace metals from aqueous solutions

The search for low-cost and effective sorbents for the removal of mercury from aqueous solutions has also directed researchers towards biosorption wherein biological materials are used as adsorbents (He and Chen, 2014; Michalak et al., 2013; Park et al., 2010; Sag and Kutsal, 2001). The main advantages of biosorption over other removal technologies include cost-effectiveness, reusability and enhanced metal selectivity, fast kinetics and high metal binding capacity (Gupta and Rastogi, 2008; He and Chen, 2014; Park et al., 2010; Rao and Prabhakar, 2011). Hence, several published works report the use of different types of biosorbents like chitosan, microbial biomass, algae and agricultural waste products to treat heavy metal polluted waters (Demirbas, 2008; Michalak et al., 2013; Romera et al., 2007; Sag and Kutsal, 2001; Tovar et al., 2015; Wang and Chen, 2009). All these types of biosorbents perform differently using varying mechanisms due to dissimilar chemical compositions (Wang and Chen, 2009).

2.3.10.1 Chitosan as a biosorbent for the sequestration of trace metals

Chitosan is a widely abundant biopolymer that can be found in shells of crustaceans, fungi, and insects (Thien et al., 2015). It is a linear amino-polysaccharide comprised of repeating units of β (1-4) 2-amino-2-deoxy-D-glucose (Fan et al., 2009; Peniche-Covas et al., 1999; Thien et al., 2015). Fig. 2.2 is an illustration of the structure of chitosan.

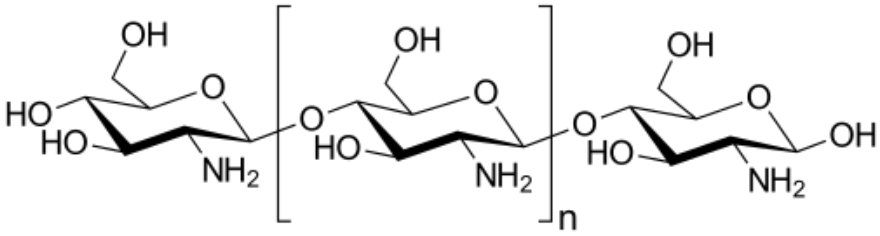

Fig. 2.2: Chemical structure of chitosan (Source: Islam et al., 2017)

Many studies have evaluated the possibility of using chitosan for removal of trace metal pollutants from aqueous solutions because it is rich in free reactive amino and hydroxyl groups on its polymeric backbone. Chitosan is also highly porous, has low toxicity and is biodegradable (Babel and Kurniawan, 2003; Metin and Alver, 2016; Miretzy and Cirelli, 2009; Peniche-Covas et al., 1999; Thien et al., 2015).

Accordingly, Thien et al., (2015) assessed the mercury adsorption capacity of chitosan under different experimental conditions. They reported the maximum adsorption capacity of the biopolymer as 5.07 mmol g^{-1} bisorbent. Adsorption by the biosorbent was also dependent on initial metal concentration, temperature and solution pH. Increasing the metal concentration enhanced metal biosorption while raising the temperature depreciated mercury removal.

Benavente et al., (2011) also studied the biosorption of Cu(II), Pb(II), Zn(II) and Hg(II) from aqueous solutions using chitosan from shrimp shells. They found that the optimum pH for all the metal ions was 6. However, maximal Hg(II) removal occurred at pH 4. The equilibrium data for all metals studied also fitted the Langmuir isotherm. The maximum adsorption capacities calculated using this

model were 79.94, 109.55, 58.71 and 47.15 mg g^{-1} for Cu, Hg, Pb, and Zn, respectively. Kinetic modeling also revealed that the binding of Cu, Zn and Pb followed the pseudo-second-order model thus indicating that chemisorption was the rate-limiting process. On the other hand, for Hg, the biosorption process followed pseudo-first order kinetics thus showing that film diffusion was rate limiting.

Nonetheless, the disadvantage of using chitosan as a metal biosorbent is that its performance is dependent on the biopolymer source, pH, particle size and ionic strength (Veglio and Beolchini; 1997; Miretzky and Cirelli, 2009). Another disadvantage of using powdered chitosan is that it has a relatively low surface area and easily dissolves in acidic medium (de Bashan and Bashan, 2010; Veglio and Beolchini; 1997; Miretzky and Cirelli, 2009).

Many studies report the physical and chemical modification of chitosan to improve these characteristics. New entities can also be grafted on the surface of the material to alter pH range tolerability and improve selectivity (Veglio and Beolchini; 1997; Miretzky and Cirelli, 2009). Accordingly, Li et al., (2005) prepared chitosan beads and appended polymerized acrylamide onto their surface. Subsequently, the adsorption capacity of the functionalized beads was compared to that of the native ones. It was found that the modified beads performed better than the unmodified ones. Optimum adsorption of mercury using the modified biosorbent occurred at pH 5 using 0.25 g L^{-1} of biosorbent, and 20 mg L^{-1} metal concentration. Equilibrium was also reached within an hour and the selectivity for mercury over lead ions was higher in the functionalized chitosan beads (Li et al., 2005).

The use of chitosan beads in industrial metal biosorption processes is still infrequent due to their fragility and instability (de Bashan and Bashan, 2008; Miretzky and Cirelli, 2009). The production of the beads also produces toxic wastes and some of the cross-linkers required for chemical modification are hazardous (Miretzky and Cirelli, 2009).

2.3.10.2 Agricultural wastes as biosorbents for mercury sequestration from wastewaters

In recent years, agricultural waste materials like bark, sawdust and leaves, rice husk, and sugar cane bagasse have gained research ground in their application as

biosorbents for heavy metals from wastewaters (Abdel-Raouf and Abdul-Raheim, 2017; Demirbas, 2008). These materials are predominantly comprised of lignin and cellulose which are rich in functional groups like amino, carbonyl and hydroxyl, phenol, carboxyl, and ether. The above-mentioned functional groups are known to have high affinities for several heavy metals and can effortlessly sequester them from solution (Demirbas, 2008; Sud et al., 2008; Bulut and Tez, 2007).

Kong et al., (2016) utilized native and modified forms of *Triplochyton Scleroxylon* sawdust as biosorbents for the removal of mercury from aqueous solutions. They showed that the degree of modification depended on temperature and materials treated at 30˚C had the highest biosorption capacity. The adsorption capacity of the treated sawdust was also far greater than that of the native one. Removal of mercury by both biosorbents was found to be pH dependent with optimal removal occurring at pH 7. However, at pH values below 6, the unmodified sorbent was found to be most effective showing that it would be most suitable for treating AMD samples.

The adsorption capacities of both types of sawdust were also found to be dependent on biosorbent dosage and optimum removal was observed at a dosage of 10 g L^{-1}. Increasing the metal concentration also improved adsorption for both biosorbents until equilibrium was reached at 30 mg L^{-1} for the native and 40 mg L^{-1} for the modified sawdust. Mercury removal was also shown to decrease in the presence of sodium, calcium and potassium ions (Kong et al., 2016).

Meena et al., (2004) also compared the biosorption of mercury by modified sawdust with that of untreated coal and treated granular activated carbon. They revealed that modified sawdust and untreated coal performed better than the activated carbon. The experimental data for the modified sawdust and untreated coal also fitted both the Langmuir and Freundlich isotherms (Meena et al., 2004). However, the downside of using sawdust for the removal of mercury is that it some of their lignocellulosic components can be leached into the water causing discoloration (Sciban et al., 2006). Hence, several authors suggest pretreatment of the sawdust with formaldehyde to minimize leaching (Sciban et al., 2006).

Ghodbane and Hamdaoui, (2008) also evaluated the bark of *Eucalyptus camaldulensis* as a potential biosorbent for mercury removal from aqueous

solutions. They found the biosorption process to be dependent on pH, sorbent dosage, and contact time, temperature and agitation speed. The kinetics of biosorption were suited to the pseudo-second-order and intraparticle diffusion models whilst equilibrium data fitted the Langmuir isotherm.

Khoramzadeh et al., (2013) also utilized sugarcane bagasse to retrieve mercuric ions from aqueous solutions. They revealed that pretreatment of biomass with sodium hydroxide had no significant impact on metal removal. The removal capacity of the biomass also depended on pH and temperature with optimal removal at pH 4 and high temperatures. Both Freundlich and Langmuir isotherms were suitable for the description of the equilibrium data whilst the kinetics fitted the pseudo-second-order model.

Al Rmalli et al., (2008) also investigated the uptake of mercury from aqueous solutions using powdered leaves of the castor tree (*Ricinus communis L*). They studied the effect of significant parameters on the biosorption performance of the sorbent. The optimum pH was 5.5 and equilibrium was reached in 40 minutes. Increasing the metal concentration improved the removal capacity and the equilibrium data fitted the Langmuir isotherm. Contrarily, the presence of chromium (III), copper (II) and cadmium (II) ions decreased mercury adsorption while lead (II) ions enhanced mercury removal. Desorption of mercury ions from the biosorbent was also achieved using 4 M hydrochloric acid. Column studies were also performed to evaluate the sorbent performance in continuous flow operations (Al Rmalli et al., 2008).

It is clear from all the above research findings that a variety of agricultural waste materials can be used to effectively treat acidic, mercury-rich aqueous solutions like AMD. In spite of this, they may require pretreatment to enhance their performance and curb leaching of lignocellulosic materials into the water being purified (Sud et al., 2008; Rizzuti et al., 2015, Sciban et al., 2006). This increases the overall cost of the technology and may entail the use of chemicals like formaldehyde which are not environmentally safe (Rizzuti et al., 2015, Sciban et al., 2006).

2.3.10.3 Microbial biomass as biosorbents for mercury sequestration from wastewaters

Recent trends show growing interest in using microbial biomass such as bacteria, fungi, and yeast as biosorbents for heavy metals like mercury (Siddiquee et al., 2015; Wang and Chen, 2009). This is mainly due to their relatively low cost and ability to bind to a vast selection of metals to different degrees (Siddiquee et al., 2015; Wang and Chen, 2009).

Microbial cells can be categorized into prokaryotes or eukaryotes with the former being smaller, simpler and having no true nucleus. In contrast, eukaryotes are larger and have a more complex morphology with a pronounced nucleus and well-defined organelles (Barsanti and Gualtieri, 2006; Wang and Chen, 2009).

- **Bacteria as biosorbents for metal uptake in aqueous solutions**

Bacterial cells are eukaryotic hence they have a very simple morphology comprised primarily of cell walls, cell membranes, ribosomes, and nucleoids. They can be spherical, rod-like or spiral in shape and their size ranges from 0.5 to 500 µm (Wang and Chen, 2009). The strength and shape of bacterial cell walls are due to the presence of peptidoglycan. Peptidoglycan is a linear polymer of N-acetylglucosamine and N-acetylmuramic acids which are rich in carboxyl groups (Wang and Chen, 2009). Carboxyl groups are known to be good ligands for binding to metals such as mercury (Kumar et al., 2016; Sag and Kutsal, 2001; Wang and Chen, 2009). Therefore, a number of research studies illustrate the use of bacterial cells for the sequestration of mercury from aqueous solutions (Green-Ruiz, 2006; Sinha et al., 2012; Von Canstein et al., 1999).

Green-Ruiz, (2006) reported the use of non-living *Bacillus sp* for the removal of mercuric ions from aqueous solutions. They found that the removal process was fast and most of the metal ions were retrieved within 20 minutes. The pH and initial metal concentration were also shown to have an impact on biosorption with maximal removal occurring at pH 4.5 and a metal concentration of 10.00 mg L^{-1} (Green-Ruiz, 2006). Experimental equilibrium data also fitted the Freundlich isotherm. The shortfalls of this research work are that the authors did not investigate the effect of biosorbent dosage and temperature on adsorption. Kinetic modeling

and thermodynamic studies were also not conducted to evaluate the thermodynamic behavior and rate of the adsorption process. The effect of co-existing metal ions in solution on the adsorption capacity of the bacterial cells was also not investigated. Continuous flow studies were also not performed to assess the industrial applicability of the biosorption system.

Sinha et al., (2012) immobilized *Bacillus cereus* bacterium in alginate beads and used it for removing mercury from aqueous solutions. They performed adsorption isotherm modeling and found the maximum adsorption capacity of the bacterial cells to be 104.1 mg g^{-1}. The Dubinin-Radushkevich isotherm gave a binding energy value of 15.8 kJ mol^{-1} signifying a chemisorptive process. The biosorbent was also used in a packed column biosorption set-up and breakthrough was attained in 11 hours (Sinha et al., 2012). Von Canstein et al., (1999) also demonstrated that cells of *Pseudomonas putida* bacterium could effectively sequester mercury from wastewater from a chloralkali plant. The biomass was found to be most effective in treating acidic effluents with metal concentrations up to 7 mg L^{-1} thus showing that it would be effective for treating AMD (Von Canstein et al., 1999). However, the authors neglected to mention the time required for attainment of equilibrium.

- **Fungi as biosorbents for metal uptake from aqueous solutions**

Fungi are eukaryotic cells with a wide variety of shapes ranging from spherical budding cells to large, branched filaments which intertwine to form tangled masses of mycelia (Wang and Chen, 2009). However, most fungi are filamentous and their cell walls are rigid to give them their structural shape. Fungal cell walls are comprised mainly of polysaccharides such as chitin which is a strong, flexible nitrogen-containing polysaccharide with N-acetylglucosamine residues. Chitin is known to play a major role in the biosorption of metal ions by fungi because it is rich in amine, hydroxyl and carboxyl groups which have high affinities for metals like mercury (Wang and Chen, 2009). Filamentous and unicellular fungi are reported to have good metal binding properties. Hence, they are the most important in biosorption applications (Wang and Chen, 2009).

Martinez-Juarez et al., (2012) compared the capabilities of 14 different fungal biomasses (*Aspergillus flavus I-V, Aspergillus fumigatus I-II, Helmionothosporium*

sp, Mucor sp I and II, Mucor rouxii IM-80 wildtype and *Candid albicans*) for removing mercury ions from synthetic wastewaters. They observed that *M. rouxii IM-80, M .rouxii mutant, Mucor sp* 1 and 2 were most efficient in removing mercury (Martinez-Juarez et al. 2012). Experimental conditions were also found to have an effect on the biosorption capacities of the biomasses and maximum removal was achieved in 24 hours at pH 5 and a temperature of 30˚C (Martinez-Juarez et al., 2012).

Svecova et al., (2006) also used waste *Penicillium oxaliam* and *Armeniaca Tolypocladium* from the fermentation industry to remove cadmium, lead, and mercury from aqueous solutions. They showed that *P. oxaliam* had higher adsorption capacities for all three metals studied. Moreover, both fungal biosorbents had a higher binding affinity for mercury compared to the other ions. Maximum removal was observed at pH 5 for all the metals studied. The experimental data was also best described by the Langmuir isotherm. Nonetheless, the effects of contact time, temperature and biosorbent dosage on biosorption of metals were not investigated (Svecova et al., 2006).

A study by Amin et al., (2016) also evaluated the biosorption of mercury by *Pleurotus eryngii* biomass and deduced that the adsorption process was rapid with attainment of equilibrium in 5 minutes. The optimum pH, biosorbent dosage, and temperature were reported as 75 mg L^{-1}, 0.25 g L^{-1} and 30 ˚C respectively. Thermodynamic studies also revealed that the biosorption process was exothermic and spontaneous in nature (Amin et al., 2016).

- **Yeast as biosorbents for metal uptake from aqueous solutions**

Yeasts are unicellular fungi which reproduce asexually through budding and transverse division. They are bigger than bacteria and can display spherical or oval morphologies. The most common are the baker's and brewer's yeasts which belong to the *Saccharomyces* genus (Wang and Chen, 2009). Even though yeasts have average biosorption capacities, they have been applied for the removal of a wide array of metals from aqueous solutions (Oyetibo et al., 2015; Sulaymon et al., 2010).

Oyetibo et al., (2015) studied the differences in mercury removal by two strains of the mercury resistant yeast *Yarrowia spp (Idd 1* and *Idd 2).* They illustrated that resting phase cells of Idd2 showed maximum removal. On the other hand, for Idd1, maximum mercury removal was achieved using growing cells (Oyetibo et al., 2015). The authors did not investigate the effect of experimental conditions on the removal of mercury by the two fungal strains. They also did not perform mechanistic studies to gain a full understanding of the binding processes used by the different strains of yeast.

Sulaymon et al., (2010) investigated the biosorption of lead, cadmium and mercury ions from multi-metal solutions using brewer's yeast. They also fitted experimental data to kinetic models and adsorption isotherm isotherms. The authors also applied the biosorption system to continuous flow operation mode and found that increasing initial metal concentration resulted in steeper breakthrough curves. On the converse, increases in flow rate were shown to decrease the breakthrough time of the column. The authors did not perform a full optimization to evaluate the effect of significant parameters like pH, contact time, temperature and biosorbent dosage on metal removal under static conditions before conducting column studies (Sulaymon et al., 2010).

2.3.11 Use of algae as biosorbents for biouptake of trace metals from aqueous solutions

Algae are eukaryotes whose cell structure is more complex than those of other microbial biomass (Barsanti and Gualtieri, 2006; Wang and Chen, 2009). They are one of the most highly abundant resources in aquatic ecosystems; hence, they are utilized in numerous industrial applications including the decontamination of heavy metal infested waters (Kumar et al., 2015; Lesmana et al., 2009). They are favored as biosorbents for the abatement of metal pollutants from industrial effluents because they have high adsorption capacities due to the presence of several functional groups like amino, carboxyl, hydroxyl and amido which can trap heavy metal ions (Bayramoglu et al., 2006; Gupta et al., 2010; Savada et al., 2014). Algae are also highly tolerant of metal pollution and can be modified to enhance selectivity for specific metals (Al-Qodah et al., 2017; Carro et al., 2013). Consequently, several published research works illustrate their use in the bioremediation of industrial

wastewaters (Bai and Abraham, 2002; Ji et al., 2012; Tabaraki et al., 2014; Verma et al., 2016).

Majority of these studies focused on the use of brown algae as metal biosorbents because they are renowned for their exceptional biosorption capabilities (Ahmady-Asbchin et al., 2012; Bermudez et al., 2012; Bhatnagar et al., 2012, Carro et al., 2013; Esmaeili et al., 2015). Non-viable biomass is also preferred over living cells because it is invulnerable to metal toxicity, does not require nutritional maintenance and has higher adsorption capacities (Kumar et al., 2015; Romera et al., 2007; Shanab et al., 2012; Sheng et al., 2004). Much of the research work also sought to determine the conditions required for equibrial metal uptake using batch adsorption studies (Carro et al., 2011; Hackbarth et al., 2011; Huang et al., 2015; Kleinubing et al., 2011; Tuzen et al., 2009; Raize et al., 2004).

2.3.11.1 Definition and properties of algae

Algae are a diverse group of aquatic, photosynthetic organisms found in the taxonomical kingdoms of Plantae and Protista (Barsanti and Gualtieri; 2006; Wang and Chen, 2009). There are approximately 1-10 million different species of algae existing in nature whose sizes range from a few microns in microalgae to several meters in giant kelps. (Barsanti and Gualtieri, 2006). They can exist as unicellular, colonial and filamentous forms (Barsanti and Gualtieri, 2006; Johnson et al., 1996; Wang and Chen, 2009). The latter are easiest to harvest and have higher mechanical stability thus making them more suitable for biotechnological applications (Barsanti and Gualtieri, 2006; Johnson et al., 1996; Kumar et al., 2016).

Algae are also versatile and can be found in a wide variety of habitats including waterbodies, snow caps and tree-trunks, hot springs, building facades and animal fur (Barsanti and Gualtier,2006; Schumann et al., 2005; Wang and Chen, 2009). In exceptional cases, they also co-exist and form symbiotic relationships with other microorganisms such as fungi (Barsanti and Gualtieri, 2006; Zeraatkar et al., 2016). Due to their extraordinary adaptability, algae are tolerant to a wide variety of pH, temperature, turbidity and redox potential conditions (Barsanti and Gualtieri; 2006; Kumar et al. 2015). These properties make them suitable for application in treating wastewaters which may have varying conditions.

2.3.11.2 Classification of algae

Traditionally, algae are categorized into three main groups (*Phaecophyta*, *Rhodophyta*, and *Chlorophyta*) depending on their evolutionary pathways and color (He and Chen, 2014; Romera et al., 2007; Verma et al., 2016). The main differences between these divisions lie in their cell wall components and variability in photosynthetic pigment constituents (Barsanti and Gualtieri, 2006; He and Chen, 2014; Zeraatkar et al., 2016). Table 2.1 gives a summary of the three algal divisions and their cellular compositions

Table 2.1: Cell wall and photosynthetic constituents of the main algal divisions

Type of algae	Photosynthetic pigments	Cell wall components
Phaecophyta	Chlorophyll a, β-carotene	Alginic acid, cellulose
	Xanthophyll, Fucoxanthin	Sulfated polysaccharides
Rhodophyta	Chlorophyll a, α and β-carotenes	Cellulose
	Xanthophyll, Phycoerythrin	Sulfated polysaccharides
Chlorophyta	Chlorophyll a, b	Cellulose
	Carotenes-α, β, γ	
	Xanthophyll	

Phaecophyta are brown, marine algae that are found in most coastal areas across the globe (Barsanti and Gualtieri, 2006; Raize et al., 2004; Verma et al., 2016). Their characteristic brown color arises from the abundance and interactions of chlorophyll a, chlorophyll c and fucoxanthin pigments in their chloroplasts (Wang and Chen, 2009; Sweetly, 2004). They have excellent metal biosorption properties due to the presence of alginates and sulfated polysaccharides on their cell surfaces which allow for selective removal of metal ions (Cazon et al., 2013; He and Chen, 2014; Kratochvil and Volesky, 1998; Raize et al., 2004; Verma et al., 2016). Therefore, they are the most extensively applied for the bioremediation of heavy metals from wastewaters compared to other algal divisions (Kumar et al., 2016; Park et al., 2010; Plaza et al., 2011; Sheng et al., 2004; Raize et al., 2004; Wang

and Chen, 2009). Of all the *Phaeophyta*, those in the *Sargassum* genus are preferred because they have the highest alginate content and therefore the highest adsorption capacities (Tabaraki et al., 2014; Verma et al., 2016).

Rhodophyta are found deep in oceans and are therefore not as abundant as brown algae (Barsanti and Gualtieri, 2006; Yu et al., 1999). They derive their reddish-purplish color from chlorophyll a, α-carotene, β-carotene and phycoerythrin photosynthetic pigments (Barsanti and Gualtieri, 2006; Yu et al., 1999). Their biosorption capability is related to the presence of sulfated polysaccharides like carrageenan on their cell wall. In spite of this, the removal capacity of red algae is much lower than that of brown algae (He and Chen, 2014; Wang and Chen, 2009). Hence, fewer research works report their use for the bio-uptake of heavy metals from polluted waters (El Hassouni et al., 2014; Esmaeili et al., 2015; Prasher et al., 2004; Tamilselvan et al., 2013).

Chlorophyta are distinctive from the other two algal divisions in that they can be found in both fresh and marine waters (Barsanti and Gualtieri, 2006; Filote et al., 2017; Skjanes et al., 2008). Their green color stems from the presence of chlorophylls a and b, α, β and γ-carotenes and xanthophyll in the cell structures (Barsanti and Gualtieri, 2006; Sweetly, 2014). Though their use in biosorption applications has increased over the past few years, there is still scope for more work (Li et al., 2012; Rajfur et al., 2013; Sag and Kutsal, 2001; Sari and Tuzen, 2001; Zeroual et al., 2003).

2.3.11.3 Algal characteristics of Cladophora sp and its potential for use in heavy metal biosorption

Cladophora sp is a genus of green, filamentous algae in the family *Cladophoraceae* (Barsanti and Gualtieri, 2006; Gupta et al., 2001). It is widely abundant and normally found growing on sticks and stones or floating in freshwaters, though some grow in marine waters as well (Barsanti and Gualtieri, 2006; Johnson et al., 1996). Fig 2.3 shows a pictorial representation of *Cladophora sp* growing on stones and a microscopic image of the alga.

Fig. 2.3: Pictorial representation and microscopic image of *Cladophora sp* alga

Most algal species in this genus are coarse in appearance and comprised of filaments bound from end to end. Each filament is in turn comprised of 6-8 daughter cells with independent metabolic functions (Barsanti and Gualtieri; 2006; Johnson et al., 1996; Lee and Chang, 2015). Reproduction in these micro-organisms is mainly asexual involving small zoospores. Sexual reproduction can also occur via biflagellate gametes which either copulate or form a new organism without uniting (Johnson et al., 1996). *Cladophora sp* also have a tendency to overgrow in conditions where vast availability of nutrients prevails. Therefore, in some coastal areas, these micro-organisms have overtaken brown algae in terms of abundance (Filote et al., 2017). The global distribution, fast growth and easy regeneration of *Cladophora sp* algae make them ideal candidates for application in metal biosorption systems (Bagda et al., 2017). Surprisingly, their exploration as metal biosorbents is only just recently gaining research interest (Bagda et al., 2017; Filote

et al., 2017). Even fewer studies report their utilization for the removal of mercury from polluted wastewaters (Ji et al., 2012; Tshumah-Mutingwende, 2014).

A study by Tshumah-Mutingwende, (2014) identified *Cladophora sp* as a possible bioindicator for mercury in acid-impacted wastewaters. They illustrated that the alga could effectively remove mercury from aqueous solutions and the optimum conditions for removal were pH 3, 20 minutes agitation time and 1 mg L^{-1} initial metal concentration. The authors also deduced that the biosorbent performed well in the presence of other divalent ions. Nonetheless, they did not characterize the alga as a possible biosorbent for mercury; nor did they perform full optimization of all the significant parameters affecting algal metal biosorption. They neglected the investigation of the impacts of biosorbent dosage and solution temperature on the adsorption capacity. In addition, the speciation of the mercury adsorbed by the biosorbent was not studied. The authors also did not elucidate the mechanism for biosorption of mercury using this algal biosorbent. Continuous flow studies were also not conducted to evaluate the industrial applicability of the algal biosorption system.

2.3.11.4 Mechanism of trace metal uptake by algae

The process for metal recovery from aqueous solutions by algae is still not fully understood due to the complexity of the organismal structures (Sag and Kutsal, 2001; Sweetly, 2014). Nevertheless, it is well-excepted in the scientific community that the process is comprised of 2 major phases commencing with a rapid stage due to non-metabolic mechanisms like physical adsorption, ion exchange, coordination, complexation, chelation and micro-precipitation (Raize et al., 2004; Sag and Kutsal, 2001; Wang and Chen, 2009). This passive adsorption phase can occur in both living cells and non-viable biomass (Kumar et al., 2015; Sag and Kutsal, 2001). Thereafter, a slower metabolic dependent stage related to metal ion transport across the cell membrane and accumulation takes place (Kumar et al., 2015; Sag and Kutsal, 2001). Intracellular accumulation is restricted to living cells and involves covalent bonding, surface precipitation, redox interactions and diffusion mechanisms (Kumar et al., 2015; Sag and Kutsal, 2001).

The contribution of each mechanism to the overall biosorption process is variable depending on the algal species, biomass preparation steps, metal speciation and solution properties (Raize et al., 2004). Many researchers agree that ion exchange is one of the most dominant mechanisms for algal biosorption of heavy metal ions and that carboxyl and sulfonate groups play a central role (Kumar et al., 2015; Maznah et al., 2012; Michalak and Chojnacka, 2010; Sag and Kutsal, 2001; Sweetly, 2014). Ion exchange entails the displacement of light metals and protons on the algal cell wall surface with heavy metals in solution (Abbas et al., 2014; Raize et al., 2004; Sag and Kutsal, 2001).

Michalak and Chojnacka, (2010) studied the biosorption of metal ions onto the surface of *Vaucheria sp* alga. FTIR analysis and potentiometric titrations revealed that carboxyl groups played a central role in the biosorption mechanism. The authors also observed the release of light metals from the algal surface into solution following the biosorption of metals by the alga thus signifying that ion exchange was the dominant mechanism (Michalak and Chojnacka, 2010) Similarly, Plaza et al., (2011) studied the mechanism for adsorption of mercury by *Undaria pinnatifida* and *Macrocystis pyrifera* algae and deduced that the process occurred mainly through ion exchange and was largely dependent on sulfonate and amine groups.

Physical adsorption is a reversible, non-metabolism dependent mechanism wherein metal ions are bound to polyelectrolytes in cell walls via electrostatic interactions like van der Waals forces, covalent bonding and redox interactions (Kumar et al., 2015). Increases in pH favor this mechanism by making the cell surface negatively charged and increasing its affinity towards metals (Kumar et al., 2015). Kuyucak and Volesky, (1988) found that the mechanism for heavy metal biosorption by dead biomass involved electrostatic interactions between the metal ions and algal cell wall surfaces. Likewise, Aksu and colleagues revealed that the metal binding onto *Chlorella vulgaris* alga was through physical adsorption by van der Waals forces (Aksu et al., 1992).

Complexation is a biosorption mechanism entailing the formation of complexes between heavy metal ions and algal cell wall binding sites via covalent coordination and electrostatic forces (Abbas et al., 2014; Raize et al., 2004; Sag and Kutsal,

2001). Aksu et al., (1992) described the adsorption of metal ions by *Chlorella vulgaris* as also involving the formation of complexes between the metal ions and the carboxyl and amino groups on the biosorbent surface. Lau et al., (1999) also determined that the biosorption of copper and nickel ions from binary solutions onto *Chlorella vulgaris* and *Chlorella miniata* was mainly via complex formation.

Microprecipitation is a distinctive mechanism that can be both independent and dependent on algal cell metabolism. In the former, especially at elevated pH values, low solubility and interactions between the metal ions and algal cell wall surface can cause metal precipitation. On the other hand, metabolism dependent precipitation occurs as a self-preservation mechanism in which metal-stressed cells release compounds like phytochelatins which facilitate precipitation of metals on their surface (Kumar et al., 2015; Sag and Kutsal, 2001). Very few studies on the significance of microprecipitation as a metal biosorption mechanism are reported in the literature (Kumar et al., 2015). Ballan-Dufrancais et al., (1991) illustrated the response of *Tetraselmis suecica* algal cells to exposure to copper and silver ions. The algal cells were found to have accumulated copper and silver coprecipitates in their vacuoles.

Metallothioneins like phytochelatins (PCs) also play a significant role in the biosorption process in algae. They are low molecular weight, cysteine-rich polypeptides that are able to complex metals into thiol clusters (Kumar et al., 2015). Most algae produce phytochelatins to aid in the chelation of toxic metals. Studies by Cobett and Goldsbrough, (2002) revealed that the formation of phytochelatins in algal cells in response to toxic metals is rapid. Moreover, Pawlik-Skowrouska, (2001) also reported the synthesis of phytochelatins by *Stigeoclonium* alga in response to heavy metals in mining effluents. The results showed that the process was dependent on pH and the concentrations of bicarbonate in the water samples (Pawlik-Skowrouska, 2001). In contrast, Perales- Vela et al., (2006) reported that the green alga *Chlamydomonas reinhardtii* adsorbed mercury ions by releasing glutathione instead of phytochelatins.

Compartmentalization of metal ions in algal cells is another significant mechanism contributing to overall biosorption of heavy metals by algae (Kumar et al., 2015).

Shanab et al., (2012) studied the biouptake of lead by three algal species (*Phormidium ambigium, Pseudochlorococcum typicum, and Scenedesmus quadricanda*) and found that the algae were tolerant to lead and could be used to remove the metal from single-metal aqueous solutions. In addition, dark, spherical bodies representing metal accumulation were observed in the vacuoles of the exposed cells (Shanab et al., 2012).

2.3.11.5 Factors affecting metal biosorption by algae

Numerous factors related to the algal biomass such as metal tolerance, size and growth stage, species and algal division, dosage and preparation method have a significant effect on the metal uptake capacity of algae (Chen et al., 2006c; Kumar et al., 2015; Prakasham et al., 1999). Hence, several studies report the investigation of the effects these parameters have on the biosorption capacities of algae (Esmaeili et al., 2015; Khoramabadi et al., 2008; Sheng et al., 2004; Priyadarshani et al., 2011; Singh et al., 2007; Yu et al., 1999).

Algal species is known to be one of the most significant biotic factors affecting the biosorption of heavy metals. Comparisons of the metal adsorption capacities and removal efficiencies of different algal species or divisions are well-represented in published works (Esmaeili et al., 2015; Sheng et al., 2004; Singh et al., 2007; Yu et al., 1999). Esmaeili et al., (2015) compared mercury removal by two different algal species (*Sargassum glaucescens* and *Glacilaria corticata*). They observed that the optimum conditions for the removal of mercuric ions by *S. glaucescens* were pH 5, 200 µg L^{-1} mercury and 90 minutes shaking time. On the converse, *for G. corticata*, maximum mercury removal was achieved at pH 7, 1000 µg L^{-1} mercury concentration and 30 minutes contact time.

Plaza et al., (2011) also assessed the biosorption of mercury using *Undaria pinnatifida* and *Macrocystis pyrifera* algae. Their findings revealed the two biosorbents had the same adsorption capacity in unitary metal solutions. The optimum pH and contact times were also shown to be 5 and 24 hours respectively for both algae. Adsorption isotherm modeling using the Langmuir isotherm also revealed that *U. pinnatifida* had a higher affinity for mercury than *M. pyrifera*.

Tolerance to metal exposure also influences the rate and extent of metal uptake by algae. Metal tolerance is an intrinsic property algae develop in response to metal contaminants like mercury. A limited number of studies in the literature have attempted to explore the effect of this parameter on the metal sequestration by algae (Kumar et al., 2015). Earlier works by Butler et al., (1980) showed that *Chlorella vulgaris* cells chronically exposed to copper (II) ions developed a tolerance for the metal. This, in turn, improved the biosorption capacity of the alga. Priyadarshani et al., (2011) also presented evidence that microalgae exposed to metal stress develop distinctive mechanisms that produce peptides that aid in metal binding.

Several works also studied the effect of biosorbent dosage on metal bioremediation by algae and reported conflicting findings (Kumar et al., 2015). Monteiro et al., (2012) suggested that metal uptake was enhanced at high algal dosages due to a higher number of available metal binding. Similarly, Ramavandi et al., (2006) showed that mercury removal by *Malva sylvestris* biomass also improved when the biosorbent dosage was increased. Abdel-Aty et al., (2013) also demonstrated that in the range 0.025 to 0.25 g L^{-1} the removal efficiency of *Anabaena sphaerica* alga was improved by increasing the biosorbent dosage. In contrast, Ghoneim et al., (2014) reported a reduction in the biosorption of cadmium by *Ulva lactuca* when the biosorbent concentration was increased from 0.1 to 0.4 g L^{-1}.

Some studies have also evaluated the effect of the composition of algae growth culture conditions on the biosorption performance of algal biosorbents (Wang and Chen, 2009). Most of these works investigated the effect of components like cysteine, glucose, sulfates, and phosphates on the metal biosorption capacity. (Khoramabadi et al., 2008; Rezaee et al., 2006; Wang and Chen, 2009; Mapolelo and Torto, 2004). Pre- sorption preparation method and treatment of algae are also known to affect their biosorption capacity. According to Rafjur, (2013), freeze-dried cells of *Spirogyra sp* alga performed better than heat-treated ones. Acid treatment of the algal cells also enhanced their metal biosorption capacities. They also suggested that conditioning the biosorbent in deionized water prior to conducting biosorption studies also improved its metal sorption performance (Rafjur, 2013).

Abiotic factors such as solution pH, metal ion speciation, and initial metal concentration, chemical composition of the solution, solution pH and temperature also impact metal biosorption by algae (Kumar et al., 2015; Kumar et al., 2016; Prakasham et al., 1999). Solution pH is known to have the largest impact on metal sorption capabilities of algae cells because it affects the availability of binding sites and metal speciation (Kumar et al., 2016; Park et al., 2010, Zeraatkar et al., 2016). For this reason, a lot of research workers take this factor into account when screening biosorbents for heavy metal uptake (Kumar et al., 2016; Shanab et al., 2012; Tuzun et al., 2005; Ramavandi et al., 2016; Zaib et al., 2016). Table 2.2 gives a summary of the findings reported for the effect of solution pH on mercury removal using different algal biosorbents.

Table 2.2: Summary of findings of studies on the effect of pH on biosorption of mercury by various algae

Biosorbent	Optimum pH	Reference
Sargassum muticum	5	Carro et al., 2011
Chlamydomonas reinhardtii	6	Tuzun et al., 2005
Spirogyra	4	Rezaee et al., 2005
Sargassum glaucescens	5	Esmaeili et al., 2012
Glacilaria corticata	7	Esmaeili et al., 2012
Cystoseira baccata	6	Herrero et al., 2005
Ulva lactuca	7	Zeroual et al., 2003
Porphyridium omentum	7	Zaib et al., 2016
Sargassum fusiforne	8	Huang and Lin, 2015

Generally, the findings show that metal sequestration by algal biosorbents is a pH-dependent process (Carro et al., 2011; Cheng et al., 2006c; Khoramabadi et al., 2008; Kumar et al., 2016;). The optimum pH for removal tends to vary with metal speciation, oxidation state, and nature of algal biomass (Cheng et al., 2006c; Gupta et al., 2010, Kumar et al., 2016). Nonetheless, it has been found that the optimum

pH for mercury removal using most algal biosorbents lies anywhere between 4 and 8 under given experimental conditions.

Initial metal concentration is an important driving force to overcome all mass transfer resistance of metal ions between the bulk solution and the solid phase (Singh et al., 2014). Consequently, it also influences the extent of metal biosorption by algae (Zeraatkar et al., 2016). In most cases, increasing the metal concentration results in an increase in algal biosorption capacity due to an increase in the number of collisions between metal ions and biosorbents (Singh et al., 2014). This improvement in biosorption capacity is attainable only up to a critical metal concentration beyond which biosorption reduces due to saturation of binding sites on biosorbent (Kumar et al., 2016; Prakasham et al., 1999, Zeraatkar et al., 2016).

Khoramabadi et al., (2008) assessed the biosorption of mercury by *Zygnema fanicum* algae at different metal concentrations. They observed that increasing the initial metal concentration up to 7.5 mg L^{-1} enhanced the adsorption capacity of the biosorbent. Further increases in initial metal concentration were shown to not have an effect on adsorption capacity (Khoramabadi et al., 2008).). On the converse, Huang and Lin, (2015) studied the biosorption of mercury and copper by *Sargassum fusiforne* biomass at metal concentrations ranging from 10 to 50 mg L^{-1}. They deduced that in this range the metal adsorption capacity of the algal biosorbent depreciated when the metal concentration was increased. This was explicable by saturation of binding sites on the sorbent surfaces (Huang and Lin, 2015).

Temperature is also known to impact the uptake of metal ions by algae biosorbents because it affects the stability of ligands on the algal surface and metal ion (Kumar et al., 2016). Studies on the effect of solution temperature on the biosorption capacity of algal biosorbents report inconsistent findings. Some showed that increasing the temperature enhances metal removal by algae while others suggest that metal uptake drops when the temperature is elevated (Aksu et al., 2001, Al-Homaidan et al., 2014; Kumar et al., 2016). Zaib et al., (2016) illustrated that the removal of mercury from aqueous solutions using *Porphyridium cruentum* biomass dropped when the temperature was increased in the range 295 -315 K. Thermodynamic studies also gave negative values of enthalpy and Gibbs free

energy thus implying that the process is exothermic and spontaneous. Conversely, Rezaee et al., (2006) showed that increasing the temperature in the range 4-37˚C reduced the extent of mercury uptake by *Spirogyra* alga. Tuzun et al., (2005) also reported that mercury removal by *Chlamydomonas reinhardtii* alga was independent of temperature in the range studied.

Metal speciation also has an influence on the biosorption rate of heavy metals by algae; yet, very few research works have attempted to evaluate the effect of metal speciation on the metal uptake capability of algal cells (Kumar et al., 2016). Doshi et al., (2007) revealed that live *Spirulina spp* alga has a higher adsorption capacity for chromium(III) than chromium(VI). Singh et al., (2014) also deduced that at low pH there was more removal of Cr(III) than Cr(VI) from aqueous solution by wild algal biomass. Figueira et al., (1999) also demonstrated differential iron species removal by non-living *Sargassum* biomass. Carboxyl groups were also found to be responsible for removing Fe(II) ions whereas sulfonate groups sequestered Fe(III) ions.

The presence of competing cations in metal solution also has a significant impact on metal sequestration by algae. However, the assessment of algal metal biosorption in multi-metal solution is still under-stated in published works (Kumar et al., 2016; Wang and Chen, 2009). Plaza et al., (2011) assessed the effect of the presence of nickel, cadmium, and zinc on the biosorption of mercury by *Undaria pinnatifida* and *Macrocystis pyrifera*. They found that the performance of both biosorbents was greatly reduced in multi-metal solutions. Carro et al., (2011) also revealed that the uptake of mercury by *Sargassum muticum* macroalga was unaffected by the presence of other divalent ions like cadmium, lead, copper, and calcium.

From all the above facts, it can be deduced that the biosorption of heavy metals by algal biosorbents is differentially affected by several biomass factors and abiotic parameters depending on the experimental conditions, properties of the target metal and algal organism used. Hence, it is vital to study them to determine the optimum values required for maximal metal uptake by a biosorbent prior to application to 'real' environmental samples.

2.3.11.6 Limitations of using algae for metal biosorption applications

Albeit, algae has received much research interest as potential biosorbents for heavy metals in aqueous solutions, their application in industry is still lagging behind (Wang and Chen, 2009). This is mainly because algae generally have low stabilities and weak mechanical strengths; hence, high mass losses are observed during biosorption processes (Carro et al., 2011; Wang and Chen, 2009). Algal biomass is also prone to swelling which can clog columns leading to pressure drops (He and Chen, 2014). Algae also leach out organic substances into the bulk solution during the biosorption process (Wang and Chen, 2009). This poses a secondary pollution threat and leads to loss of some beneficial adsorptive materials (He and Chen, 2014; Kumar et al., 2015; Wang and Chen, 2009). Additionally, once biosorption is completed, algae require costly methods like centrifugation and filtration to separate them from solution (Moreno-Garrido, 2008). The regeneration and recycling of algal biosorbents are also problematic (Michalak et al., 2013).

Many scientists recommend the use of chemical or physical pretreatment techniques to overcome these challenges (Chen and Yang, 2006; He and Chen, 2014; Zeraatkar et al., 2016). The most popular methods for pre-treating algal biomass are surface modification and encapsulation (Chen and Yang, 2006; He and Chen, 2014). Chemical modification involves treating the algal surface with reagents such as acids, formaldehyde, and glutaraldehyde. The additional advantage of this method is that modified cells often perform better than native algal cells (He and Chen, 2014; Chen and Yang, 2006). Chen and Yang, (2006) reported a reduction in organic leaching from *Sargassum sp* alga following pretreatment with glutaraldehyde. The biosorption performance of the alga was also enhanced by modification (Chen and Yang, 2006).

Encapsulation, on the other hand, involves the use of immobilizing agents like alginate, agar, silica gel, polyacrylamide to trap the algal cells during biosorption. The benefits of this method are that it utilizes non-toxic chemicals, shields living cells from toxic metal pollutants and facilitates the use of algal biosorption technology in column applications (Bayramoglu and Arica, 2009; Chen and Yang, 2006).

2.3.11.7 Immobilization of algae on solid supports for biosorption applications

Techniques for immobilizing algal cells on solid matrices are basically categorized as passive or active techniques (de Bashan and Bashan, 2010). Passive or physical immobilization is a reversible process based on algae's natural propensity to adhere to surfaces and grow on them (de Bashan and Bashan, 2010; Moreno-Garrido, 2008). In this process, algae can attach to natural or synthetic carriers; but, the former are preferred because they are non-toxic, inert and cheap, mechanically strong and remain stable for long durations (de Bashan and Bashan, 2010; Moreno-Garrido, 2008). The possibility of cells detaching from the support limits the large-scale application of this technique (de Bashan and Bashan, 2010; Mallick, 2002; Moreno-Garrido, 2008).

Active immobilization, on the other hand, involves the use of flocculating agents, chemical attachment and gel entrapment to trap the algal cells (de Bashan and Bashan, 2010; Moreno-Garrido, 2008). Flocculating agents like chitosan are used to bypass the tedious and costly filtration step after biosorption. The downside of using chitosan is its inherent weak stability. On the contrary, chemical entrapment involves interactions of cells with chemicals like glutaraldehyde which can be toxic to living cells or damage algal surfaces (Moreno-Garrido, 2008).

Consequently, gel entrapment is the most extensively used technique for algal cell immobilization (Bayramoglu et al., 2006; Mallick, 2002; Moreno-Garrido, 2008). It can be carried out using a variety of immobilizing agents including polysulfone, polyacrylamide and polyurethanes, agars, alginates, silica gel and carrageenan (de Bashan and Bashan, 2010; Mallick, 2002; Moreno-Garrido, 2008; Wang and Chen, 2009). Natural matrices like alginates are the most commonly used because they are environmentally safe, have high diffusivity and their production is least hazardous (de Bashan and Bashan, 2010; Moreno-Garrido, 2008). Alginates are salts of alginic acid which is a heteropolysaccharide comprised of α-L-guluronic and β-mannuronic acid monomers (Aravindhan et al., 2007; Bayramoglu et al., 2006; Park et al., 2010; Sinha et al., 2012). The most extensively used alginate for immobilization of algal cells is calcium alginate because its preparation steps are simple and it is non-toxic to living cells (Abu Al-Rub et al., 2004; Bayramoglu et al., 2006). Fig. 2.4 shows the chemical structure of calcium alginate.

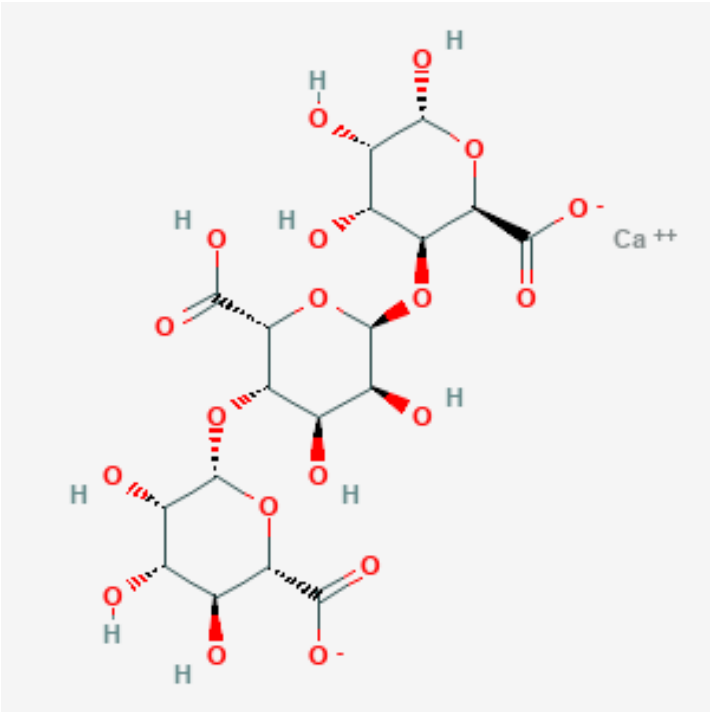

Fig. 2.4: Chemical structure of calcium alginate (Source: Leick et al., 2010)

Accordingly, Bayramoglu et al., (2006) reported the immobilization of *Chlamydomonas reinhardtii* alga on calcium alginate beads and their subsequent use for the removal of mercury, cadmium and lead ions from unitary aqueous solutions. They observed that immobilization improved the adsorption capacity of the alga and the immobilized beads could effectively remove all three metals and the optimum pH for removal was in the range 5-6 (Bayramoglu et al., 2006). The entrapped cells were also found to be reusable after regeneration with 2M NaCl (Bayramoglu et al., 2006). However, the performance of the immobilized beads in multi-elemental solutions was not investigated.

Abu-Al Rub et al., (2004) also immobilized *Chlorella vulgaris* algal cells in calcium alginate beads and used the biosorbents to remove nickel ions from aqueous solution. They too found that immobilization improved the adsorption capacity of the alga. Increasing the pH from 2 to 5 and increasing the metal concentration enhanced the adsorption capacity of the immobilized biosorbents. The alga immobilized in the alginate beads was also reusable up to 3 cycles using 0.1 M HCl

as the desorption medium. In addition, the experimental data fitted the pseudo-second-order kinetic model and both the Freundlich and the Langmuir isotherm (Abu-Al Rub et al., 2004). The shortfalls of the study were that the authors did not evaluate the effects of biosorbent dosage and temperature on the adsorption capacity of the test biosorbent. Column studies were also not performed to assess the industrial applicability of the biosorption system.

Synthetic polymers like silica gel have also been used for the immobilization of algae for metal removal purposes (Moreno-Garrido, 2008). Suharso et al., (2010) reported the immobilization of *Sargassum duplicatum* biomass on silica gel and used the resultant material to sequester copper, cadmium and lead ions in continuous flow mode. They demonstrated that maximum column operation was at a flow rate of 1.3 mL min^{-1}. The maximum adsorption capacities of the metals were found to be 280, 130 and 113 mmol g^{-1} sorbent for copper, cadmium, and mercury respectively. In addition, metals could easily be desorbed from sorbent surface using 2 mM hydrochloric acid (Suharso et al., 2010).

2.3.12 Theoretical treatment of batch biosorption data

Most metal biosorption studies using algae as biosorbents report the use of batch equilibrium studies wherein known amounts of sorbent and fixed volumes of the metal solution under specified conditions are held in closed setups (Kumar et al., 2016; Wang and Chen, 2009). These studies offer valuable information on algal metal biosorption systems such as the kinetics of the process, the effects of environmental factors and the biosorption performance of the biosorbents (Kumar et al., 2016; Park et al., 2010). The performance of the algal biosorption system is one of the most significant outcomes because it gives an indication of the suitability of the test biosorbents for metal removal applications (Kumar et al., 2016).

2.3.12.1 Evaluation of the performance of algal biosorbents

The method that is commonly used for the evaluation of the performance of algal biosorbents is that of calculation of their adsorption capacities (q) and removal efficiencies (Abdi and Kazemi, 2015; Kratochvil and Volesky, 1998). According to Abdi and Kazemi, (2015), a good biosorbent has high values of both adsorption

capacity and removal efficiency. But, some authors argue that evaluation of biosorbent performance using these parameters is inadequate and suggest that their application should be limited to quick approximations for preliminary screening of biosorbents (Kratochvil and Volesky, 1998; Wang and Chen, 2009). In most cases, it is recommended that these calculations should be followed by adsorption isotherm modeling to provide a scientific basis for selecting biosorbents for metal removal (Kumar et al., 2016; Wang and Chen, 2009).

2.3.12.2 Adsorption isotherm modeling of batch biosorption data

Adsorption isotherms are characterized by specific constants whose values represent surface properties of biosorbents and their affinities to target metal ions (Donmez et al., 1999). Hence, they can be used to evaluate the biosorption potential of biosorbents and quantify variations between different sorption systems (Dada et al., 2012; Vijayaraghavan et al., 2006). Essentially, they are plots of adsorption capacity (q) against final or equilibrium concentration (C_e) of metal ions in bulk solution (Abdi and Kazemi, 2015; Vijayaraghavan et al., 2006). Langmuir and Freundlich models are the two most widely applied equilibrium isotherms for the assessment of single metal biosorption systems (Abdi and Kazemi, 2015; Dada et al., 2012; Vijayaraghavan et al., 2006; Wang and Chen, 2009).

The Langmuir isotherm assumes metal sorption onto a homogeneous surface comprised of active sites with equivalent energies. On the other hand, the Freundlich model is an empirical model proposing that metal binding occurs on a heterogeneous surface with active sites of different energies. The limitations of above models are that they do not provide information on the mechanism of the biosorption process adsorption and do not sufficiently express the heterogeneity in dispersal of active sites on biomass (Kumar et al., 2016; Park et al., 2010; Wang and Chen, 2009). As a consequence, they are used in conjunction with the Dubinin-Radushkevich model to provide supplementary information (Dada et al., 2012; Gin et al., 2002; Kumar et al., 2016; Vijayaraghavan et al., 2006). The Dubinin-Radushkevich isotherm is often used for expressing the mechanism for biosorption onto a heterogeneous surface with a Gaussian energy distribution; it is most applicable for intermediate and high concentration aqueous solutions (Dada et al., 2012).

2.3.12.3 Kinetic modeling of batch biosorption data

Kinetic studies are invaluable to the development of novel biosorption systems and improving existing ones because they provide information on the rate of the overall process (Wang and Chen, 2009; Tuzen et al., 2009).The majority of the kinetic studies reported in the literature focus on Lagergren's pseudo-first order and Ho's pseudo-second order models (Kumar et al., 2016; Wang and Chen, 2009; Tuzen et al., 2009). Lagergen's pseudo-first order model is applied when the rate of adsorption depends only on the number of metal binding sites available on the sorbent. Contrarily, Ho's pseudo-second order model assumes that the removal rate is dependent on the square root of the number of available sites (Tuzun et al., 2009). Results from several research works illustrate that pseudo- second order kinetics fit experimental data from a wide array of biosorption systems (Chojnacka et al., 2005; Gonzalez-Bermudez et al., 2011; Preetha and Viruthagiri, 2007; Samuel et al., 2013; Vijayaraghavan et al., 2005; Wang and Chen, 2009).

The main disadvantage of these models is that they ignore the contribution of diffusion mechanisms like intraparticle diffusion. The above models also work on the pretext of fixed sorption mechanisms and pre-existing equations (Wang and Chen, 2009); but, that may not the case for biosorbents like algae. Therefore, in some works, the Webber-Morris intraparticle diffusion model is used to gain perspective on the influence of diffusion on the overall biosorption mechanism (Apiratikul and Pavasant, 2008; Park et al., 2010).

2.3.13 Continuous flow operation for algal-based metal biosorption systems

Despite their many benefits, batch systems are problematic to adopt at a large scale. They are also not suitable for treatment of large volumes of water. In this way, continuous flow systems are preferable (Kumar et al., 2016). Of the many column flow systems described in the literature, packed bed columns are the most broadly utilized because they have minimal energy requirements, are easy to operate, offer high degrees of purification and automatically harvest biomass from metal solution (Ghasemi et al., 2011; Gokhale et al., 2009; Kumar et al., 2016; Lodeiro et al., 2006; Park et al., 2010).

The results of continuous flow biosorption studies are represented as breakthrough curves which are basically plots of the ratio of the effluent and influent metal concentrations (C_e/C_i) against time or volume (Kumar et al., 2016; Orguz and Ersoy, 2014; Singh et al., 2012). From these curves, the breakthrough time (t_b) or volume (v_b) which represent the time or volume at which the binding sites on the biosorbent are just starting to get saturated can be deduced (Kumar et al., 2016; Singh et al., 2012). These values are indicators of the performance of the column and depend on experimental conditions such as bed height, flow rate and inlet metal concentration. Many research studies have focused on evaluating the effects of bed height, flow rate, metal ion type and metal concentration on the breakthrough and saturation times (Apiratikul and Pavasant, 2008; Kumar et al., 2012; Kumar et al., 2016; Naja and Volesky, 2006; Pradhan and Rai, 2001).

Fig. 2.5 gives an illustration of the typical set up of a packed bed column.

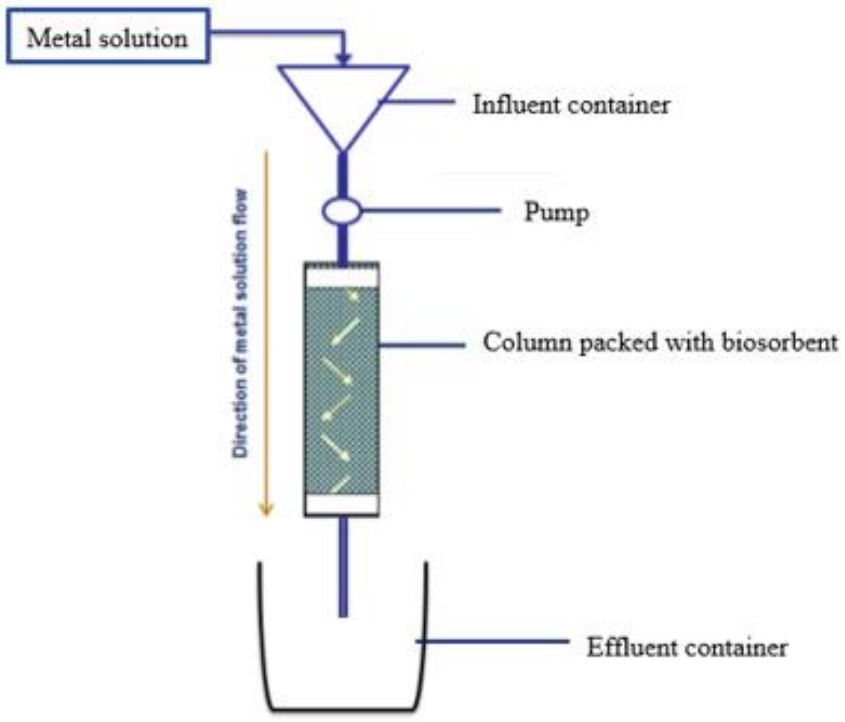

Fig.2.5: Schematic diagram of a packed bed column (Source: Kumar et al., 2016)

Even though, some work has been done regarding the removal of metals by algae in continuous flow systems. Knowledge is still lacking on their performance in multi-elemental solutions. But, most industrial effluents like AMD are comprised of many metals which could impact the removal efficiencies of the continuous flow systems (Mahanadi et al., 2015; Park et al., 2010).

2.3.14 Prediction of breakthrough behavior of fixed bed columns

Prediction of breakthrough behavior of packed bed columns is essential because it facilitates the scaling of algal-metal biosorption systems for industrial application (Baral et al., 2009; Ghasemi et al., 2011; Lodeiro et al., 2006). Therefore, many research workers illustrate the prediction of large scale industrial behavior of biosorption columns. The most commonly used methods for modelling experimental biosorption data are the Bed Depth Service Time (BDST), Adams-Bohart, Thomas and Yoon-Nelson models (Orguz and Ersof, 2014; Singh et al., 2012; Jeon et al., 2009).

The Adams-Bohart Model is often used for the description of the initial stages of breakthrough curves and focuses on the determination of the adsorption capacity of the biosorbent and the kinetic rate constant (Oguz and Ersoy, 2014; Samuel et al., 2013). On the other hand, the BDST model is used to predict the relation between the service time of the column and the height (Babu et al., 2015). It also assumes that the column biosorption kinetics are governed by the surface interactions between the metal and the biosorbent. Even though the model is useful for the comparison of column performances under different experimental conditions, it does not factor in intra-particle diffusion or external mass resistance (Baral et al., 2009, Gokhale et al., 2009, Preetha and Viruthagiri, 2007).

Unlike the two above-mentioned methods, the Thomas model seeks to give a generalized description of the overall performance of fixed bed columns. It assumes that the biosorption follows the Langmuir isotherm and pseudo-second order kinetics (Baral et al., 2009, Ghasemi et al., 2011). In the same way, the Yoon Nelson model describes the entire breakthrough curve. It is less complex than the Thomas model and requires minimal input data from the experimental results. Moreover, it is based on the assumption that the rate of decrease in the likelihood of biosorption

of metal ions on the biosorbent surface depends solely on the probability of biosorption and attainment of breakthrough (Crhribi and Chlendi, 2011; Trgo et al., 2011).

2.3.15 Commercial application of metal-algae biosorption systems

In addition to the many studies in the literature illustrating the potential of use of algae for metal biosorption in laboratory scale operations, there have also been reports of commercialization and patenting of some metal-algae biosorption systems. For instance, systems such as ALGASORB™, Biofix, B.V Sorbex and AMT-Bioclaim™ have been patented for commercial applications in North America (Park et al., 2010).

Prasad et al., (2006) described the use of an ALGASORB column formed by immobilization of *Spirogyra sp* alga on polyelectrolyte modified silica gel for removal of As (III) in multi-metal solutions. They found the system could be recycled for 59 cycles. Jeffers et al., (1991) utilized Biofix technology based on *Spirulina sp* in polysulfone beads for retrieving As, Cd, Cu and Pb. The authors reported removal efficiencies greater than 95% for all metals studied. Gupta et al., (2000) also reported the use of AMT Bioclaim comprised of granulated *Bacillus sp* for biouptake of Co, Zn and Mn from wastewater. They found that the biosorption system was not selective and could retrieve up to 99% of the metal pollutants from solution.

However, all these works only demonstrated laboratory scale applications. In fact, until this date, not a single industrial facility uses these systems for commercial scale metal uptake from wastewaters (Park et al., 2010). Also, according to the author's knowledge, none of the studies on metal biosorption using algae report the use of the biosorption systems to build 'tea-bag like' biotraps for large scale remediation of mercury.

2.4 Gaps in the literature

From the literature review conducted, it was deduced that even though wetlands are effective technologies for the remediation of AMD, their major limitation is their inability to effectively remove mercury. They convert the pollutant to a more toxic form (MeHg) which can bioaccumulate in food webs thus ultimately causing severe

human health disorders and negatively impacting biodiversity in aquatic ecosystems. Hence, many researchers report the utilization of conventional methods such as chemical precipitation, coagulation, membrane filtration and ion exchange for mercury remediation in these ecosystems. However, these techniques are costly, ineffective at low metal concentrations and produce hazardous secondary wastes. Therefore, it would not be feasible to adopt these techniques in developing countries such as South Africa.

Biosorption using algae as biosorbents is being considered as a plausible replacement technique or at least as a method for augmenting the efficiency of wetland systems. However, most of the research works in the literature report the use of brown algae (Bhatnagar et al., 2012; Cazon et al., 2013; Huang et al., 2015; Mata et al., 2009). Hence, there is still scope for the evaluation of the biosorption capabilities of green algae such as *Cladophora sp* (Zeroual et al., 2003). In fact, *Cladophora sp* is more abundant and accessible than most brown algae because it is found in most fresh and marine waters across the globe. In spite of this, only a few studies demonstrate its use for treatment of mercury laden wastewaters (Ji et al., 2012; Tshumah-Mutingwende, 2014). The emphasis of these few studies was also on investigating the effects of significant solution and biosorption parameters on the biosorption capabilities of the algal biosorbent using batch equilibrium studies. Even then, the studies were incomplete and left out significant operational parameters such as biosorbent dosage and temperature. The studies also did not attempt to characterize the alga for biosorption of mercury. Characterization is vital because it provides information on the chemical properties of the biosorbent that have a huge impact on their biosorptive performance.

The performance of the algal biosorbents in continuous flow operations was also not evaluated. But, most industrial wastewater treatment plants are based on continuous flow mode. Furthermore, the mechanism for biosorption of metals is also still vaguely understood because very few works in the literature report attempts to elucidate it. The focus of these limited studies has also been on other metals excluding mercury. Mercury has unique chemical and physical properties that affect its interaction with algal biosorbents during biosorption; hence, it is important to study its mechanism specifically.

The majority of biosorption studies also do not comprehensively evaluate the speciation of the biosorbed metals by alga thus making it difficult to differentiate between adsorption and precipitation on the algal surfaces. Not a single study in the literature demonstrate the application of algal-metal biosorption systems to build ‘teabag’ biotraps for the utilized remediation of mercury from environmental samples.

CHAPTER 3: AIM AND OBJECTIVES

This chapter describes the general aim and specific objectives of the study. It also gives a synopsis of the research questions the study seeks to resolve and hypothesizes on the findings and trends that will be uncovered. A brief account of the novelty of the study is also given.

3.1 General aim and specific objectives

3.1.1 General aim of the study

The aim of this study was to prepare modified biosorbents based on *Cladophora sp* alga, optimize them for mercury retrieval from synthetic aqueous solutions and utilize them to develop biotraps for application in real environmental waters.

3.1.2 Specific objectives

The main aim of the study was achieved by addressing the following specific objectives:

i) To modify *Cladophora sp* alga by immobilization in calcium alginate beads and silica gel and use the resultant biosorbents for removal of mercury from aqueous solutions.

ii) To characterize the biosorbents for mercury biosorption from aqueous solution and optimize them for pertinent parameters affecting the removal of mercury from aqueous solutions under batch and continuous flow modes.

iii) To conduct speciation and mechanistic studies to elucidate the species of mercury adsorbed onto the pristine *Cladophora sp* alga and the mechanism of the biosorption process using all the biosorbents

iv) To model the experimental batch equilibrium and column data against the relevant kinetic, adsorption isotherm and breakthrough prediction models

v) To develop biotraps based on the modified biosorbents and utilize them to treat acid impacted environmental water.

3.2 Hypothesis

It is hypothesized that both the pristine and modified forms of *Cladophora sp* are effective in sequestering mercury from aqueous solutions. The performance of the

biosorbents is also influenced by numerous biomass and solution parameters. The adsorption of mercury by the pristine alga and modified biosorbents also occurs via complex processes comprised of many mechanisms involving several functional groups. Application of the developed biotraps to environmental waters causes the mercury concentration in the samples to decrease significantly.

3.3 Key research questions

The study seeks to address the following research questions:

i) Which characteristics of the pristine alga and modified biosorbents make them suitable for the biosorption of mercury from wastewaters?
ii) What are the optimum parameters (pH, biosorbent dosage, agitation time etc.) required for the effective removal of mercury from aqueous solutions by the pristine alga and modified biosorbents in batch mode operations?
iii) What are the optimum conditions for the removal of mercury from aqueous solutions using a continuous flow mode column packed with the modified biosorbents?
iv) What is the speciation of the mercury by the pristine alga?
v) Which mechanisms play a significant role in the binding of mercury to the pristine and modified forms of *Cladophora sp* alga?
vi) Will the designed biotraps be effective in removing mercury from environmental samples?

3.4 Novelty of the study

To the best of the author's knowledge, no study has been previously undertaken to modify *Cladophora sp* by immobilization in alginate beads and silica gel for utilization in bioremediation of mercury from environmental waters. In addition, no other research work reports the elucidation of the mechanism of mercury biosorption by pristine and modified forms of *Cladophora sp* alga. This study is also the first to show the use of the modified algal biosorbents to develop 'teabag' biotraps for the remediation of mercury from environmental waters.

CHAPTER 4: MATERIALS AND METHODS

This chapter gives an in-depth description of all the methods, protocols and materials utilized to achieve the aim and specific objectives of the study.

4.1 Chemicals and reagents

All the chemicals and reagents used in this study were of analytical grade or better and were procured from Sigma Aldrich, South Africa. They were used as supplied without any further purification or treatment.

4.2 Preparation of solutions

1000 mg L^{-1} stock solutions were prepared by dissolving the required amounts of the nitrate salts of Hg^{2+}, Pb^{2+}, Ni^{2+}, Co^{2+}, Cu^{2+}, Fe^{3+} and Cd^{2+} in deionized water (Milli-Q, 18.2 MΩ.cm at 25˚C) purified using a Millipore Direct UV-3 (France) water purification system. Thereafter, working solutions of desired concentrations were prepared by serial dilution of the stock solutions.

4.3 Sample collection

Cladophora sp algae samples were collected from random points at Alexander Dam, Springs, East Rand, Johannesburg, South Africa (GPS coordinates: Latitude S26˚12.6732′, Longitude E028˚ 24.8721’) using the method described by Amde et al., (2014). First, prewashed 1 L PTFE sampling bottles were thoroughly rinsed and partially filled with dam water. *Cladophora sp* algal samples were then handpicked and placed in the bottles until they were filled to capacity. The bottles containing the samples were then tightly sealed and placed in polyethylene bags which were then stored on ice for transportation to the laboratory.

Samples of the water from which the alga was harvested were also collected from the same points in prewashed 1 L PTFE bottles. The bottles were rinsed thoroughly with dam water prior to being filled to the brim and closed whilst still fully submerged in the water. A Thermo - Scientific Orion Star (USA) multi-probe field meter was then used to measure the hydrochemical characteristics (pH, temperature, redox potential, salinity and conductivity) of the water samples on site. The water sample bottles were then tightly sealed, placed in polyethylene bags and stored on

ice for transportation to the laboratory. Fig. 4.1 is a pictorial representation of some of the procedures executed during sampling excursions.

Fig. 4.1: Sample collection at Alexandra, Dam, Springs, Gauteng, South Africa

4.4 Sample preparation

Upon arrival at the laboratory, the water samples were divided into two portions of equal volumes and transferred to 500 mL Schott reagent bottles. One portion of each sample was left as is for analysis for anion composition while the other was treated with a few drops of concentrated nitric acid to preclude metal precipitation. Both the treated and untreated water samples were stored at 4˚C for use in forthcoming experiments. Conversely, the algal samples were removed from the PTFE bottles and washed thoroughly with running tap water to remove any foreign bodies and debris adhered to their surfaces. Afterwards, the algae were washed thrice with deionized water before being placed in Ziploc bags and stored at 4˚C for later use.

4.5 Physicochemical characterization of the water samples collected

The water samples collected from Alexandra Dam were characterized in terms of their field parameters (pH, electrical conductivity, total dissolved solids and redox potential), total metal concentrations and anionic contents. Field parameters were measured on site using a Thermo-Scientific Orion Star (USA) field meter. The total

metal concentrations of the samples were determined using the mercury analyzer and ICP-OES systems as per the methods in sections 4.18.1 and 4.18.2, respectively. Correspondingly, the anionic content was determined using ion chromatography as shown in section 4.19.

4.6 Preparation of algal growth medium

Bold's acidic medium (BAM) was prepared as per the chemical composition illustrated in Table 4.1.

Table 4.1: Composition of BAM

Essential elements	Concentration ($g\ L^{-1}$)	Trace Elements	Concentration ($mg\ L^{-1}$)
$NaNO_3$	25.0	*$FeCl_3.\ 6H_2O$	97.0
$Mg\ SO_4.\ 7H_2O$	7.5	$MnCl_2.\ 4H_2O$	41.0
NaCl	2.5	*$ZnCl_2.\ 6H_2O$	5.0
$K_2HPO_4.\ 3H_2O$	7.5	$CoCl_2.\ 6H_2O$	2.0
KH_2PO_4	17.5	$Na_2MoO_4.\ 2H_2O$	4.0
$CaCl_2.\ 2H_2O$	2.5		

*replaced by $FeSO_4$ and $ZnSO_4$ respectively in modified BAM

10 mL of each of the essential elements was first added to a 1 L volumetric flask containing 800 mL of deionized water and 250 mg NH_4SO_4. In another volumetric flask, 0.75 g of Na_2 EDTA was dissolved in 1000 mL deionized water containing the trace elements as per the list in Table 4.1. Thereafter, 6.0 mL of the trace elements solution was added to the volumetric flask containing NH_4SO_4 and essential elements. The pH of the resultant mixture was then adjusted to that of the dam water (7.21) before the volume was made to the 1000 mL mark using deionized water. The medium was then autoclaved at 100˚C in a WiseCube Fuzzy control system (Germany) for an hour to eliminate bacterial contamination. Modified BAM was also prepared in the same manner except that in this case, $FeCl_3$ and $ZnCl_2$ salts in the essential elements list were replaced by sulfate salts i.e. $FeSO_4$ and $ZnSO_4$.

4.7 Cultivation of the algae in growth medium

Cladophora sp algae were cultivated in the media using the method described by Ji et al., (2012) whereby approximately 20 g of 'wet' algae were placed in 500 mL Schott reagent bottles filled with growth medium viz. BAM or modified BAM. The bottles were then sealed using parafilm with small holes pierced on it to allow the influx of oxygen. Subsequently, the sample bottles were placed on a window ledge in a room permitting light capture by algae while protecting them from harsh environmental conditions. After 2-3 days the algae were removed from media and acclimated in de-ionized water for 24 hours.

The samples were then placed on filter papers to remove excess moisture and later divided into 3 portions. Two of these portions were marked for modification by immobilization in silica gel and calcium alginate beads in later experiments while the third one was left unaltered as 'pristine *Cladophora sp* alga' to be used for mercury biosorption as is.

4.8 Modification of *Cladophora sp* alga

The *Cladophora sp* algal samples marked for modification were immobilized in calcium alginate beads and silica gel as per the procedures described in sections 4.8.1 and 4.8. 2, respectively.

4.8.1 Immobilization of *Cladophora sp* alga in alginate beads

This was achieved using a modified version of the method described by Bayramoglu et al., (2006). 2 g of sodium alginate was dissolved in 50 mL deionized water with the aid of heating. The resultant solution was then cooled to room temperature and mixed with an algal suspension comprised of 1.0 g of alga in 50 mL deionized water. Afterwards, the mixture was added dropwise to 50 mL of 0.1 M $CaCl_2$ while agitating to form beads of approximately 2 mm diameter. The beads were then left in solution for 90 minutes for complete gel formation and subsequently stored at 4˚C in 5 mM $CaCl_2$ for future use. Blank alginate beads were also prepared in the same manner; but, without the addition of *Cladophora sp* alga.

4.8.2 Immobilization of *Cladophora sp* alga in silica gel

Cladophora sp alga was immobilized in silica gel using the method described by Akar et al., (2009). 5 g of silica gel was dissolved in 50 mL of 7% (w/v) aqueous solution of KOH with the aid of heating. After cooling to room temperature, the solution was added to and mixed with an algal suspension made up of 2.5 g of alga in 100 mL of deionized water. A few drops of 20% (v/v) phosphoric acid were then added to facilitate gel formation. The gel formed was then dried in a WiseCube Fuzzy control (Germany) incubation system set at 60˚C for 24 hours. Subsequently, the dry gel was ground and sieved to a powder with particles of size 0.5 -1.0 mm and stored in 50 mL PTFE centrifuge tubes at 25˚C until further use. Blank silica gel was also prepared using the same procedure; but, without the addition of *Cladophora sp* alga.

Throughout this study, the *Cladophora sp* alga immobilized in silica gel and calcium alginate beads will be collectively referred to as 'modified forms of the alga', 'modified biosorbents' or 'synthesized biosorbents'.

4.9 Characterization of pristine and modified forms of *Cladophora sp* alga

The pristine and modified forms of *Cladophora sp* alga were characterized by determination of moisture content, Fourier transform infrared spectroscopy (FTIR), Braunner-Emmett-Taylor (BET) analysis, Thermogravimetric analysis (TGA) and Scanning electron microscopy (SEM) coupled with Electron dispersive X-ray spectroscopy (EDX).

4.9.1 Determination of the moisture content of pristine *Cladophora sp* alga and *Cladophora sp* alga immobilized in alginate beads

The moisture contents of pristine *Cladophora sp* alga and the alga immobilized in alginate beads were determined using the protocols described by da Silva et al., (2008) and Rocher et al., (2008) respectively. For the pristine alga, 4.0 g of the 'wet' biosorbent was weighed using a Precisa 180A (Switzerland) analytical balance and oven-dried at 60˚C for 48 hours (da Silva et al., 2008). The alga was then re-weighed after drying and the percent moisture was calculated using eqn. 2 below (da Silva et al., 2008).

$$\%\ \text{moisture content} = \{(M_{bd} - M_{ad})/M_{bd}\} * 100\% \qquad (4.1)$$

where M_{bd} and M_{ad} are the masses of the biosorbents (in g)before and after drying respectively.

On the contrary, in the case of the alga immobilized in alginate beads, 50 beads were weighed using the same balance and oven-dried at 60˚C for 48 hours. The dried beads were then weighed and their percent moisture was also calculated using eqn. 4.1. Subsequently, the calculated moisture contents of the pristine alga and alga immobilized beads were used to determine their 'dry' weights. Therefore, henceforth in this work, unless otherwise stated, any mass of these two biosorbents reported will be their dry mass.

It is worth noting that in the case of the pristine alga and alga immobilized in alginate, drying completing changed their texture. Hence, their 'wet' form was used for the biosorption studies and their dry masses was computed using their percent moisture values. On the other hand, for the alga immobilized in silica gel, the biosorbent could be dried effectively without loss in integrity and could, therefore, be used for biosorption in this form. Therefore, percent moisture calculations were not necessary in this instance.

4.9.2 Functional group identification

The functional groups on the surfaces of the pristine alga and modified biosorbents were identified using a Bruker Tensor 27 FTIR spectrometer, (Germany). Biosorbent samples were first oven-dried at 60˚C for 48 hours and finely ground to a powder of particle size 0.5-1.0 mm. In preparation for analysis, the sample holder and probe on the FTIR spectrometer were thoroughly cleaned using ethanol sprayed on a soft Kleenex tissue. Thereafter, powdered biosorbent samples were successively placed on the sample holder and scanned in the range 500– 4000 cm^{-1} while data was collected on a personal computer using the Opus software (Bruker, Germany). FTIR spectra were then drawn from the data point table using Microsoft Office EXCEL.

4.9.3 Surface morphology studies

The surface morphologies of the pristine and modified forms of *Cladophora sp* alga were studied using an FEI Quanta 200 ESEM (USA) scanning electron microscope equipped with an Electron Dispersion X-ray (EDX) spectrometer. Firstly, powdered

samples of the biosorbents were placed on carbon tape adhered to specimen stubs until the tape was entirely covered. Any unattached sample particles were then removed from the tape by gently tapping on the stub several times. The adhered samples were then coated with 5 nm gold and palladium alloy under argon vacuum to improve their electrical conductivities and protect them from being damaged by the electron beam.

The settings on the microscope were then changed to high vacuum mode and the specimen chamber was vented to ensure that vacuum conditions prevailed during analysis. A single specimen stub with biosorbent sample attached to it was then positioned on the microscope stage where it was held tightly in place using screws. Subsequently, the stage was raised upwards until a working distance of 10 +/- 1 mm was achieved. Scanning analysis of the sample was then initiated by bombardment with electrons at 10 eV while tuning the magnification, contrast and color settings of the microscope to obtain a clear micrograph. The best quality image was then captured via an inbuilt camera and stored on a personal computer. This procedure was repeated until all the samples had been analyzed.

4.9.4 Determination of the surface areas and pore volumes of the biosorbents

The surface areas and porosities of the pristine and modified forms of *Cladophora sp* alga were measured using the Braunner-Emmett-Taylor (BET) technique on a Micrometrics Trista 3000 (USA) analyzer. Initially, approximately 0.2 g of sample was degassed in N_2 gas overnight using a Micrometrics flow prep 060 (USA) sample degasser to ensure complete vacation of the pores. The samples were then transferred to the BET instrument for analysis and all measurements were performed under isothermal conditions (-196˚C) using liquid N_2. Moreover, the surface area measurements were determined in the relative pressure range P/P_0 =0.05-0.30 while the pore volumes were determined at a relative pressure P/P_0 =0.995.

4.9.5 Thermostability studies

The thermostabilities of the biosorbents were evaluated using thermogravimetric analysis (TGA) on a Perkin Elmer STA 600 (USA) thermal analyzer. Powdered samples were placed on a sample pan attached to a precision balance and heated

from 0 -900˚C at a rate of 10˚C min^{-1} under nitrogen. The weight loss in the samples was then recorded as a function of temperature.

4.10 Batch biosorption studies

Batch biosorption studies were conducted in 100 mL Erlenmeyer flasks containing 0.5 g biosorbent suspended in 50 mL of metal solution of known concentration and pH. The reaction vessels were then agitated at 150 rpm on a Labcon 3100E (USA) rotary shaker for prescribed time periods. After completion of the biosorption process, the biosorbents were separated from the bulk solution using gravimetric filtration. In the case of the modified biosorbents, the filtrates obtained were directly analyzed for mercury. However, for the pristine alga, the algal samples were solubilized using micro-assisted digestion as per the method described in section 4.10.1 and the digests were analyzed for mercury content.

The biosorption capacities (q) of all the test biosorbents were determined using eqn. 4. 2 below (Lee and Chang, 2011; Tuzen et al., 2009).

$$q = (C_0 - C_e) \times V/M \quad (4.2)$$

where q is the adsorption capacity (mg g^{-1}), C_0 and C_e are the initial and equilibrium metal concentrations (mg L^{-1}), V is the volume of solution (L) and M is the mass of sorbent (g).

The removal efficiency (r) was determined using eqn. 4.3 below (Lee and Chang, 2011; Tuzen et al., 2009).

$$r = \{(C_0 - C_e)/C_0\} * 100\% \quad (4.3)$$

For all biosorption studies, all experiments were performed in triplicates. Therefore, the results reported are averages of replicate values and the error is expressed in terms of the standard deviation.

4.10.1 Microwave-assisted digestion of pristine *Cladophora sp* alga

Solubilization of the mercury-loaded pristine *Cladophora sp* algal samples was achieved through digestion in an automated Anton Paar Microwave Go, (USA) digestion system. 0.1 g of the powdered algal samples (particle size 0.5-1.0 mm) was placed in 50 mL Teflon digestion tubes containing 8 mL HNO_3 and 2 mL H_2O_2

reagents. The tubes containing the algae and reagents mixtures were then inserted in designated positions on the microwave rotor. Thereafter, the rotor was slotted at the appropriate place in the digestion system and exposed to 2 bar pressure and a temperature of 150˚C for 20 minutes.

Following the completion of the digestion process, the vessels were left to cool to room temperature. The resultant algal digests were then analytically transferred to 50 mL centrifuge tubes and diluted by a factor of 5 using deionized water. Pristine *Cladophora sp* alga which had not been exposed to mercury was also digested in the same manner. All the digested algal samples were then stored in a refrigerator set at 4˚C prior to metal analysis.

4.10.2 Optimization of the significant factors affecting the biosorption of mercury by pristine and modified *Cladophora sp* algal biosorbents

The effects of various significant parameters (solution pH, agitation time and initial metal concentration, the presence of competing cations, temperature, biosorbent dosage and composition of algal growth media) on the biosorption capacities of the pristine alga and modified biosorbents were also evaluated. This was achieved by varying one parameter whilst keeping the rest constant as per the procedures described in sections 4.10.2.1 – 4.10.2.7.

4.10.2.1 Effect of the composition of the algal growth medium

To investigate the effect of the composition of algal growth medium on the biosorption performance of pristine *Cladophora sp* alga, algal samples were first grown in either BAM or modified BAM as per the method described in section 4.7. After this, the pristine algae were harvested, acclimated in deionized water and used for biosorption studies as per the procedure described in section 4.10. The mercury-loaded algal samples were then separated from the solution, digested and analyzed for mercury content. The adsorption capacities of the algae grown in the two types of media were then calculated and compared.

4.10.2.2 Effect of pH

The effect of pH on the adsorption capacities of the biosorbents was evaluated using four different experimental setups. Each experiment was comprised of 0.5 g of biosorbent suspended in 50 mL of 1 mg L^{-1} Hg^{2+} solutions held at a specific pH

value within the range 3 – 8.5. All pH measurements were made using a Mettler Toledo (USA) pH meter which had been calibrated before use and pH adjustments were made using 0.1 M NaOH and 0.1 M HNO_3.

The reaction mixtures were then agitated at 150 rpm on the rotary shaker for 120 minutes whilst maintaining the temperature of the solution at 25˚C. After completion of the process, the biosorbents were harvested from solution using filtration and their adsorption capacities at different pH values were determined.

4.10.2.3 Effect of agitation time

The influence of agitation time on the biosorption capabilities of the pristine and modified forms of *Cladophora sp* was investigated in the range 0-120 minutes. Batch biosorption studies were performed using different vessels containing 0.5 g of biosorbent in 50 mL of 1 mg L^{-1} metal solution held at pH 5. The reaction vessels were then agitated at 150 rpm on a rotary shaker for prescribed time values in the test range while the temperature was kept constant at 25˚C. Next, the algal-based biosorbents were separated from the bulk solution and their adsorption capacities at the various agitation times were determined.

4.10.2.4 Effect of initial metal concentration

The effect of initial metal concentration on the adsorption capacities of the biosorbents was evaluated using eight different values i.e. 1, 2, 5, 10, 20, 50 and 100 mg L^{-1}. Several reaction mixtures comprised of 0.5 g biosorbents in 50 mL metal solutions of varying initial concentrations were agitated simultaneously on the rotary shaker for given time periods i.e. 20 minutes for the pristine alga and 30 minutes for the modified biosorbents. Throughout the experiments, the pH, agitation speed, and temperature were held at pH 5, 150 rpm and 25˚C, respectively. The adsorption capacities of the biosorbents at different initial metal concentrations were also determined.

4.10.2.5 Effect of biosorbent dosage

The dependence of the adsorption capacities of the pristine and modified forms of *Cladophora sp* alga on the biosorbent dosage was studied in the range 0-50 g L^{-1}. A number of experimental set-ups comprised of different masses of biosorbent in 50 mL of 1 mg L^{-1} metal solution held at pH 5 were agitated on the rotary shaker

for specified times (20 minutes for the pristine alga and 30 minutes for the modified biosorbents). Thereafter, the biosorbents were separated from the solution and their adsorption capacities at different biosorbent dosages were determined.

4.10.2.6 Effect of temperature

The relation between the temperature and the biosorption capacities of pristine and modified *Cladophora sp* alga was studied using four different values (16, 25, 30 and 40˚C). Reaction vessels containing 0.5 g of biosorbent in 50 mL of 1.0 mg L^{-1} mercury solution were agitated on the incubator shaker system for given time periods. The temperature of the solutions used was varied between the four test values while all the other parameters were kept constant. Thereafter, biosorbents were harvested from solution and their adsorption capacities at different temperatures were determined.

4.10.2.7 Effect of competing ions

The effect of the presence of competing ions on the adsorption capacities of pristine and modified forms of *Cladophora sp* alga was studied by bringing 0.5 g biosorbent in contact with 50 mL of a multi-metal solution comprised of 1 mg L^{-1} each of Hg^{2+}, Fe^{3+}, Ni^{2+}, Cu^{2+}, Cd^{2+}, Co^{2+} and Pb^{2+} ions held at pH 5. The reaction mixtures were agitated at 150 rpm on the rotary shaker for prescribed times (20 minutes for the pristine alga and 30 minutes for the modified biosorbents) while keeping the temperature and biosorbent dosage constant at 25˚C and 10 g L^{-1}, respectively.

The selectivity of the biosorbents was evaluated using the distribution co-efficient (K_D) whose value was determined using eqn. 4.4 (Lee and Chan, 2011; Tuzen et al., 2009).

$$K_D = (C_0 - C_f / C_f) \quad (4.4)$$

where K_D is the distribution co-efficient, C_0 and C_f are the initial and final concentration, V is the volume of solution and M is the mass of biosorbent

4.10.3 Reusability of the biosorbents

The recyclability of the pristine alga and modified biosorbents was studied using a two-stage process beginning with regeneration using suitable desorption media. Thereafter, the biosorbents were reused and their biosorption capacities were

evaluated after several successive adsorption-desorption cycles. The method for the selection of the best medium for eluting mercury from the biosorbents is described in section 4.10.3.1 while that for the recycling and reuse of the biosorbents is shown in section 4.10.3.2.

4.10.3.1 Selection of the best desorption medium

To achieve this, mercury was first biosorbed onto the biosorbents under optimum conditions using the method described in section 4.10. The biosorbents loaded with mercury were then separated from the solution and washed thoroughly using deionized water. Thereafter, desorption of mercury from the biosorbents was performed using a modified version of the method described by Gupta and Rastogi, 2009. The mercury-loaded biosorbents were placed in 50 mL Erlenmeyer flasks containing 10 mL of either 0.1 M HCl, 0.1 M HNO_3 or 0.1 M NaCl. The mixtures were then agitated at 200 rpm for 2 hours on the rotary shaker. Following this, the biosorbents were removed from the desorption medium and the concentration of mercuric ions remaining in the medium was determined. Finally, the desorption capabilities of the different desorption media were compared using their desorption ratios which were determined using eqn. 4.5 below (Guler and Sarioglu, 2013; Kacar et al., 2002).

$$Desorption\ ratio = (C_M/C_B) \times 100\% \quad (4.5)$$

where C_M is the concentration of mercury remaining in sorption medium and C_B is the concentration of mercury adsorbed by biosorbent.

The desorption medium with the highest eluting power (desorption ratio) was then used for the regeneration of the biosorbents in subsequent experiments

4.10.3.2 Recycling and reuse of the biosorbents

Recycling and reuse of the test biosorbents were performed by first adsorbing mercury onto the surfaces of the biosorbents under optimal conditions using the method described in section 4.10. The biosorbents with mercury bound to them were then separated from the bulk solution and rinsed thoroughly with deionized water. Next, the biosorbents were regenerated by shaking for 2 hours in 10 mL of 0.1 M HCl. The algal-based biosorbents were then separated from the desorption

medium and washed with deionized water. The recycled biosorbents were then reused for biosorption before being regenerated again. Repeated reuse and regeneration of the biosorbents was continued for 3 successive adsorption-desorption cycles while determining the removal efficiencies of the biosorbents after each cycle as per equation 4.2.

4.11 Speciation studies

Speciation studies were performed to determine the fraction of mercury biosorbed on pristine *Cladophora sp* alga that is converted to methylmercury. This was achieved using the procedure prescribed by Calderon et al., (2013) whereby 0.2 g of powdered alga was first mixed with 10 mL hydrobromic acid in a 50 mL PTFE centrifuge tube. Next, 20 mL toluene was added and the resultant mixture was centrifuged for 10 minutes on a Restek Q-SEP 3000 (USA) centrifuge set at 3000 rpm. 15 mL of the organic (top) phase was then removed and placed in another 50 mL centrifuge tube containing 6 mL of 1% (w/v) L-cysteine solution.

An additional extraction of the algal sample was performed by adding 15 mL of toluene to the first centrifuge tube with hydrobromic acid and centrifuging the mixture at 3000 rpm for another 10 minutes. The organic phase formed at the top was again removed and added to the solution with L-cysteine. Thereafter, the solution with the organic phases and L-cysteine was agitated manually for 2 minutes before being centrifuged at 3000 rpm for 10 minutes. A 3 mL aliquot of the lower phase formed in this instance was then withdrawn using a Pasteur pipette and transferred to a 50 mL glass vial. The sample vial was then tightly sealed and stored at 4˚C for up to 7 days before being analyzed for mercury content. The mercury determined in this instance translated to the quantity of methylmercury in the sample. This experiment was performed in triplicate and the results reported thereof are averages of these replicates.

4.12 Mechanistic studies

Mechanistic studies were conducted to elucidate the mechanisms involved in the biosorption of mercury from aqueous solutions using pristine and modified forms of *Cladophora sp* alga. The techniques that were used for the elucidation of the

mechanism are FTIR analysis, determination of metal content, SEM-EDX analysis, chemical modification and potentiometric titrations.

4.12.1 FTIR analysis

FTIR analysis was used to identify the functional groups responsible for mercury binding in the pristine *Cladophora sp* alga. In this instance, batch biosorption studies were first conducted using the optimum conditions and the protocol described in section 4.10. The biosorbents with mercury bound onto their surfaces were then separated from the solution, oven-dried at 60˚C for 48 hours and ground to a powder of particle size 0.5 -1.0 mm. For comparison, the same mass of biosorbents that had not undergone biosorption was also oven-dried and ground to powders with particles of the same size. The FTIR spectra of the biosorbents before and after mercury binding were obtained using the procedure described previously in section 4.9.2.

4.12.2 SEM-EDX analysis

SEM-EDX analysis was also utilized to gain insight on the mechanism for biosorption of mercury onto the pristine and modified forms of *Cladophora sp* alga. First, biosorption studies were performed using the biosorbents as per the method and conditions stated in section 4.10. The alga was then separated from the solution, rinsed and ground to fine particles (0.5 -1.0 mm). Similarly, equivalent amounts of biosorbents which had not been exposed to mercury were also ground to powder. The SEM micrographs and EDX data of the biosorbents before and after metal biosorption were then obtained using the method shown in section 4.9.3. EDX data was collected from 7 areas on the biosorbents and the results reported are averages of those obtained from the targeted points.

4.12.3 Determination of total metal content of pristine *Cladophora sp* alga

In order to evaluate the contribution of ion exchange to the overall mechanism of mercury biosorption by pristine *Cladophora sp*, the total metal content of the alga before and after biosorption were determined. Initially, batch adsorption tests using pristine *Cladophora sp* were conducted as per the method described in section 4.10. After this, the algal samples were harvested from solution and oven-dried for 48 hours. Concurrently, pristine *Cladophora sp* without any prior exposure to mercury

was oven-dried for the same time period. The dried algae were then powdered, digested and analyzed for total metal content. Mass balance equations were then used to determine if ion exchange was the dominant mechanism.

4.12.4 Chemical modification of the functional groups

The carboxyl, hydroxyl, sulfonate, and amine functional groups on the surface of pristine *Cladophora sp* alga were chemically modified to gain insight on their contribution to the overall process of the biosorption of mercury.

4.12.4.1 Esterification of carboxyl groups

The esterification of the carboxyl groups on the surface of pristine *Cladophora sp* alga was achieved using the protocol described by Carro et al. (2013). 3 g of the alga was mixed with 200 mL of absolute methanol and 1.8 mL concentrated HCl. The resultant mixture was then agitated at 150 rpm for 24 hours on the rotary shaker and the alga was separated from the solution by filtration thereafter. The algal residue was then thoroughly rinsed with deionized water and used for mercury biosorption as per the procedure described in section 4.10. The mercury-loaded alga was then separated from the solution and digested using the microwave digestion system. Similarly, pristine *Cladophora sp* alga was used for biosorption, separated from the solution and digested. The adsorption capacities of the pristine and esterified algae were then determined and compared.

4.12.4.2 Esterification of the sulfonate groups

Esterification of the sulfonic acid groups on the surface of the pristine alga was performed using the method prescribed by Hackbarth et al., (2014). 2 g of the alga was suspended in 130 mL methanol and 12 mL HCl and the resultant mixture was agitated on the rotary shaker at 150 rpm for 48 hours. After this, the methanol and HCl were refreshed and the mixture was agitated for another cycle. This was repeated for 4 cycles before the alga was removed and rinsed thoroughly with deionized water. The modified alga was then used for mercury biosorption as per the procedure in section 4.10. Thereafter, the alga was separated from the mercury solution and digested. Pristine unmodified alga was also used for biosorption, digested and analyzed for mercury content. The adsorption capacities of the pristine and modified alga were then compared.

4.12.4.3 Acetylation of amine and hydroxyl groups on Cladophora sp alga

The total acetylation of amino and hydroxyl groups on *Cladophora sp* alga was achieved using a modernized and microwave-assisted version of the method described by Bai and Abraham, (2002). 3 g of pristine alga was suspended in a G30 glass sample vial containing 20 mL of acetic anhydride. The mixture was then refluxed uniformly for 1 hour in an Anton Paar Monowave 400 Microwave Reactor (USA) connected to an argon gas supply using the program shown in table 4.2.

Table 4.2: Settings and parameters for the microwave-assisted acetylation of the amine and hydroxyl groups in *Cladophora sp* alga

Step	Temperature (˚C)	Time (h)	Stirrer speed (rpm)
1) Heat as fast as possible	80	0.10	800
2) Hold time	80	1.00	800
3) Cooling	45	0.45	800

After completion of the program and cooling of the system, the algae were separated from the solution and washed thoroughly using deionized water. The algal samples were then used for Hg^{2+} biosorption using the method prescribed in section 4.10. The mercury-bound algae samples were then separated from the solution, digested and analyzed for metal content. Unaltered *Cladophora sp* alga was also used for biosorption and its metal uptake was compared with that of the acetylated alga. These experiments were also performed in triplicates and the results reported are averages.

4.12.5 Potentiometric titrations

Potentiometric titrations of the pristine alga were performed using the method prescribed by Andrade et al., (2005) to determine the dissociation constants and total concentrations of the functional groups on the surfaces of the biosorbents. First, an algal suspension was prepared by mixing 2.5 g alga in 50.0 mL 0.05 M

$NaNO_3$. Thereafter, 10 mL of the suspension was acidified to pH 2 and deaerated using nitrogen gas for 2 hours. The degassed suspension was allowed to equilibrate and then titrated by stepwise addition of 0.25 M NaOH via a Metrohm Dosimat 756 (Switzerland) automated burette. The pH of the solution was measured after each addition of NaOH and all readings were taken after the meter had completely stabilized. The titrations were performed in triplicates and the results reported are averages. Fig. 4.2 gives an illustration of the auto-burette used.

4.13 Theoretical treatment of batch biosorption data

The experimental data obtained from the batch biosorption studies was modeled against kinetic models, adsorption isotherms and thermodynamic models as per the protocols shown in sections 4.13.1, 4.13.2 and 4.13. 3, respectively.

Fig. 4.2: The auto-burette used for potentiometric titrations

4.13.1 Kinetic modeling

The kinetic data for the biosorption of Hg^{2+} ions onto pristine *Cladophora sp* alga, *Cladophora sp* alga immobilized in alginate beads and *Cladophora sp* alga immobilized in silica gel were modeled against Lagergren's pseudo-first-order, pseudo-second-order and Webber-Morris intraparticle diffusion models. The linear mathematical expressions of the models are given in eqns. 4.6, 4.7 and 4.8, respectively (Apiratikul and Pavasant, 2008; Tran et al., 2017; Tuzen et al., 2009).

$$\ln(q_e - q_t) = -k_1 t + \ln(q_e) \quad (4.6)$$

where q_t and q_e are the adsorption capacities at time t and equilibrium respectively (mg g^{-1}), k_1 is the rate constant for pseudo- first-order kinetics (min^{-1}).

The values of k_1 and q_e were obtained from the slope and intercept of the linear plot of $\ln(q_e - q_t)$ versus t.

$$t/q_t = 1/k_2 {q_e}^2 + 1/q_e\, t \quad (4.7)$$

where k_2 is the rate constant (g mg^{-1} min^{-1}), q_t is the biosorption capacity at time *t*, q_e is the biosorption capacity at equilibrium and the values of k_2 and q_e were deduced from the slope and intercept of the linear plot of $\frac{t}{q_t}$ against t.

$$q_t = k_p \sqrt{t} \quad (4.8)$$

where k_p is the intraparticle diffusion rate constant (mg g^{-1} $min^{-0.5}$), q_t is amount metal adsorbed (mg g^{-1}), t is the time in minutes and k_p was determined from the slope of q_t versus t.

4.13.2 Adsorption isotherm modeling

The equilibrium data for the biosorption of mercuric ions using pristine and modified forms of *Cladophora sp* alga were modeled against the Freundlich, Langmuir and Dubinin-Radushkevich isotherm whose linear mathematical expressions are given as eqns. 4.9, 4.10 and 4.12 respectively (Dada et al., 2012; Tuzen et al., 2009).

$$log q_e = log K_F + n.\, log C_e \quad (4.9)$$

where q_e is the adsorption capacity of the sorbent at equilibrium (mg g^{-1}), C_e is the concentration of metal ions in solution at equilibrium (mg L^{-1}), K_F is the Freundlich constant indicative of the adsorption capacity and n is the adsorption intensity.

The values of n and K_F were determined from the slope and intercept of the linear graph of log q_e against log C_e

$$C_e/q_e = 1/b.q_m + C_e/q_m \quad (4.10)$$

where q_m is maximum adsorption capacity (mg g^{-1}) and b is the Langmuir constant related to the suitability of sorbent-sorbate system.

The values of q_m and b were deduced from the slope and intercept of the linear plot of C_e / q_e versus C_e. The separation factor (R_L) was also calculated using equation 4.11 (Dada et al., 2012; Tuzen et al., 2009)

$$R_L = {}^{1}/_{(1 + C_0)} \quad (4.11)$$

$$ln\ q_e = lnx_m - \beta\varepsilon^2 \quad (4.12)$$

wherex_m is the maximum adsorption capacity, β is the activity co-efficient related to energy and ε is the Polanyi potential given by $RT = \ln(1 + 1/C_e)$

The values of β and q_m were calculated from the slope and intercept of the linear plot of ln q_e versus ε^2 and the energies of sorption (E_s) values for the biosorption processes using all three test biosorbents were calculated using eqn. 4.13 (Dada et al., 2012).

$$E_s = 1/(\sqrt{2\beta}) \quad (4.13)$$

4.13.3 Thermodynamic modeling

Thermodynamic parameters provide insight pertaining to the thermal feasibility of biosorption processes and the associated energy changes. Therefore, the values of Gibb's free energy for the biosorption of Hg^{2+} by pristine and modified forms of *Cladophora sp* alga were determined using eqn. 4.14 (Tuzen et al., 2009).

$$\Delta G^{\circ} = -RT \ln K_D \quad (4.14)$$

where ΔG° is Gibb's free energy (kJ mol^{-1}), R is the universal gas constant (8.314 J K^{-1} mol^{-1}), T is the temperature (K), K_D is the partition coefficient = (C_e/q_e).

Similarly, the values of the enthalpy (ΔH°) and entropy (ΔS°) were calculated using eqn. 4.15 (Dada et al., 2012).

$$ln\ K_D = \Delta S^{\circ}/R - \Delta H^{\circ}/RT \quad (4.15)$$

where ΔH° and ΔS° are determined from the slope and intercept of the Vant Hoff plot of ln K_D versus 1/T

4.15 Continuous flow studies

Continuous flow studies for the biosorption of Hg^{2+} from aqueous solutions were only performed using the *Cladophora sp* alga immobilized in alginate beads because it had a higher mechanical strength than the other two test biosorbents. Moreover, the alga immobilized in alginate beads was much easier to handle and had a higher biosorption capacity than both the pristine alga and the alga immobilized in silica gel.

The column studies were conducted in a small-scale Pyrex glass column with an internal diameter of 1.5 cm and a length of 15 cm. A sintered filter (porosity 1) was infused at the bottom of the column to prevent loss of biosorbent yet permitting a uniform flow of solution. *Cladophora sp* alga immobilized in alginate beads was then tightly packed in the column up to the desired bed height. After this, a layer of glass beads (1 cm) was placed on top of the biosorbent to prevent the beads from floating around the column thus reducing the pressure in the column during experiments.

Deionized water was then flushed through the packed column for 1 hour to remove any light metals adhered to the biosorbent. Subsequently, metal solution of known concentration held at pH 5 was fed from the top of the column at a specific flow rate using a Pole Carmer Instrument Company Masterflex LS (USA) peristaltic pump. Successive aliquots of 5 mL of effluent were collected at the bottom of the column in glass sample vials and the concentration of mercury in the collected samples was determined. The collection of effluent samples and their subsequent analysis for metal content was continued until the ratio of the concentration of

mercury in the effluent to that in the inlet solution (C_e/C_i) was approximately 0.95. The experimental setup of the packed biosorption columns used is illustrated in Fig. 4.3.

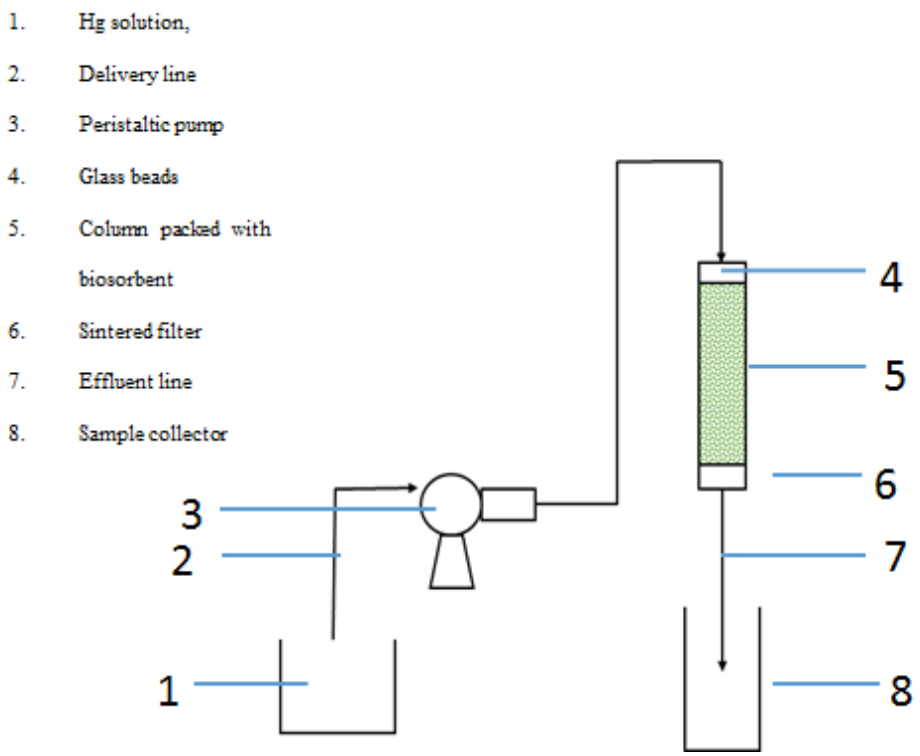

Fig. 4.3: Schematic diagram of the column packed with *Cladophora sp* immobilized in alginate beads for continuous flow studies

4.15.1 Optimization of the performance of the biosorption column packed with *Cladophora sp* alga immobilized in alginate beads

The efficiency and the performance of the biosorption used were optimized by evaluating the effects of bed height, flow rate and metal inlet concentration as per the protocols described in 4.15.1.1, 4.15.1.2 and 4.15.1.3, respectively.

4.15.1.1 Effect of bed height

The effect of bed height on the removal of mercury from aqueous solutions was investigated using three different column set-ups packed with biosorbent up to 3, 5 and 7 cm. Mercury solution (2 mg L^{-1}) was then pumped through the columns at a

flow rate of 2 mL min^{-1} while maintaining the solution pH and temperature at 5 and 25˚C respectively. 5 mL aliquots of effluent were consecutively collected and analyzed for mercury content. Effluent collection and their subsequent analysis were continued until the ratio of C_e to C_i was close to 0.95.

4.15.1.2 Effect of flow rate

The effect of flow rate on the biosorption performance of the biosorbent in continuous flow operation was also studied using two columns with the same dimensions (internal diameter, length 15 cm) packed with biosorbent up to a bed height of 7 cm. In one column, the rate of flow of metal solution was kept at 2 mL min^{-1} while in the other, the flow rate was increased to 4 mL min^{-1}. However, in both cases, solution pH, inlet metal concentration, and temperature were kept constant at 5, 2 mg L^{-1} and 25˚C respectively. Effluents were collected at the bottom of each column and analyzed for mercury concentration. Sample collection was continued until a C_e/C_i value of 0.95 was reached.

4.15.1.3 Effect of inlet metal concentration

The effect of inlet metal concentration was also studied using three column set-ups with bed heights of 7 cm. Metal solutions of varying concentrations (1, 2 and 5 mg L^{-1}) were pumped through the columns at a flow rate of 2 mL min^{-1} using the pump. 5 mL samples were collected at the bottom of the column and analyzed for metal content until C_e/C_i was 0.95.

4.15.2 Evaluation of the performance of the biosorption column

The performance or efficiency of the fixed bed columns packed with *Cladophora sp* immobilized in alginate was evaluated in terms of the breakthrough time (t_b), exhaustion time (t_e), total percent removal (r %) and maximum specific uptake (q) which were computed using eqns. 4.16, 4.17, 4.18 and 4.21, respectively (Gonen and Aksu, 2003; Mishra et al., 2012).

$$t_b = V_b/F \tag{4.16}$$

where t_b is the breakthrough time (minutes), V_b is the volume of solution treated when the ratio of the effluent concentration to the inlet concentration is 0.05 and F is the flow rate (mL min^{-1})

$$t_e = V_e/F \quad (4.17)$$

where t_e is the exhaustion time (minutes), V_e is the volume of solution treated when the ratio of the effluent metal concentration to the inlet metal concentration is 0.95

$$r\% = q_{total}/m_{total} \quad (4.18)$$

where r% is the total percent removal (%), q_{total} is the total amount of Hg^{2+} adsorbed (mg) calculated using eqn. 4.19 and m_{total} is the total amount of Hg^{2+} ions fed into the column (mg) calculated using eqn. 4.20 (Gonen and Aksu, 2003)

$$q_{total=F/1000}\int_0^t C_{ad}dt \quad (4.19)$$

where q_{total} is the total amount of Hg^{2+} adsorbed in the packed column (mg), F is the flow rate (mL min^{-1}) and C_{ad} is the adsorbed concentration (mg L^{-1})

$$m_{total} = C_eFt_{total}/1000 \quad (4.20)$$

where m_{total} is the total amount of Hg^{2+} ions fed into the column (mg), C_e is the concentration of metal in effluent and t_{total} is the total time the solution was running through the column

$$q = q_{total}/X \quad (4.21)$$

where q is the maximum specific uptake (mg g^{-1}), q_{total} is the total amount of Hg^{2+} adsorbed (mg) and X is the mass of biosorbent used (g)

4.15.3 Selectivity of the biosorption column packed with *Cladophora sp* alga immobilized in alginate beads

The selectivity of the biosorption column was evaluated by using it to treat multi-elemental solutions. In this instance, biosorption of mercury using the packed column was performed in the manner described in section 4.15 except that the inlet solution was comprised of 1 mg L^{-1} each of Hg^{2+}, Cd^{2+}, Cu^{2+}, Fe^{3+} and Pb^{2+}ions. The glass column was packed with biosorbent up to a bed height of 7 cm and the flow rate of the metal solution through the column was maintained at 2 mL min^{-1}.

4.16 Prediction of the breakthrough behavior of the biosorption column packed with *Cladophora sp* immobilized in alginate beads

The breakthrough behavior of the biosorption column was modeled against the Bed Depth Service Time (BDST) Thomas, Adams-Bohart and Yoon-Nelson models to predict the scale-up design parameters. Linear expressions of the models are given in eqns. 4.22, 4.23, 4.24 and 4.25, respectively (Mishra et al., 2012; Preetha and Viruthagiri, 2007).

$$t = N_0 Z/C_i V - 1/K_a C_i[\ln(C_i/C_b - 1)] \quad (4.22)$$

where t is the service time (minutes), C_i and C_b are the inlet and breakthrough metal concentrations (mg L^{-1}), N_0 is the sorption capacity of the bed (mg g^{-1}), V is the velocity of fluid flowing through the column (cm min^{-1}), K_a is the rate constant (L mg^{-1} min^{-1}), Z is bed height of the column (cm).

The values of N_0 and K_a were determined from the slope and intercept of the linear graph of T versus Z

$$\ln(C_i/C_e - 1) = K_{TH} C_e q_0 m/F - K_{TH} C_i/F \ (V_{\text{eff}}) \quad (4.23)$$

where C_i and C_e are the influent and effluent metal concentrations (mg L^{-1}), K_{TH} is the Thomas rate constant (mL min^{-1} mg^{-1}), q_0 is the equilibrium metal uptake (mg g^{-1}), m is the amount of biosorbent in column (g), F is the flow rate (mL min^{-1}) and V_{eff} is the effective volume of the solution (mL).

The values of K_{TH} and q_0 were calculated from the slope and intercept of the linear plot of ln (C_e/C_i -1) against V_{eff} at various values of inlet metal concentration, flow rate, and bed height.

$$\ln(C_e/C_i) = K_{AB} C_i t - K_{AB} N_0 (Z/U_0 \quad (4.24)$$

where C_i and C_e are the influent and effluent metal concentrations (mg L^{-1}), K_{AB} is the Adams-Bohart kinetic constant (L mg^{-1} min^{-1}), t is the time (minutes), N_0 is the saturation concentration (mg L^{-1}), Z is the bed height (cm) and U_0 is the superficial velocity (cm min^{-1}).

The values of K_{AB} and N_0 were determined from the intercept and slope of the linear graph of ln (C_e/C_i) versus time.

$$\ln(C_e/C_i - C_e) = K_{YN}t - \tau K_{YN} \quad (4.25)$$

where K_{YN} is the Yoon-Nelson rate constant (min^{-1}), τ is 50% of the time required to reach breakthrough (minutes) and t is the time the column was running (minutes).

The values of K_{YN} and τ were determined from the slope and intercept of the linear plot of ln (C_e/ (C_i –C_e)) at the various inlet metal concentrations, flow rates, and bed heights studied.

4.18 Design and development of biotraps and their application for the treatment of environmental samples

The design of biotraps from the alga immobilized in alginate beads and their subsequent application for the treatment of AMD samples was done as per the methods described below.

4.18.1 Design and development of biotraps

Biotraps for the remediation of mercury from environmental samples were developed based on the *Cladophora sp* immobilized in alginate beads because the results obtained for the biosorption studies revealed that the biosorbent had the highest biosorption capability. In addition, the alga immobilized in alginate beads had the highest mechanical strength and were the easiest to handle and separate from water. Column studies had also demonstrated that the biosorbent could effectively be utilized for mercury removal under pseudo-industrial conditions.

The biotraps were constructed by enclosing the alga immobilized in alginate beads in 'teabag-like' mesh bags made from nylon mesh fabric with pores of size 2 mm. Fig. 4. 4 is an illustration of the nylon mesh material sheets used.

Firstly, the mesh material was cut into square-shaped pieces of dimensions 5 cm x 5 cm. The pieces were then hand-sewn together using nylon thread to make mesh bags with their tops left open. Subsequently, the mesh bags were filled with *Cladophora sp* alga immobilized in alginate beads and hand stitched at the top. A piece of nylon string was then tied attached to the top to form a 'teabag-like' device.

Fig. 4.4: Nylon mesh fabric used for constructing biotraps

4.18.2 Application of the biotraps for the treatment of environmental samples

First, 5 g of environmental salt crusts was dissolved in 1000 mL of deionized water to form acid mine water. The pH, TDS and the EC of the resultant waters were then determined using the field meter. The water samples were then filtered using 0.45 μm filters their total metal contents were determined using the ICP-OES and mercury analyzer systems. Thereafter, three different experiments were set up wherein 100 mL of the environmental water samples was brought in contact with a single biotrap containing approximately 1.0 g of the biosorbent. The mixtures were then agitated at 150 rpm on the incubator shaker set at 25˚C for 1 hour. After completion of the biosorption process, the biotraps were removed from the solution and the total concentration of metals remaining in the solution was determined.

4.19 Metal analysis

The metal contents of all the metal solutions, algal digests, and water samples were determined using either a Perkin Elmer FIMS 400 mercury analyzer (USA) or Spectro Genesis FEE (Germany) Inductively Coupled Plasma Optical Emission Spectroscopy (ICP-OES). The methodologies for analysis using the two instruments are given in section 4.19.1 and 4.19.2 respectively.

4.19.1 Determination of total mercury content (Hg_{total}) in metal solutions and algal digests

The mercury concentrations in all the metal solutions and algal digests were measured using a Perkin Elmer FIMS 400 (USA) mercury analyzer equipped with an autosampler. Fig. 4.5 shows a photographic representation and schematic diagram of the significant functional parts of the instrument. Samples were introduced into the system via a 5-port valve and 3% puriss HCl was used as a carrier to convey them to the mixing section. At the mixing section, 1.1% $SnCl_2$ then reacted with the samples and reduced any mercury present to the elemental species. Subsequently, the vaporous mercury formed was separated from the liquid components of the sample by passage of the sample stream through a gas/liquid separator. The vapor was then transported to the adsorption cell via argon gas carrier for determination and quantification. The operation of the system was automated and controlled using the Perkin Elmer WinLab 32 (USA) software.

Table 4.3 is an illustration of the program used for the automated analysis of mercury using the mercury analyzer. Data processing and quantification were also performed automatically using the same software. The height and area of the analytical signal produced were then used to determine the concentration of mercury in the sample.

Table 4.3: Program for determination of Hg_{total} using the FIMS 400 mercury analyzer system

Step	Time (s)	Valve position	Read
Prefill	15	Fill	No
1	10	Fill	No
2	15	Inject	Yes
3	0	Fill	No

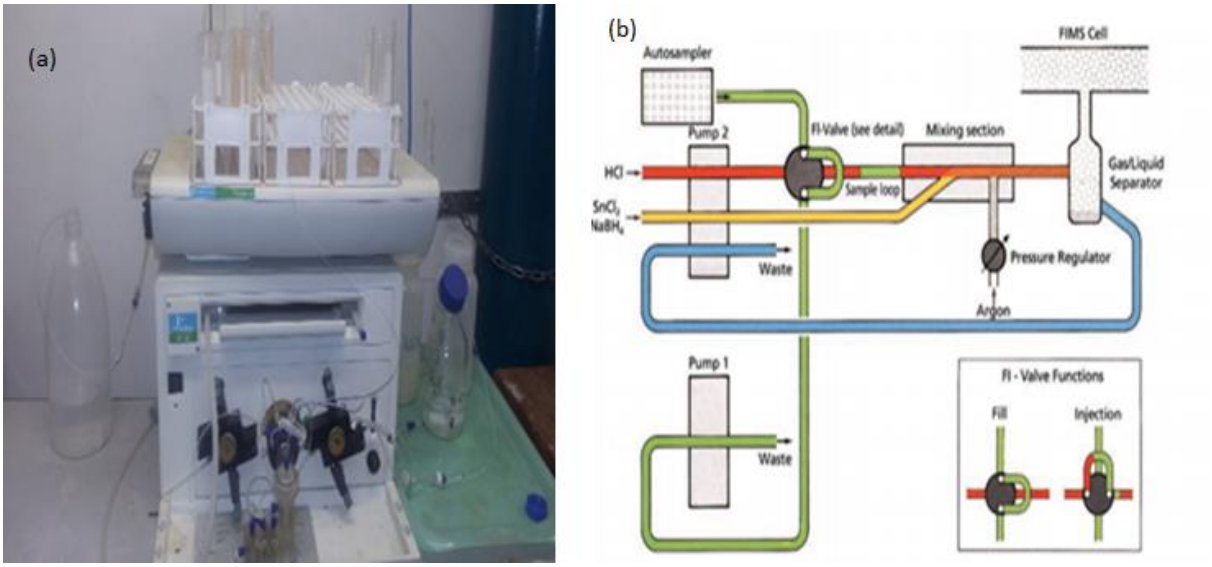

Fig.4.5: Photographic image (a) and schematic diagram (b) of the FIMS 400 mercury analyzer

4.19.2 Determination of the total metal concentrations in metal solutions, water samples, and algal digests

The total concentrations of all the other metals (excluding mercury) were determined using the ICP-OES technique. Fig 4.6 gives a pictorial representation and schematic diagram of main functional components of the equipment used.

The instrument was first automatically conditioned for the simultaneous measurement of the metals of interest using Intelligent Calibration Logic (ICAL). The elemental composition of the ICAL solutions was 10 µg mL^{-1} (Ni, Ce, P, Cu, Fe, Si, K, Ti, V, Y and Zr), 5 µg mL^{-1} (Na, Sc, Mn and Mo), 2 µg mL^{-1} (Be, Sr and Li) and 1 µg mL^{-1} (Ca). The operational conditions were also set to those shown in Table 4.4 and all the analysis steps were controlled Spectro Smart Analyzer Vision software (Germany).

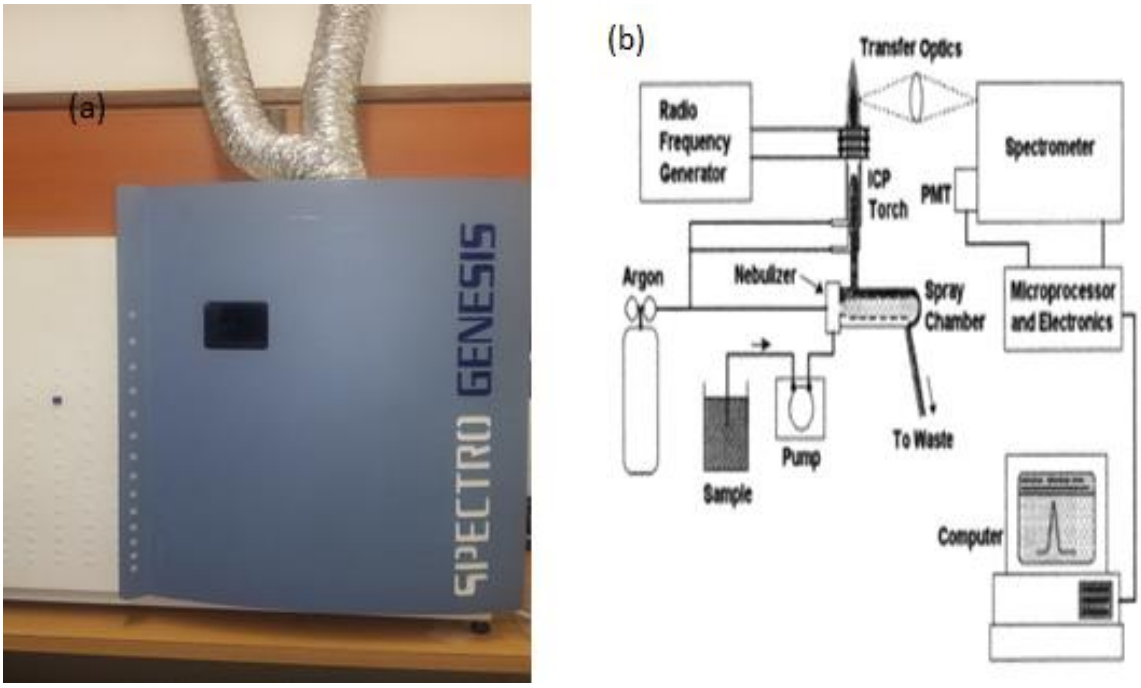

Fig 4.6: Pictorial representation (a) and schematic diagram (b) of the ICP-OES

Table 4.4: Optimum operating conditions for the determination of total metal concentrations using the Spectro Genesis ICP-OES

Parameter	Value
Power	1450 W
Auxiliary flow	0.7 L min^{-1}
Nebulizer flow	0.8 L min^{-1}
Sample aspiration rate	2.0 mL min^{-1}
Plasma	Quartz, 3.0 mm, injector time
Nebulizer	Modified Licht

4.19.3 Determination of anionic concentration in water samples

The total concentrations of all the anions in the water samples were determined using Ion Chromatography (IC) on a Metrohm 761 Compact (Germany) system. Figure 4.7 gives an illustration of the equipment used.

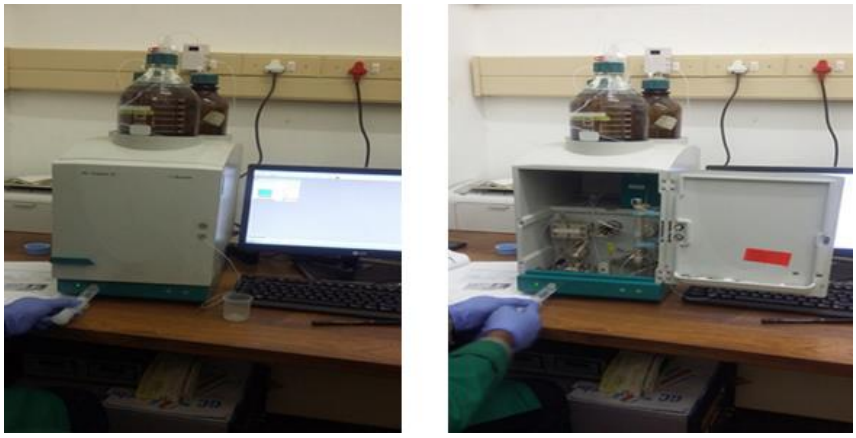

Fig.4.7: IC system used for anion content determination

The major components of the system that are significant for analysis are the separation center, detector, interface, suppressor module and pump. Moreover, data collection was performed using the IC Net 2B (Metrohm, Germany) software. The eluent solution used during analysis was a mixture of 1.0 mM $NaHCO_3$ and 3.2 mM Na_2CO_3 while the conducting suppressor reagent solution was 50 mM H_2SO_4. Both solutions were sonicated and filtered using 0.45 μm filter paper before use. Sample introduction into the system was through a 5 mL syringe. A multi-component standard solution containing 1000 mg L^{-1} each of F^-, Cl^-, NO_2^-, NO_3^-, PO_4^{3-} and SO_4^{2-} was also prepared by dissolving the required amounts of the Na salts in deionized water. The solution was then filtered and used for the preparation of working standards with concentrations in the range 1-20 mg L^{-1}. Subsequently, the working standards were used for calibration of the system. The water samples were then filtered, diluted and analyzed for anionic content.

4.20 Quality control and quality assurance

Quality assurance and quality control procedures were undertaken starting from the sample collection stage through to the metal analysis phase to ensure the validity of the results acquired. During sample collection, nitrile gloves were worn at all times to limit the contamination of samples. All algal and water samples were collected and stored in glass and PTFE containers to minimize the adherence of mercury onto the surfaces of the containers. The water samples were also acidified with concentrated nitric acid to prohibit metal precipitation.

Furthermore, all the containers and glassware used during the sampling, sample preparation and analysis stages of the experiments were prewashed using the method prescribed by Amde et al., (2016). The vessels were first washed thoroughly using detergent water and rinsed before being soaked in 10% HNO_3 for 24 hours. Next, the vessels were rinsed thoroughly rinsed with deionized water just before use. All samples were also stored in a refrigerator at 4˚C to maintain their integrity.

During the sample analysis phase, quality assurance and quality control were observed via the measurement of the recoveries, linearity, precision, and accuracy, limit of detection (LOD) and limit of quantification (LOQ). The linearity of the methods used was tested by the construction of calibration curves using different concentrations of working standards prepared by serial dilution of either a multi-elemental standard (1000 mg L^{-1}, Ultraspec, Germany) for ICP-OES analysis or a mercury standard (1 mg L^{-1}, Ultraspec, Germany) for mercury analysis. Calibration blanks and standards were also included in the sampling analysis procedure to periodically verify the instrumental performance. The standard blank measurement was also used for the determination of the LOD and LOQ of the analytical instruments using eqns. 4.26 and 4.27, respectively.

$$LOD = 3\ X\ SD_{blank} \tag{4.25}$$

$$LOQ = 10\ XSD_{blank} \tag{4.26}$$

where SD_{blank} is the standard deviation of 20 blank measurements

The accuracy of the methods used was also assessed utilizing a certified reference material (BCR 482 for trace elements in lichens). For each digestion run, vessels containing a known amount of CRM was exposed to the same digestion program as the algal samples. Similarly, procedural blanks were also used wherein vessels containing digestion reagents without the addition of sample were digested in the same manner to substantiate if any contamination of samples had occurred during their preparation and treatment. Subsequently, the amount of mercury in the blanks and CRM was measured and compared to the expected values. The precision of the method was also evaluated by analysis of the samples three times and determining the standard deviations of the replicate measurements.

CHAPTER 5: RESULTS AND DISCUSSION

This chapter presents the statement, discussion, and analysis of the results obtained for all the experiments conducted in the study.

5.1 Optimization of the mercury analyzer for the determination of Hg_{total} in water samples, algal digests, and synthetic mercury solution

The results for the optimization of the mercury analyzer are given in Fig. 5.1 and Table 5.1. Fig. 5.1 gives an illustration of the calibration curve obtained using the mercury analyzer. The calibration curve displayed excellent linearity with an R^2 value very close to unity (0.99984).

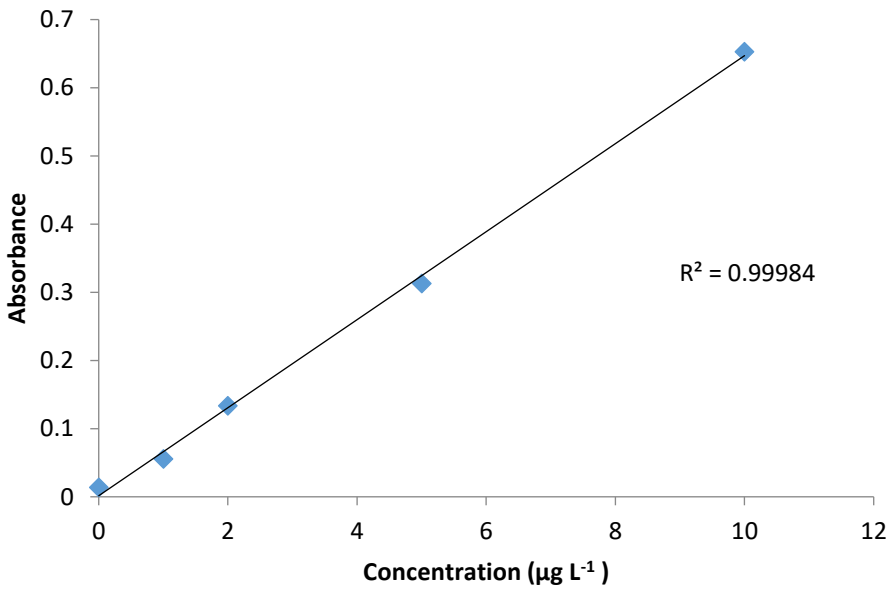

Fig. 5.1: Calibration curve for the determination of total mercury concentrations (Hgtotal) using the mercury analyzer

On the other hand, Table 5.1 provides a summary of all the calibration parameters obtained. These findings showed that the values of LOD and LOQ were sufficiently low thus indicating that the system allows for measurement of very low values of Hg_{total}. The range also showed that the equipment could be utilized for analysis of

samples with concentrations between 0.02 and 10.00 μg L^{-1}. Hence, it is reasonable to conclude that the set instrumental parameters were optimal for the quantification of mercury totals in water samples, algal digests and synthetic mercury solutions containing trace levels of mercury.

Table 5.1: Calibration parameters for the FIMS 400 mercury analyzer

Parameter	Hg_{total}
Correlation coefficient	0.9998
LOD (μg L^{-1})	0.02
LOQ (μg L^{-1})	0.06
Range (μg L^{-1})	0.02 -10.00

5.2 Optimization of the ICP-OES system for determination of total metal concentrations in water samples, algal digests, and mercury solutions

The results for the optimization of the ICP-OES are illustrated in Fig. 5.2 and Table 5.2. From these results, it was deduced that the ICP-OES system generally gave good linearity for the metals studied. Fig 5.2 shows the calibration curves for some of the metals (Cd, Ni, and Fe) analyzed using the ICP-OES system. The curves showed good linearity with R^2 values very close to 1 i.e. 0.9997, 0.9924 and 0.9998 for Cd, Fe, and Ni respectively. Table 5 also provides a summary of the calibration parameters for 6 of the metals determined using the ICP-OES system. From this, it was deduced that the R^2 values for Cu, Co and Pb were also close to unity. In addition, the LOD and LOQ values determined were reasonably low. The ranges of concentrations that the system could measure were also sufficiently wide. Hence, it can be deduced that under the set conditions, the ICP-OES system was also well-suited for the determination of total metal concentrations in the environmental samples used in this study.

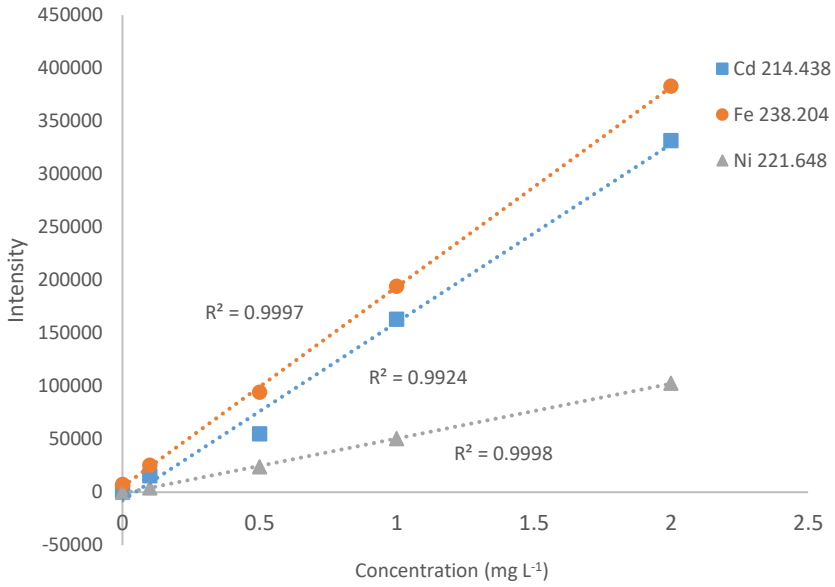

Fig. 5.2: Calibration curves for some of the metals (Cd, Ni, and Fe) studied using the ICP-OES system

Table: 5.2: Calibration parameters for different metals using the ICP-OES

Metal	R^2	LOD (mg L^{-1})	LOQ (mg L^{-1})	Range (mg L^{-1})
Cd	0.9997	0.15	0.25	0.15-2.00
Co	0.9998	0.16	0.18	0.16-2.00
Cu	0.9998	0.12	0.17	0.12-2.00
Fe	0.9999	0.12	0.14	0.12- 2.00
Pb	0.9998	0.13	0.14	0.13-2.00
Ni	0.9998	0.15	0.16	0.15 -2.00

5.3 Validation of the analytical method used

The validity of the analytical method was assessed through the analysis of the total mercury and metal concentration in a certified reference material (BCR 482 for lichens) using the mercury analysis and ICP-OES systems respectively. Table 5.3

presents the results for the validation of the method for determination of total mercury content.

Table 5.3: Hg_{total} content in CRM BCR 482 lichen using the FIMS 400 Hg analyzer

CRM	Hg_{total} measured ($\mu g\ kg^{-1}$)	Hg_{total} certified ($\mu g\ kg^{-1}$)	RSD (%)	Recovery (%)
BCR 482	0.47 ± 0.03	0.48 ± 0.02	2.86	98.58

According to these findings, the total mercury content in the CRM determined experimentally (0.47) was very close to the certified value (0.48). Hence, the recovery of the method was very close to 100% i.e. 98.58%. This signified that the accuracy of the analytical method for determination of Hg_{total} was good. The precision of the method was also exceptionally good because the relative standard deviation (RSD) between replicate measurements was lower than 5%. This indicated that the sample preparation steps used were very efficient and resulted in minimal sample loss or contamination. Therefore, it can be inferred that the results obtained using this method are reliable.

The validity of the method using the ICP-OES system was also evaluated and the results are displayed in Table 5.4. These findings also revealed that experimental values for the total concentrations of all metals studied were congruent to those certified by in the CRM data sheet. In addition, the recoveries for all the metals were close to 100% thus showing that the accuracy of the analytical method was high. The RSD values of replicate measurements for all the metals under study were also below 5% thus signifying that the precision of the method was high. The above results reaffirmed that the sample preparation steps undertaken before analysis were efficient and the analytical methods chosen were suitable for the analysis of total metal concentration in water samples, algal digests, and multi-elemental aqueous solutions.

Table 5.4: Metal content in BCR 482 lichen CRM using the ICP-OES system

Metal	Certified value (mg kg^{-1})	Measured value (mg kg^{-1})	RSD (%)	Recovery (%)
Al	1103.00 ± 24.00	1093.00 ±8.33	3.82	99.09
As	0.85 ± 0.07	0.82 ± 0.04	3.46	96.69
Cd	0.56 ± 0.02	0.51 ± 0.06	4.59	91.07
Cr	4.12± 0.15	4.06 ± 0.09	2.22	98.50
Cu	7.03 ± 0.19	6.88 ± 0.24	3.03	97.79
Ni	2.47 ± 0.07	2.35 ± 0.01	3.58	95.06
Pb	40.90 ±1.40	40.3 ± 0.32	4.01	98.43

5.4 Physicochemical characterization of the water samples collected from Alexander Dam

The water samples collected from the dam were characterized using their field parameters and total metal ion concentrations. Table 5.5 gives a summary of the results obtained for the field parameters of the water samples. According to these results, the pH of the water was neutral i.e. between 7.01 and 7.57. The values of total dissolved solids (TDS) and electrical conductivity (EC) measured were also relatively low. This implied that the water samples had low levels of metal and organic solutes. The values of dissolved oxygen (DO) and redox potential (ORP) also revealed that the water was oxidizing and supported the habitation of living microbial organisms like bacteria and algae. From this, it can be concluded that the algal samples were found growing in freshwater with minimal metal contaminants thus favoring their survival. The fact that the algae were harvested from freshwater containing minimum metal contaminants also suggests that some of the binding sites on their surfaces are free for metal interactions during metal biosorption.

Table 5.5: Field parameters of the water samples

Parameter	Sample 1	Sample 2	Sample 3
Temperature (˚C)	24.5	22.7	24.4
pH	7.01	7.57	7.15
Total dissolved solids (mg L^{-1})	384	365	411
Redox potential (mV)	118.6	80.1	114.1
Dissolved oxygen (mg L^{-1})	94	76	38
Electrical conductivity (µS cm^{-1})	605	559	638

In the same way, the results for the determination of the total metal and anion concentrations of the water samples are shown in Table 5.6. According to these findings, the water samples studies had low levels of metallic solutes. This correlated with the results for the field measurement of pH, TDS, and EC which also predicted that the water samples had low concentrations of metal and organic contaminants. The concentrations of the alkali and alkaline earth metals in the water samples far exceeded those of the other metals. In fact, Na was most abundant followed by K, Mg and then Ca. Slightly elevated levels of Al and Fe were also found in the water samples while only trace amounts of transition metals such as Hg, As and U were determined. This trend is typical for the concentration of metals in freshwater samples with minimal pollution (Öztürk et al., 2009; van Loof and Duffy, 2009). The high levels of Fe and Al can be attributed to the natural abundance of these metals are found in higher concentrations than the above-mentioned trace metals.

The results for the anion content of the water samples reveal that SO_4^{2-} and Cl^- ions were the most abundant. This observation is typical of the concentrations of these anions in freshwater samples (Öztürk et al., 2009; van Loof and Duffy, 2009).

Table 5.6: Total metal and anion content of water samples collected from Alexander Dam

Metal	Concentration (mg L^{-1})
Li	0.04 ± 0.01
Na	44.58 ± 1.22
Mg	15.63 ± 0.14
K	14.85 ± 0.22
Ca	4.22 ± 0.54
Mo	0.18 ± 0.03
Fe	0.90 ±0.08
Zn	0.05 ± 0.01
Hg	0.09 ± 0.01
Al	2.63 ± 0.28
As	0.03 ± 0. 01
U	0.05 ± 0.01
F^-	0.26 +/- 0.01
Cl^-	37.42+/-0.38
PO_4^{3-}	Not detected
SO_4^{2-}	54.31+/-1.60
NO_3^-	1.20 +/-0.35

5.5 Synthesis of the modified forms of *Cladophora sp* alga

Pristine *Cladophora sp* alga was modified by immobilization in alginate beads and silica gel to form 'modified biosorbents'. Fig. 5.3 shows the pristine alga before and after immobilization in alginate beads and silica gel. From the figures above, it is apparent that the physical appearances and characteristics of the pristine alga differ profusely from those of the modified biosorbents. Firstly, pristine *Cladophora sp* alga is dark green in color and comprised of several intertwined filaments which are very difficult to separate from water. On the contrary, the alga immobilized in

calcium alginate was in the form of beads which were greenish-yellow in color due to the color contributions of both the alga and alginate support.

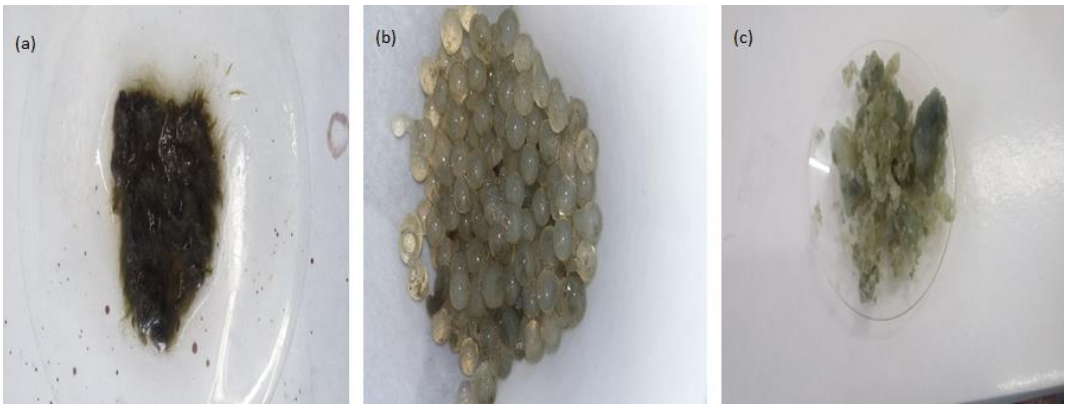

Fig. 5.3: Pristine *Cladophora sp* alga before (a) and after immobilization in alginate beads (b) and (c) silica gel

The beads were easily separated from water and had an average diameter of approximately 2.3 mm. The alga immobilized in silica gel was in the form of a yellowish-green gelatinous solid which was also easily harvested from water and much easier to handle than the pristine alga. This verified that the pristine alga had been successfully modified by immobilization in alginate beads and silica gel. The fact that the modified biosorbents were much easier to handle and had improved stabilities also proved that indeed immobilization of algae improved their physical properties.

Haydar et al., (2016) also immobilized the biomass of *Candida lipolytica, Candida tropicalis* and *Candida utilis* in alginate beads for the biosorption of Ni (II) ions from aqueous solutions. They also discovered that immobilization improved the mechanical properties of the biosorbents. The physical properties of the resultant beads differed from those of the beads synthesized in the present study. For instance, the diameter of the beads produced by Haydar et al., (2016) ranged between 1.18 and 1.83 mm while the beads synthesized in the current work had an average diameter of 2 mm. Barquilha et al., (2017) also immobilized *Sargassum sp* alga in alginate for the retrieval of Ni(II) and Cu(II) from aqueous solutions. They

found that the beads formed were much easier to separate from water than the unmodified alga. The beads also had an average diameter of 2.5 mm. The differences in the properties of the biosorbents synthesized in the different studies are explicable by the utilization of differing microbial biomass and preparation methodologies.

5.6 Characterization of the pristine and modified forms of *Cladophora sp* alga for the biosorption of mercury from aqueous solutions

Prior to their utilization for biosorption studies, all the test biosorbents were characterized using various techniques and the results are described in detail in subsections 5.6.1 -5.6.5 below.

5.6.1 Determination of moisture contents of the pristine alga and alga immobilized in alginate beads

The moisture contents of the pristine alga and alga immobilized in alginate beads were determined so as to get an indication of the quantity of sample to be weighed out to attain the dry masses required for biosorption studies. The results are shown in Table 5.7. As shown in the table, the moisture contents of the pristine alga and alga immobilized in alginate beads were 80.76 +/- 1.49% and 96.50 +/- 1.76% respectively. Hence, when weighing the masses of these two biosorbents for biosorption these values were taken into consideration.

Table 5.7: Moisture contents of pristine *Cladophora sp* alga and *Cladophora sp* immobilized in alginate beads

Biosorbent	% moisture
Pristine *Cladophora sp* alga	80.76 ±1.49
Cladophora sp alga immobilized in alginate beads	96.50 ±1.77

da Silva et al., (2003) also reported the moisture contents of *Ulva lactuca, Padina sp*, *Dictiospheria versluysii*, *Caulerpa racemosa*, *Caulerpa cupressoide* and *Sargassum vulgare* algae as 76.0, 83.7, 91.7, 95.0, 86.5 and 78.5% respectively. On

the other hand, Lopes et al., (2017) modified *Lactobacillus rhamnosus* by entrapment in alginate beads and characterized the resultant biosorbent. They deduced that the moisture content of the immobilized biomass was 97.70 ± 0.03%. Barquilha et al. (2017) also immobilized *Sargassum sp* alga in alginate for the retrieval of Ni(II) and Cu(II) from aqueous solutions. Characterization of the resultant beads revealed that they had a moisture content of 94.83%. Differences between the results found in the aforementioned studies and those of the current work are mainly due to the variations in the taxonomy of the algal species used and methods used for biosorbent preparation.

5.6.2 Functional group identification

FTIR spectroscopy was used for the identification of the functional groups on the surfaces of the biosorbents and the results are shown in Fig. 5.4. It is evident from this figure that the spectrum for the pristine alga had four prominent peaks corresponding to the overlapping stretching of –OH and –NH functional groups (2908 cm^{-1}), symmetric and asymmetric stretching of the -C=O group (1739 and (1126 cm^{-1}), respectively.

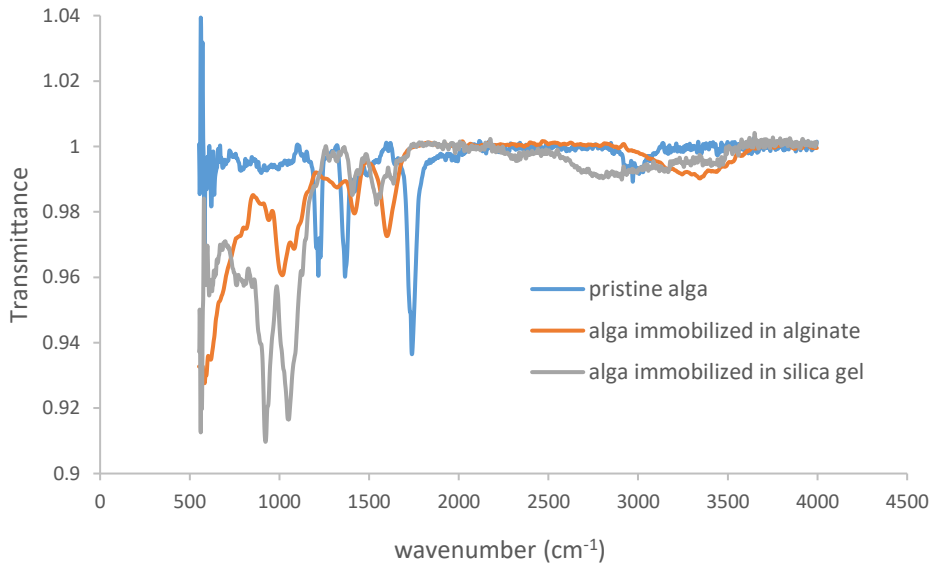

Fig. 5.4: FTIR spectra of pristine and modified forms of *Cladophora sp* alga

The results also showed that the spectrum for the *Cladophora sp* alga immobilized in alginate was slightly different from that of the pristine alga. Though it had conspicuous bands at 3408, 1602, 1419 and 1020 cm^{-1} corresponding to the –OH, -NH and C=O as in the pristine alga, it also had an additional peak due to –C-O-C vibration stretching respectively (Petrovic and Simonic, 2016). These bands were characteristic of functional groups originating from both the alga and the alginate support matrix thus further verifying that immobilization had successfully been performed. It is also notable that the immobilization of *Cladophora sp* alga onto alginate beads resulted in the reduction in the intensities and shifting of the peaks due to the –C=O, N-H and –O-H functional groups. This observation suggests that these groups interact with functional groups in alginate during immobilization.

Similarly, Fig. 5.4 illustrated that the FTIR spectrum of the alga immobilized in silica gel differed substantially from those of the pristine alga and alga immobilized in alginate beads. The spectrum showed 5 prominent bands at 3010, 1739, 1367, 1217 and 640 cm^{-1}. These peaks were assigned to the overlapping of the –OH and–NH groups, asymmetric and symmetric stretching vibration of the – C=O group, and -Si-O-Si groups respectively (Akar et al., 2009; Hammud et al., 2014).This indicated that as in the case of the alga immobilized in alginate beads, this biosorbent also had functional group contributions from both the alga and the silica gel support matrix. This provided further verification that the alga had indeed been successfully immobilized in the silica gel support.

Comparisons of these findings with those of other works showed marked differences. For instance, Gupta et al., (2008) examined acid treated *Oedogonium hatei* alga for the biosorption of Ni(II) ions. FTIR analysis revealed peaks at 3390 and 1648 cm^{-1} corresponding to the –OH, -NH and –C=O functional groups respectively. However, unlike in the case of the *Cladophora sp* utilized in the current study, the FTIR spectrum did not show the presence of the $–SO_3$ group as in the case of the *Cladophora sp* alga utilized in the current study. Instead, the authors observed a peak at 1248 cm^{-1}which they attributed to the phosphoryl function group.

Bayramoglu and Arica, (2009) also reported biosorption of Cu, Zn, and Ni using *Scenedesmus quadricauda* alga immobilized in alginate beads. Characterization of the resultant biosorbent using FTIR spectroscopy revealed the presence of –OH, -N-H, -C=O and -C-OH functional groups on its surface. However, an additional peak was also observed at 2932 cm^{-1} which were assigned to the phenolic functional group. The authors also did not attempt to use FTIR to compare the functional groups on the native alga with those on the modified biosorbents. The results reported by Suharso et al., (2010) for the immobilization of *Sargassum duplicatum* in silica gel also showed that the resultant biosorbent had characteristic functional groups originating from both the alga and silica gel. Notwithstanding, the peaks due to the different functional groups were slightly shifted compared to those reported for the biosorbent synthesized in the present study. The authors also observed the presence of a peak due to the Si-O- group at 470 cm^{-1}. Disparities between the results obtained in the above-mentioned studies are explicable by the use of different algal biomass with dissimilar cell wall compositions. The properties of the test metals and solution parameters also varied between the various research works.

5.6.3 Surface morphology studies

SEM was used to evaluate the surface morphologies and textures of the pristine and modified forms of *Cladophora sp* alga and the results are shown in Figs. 5.5 and 5.6, respectively. Fig. 5.5 shows the morphology of the pristine alga at different magnifications. As illustrated above, at low magnification (Fig 5.5 (a)), the algal surface appears as a complex network of intertwined filaments arranged in a net-like format. However, increasing the magnification to x9237(Fig. 5.5 (b)) placed focus on a single filament whose surface was relatively smooth and homogeneous. These results differed from those reported by Sarada et al., (2014) for the characterization of *Caulerpa fastigiata* alga for the biosorption of Cd ions. SEM analysis revealed that the surface of *C. fastigiata* was not as complex as that of *Cladophora sp* alga. The surface was also uneven, heterogeneous and showed pores for metal bioaccumulation (Sarada et al., 2014).

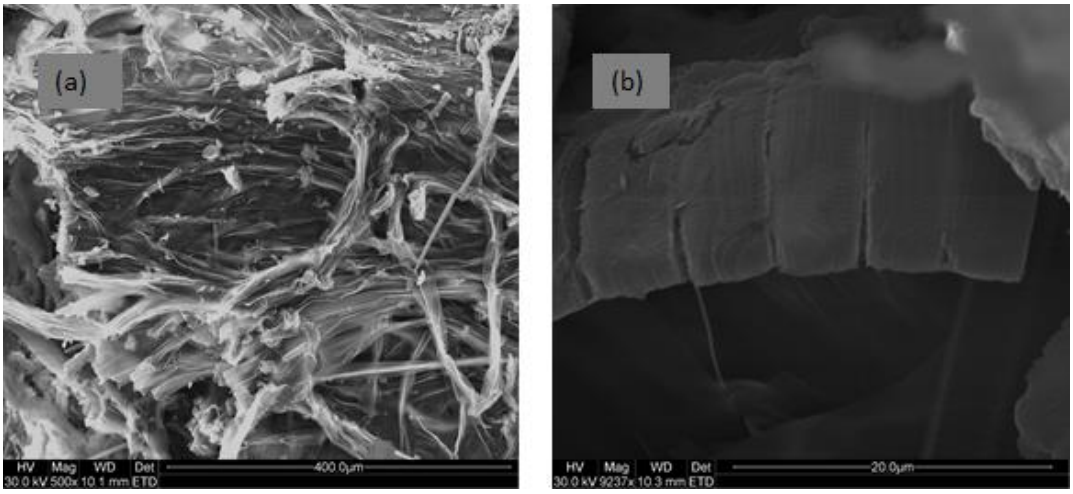

Fig. 5.5 SEM micrographs showing the morphology of pristine *Cladophora sp* alga at (a) x 500 and (b) x 9237 magnification

Mata et al., (2008) also assessed the capability of *Fucus vesiculosus* as a biosorbent for Cd, Pb, and Zn. SEM studies revealed that the alga had both regular and irregular surface morphologies (Mata et al., 2008). The differences between the morphology of the alga studied in the present work and those of other algal biosorbents in the literature can be attributed to the varying physiological and biochemical properties spanning across the various algal taxonomical divisions and species.

The morphologies of the modified biosorbents were also examined and the SEM micrographs attained are illustrated in Fig. 5.6. Fig 5.6 showed that the immobilization of the alga onto polymeric supports altered its morphology. The micrograph for the alga immobilized in silica gel (Fig. 5.6 (a)) demonstrated that the biosorbent surface had clumps of algal filaments irregularly attached to the surface of silica gel. On the converse, Fig. 5.6 (b) revealed that immobilizing *Cladophora sp* alga in alginate resulted in a regular 3-D network with a few cracks due to distortion of alginate by algal filaments. Pores were also seen on some parts of the algal biosorbent surface. Nevertheless, in both cases, immobilization of the alga yielded a more rugged texture and morphology which is more suitable for metal biosorption.

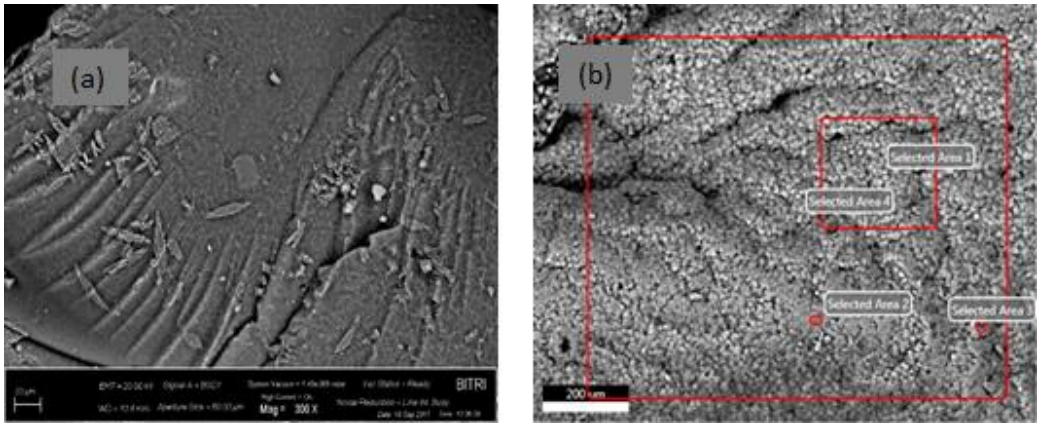

Fig. 5.6: SEM micrographs showing the morphology of *Cladophora sp* alga immobilized in (a) silica gel and (b) alginate beads (Magnification X300)

Carrilho et al., (2003) also immobilized *Pilayella littoralis* alga in silica gel and characterized the resultant biosorbent for metal preconcentration. Even though, SEM studies revealed that the surface of the resultant biosorbent was also rough, the alga covering the silica gel surface was not comprised of intricate filament networks. Equally, Mata et al. (2009) modified *Fucus vesiculosis* alga by immobilizing it in alginate beads and drying the resultant bisorbents to form xerogels. The xerogels were studied using SEM and the resultant micrographs showed that the surface morphology was heterogeneous with a number of cracks due to algal entrapment. In some instances, the alga and support matrix could be distinguishable. The differences observed in biosorbents studied is explicable by variations in the algae used, algal immobilization method and pre-treatment of the modified biosorbents prior to their evaluation.

5.6.4 Determination of the surface areas and pore volumes of the pristine and modified forms of *Cladophora sp* alga

BET analysis was utilized to determine the surface areas and pore volumes of the pristine and modified forms of *Cladophora sp* alga. The results are presented in Table 5.8.

These findings showed that pristine alga had a surface area of 8.283 $m^2 g^{-1}$ and a pore volume of 0.047 $cm^3 g^{-1}$. The surface area of the alga was greater than those reported for other algae utilized in other studies in the literature. Gupta and Rastogi, (2008) characterized *Oedogonium sp* and *Nostoc sp* for the uptake of Pb (II) from aqueous solutions and revealed that the surface areas of the algal biosorbents were 1.22 and 1.14 $m^2 g^{-1}$, respectively.

Table 5.8: Surface areas and pore volumes of pristine and modified forms of *Cladophora sp* alga before and after metal binding

Biosorbent	Surface area ($m^2 g^{-1}$)	Pore volume ($cm^{-3} g^{-1}$)
Pristine *Cladophora sp*	8.283	0.047
Pristine *Cladophora sp* after biosorption	5.044	0.030
Cladophora sp immobilized in alginate beads	6.234	0.025
Cladophora sp immobilized in alginate bead after biosorption	3.961	0.013
Cladophora sp immobilized in silica gel	5.862	0.024
Cladophora sp immobilized in silica gel after biosorption	4.991	0.010

In another study, Ahmady-Asbchin et al., (2008) deduced that the BET surface area of *Fucus serratus* alga was 1.79 +/-0.22 $m^2 g^{-1}$. The variation of the surface areas reported in the above-mentioned studies can be attributed to differential surface properties among the biosorbents used.

The results in Table 5.8 also revealed that immobilization of the alga in alginate beads led to the surface area and pore volumes depreciating to 6.234 $m^2 g^{-1}$ and 0.025 $cm^3 g^{-1}$ respectively. Similarly, the surface area and pore volume of the alga immobilized in silica gel also dropped to 5.862 $m^2 g^{-1}$ and 0.024 $cm^3 g^{-1}$

respectively. The decline in surface area and pore volume observed after immobilization is mainly due to the inhibition of nitrogen passage through some of the pores on the modified biosorbents by pendant groups from the solid support matrices (Song et al., 2016). Despite this, the surface areas and pore volumes of the immobilized biosorbents used in this study were much higher than those reported for other hybrid biosorbents utilized in other research works.

For instance, Bayramoglu and Arica, (2009) revealed that the BET surface area of *Scenedesmus quadricauda* immobilized in alginate beads was 0.97 m^2 g^{-1}. Kapoor and Viraraghavan, (1998) also reported that the BET surface area of the biosorbent prepared by immobilizing *Aspergillus nigger* biomass in polysulfone beads was 3.40 m^2 g^{-1}. Sheng et al., (2008) also prepared a low-cost biosorbent comprised of *Sargassum sp* alga immobilized in PVA cryogel beads for biosorption of Cu(II). They revealed that the surface area of the biosorbent was 1.71 m^2 g^{-1}. The differences in the surface areas of biosorbents utilized in these studies are explicable by variations in properties of the polymeric support matrices and algal biomass. The methods used for the pretreatment of the algae and preparation of modified biosorbents also varied (Sheng et al., 2008).

The results from the current study (Table 5.8) also demonstrated that mercury biosorption onto the pristine and modified forms of *Cladophora sp* alga also negatively impacted their surface areas and pore volumes. The surface area and pore volume of pristine *Cladophora sp* alga dropped to 5.044 m^2 g^{-1} and 0.030 cm^3 g^{-1}, respectively. Likewise, the surface areas and pore volumes of the alga immobilized in alginate beads depreciated to 3.961 m^2 g^{-1} and 0.013 cm^3 g^{-1} respectively while those for the alga immobilized in silica gel dropped to 4.991 m^2 g^{-1} and 0.010 cm^3 g^{-1} , respectively. The decline in surface area and pore volume in both forms of *Cladophora sp* alga after biosorption is explicable by the occupation of some of the pores on the biosorbent surface by mercury. Moreover, the metal ions blocked nitrogen access to these pores during BET analysis and thus causing a decrease in surface area and pore volume (Ahmady-Asbchin et al., 2012; Gupta and Rastogi, 2008).

5.6.5 Thermal stabilities of the pristine and modified forms of *Cladophora sp*

The thermographs for the TGA characterization of the biosorbents are shown in Fig. 5.7. According to these results, the thermal decomposition of pristine alga occurred via three steps. The first step (25-240˚C) was due to moisture loss and was succeeded by the combustion of carbohydrates in the range 240-330˚C. Lastly, protein degeneration occurred in the temperature range (330-470˚C) (Ibrahim et al., 2016). These results were slightly different to those reported by Gupta and Rastogi (2008) for the thermal degradation of *Oedogonium sp* and *Nostoc sp* algae. The authors found that moisture loss occurred in the range 20 -150˚C and accounted for only 5% of the total weight loss. In addition, the weight loss due to decomposition of the organic components of the alga occurred in 2 phases i.e. at the range 200-400˚C and 600-700˚C.

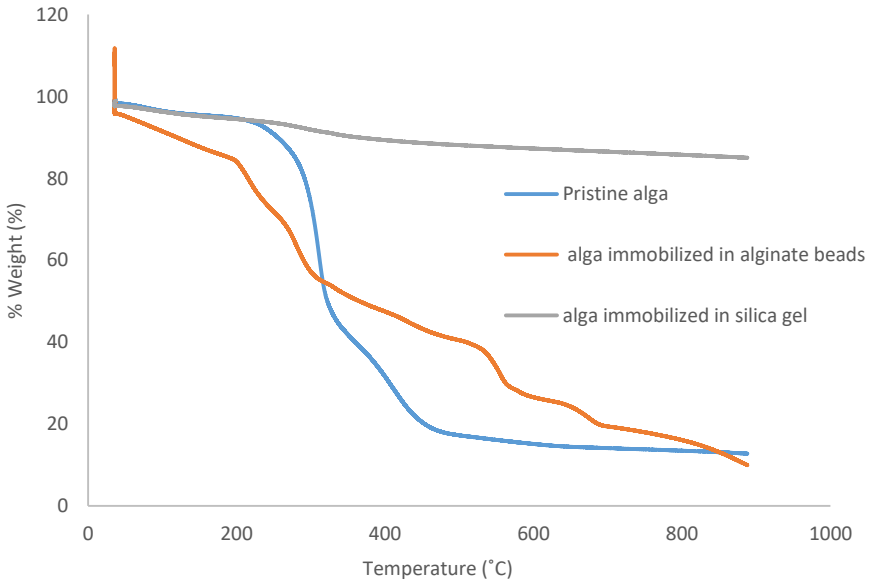

Fig. 5.7: Thermographs showing thermal stability of pristine *Cladophora* sp alga and *Cladophora sp* alga immobilized in alginate beads and silica gel

Further inspection of Fig. 5.7 also showed that thermal degradation of the alga immobilized in alginate beads entailed four major steps. As in the case of the

pristine alga, moisture loss was observed in the temperature range 25-240˚C. However, the weight lost as moisture was higher in the case of the alga immobilized in alginate beads (23.69%) than for the pristine alga. Next, a sharp dip in mass occurred in the range 240-270˚C and was attributed to destruction of glycosidic bonds in the alginate component of the biosorbent. The glycosidic bonds were then degraded between 270 and 330˚C; thereafter, gradual degradation of all previously formed intermediate carbonaceous materials commenced and continued until 530˚C (Chen et al., 2014; Patel et al., 2016). In another study, Qiusheng et al., (2015) accessed the thermal stability of zirconium alginate beads and observed slightly different behavior. There was no change in the weight of the biosorbent observed until a temperature of 81.25˚C was reached. Thereafter, water evaporation occurred up till 204.15˚C. Degradation of alginate only began at 204.15 and ended at 463.15˚C. The last phase of the process was the decomposition of other carbonaceous materials which occurred at temperatures greater than 463.15˚C (Qiusheng et al., 2015).

The thermograph for the alga immobilized in silica gel used in this study (Fig. 5.7) was very simple compared to those of the pristine alga and the alga immobilized in alginate beads. It showed that thermal degradation of the biosorbent occurred in two steps. The first step was due to the loss of physisorbed water (50 -150˚C) and accounted for 6.65% weight loss. On the other hand, the second phase (200 -800˚C) was attributed to the degradation of organic moieties and condensation of silanol groups and resulted in 13.9% weight loss. The thermograph of this biosorbent was compared with that obtained by Mureseanu et al., (2011) for a hybrid biosorbent developed by immobilizing copper-metallothioneins from baker's yeast onto mesoporous silica. The authors found that even though the biosorbent degraded via a 2 step process, mass loss, in this case, occurred in the range 20-120˚C. Degradation of the organic components was also observed between 150 and 800˚C. These slight variations in the TGA profiles of the biosorbents are mainly due to the use of different biomass components and polymeric support matrices.

5.7 Batch biosorption studies

Batch biosorption studies were conducted to evaluate the effects of significant parameters on the performances of the test biosorbents and compare their biosorption capabilities. The results are presented in the subsections below.

5.7.1 Effect of the composition of algal growth medium on the biosorption capacity of pristine *Cladophora sp* alga

The effect of the composition of growth medium on the biosorption capacity of pristine *Cladophora sp* was evaluated and the findings are illustrated in Fig. 5.8.

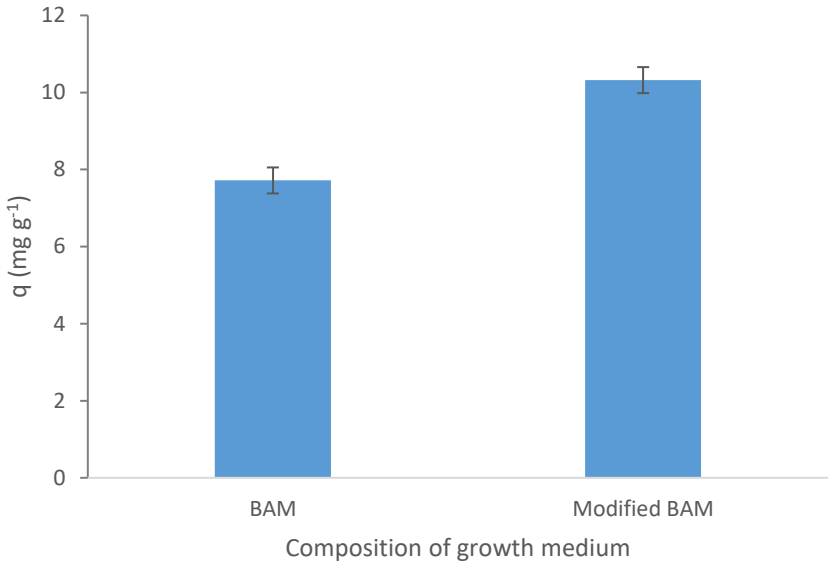

Fig. 5.8: Effect of composition of algal growth medium on the biosorption capacity of pristine *Cladophora sp* alga for removal of mercury from aqueous solutions

According to the results shown in 5.8, modification of BAM by increasing the sulfur group content impacted the biosorption capacity of *Cladophora sp* alga significantly. The biosorption capacity of the alga grown in modified BAM was higher than that of the alga cultured in unmodified BAM. This observation is explicable by Pearson's Hard Soft Acid and Base (HSAB) theory which classifies mercury as a soft metal which will have a high affinity for soft ligands or bases such as those bearing sulfur or nitrogen (Apiratikul and Pavasant, 2008; Fomina and Gadd, 2014; Park et al., 2010). Hence, the modification of the algal growth medium

by increasing sulfur-containing materials will increase the sulfur content of the algal cell wall surface and thus enhance the uptake of mercury by alga grown in this medium. Therefore, for the rest of the study, all the experiments were performed using algae grown in modified BAM.

In another study, Chojnacka et al., (2005) compared the capabilities of commercial *Spirulina sp* alga, *Spirulina sp* grown in unmodified Zarrouk growth medium and alga grown in Zarrouk medium spiked with 1 g L^{-1} glucose for biosorption of Cr^{3+}, $Cd^{2+,}$ and Cu^{2+}. They deduced that the commercial grade *Spirulina sp* alga had the highest biosorption capacity for Cr^{3+} (9 mEq g^{-1}) and Cu^{2+} (5 mEq g^{-1}). On the other hand, *Spirulina sp* grown in the unaltered medium had the highest capacity for Cd^{2+} (2.5 mEq g^{-1}). The alga grown in the modified medium had the lowest biosorption capacity for both Cr^{3+} (1 mEq g^{-1}) and Cu^{2+} (0.5 mEq g^{-1}) while its capacity for removal of Cd^{2+} (0.8 mEq g^{-1}) was higher than that of commercial grade *Spirulina sp* (0.5 mEq g^{-1}). These results showed that the effect of algal growth medium on the biosorption capabilities of algae depends not only on the chemical properties of the components of the media but also on the properties of the target metal.

5.7.2 Effect of pH

Solution pH is one of the most significant parameters affecting metal biosorption by algae and algal-based biosorbents because it affects metal speciation and surface properties of the biosorbent (Bulgariu and Bulgariu, 2012; Park et al. 2010; Wang et al., 2016). Hence, the effect of pH on the biosorption of mercury onto pristine and modified forms of *Cladophora sp* was investigated and the results are shown in Fig. 5.9. The results clearly showed that the biosorption of mercuric ions onto pristine *Cladophora sp* and the modified biosorbents is pH-dependent. The adsorption capacities of all the three biosorbents were lowest at pH 3. This is because, at low pH values, there are abundant protons which compete with the metal ions for available binding sites on the biosorbents. Protonation of active binding sites on the biosorbent also reduced their metal binding capacities due to the repulsion of the Hg(II) ions (Gupta et al., 2006; Zhu et al., 2009).

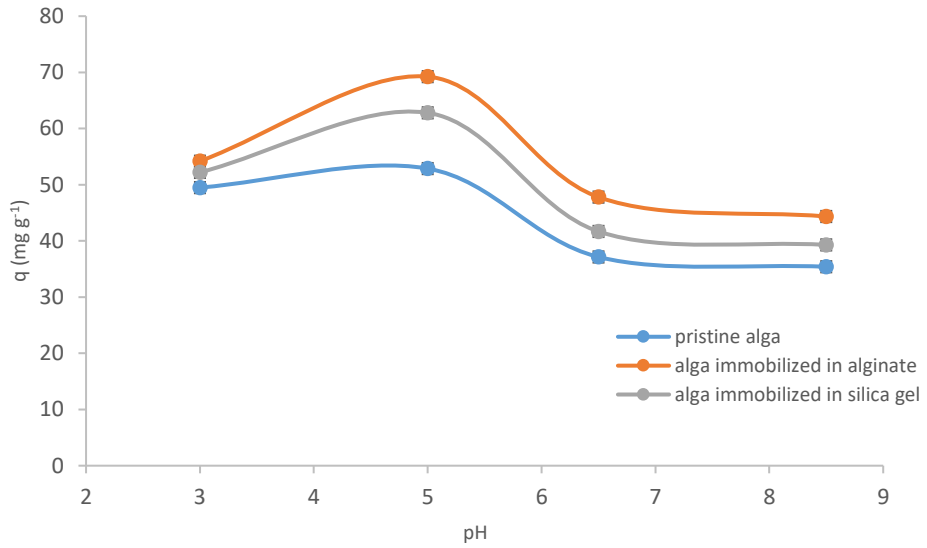

Fig. 5.9: Effect of pH on the biosorption of mercury by pristine and modified forms of *Cladophora sp* alga (Temperature 25˚C, initial metal concentration 10 mg L^{-1}, agitation time 120 minutes, biosorbent dosage 10 g L^{-1})

Accordingly, increasing the pH to 5 improved the biosorption capacities of the test biosorbents. However, further increases in pH up to 6.5 and 8.5 negatively impacted the adsorption capacities of the pristine and modified forms of *Cladophora sp.* This trend was attributed to the predominance of metal precipitation at high pH values which reduced the concentration of free metal ions available for binding (Bayramoglu et al., 2003; Herrero et al., 2005; Singh et al., 2009). Hence, the observed decrease in adsorption capacities of both the pristine and modified forms of *Cladophora sp* alga at these pH values.

Consequently, optimum pH value for the sequestration of mercury by pristine *Cladophora sp* alga, *Cladophora sp* alga immobilized in alginate beads and *Cladophora sp* immobilized in silica gel was set as 5. All subsequent biosorption studies in this work were performed at this pH. It is also worthwhile to mention that, for all the pH values studied, the adsorption capacity of the pristine alga was lower than that of the modified forms. This can be attributed to the surface contribution of the silica gel and alginate beads to the overall biosorption (Abu-Al Rub et al., 2004; Sheikha et al., 2008; Wang et al., 2016). However, the adsorption capacity of

the alga immobilized in alginate beads was higher than that of the alga entrapped in silica gel. This is because the oxygen atoms in the silanol (=Si-OH) and siloxane groups on the surface of silica gel are poor electron donors compared to those in the carboxyl group of alginates (Suharso et al., 2010).

Montazer-Rahmati et al., (2011) studied the impact of pH on the biosorption of Ni, Cd, and Pb using four different brown algae. They also found that biosorption using all the algal biosorbents was pH dependent and varied between metals. Moreover, for all the algae studied, the optimum pH values for removal of Ni, Cd, and Pb were 6.0, 5.5 and 5.5, respectively. Donmez et al., (1999) also studied the effect of pH change on the biosorption of Cu(II), Ni(II) and Cr (VI) onto *Scenedesmus obliquus* and *Synechocystis sp* biomass. They found that for both biosorbents studied, increasing the pH up to pH 5favored the biosorption of Cu(II) and Cr (VI). On the other hand, increasing the pH improved Ni(II) until a plateau was reached at pH 4.5. The disparities in the values of optimum pH are attributed to the fact that the properties of the various biosorbents and target metals used were differently affected by changes in solution pH.

5.7.3 Effect of agitation time

The effect of agitation time on the biosorption performance of pristine *Cladophora sp* alga and modified *Cladophora sp* alga was also investigated and the time profiles are depicted in Fig 5.10. For all the three biosorbents studied, it was deduced that mercury biosorption was fastest during the initial stages of the biosorption process. Hence, most of the mercuric ions in solution were adsorbed within 30 minutes. This was due to the abundance of metal binding sites at the start of the process (Bayramoglu et al., 2006). As time progressed, though more mercury was adsorbed, the rate of increase of adsorption capacity decreased due to the exhaustion of binding sites on the biosorbent surfaces (Apiratikul and Pavasant, 2008). Ultimately, a plateau was reached at 20 minutes for the pristine alga and 30 minutes for the modified biosorbents. Increasing the agitation time beyond these points had no significant impact on the biosorption capacities of the test biosorbents. Consequently, the agitation of the reaction vessels for 20-30 minutes would be ideal for attaining equilibrium using both forms of *Cladophora sp* alga.

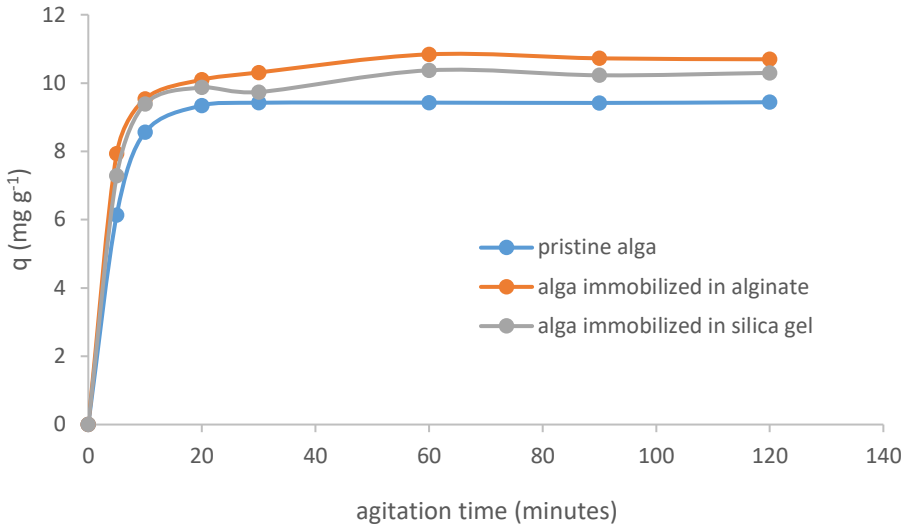

Fig. 5.10: Effect of agitation time on the biosorption of mercury by pristine and modified forms of *Cladophora sp* alga (Temperature 25˚C, initial metal concentration 1 mg L^{-1}, pH 5, biosorbent dosage 10 g L^{-1})

Moreover, under the conditions studied, the adsorption capacities of the biosorbents at equilibrium were 9.35, 10.94 and 10.37 mg g^{-1} for the pristine alga, alga immobilized in alginate beads and alga immobilized in silica gel respectively. This reaffirmed the fact that the immobilization of *Cladophora sp* alga onto the selected polymeric supports enhanced biosorption performance.

Rahman and Sathasivam, (2015) also assessed the biosorption of Pb(II), Cu(II), Fe(II) and Zn(II) onto *Kappaphycus sp* alga at different agitation times. The authors revealed that biosorption capacity of the alga for all metals improved with increases in contact time until maximum uptake was attained in 90 minutes. The maximum removal efficiencies of the metals were 83.88, 85.98, 21.27 and 54.13% for Pb(II), Cu(II), Fe(II) and Zn(II) respectively. Furthermore, a decrease in adsorption capacity was observed when the reaction mixtures were agitated for longer than 90 minutes. Cazón et al., 2013 also observed that the biouptake of Zn(II) and Cd(II) by the marine alga *Undaria pinnatifida* was rapid within the first 60 minutes and later slowed down until equilibrium was reached in 120 minutes. Ahmady-Asbchin et

al., (2008) also revealed that equilibrium uptake of Cu(II) from aqueous solutions by Fucus serratus alga occurred at a contact time of 350 minutes. The difference in the equilibrium times obtained in the various studies is mainly due to the variations in the contributions of external surface binding and intra-particle diffusion to the overall mechanism (Ahmady-Asbchin et al., 2008).

5.7.4 Effect of initial metal concentration

The relation between the biosorptive behavior of the test biosorbents and the initial metal concentration was also studied. As per the results in Fig 5.11, the initial metal concentration also had a huge impact on the biosorption of mercury by the pristine and modified forms of *Cladophora sp* alga.

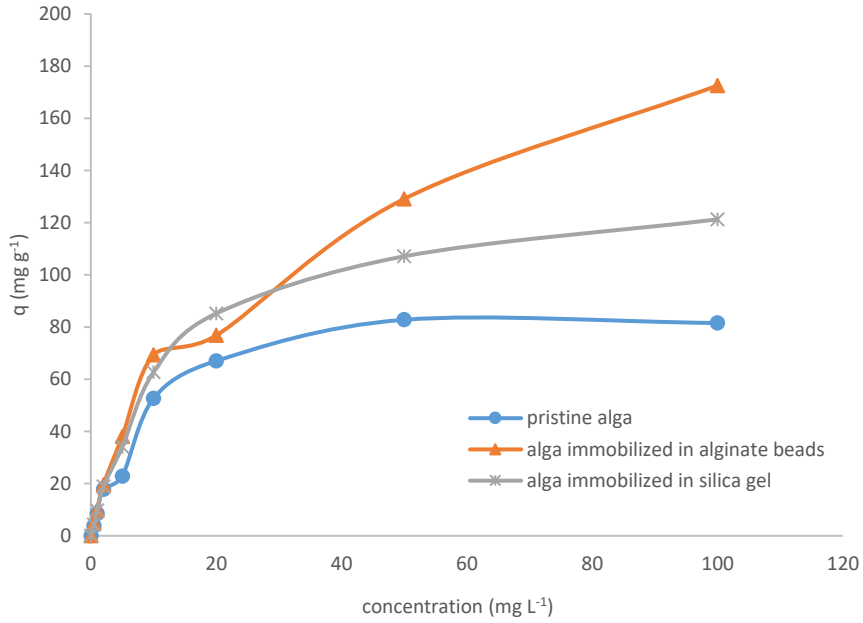

Fig. 5.11: Effect of initial metal concentration on the biosorption of Hg^{2+} by pristine *Cladophora sp* alga, *Cladophora sp* alga immobilized in alginate beads and *Cladophora sp* immobilized in silica gel (Temperature 25˚C, pH 5, biosorbent dosage 10 g L^{-1})

Clearly, increasing the initial metal concentration resulted in the enhancement of the biosorption performance of the biosorbents. This trend can be attributed to higher probabilities of interaction between metal ions and binding sites at higher

metal concentrations (Kumar and Oommen, 2012). Nevertheless, for the pristine alga, a maxima was reached at 50 mg L^{-1} corresponding to the saturation of binding sites on the biosorbent at higher concentrations (Wang et al., 2016). Hence, the optimum initial metal concentration for the biosorption of mercury by pristine alga was set at 50 mg L^{-1}. On the converse, for the modified biosorbents, the increase in metal uptake with increases in initial metal concentration continued up to 100 mg L^{-1}. Therefore, the optimum initial metal concentration for mercury biosorption by *Cladophora sp* alga immobilized in alginate beads and *Cladophora sp* immobilized in silica gel was set at 100 mg L^{-1}. The maximum adsorption capacities of the biosorbents were 82.93, 121.31 and 183.42 mg g^{-1} for the pristine *Cladophora sp* alga, *Cladophora sp* alga immobilized in silica gel and the *Cladophora sp* alga immobilized in alginate beads respectively.

Bayramoglu et al. (2006) also studied the effect of initial metal concentration on the biosorption of Hg (II), Cd (II) and Pb (II) ions using *Chlamydomonas reinhardtii* biomass immobilized in calcium alginate beads. They found that for all the metals studied, increasing the metal concentration in the range 0-100 mg L^{-1} enhanced the biosorption capacity of the biosorbent. Though the equilibrium concentration for all the metals was around 150 mg L^{-1}, the biosorption capacities of the biosorbent were 106.61, 79.70 and 308.70 mg g^{-1} for Hg(II), Cd(II) and Pb(II) respectively. Similarly, Karthikeyan et al., (2007) investigated the effect of increasing the initial metal on the sequestration of Cu from aqueous solutions using *Ulva fasciata* and *Sargassum sp* algae. They found that increasing the initial metal from 2.5 to 70 mg L^{-1} improved the biosorption capacities of both biosorbents. The maximum adsorption capacities were 55 and 60 mg g^{-1} for *Ulva fasciata* and *Sargassum sp* respectively. On the contrary, Abdel-Aty et al., (2013) observed that increasing the initial metal concentration in the range 50-300 mg L^{-1} led to the depreciation in the capacity of *Anabaena sphaerica* alga to remove Cd and Pb from aqueous solutions. These variable results can be attributed to the chemistry of the different metals biosorbed, algal biosorbents and the ranges of concentration studied.

5.7.5 Effect of biosorbent dosage

The results for the effect of biosorbent dosage on the biosorption performances of pristine and modified forms of *Cladophora sp* alga are illustrated in Fig. 5.12.

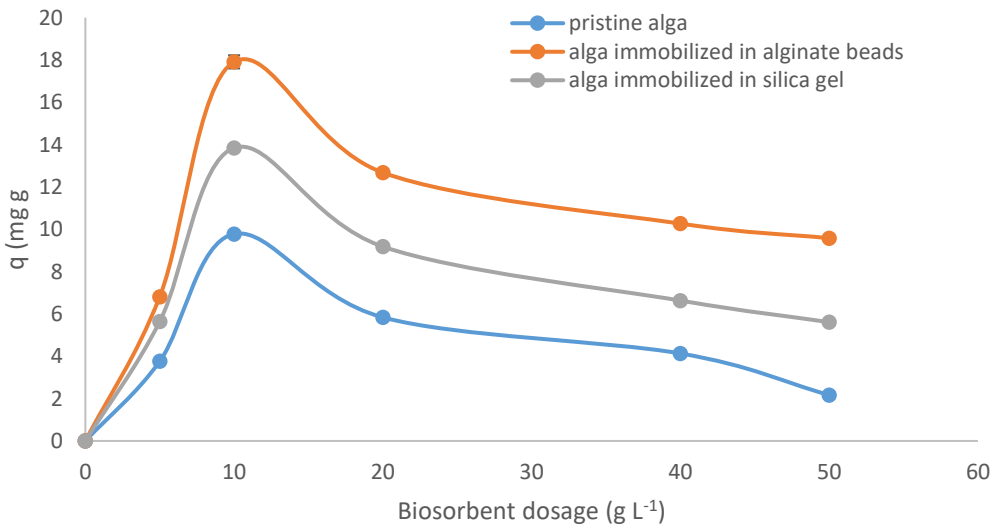

Fig. 5.12: Effect of biosorbent dosage on the biosorption capacity of pristine *Cladophora sp* alga, *Cladophora sp* immobilized in silica gel and *Cladophora sp* immobilized in silica gel for the removal of Hg^{2+} (Temperature 25˚C, initial metal concentration1 mg L^{-1}, pH 5)

From the results, it is evident that the adsorption capacities of the pristine and immobilized forms of *Cladophora sp* alga are influenced by the biosorbent dosage. Increasing the dosage from 5 to 10 g L^{-1} enhanced the adsorption capacities of the algal biosorbents. Nonetheless, further increases in biosorbent dosage led to a decline in the adsorption capacities of all the biosorbents studied. The observed trends are explicable by the aggregation of biosorbent particles at higher dosages thus diminishing the surface area available for interaction with metal ions. Moreover, enhanced inter-particle interaction at higher dosages could have promoted the detachment of some metals that were loosely held to sorption sites (Manohar et al., 2002).

Gupta et al., (2010) also studied the biosorption of Ni(II) from aqueous solution using native and treated *Oedogonium hatei* alga. They found that changing the biomass dosage in the range 0.1 to 1.0 g L^{-1} influenced the biosorption performance of both forms of the alga. Increasing the dosage from 0.1 to 0.7 g L^{-1} improved the biosorption of the algal biosorbents. Further increases in biosorbent dosage had no significant impact on the biosorption performance of both forms of the alga. El-Sikaily et al., (2011) also evaluated the effect of biosorbent dosage on the biosorption of copper by *Pterocladia capillacea*. Their findings revealed that the biosorption capacity of the alga depreciated from 14.5 to 3 mg g^{-1} when the biosorbent dosage was increased from 2 to 15 g L^{-1}. The contradictory results obtained in the different research works are explicable by the use of different biosorbents with dissimilar functional groups and properties of the target metals studied.

5.7.6 Effect of temperature

The effect of temperature on the biosorption capabilities of the test biosorbents was evaluated in the range 16-40˚C and the findings are displayed in Fig. 5.13. As clearly depicted in the figure, the biosorption performances of the biosorbents was affected by temperature in the range studied. Increasing the temperature from 16 to 40˚C led to biosorption capacity of the pristine alga dropping from 37.23 to 12.71 mg g^{-1}. Similarly, the biosorption capacity of the alga immobilized in alginate decreased from 43.87 to 16.13 mg g^{-1} while the biosorption capacity of the alga immobilized depreciated from 39.47 to 17.43 mg g^{-1}. This observed trend indicated that the biosorption of mercury using pristine and modified forms of Cladophora sp alga occurred via an exothermic process. This suggested that the biosorption systems studied would be most effective during the early mornings and night time when temperatures are generally lowest. Al-Homaidan et al., (2014) also investigated the uptake of copper ions by *Spirulina platensis* biomass at different temperatures. Their findings demonstrated that the metal removal efficiency of the algal biosorbent increased from 78.8% to 90.61% when the temperature was increased from 20-37˚C. Further increases in temperature up to 60˚C led to the removal efficiency dropping to 85%. This showed that the biosorption process was endothermic and maximum uptake occurred at 37˚C.

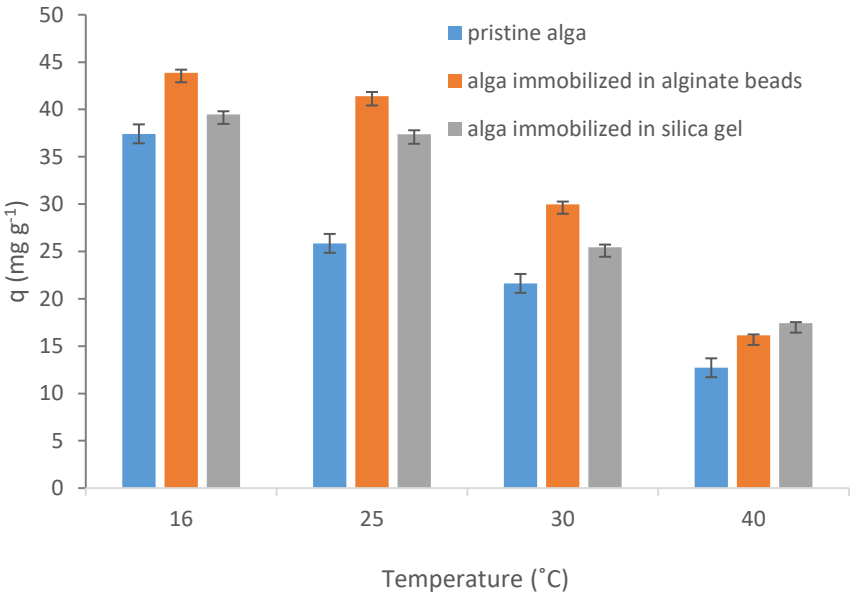

Fig. 5.13: Effect of temperature on the biosorption capacities of pristine *Cladophora sp*, *Cladophora sp* immobilized in alginate beads and *Cladophora sp* immobilized in silica gel

Aksu, (2001) also studied the influence of temperature on the biosorption Cd (II) from aqueous solutions using *Chlorella vulgaris* biomass. The authors found that the biosorption capacity of the alga decreased from 85.3 to 51.2 mg g^{-1} when the temperature was increased from 20 to 50˚C. This suggested that the biosorption process using *Chlorella vulgaris* was exothermic. Hence, from the results of the aforementioned studies it can be deduced that the effect of temperature on biosorption depends on the metal-biosorbent system.

5.7.7 Effect of competing ions

The results for the effect of competing ions on the biosorption of mercury using pristine and modified forms of *Cladophora sp* are summarized in Tables 5.9. Table 5.9 gives a summary of the performance and selectivity parameters for the pristine and modified forms of the alga in unitary and multi-metal solutions.

Table 5.9: Performance and selectivity parameters for the biosorption of Hg^{2+} from multi-metal solutions using pristine and modified forms of *Cladophora sp* alga

	Pristine alga		Alga immobilized in alginate beads		Alga immobilized in silica gel	
	q (mg g^{-1})	K_D (L g^{-1})	q (mg g^{-1})	K_D (L g^{-1})	q (mg g^{-1})	K_D (L g^{-1})
Cd^{2+}	2.84	3.97	2.21	2.83	2.64	3.59
Co^{2+}	4.41	7.90	3.09	4.32	3.73	5.94
Cu^{2+}	4.94	9.76	4.34	7.65	4.71	8.90
Fe^{3+}	4.23	7.48	3.56	5.55	3.93	6.46
Hg^{2+}	5.82	13.89	6.86	20.01	5.84	14.88
* Hg^{2+}	8.95	85.61	8.99	89.70	8.97	86.88
Ni^{2+}	4.79	9.19	4.03	6.75	4.28	7.49
Pb^{2+}	5.47	12.06	4.98	9.91	5.21	10.89

* Shows the performance and selectivity parameters for Hg^{2+} in unitary solution

As per the results in Table 5.9, the presence of competing ions cations negatively impacted the biosorption performance of pristine and modified forms of *Cladophora sp* alga. The adsorption capacity of the pristine alga for mercury reduced from 8.95 mg g^{-1} in the unitary solution to 5.82 mg g^{-1} in the multi-elemental solution. This was mainly due to the competition among the metal ions for the fixed number of binding sites available on the biosorbents (Singh et al., 2007; Sheng et al., 2007). The K_D value for mercury also dropped from 85.61 L g^{-1} in the unitary solution to 13.89 L g^{-1} in the multi-metal solution. It was also observed that the K_D and, q values for mercury in the multi-metal solution were higher than those for other metal components. This signified that pristine *Cladophora sp* alga was more selective for mercury over all the other metal components of the solution.

The results in Table 5.9 also showed that the biosorption capability of *Cladophora* was also affected by the presence of competing ions in solution. The adsorption capacity of the biosorbent decreased from 8.99 mg g^{-1} in the single-metal solution to 6.86 mg g^{-1} in the multi-elemental solution. This observation was also a

consequence of the metal ions in solution competing for sites on the biosorbent surface.

The K_D value for mercury using this biosorbent also declined from 89.70 L g^{-1} in the unitary solution to 20.01 L g^{-1} in the solution containing competing metal ions. As in the case of the pristine alga, the K_D and q values for the target metal ion were higher than those of the competing ions thus showing that *Cladophora sp* alga immobilized in alginate beads was more selective for mercury than the other metals. The K_D values for mercury using this biosorbent were also higher than those obtained using the pristine alga. This showed that the *Cladophora sp* alga immobilized in alginate beads was more selective for mercury than pristine *Cladophora sp* alga.

The findings in Table 5.9 also demonstrate that the adsorption capacity of *Cladophora sp* alga immobilized in silica gel reduced from 8.97 mg g^{-1} in the unitary solution to 5.84 mg g^{-1} in the multi-metal solution. The value of K_D for mercury also dropped from 86.88 to 14.88 L g^{-1} under the same circumstances. Comparison of the K_D and q values for mercury with those of the other ions in the multi-metal solution also showed that *Cladophora sp* alga immobilized in silica gel was more selective for mercury over the competing ions. Albeit, the K_D values for the alga immobilized in silica gel were higher than those of the pristine alga, they were lower than those of the alga immobilized in alginate beads. Hence, the selectivity of the test biosorbents followed the order pristine alga < alga immobilized in silica gel < alga immobilized in alginate beads.

A comparison of the values of q and K_D values for mercury using the pristine alga and modified biosorbents also showed that those of the latter far exceeded those of the pristine alga in both unitary and multi-metal solutions. This indicated that under the conditions studied, immobilization not only enhanced the biosorption capacity of the alga but also improved selectivity towards mercury.

Notwithstanding, for all biosorbents studied, the affinities for the metal ions in solution followed the order $Hg^{2+} > Pb^{2+} > Cu^{2+} > Fe^{3+} > Co^{2+} > Cd^{2+}$. The differences in affinities of the metal ions was attributed to varying ionic radii, electronegativities and redox potentials (Donmez et al., 1999, Mishra et al., 2016).

Moreover, Cd and Co often only bind to one type of ligand (amine) on the biosorbent surface while Hg and Pb are able to bind to a variety of the functional groups on the biosorbent surfaces (Mishra et al., 2016).

Sheng et al., (2007) also evaluated the uptake of Pb, Cu and Cd in single component and ternary aqueous solutions using *Sargassum sp* alga. They revealed that the biosorption capacities of the metals in the unitary solution were 1.16, 1.07 and 0.76 mmol g^{-1} for Pb, Cu and Cd respectively. However, in the solution containing all three metals, the biosorption capacities dropped to 0.87, 0.29 and 0.12 mmol g^{-1} respectively. This showed that the presence of competing ions also had an antagonistic effect on metal removal using *Sargassum sp* alga. However, the degree of the impact was dependent on the metal species studied. The extent of the impact was also lower than that observed for the *Cladophora sp* alga based biosorbents used in this study.

Fan et al., (2008) also assessed the effect of competing ions on the biosorption of Cd, Zn and Pb by *Penicillium Simplicissimum*. They revealed that the biosorption capacities of metals in the mono-metal solution were 21.50, 25.54 and 30.37 mg g^{-1} for Cd, Zn and Pb respectively. These values decreased to 6.94, 18.72 and 13.38 respectively in the multi-metal solution thus showing that Cd was the least affected followed by Zn and then Pb. The results from the various studies showed that the effect of competing ions on biosorption of a specific metal differs with respect to properties of the metal studied and surface properties of the algal biosorbents used.

5.7.8 Reusability studies

In order to effectively use algal based biosorption systems in industrial applications, it is essential to study the reusability of the biosorbents (Gupta and Rastogi, 2008). Hence, the reusability of the pristine and modified forms of Cladophora sp alga were evaluated and the results are illustrated in sections 5.8.8.1 and 5.8.8.2 below.

5.7.8.1 Selection of the suitable desorption medium

The results for the evaluation of the eluting capabilities of 0.1 M HCl, 0.1 M HNO_3 and 0.1 M NaCl in removing bound mercury from the surfaces of the pristine alga, alga immobilized in alginate beads and alga immobilized in silica gel are illustrated in Fig. 5.14.

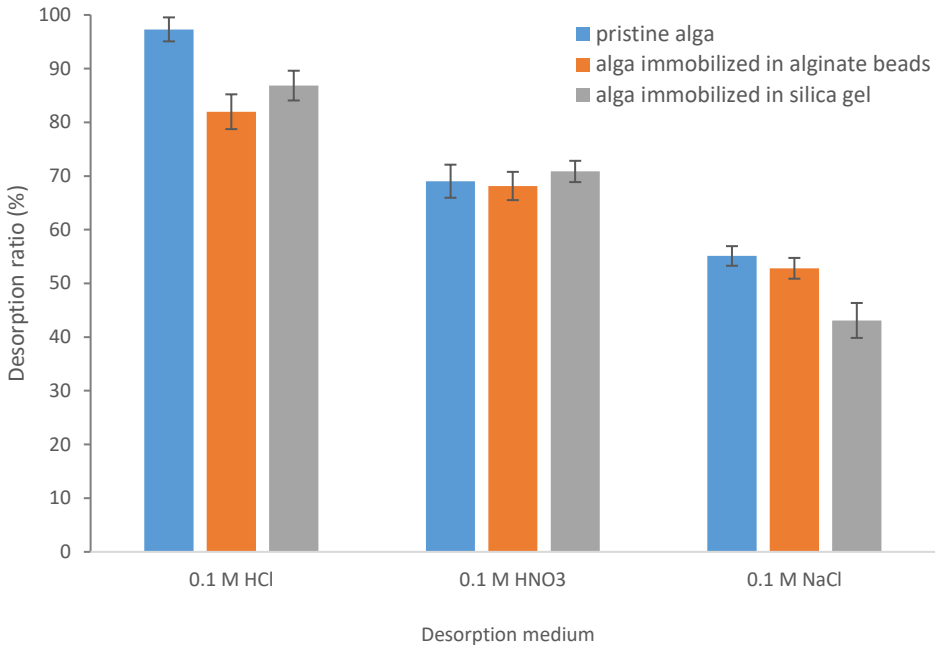

Fig. 5.14: Regenerability of pristine and modified forms of *Cladophora sp* alga using different desorption media

According to these findings, for all the biosorbents studied, the mineral acids had a higher eluting power than NaCl. This was attributed to the lowering of pH thus leading to desorption of mercury from the biosorbent surfaces (Ferraz et al., 2004). Nonetheless, among the acid eluents, 0.1 M HCl had the highest desorption ratio because mercuric ions have a higher affinity for Cl^- than NO_3^-. Hence, under the conditions studied, 0.1 M HCl desorbed 97.81, 81.97 and 86.84 % of the mercury biosorbed by pristine alga, alga immobilized in alginate beads and alga immobilized in silica gel, respectively. Therefore, subsequent regeneration and recycling was performed using 0.1 M HCl as the desorption medium for all the test biosorbents. Hence, it was used for the regeneration of the biosorbents in subsequent experiments.

Similarly, Li et al., (2015) investigated the desorption of Uranium(VI) from amidoxine modified *Aspergillus niger* using 5 different media i.e. 0.1 M HCl, HNO_3, NaOH, Na_2CO_3 and EDTA-Na. They also found that 0.1 M HCl was the

best desorption and effectively removed 94.67% of uranium ions bound to the surface of the biosorbent. However, this value was slightly lower than that removed from pristine *Cladophora sp* alga in the current study (97.31%). On the contrary, Gupta and Rastogi, (2008) studied the biosorption of Cr(VI) from aqueous solutions using *Nostoc muscorum* alga. They also evaluated the capabilities of 10 eluting agents (0.1M HCl, 0.1 M HNO_3, 0.1 M H_2SO_4, 0.2 M $CaCl_2$, 0.2 M $MgCl_2$, 0.5 M KOH, 0.1M NaOH and 0.1M EDTA) in removing the biosorbed metal ions from the algal surface. Their findings revealed that 0.1 M EDTA and 0.1 M HNO_3 had the highest eluting powers. Chojnacka et al., (2005) also investigated the potential of using 0.1 M EDTA, 0.1M HNO_3 and deionized water as eluents for desorbing Cr and Cd from Spirulina sp alga. They deduced that 0.1 M HNO_3 was most effective and removed 93% of the biosorbed metal ions while 0.1 M EDTA removed only 53% of the bound metal ions. The contradictory findings reported in these studies are mainly due to the differences in the surface characteristics of the biosorbents used and the metals studied.

5.7.8.2 Recycling and reuse of the biosorbents

The recyclability and reuse of the biosorbents was assessed for 3 successive adsorption-desorption cycles using 0.1 M HCl as the eluting agent. The results for the reusability of the pristine and modified forms of the alga are illustrated in Fig 5.15. It is clear from this figure that the removal efficiency of pristine *Cladophora sp* alga remained over 90% after the first cycle and dropped to 80% after completion of the second cycle. The removal efficiency decreased even further to 67% after the third cycle. This showed that even though the performance of the alga decreased with increasing number of cycles, the alga still had a reasonable removal efficiency after 3 consecutive cycles. Fig. 5.15 also demonstrated that the desorption behavior of the alga immobilized in alginate beads differed slightly from that observed for the pristine alga. First, the removal efficiency of the alga immobilized in alginate beads was enhanced after completion of the first adsorption-desorption cycle. This was attributed to the fact that the acidic medium was able to remove the contaminants adhered to the binding sites on the biosorbent thus freeing them for mercury binding (Abu-Al Rub et al., 2004). Moreover, after completion of the first cycle, there was a gradual reduction in the efficiency of the biosorbent with

increases in the number of adsorption-desorption cycles. In fact, *Cladophora sp* alga immobilized in alginate beads retained an efficiency greater than 80% even after 3 cycles.

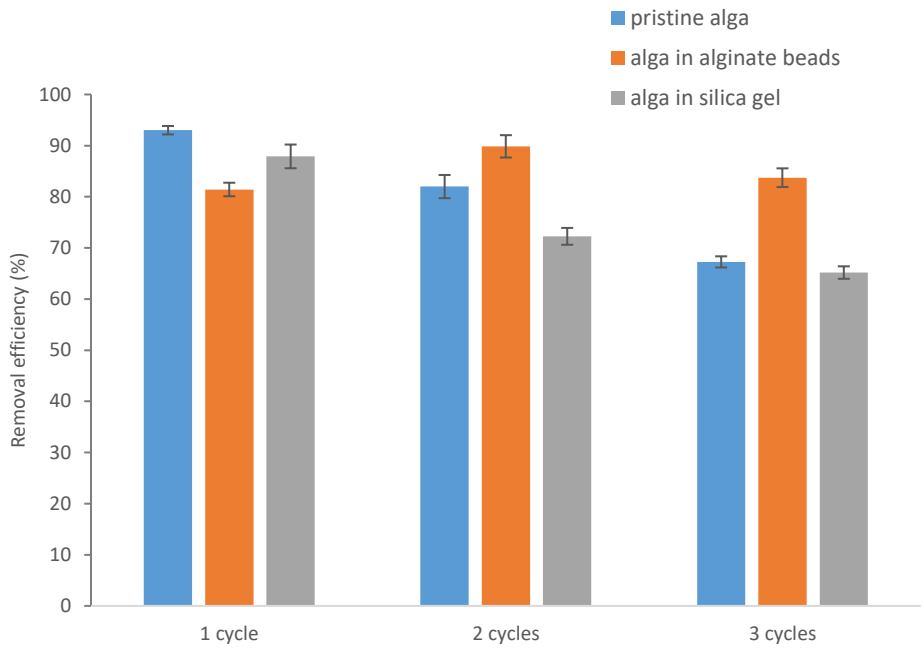

Fig. 5.15: Reusability of pristine and modified forms of *Cladophora sp* alga (Eluent 0.1 M HCl, Temperature 25˚C, initial metal concentration 1 mg L^{-1}, pH 5, biosorbent dosage 10 g L^{-1})

On the other hand, reusability of the alga immobilized in silica gel displayed a trend similar to the one observed for the pristine alga. The removal efficiency of the alga immobilized in silica gel depreciated to 87.89% after the first cycle then 72.26 % after 2 cycles before finally dropping to 65.18% in the third cycle. Thus, it can be resolved that all the biosorbents under study could be re-used repeatedly for up to three cycles to remove mercury from aqueous solutions without significant deterioration in their biosorption capabilities.

Tuzun et al., (2005) also investigated the reusability of *Chlamydomonas reinhardtii* alga for biosorption of Hg(II), Pb(II) and Cd(II) after regeneration with 0.1 M HCl.

They found that the acid could remove upto 80% of the metal biosorbed onto the biosorbent surface. However, recyclability studies revealed that the adsorption capacity of the alga dropped to around 20% after 6 consecutive adsorption-desorption cycles thus showing that the acid had a negative impact on the binding sites on the biosorbent. Kapoor et al., (1999) also evaluated the reusability of *Aspergillus niger* for the removal Cd and Cu from aqueous solutions. They found that the biosorbent could be reused upto five cycles after regeneration with 0.05 N HNO_3. The biosorption capacity of the biomass dropped by 50% after the first cycle; but, it remained constant thereafter.

5. 8 Speciation studies

Speciation studies were conducted to determine the proportion of the mercury biosorbed by the pristine alga that is converted to the toxic species MeHg. The results are illustrated in Table 5.12.

Table 5.10: Hg_{total} and MeHg concentrations in pristine *Cladophora sp* alga before and after metal biosorption (Temperature 25˚C, initial metal concentration 1 mg $L^{-1,}$ pH 5, biosorbent dosage 10 g L^{-1}, agitation time =20 minutes)

Biosorbent	Concentration (mg L^{-1})
Hg_{total} in pristine *Cladophora sp* alga (before biosorption)	0.068 +/- 0.008
MeHg in pristine *Cladophora sp* alga (before biosorption)	0.004 +/- 0.001
Hg_{total} in pristine *Cladophora sp* alga (after biosorption)	1.043 +/- 0.296
MeHg in pristine *Cladophora sp* alga after (biosorption)	0.033 +/-0.002

The findings revealed that prior to exposure to mercury solutions, the total mercury content in the alga was 68 ± 8 μg L^{-1}. Of this quantity, only 4 ± 1 μg L^{-1} was MeHg thus showing that of all the mercury originally present in the alga, only 5.88% was MeHg. After biosorption, the levels of total mercury in the alga increased to 1.04 ± 0.30 mg L^{-1} while the concentration of MeHg in the alga rose to 33±2 μg L^{-1}. This

signified that of all the mercury adsorbed by the alga, only 2.78% was converted to MeHg. The ratio of Hg_{total} to MeHg in the alga also decreased from 5.88 to 3.16%. From these results, the adsorption capacities of the alga for inorganic mercury and MeHg were 9.461 mg g^{-1} and 0.29 mg g^{-1} respectively. Though these results might suggest that only a small fraction of the mercury bound by pristine *Cladophora sp* is MeHg, this value is still significant because it can be biomagnified to high values in food webs.

Bravo et al., (2014) also traced the speciation and transformation of mercury in *Chlamydomonas reinhardtii* during biosorption using isotope-specific mercury solutions after biosorption. They found that exposing the alga to mercury for 48 hours resulted in the total mercury concentration increasing. However, contrary to the results observed in the current study, they observed that the ratio of inorganic mercury to MeHg increased from 0.25 ± 0.01 to 1.70 ± 0.1 pM after biosorption. Gokhale et al., (2009) also investigated the speciation of Cr adsorbed from aqueous solution using *Spirulina platensis sp* alga immobilized in alginate beads. They revealed that the biosorbent had a higher biosorbent capacity for Cr (III) than Cr(VI). The proportion of Cr(VI) converted to Cr(III) during the process was also lower than 12%. These findings also deviated from those for the mercury-*Cladophora sp* system used in the present study mainly because of metals studied. The variations in the results obtained could be due to the in inherent characteristics of the algae used and experimental conditions.

5.9 Mechanistic studies

According to the author's knowledge, no research works in the literature report the evaluation of the mechanism for the biosorption of mercury by *Cladophora sp* alga. Hence, mechanistic studies were conducted using different techniques to elucidate the mechanism of biosorption of mercury onto the surfaces of pristine and modified forms of *Cladophora sp* alga. The results are shown in the subsections below.

5.9.1 FTIR analysis

FTIR spectroscopy is one of the most powerful tools for elucidating the mechanism of biosorption and identifying the functional groups responsible for metal biosorption (Abdi and Kazemi, 2015; Figueira et al., 1999). The FTIR spectra of

the pristine alga, alga immobilized in alginate beads and alga immobilized in silica gel before and after metal binding were compared to determine the functional groups responsible for mercury biosorption. Fig 5.16 below gives the FTIR spectra of pristine *Cladophora sp* alga before and after mercury binding.

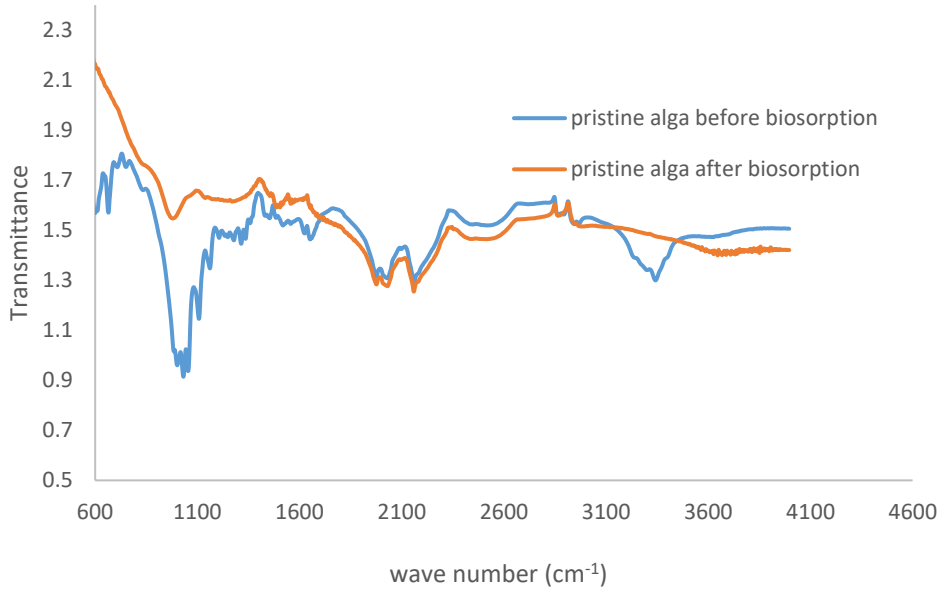

Fig. 5.16: FTIR spectra for pristine *Cladophora sp* alga before and after mercury biosorption

It is clear from the figure that the peak due to –NH and –OH (3340 cm^{-1}) was suppressed in the spectrum of the mercury-loaded alga. This showed that these functional groups are major contributors to the biosorption mechanism. Likewise, the intensity of the band due to the carboxyl group (1652 cm^{-1}) also diminished and shifted to 1699 cm^{-1} showing the group's participation in the biosorption process. The peak due to the sulfonate group (1049 cm^{-1}) also became less intense showing its involvement in the mechanism for mercury biosorption. The changes in the intensities of the peaks due to the amine, hydroxyl and sulfonate groups far exceeded those observed for the carboxyl group. This suggested that that the amine, hydroxyl and sulfonate groups played a more signicant role in the biosorption mechanism compared to the carboxyl functional group.

Earlier work by Mata et al., (2008) also reported the use of FTIR analysis for evaluating the mechanism of biosorption of Cd, Pb and Cu using *Fucus vesiculosis*. The FTIR spectra obtained revealed that the most apparent change due to metal biosorption was the shifting of the peaks due to the carboxyl group from 1625 to 1618 cm^{-1}. This signified the major involvement of the functional group in the biosorption of the heavy metals by *Fucus vesiculosis*. Mishra et al., (2016) also revealed that the biosorption of Ni (II) and Cr(VI) onto the surface of modified *Hydrilla reticulata* altered its FTIR spectra. The bands at 3393 and 1646 cm^{-1} shifted to 3411 and 1646 cm^{-1} , respectively thus signifying the involvement of amine and hydroxyl functional groups in the biosorption of the metal ions. Raize et al., (2004) also reported the biosorption of heavy metals using *Sargassum vulgaris* alga. FTIR analysis of the alga before and after metal binding showed the significance of amine and carboxyl functional groups in the biosorption process. The differing findings between studies are mainly due to the variations in the chemical composition of the algal biosorbent used and the properties of the target metals (Abdi and Kazemi, 2015).

The results for the FTIR analysis of *Cladophora sp* alga immobilized in alginate beads are also shown in Fig. 5.17. The biosorption of mercury onto *Cladophora sp* alga immobilized on alginate beads also altered the FTIR spectrum of the biosorbent. Mercury binding onto the biosorbent resulted in the suppression of the peak at 3408 cm^{-1} and the depreciation in the intensities of the bands at 1606 and 1409 cm^{-1}. This suggested that the –OH, -NH and –C=O groups were major contributors in the mechanism for the biosorption of mercury onto *Cladophora sp* alga immobilized in alginate beads. The most significant change brought forth by the binding of mercury onto this biosorbent was the reappearance of the peak at 2356 cm^{-1} due to the –CH group in alginate (Daemi and Barikani, 2012). This was explicable by the fact that during metal binding, mercury which has a higher affinity for nitrogen-containing groups replaced the –C-O-C- functional group which previously interacted with the amine group thus resulting in the formation of a new –CH bond (Daemi and Barikani, 2012).

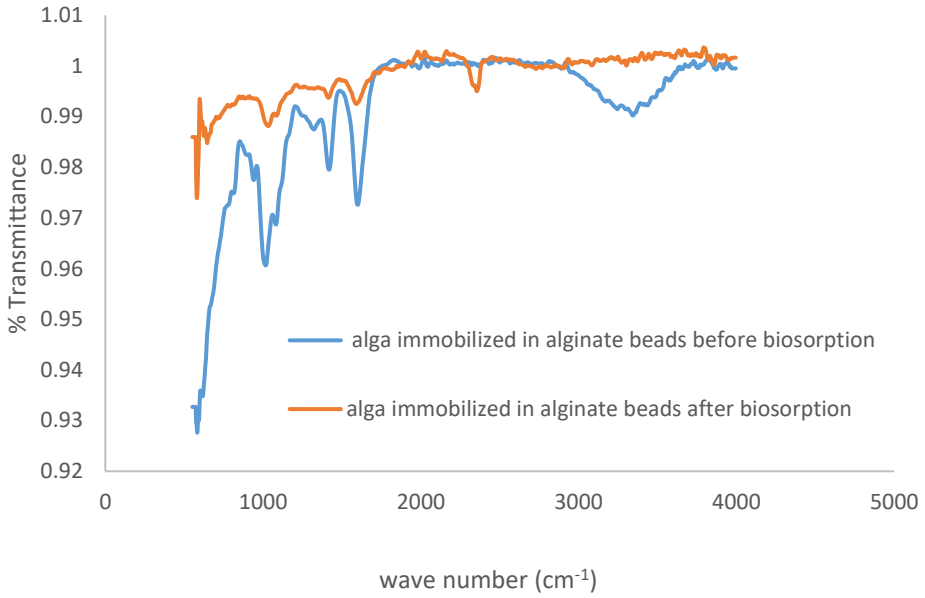

Fig. 5.17: FTIR spectra for *Cladophora sp* alga immobilized in alginate beads before and after biosorption of mercury

Mata et al., (2009) also investigated the mechanism for the biosorption of Cd, Pb and Cu using *Fucus vesiculosus* alga immobilized in calcium alginate xerogels. Through FTIR analysis, they discovered that the major functional groups participating in the biosorption process were carboxyl and hydroxyl. In addition, the contribution of the hydroxyl group to the mechanism was highest in case of Pb than Cd and Cu. Bishnoi et al., (2009) also utilized FTIR analysis to study the process for the sequestration of Cr(VI) from aqueous solution by *Trichoderma viride* biomass immobilized in alginate beads. They observed that the peaks corresponding to the amine, hydroxyl and carboxyl groups shifted during metal binding thus indicating their involvement in the biosorption mechanism.

The FTIR spectra for the alga immobilized in silica gel are also illustrated in Fig. 5.18. Mercury binding onto the alga immobilized in silica gel resulted in in the suppression of the peaks at 3010, 1739, 1367 and 1217 cm^{-1} thus implying that the –OH, -NH, Si-O- and –C=O- participated in the process for the biosorption of mercury by this biosorbent. The most conspicuous indication of mercury

biosorption onto the surface of *Cladophora sp* immobilized in silica gel was the appearance of a new peak at 1066 cm^{-1}.

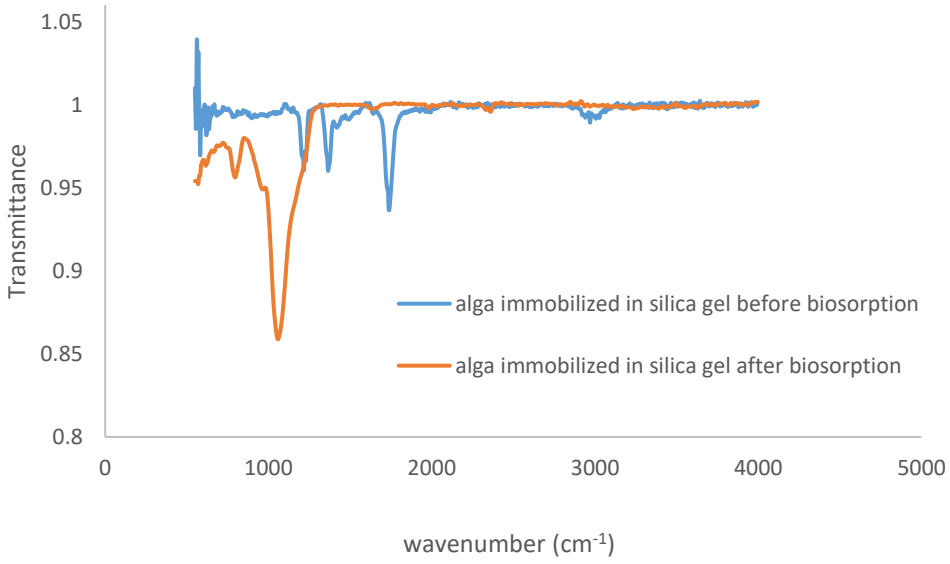

Fig. 5.18: FTIR spectra for *Cladophora sp* alga immobilized in silica gel before and after mercury biosorption

This was attributed to the reappearance of the Si-OH group in silica gel due to loss of interaction of Si-O- with the amine group (Akar et al., 2009). This observation provided additional proof that the –NH group is one of the major contributors towards the biosorption of mercury from aqueous solutions by *Cladophora sp* alga immobilized in silica gel.

Akar et al., (2009) immobilized *Phaseolus vulgaris L* biomass in silica gel and utilized the resultant biosorption for retrieval of Ni (II) from aqueous solutions. Inspection of the FTIR spectra of the biosorbent before and after metal biosorption revealed that the intensities of the bands due to the amine, hydroxyl and carboxyl groups diminished during biosorption. This indicated that these functional groups participated in the biosorption mechanism. New peaks due to the interactions of the metal ions with sulfur groups were also observed at 800, 570 and 578 cm^{-1}. The slight disparities between the results reported by Akar et al., (2009) and those found in the present work can also be explicable by the complexity of the structural and

functional properties of the different biosorbents used. The varying contribution of functional groups is also due to their accessibility and affinities for the target metals (Abdi and Kazemi, 2015).

5.9.2 SEM-EDX analysis

SEM-EDX was used to assess effect of metal binding on the morphologies and elemental compositions of the test biosorbents. The results are illustrated in sections 5.9.2.1 and 5.9.2. 2, respectively.

5.9.2.1 Evaluation of the morphologies of the biosorbents before and after mercury biosorption

The surface morphologies of the pristine and modified forms of *Cladophora sp* before and after mercury binding were studied to gain insight on the mechanism and the results are depicted in Figs. 5.19-5.21. Fig. 5.19 illustrates the morphology of the pristine alga before and after exposure to mercury.

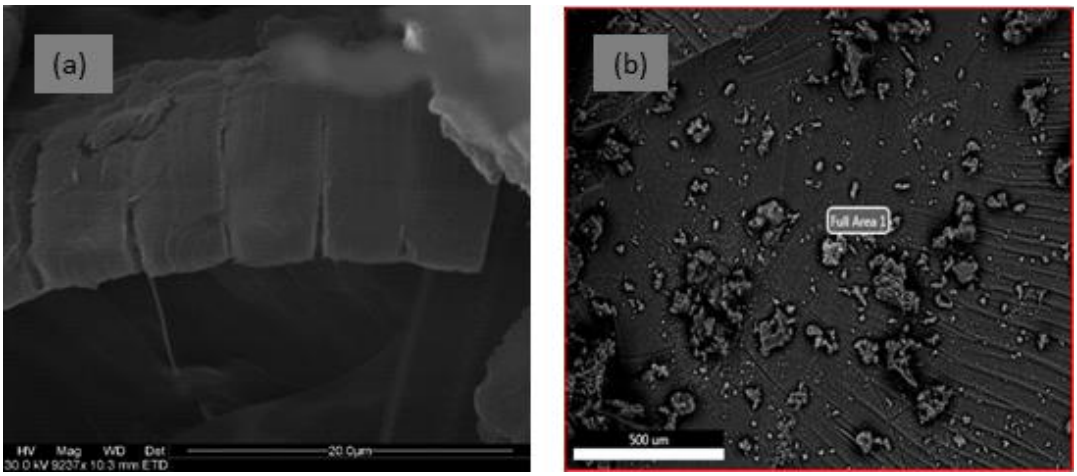

Fig. 5.19: SEM micrographs showing the morphology of pristine *Cladophora sp* alga before (a) and (b) after mercury biosorption (Magnification: X9273)

It is clear from Fig. 5.19 that there is dissimilarity between the morphologies of the pristine alga before and after mercury binding. The algal filaments started off smooth with a well-defined morphology. After biosorption, the surface of the biosorbent became rough and heterogeneous indicative of mercury exposure.

Particle and crystalline-like depositions were also observed on the surface of the alga. These observations provided confirmation that indeed mercury had adsorbed onto the surface of the pristine alga.

The surface morphologies of *Cladophora sp* alga immobilized in alginate beads before and after metal biosorption (Fig. 5.20) demonstrate that the surface of the bisorbent started off as a detailed 3-D network with a few cracks. However, mercury biosorption resulted in the biosorbent becoming more distorted and less structured. Uneven distribution of particular deposits in the pores and surface of the biosorbent also gave proof that mercury biosorption had occurred.

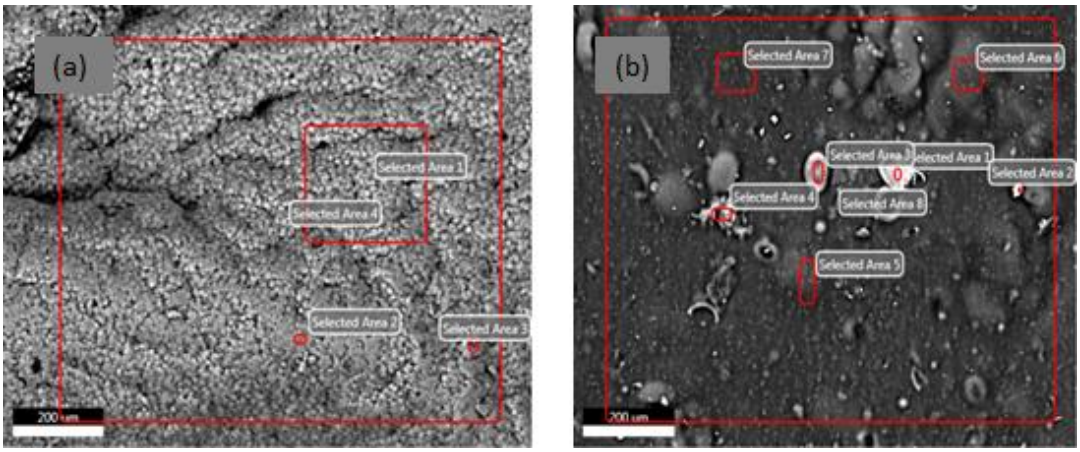

Fig. 5.20: SEM micrograph of *Cladophora sp* alga immobilized in alginate beads (a) before and (b) after mercury biosorption (Magnification: X300)

Fig. 5.21 presents the surface morphologies of *Cladophora sp* alga immobilized in silica gel before and after mercury biosorption. According to Fig. 5.21, the surface of the alga immobilized in silica gel was originally organized and comprised of algal filaments attached to the surface of silica. After mercury binding, the surface became rugged and showed an irregular distribution of particle and crystalline deposits adhered to it. These changes in morphology were attributed to exposure of the biosorbent surface to mercury. The distortion of the surfaces of the pristine and modified forms of *Cladophora sp* alga and the uneven distribution of particles on the biosorbent surfaces after mercury biosorption reveal that surface binding

contributed to the overall biosorption process (Das et al., 2007). The participation of surface binding as a mechanism is also supported by the rapid metal uptake kinetics observed for all three biosorbents. However, the relatively low values of BET surface areas of the biosorbents reported with respect to their adsorption capacities indicate that surface binding occurs in combination with other mechanisms.

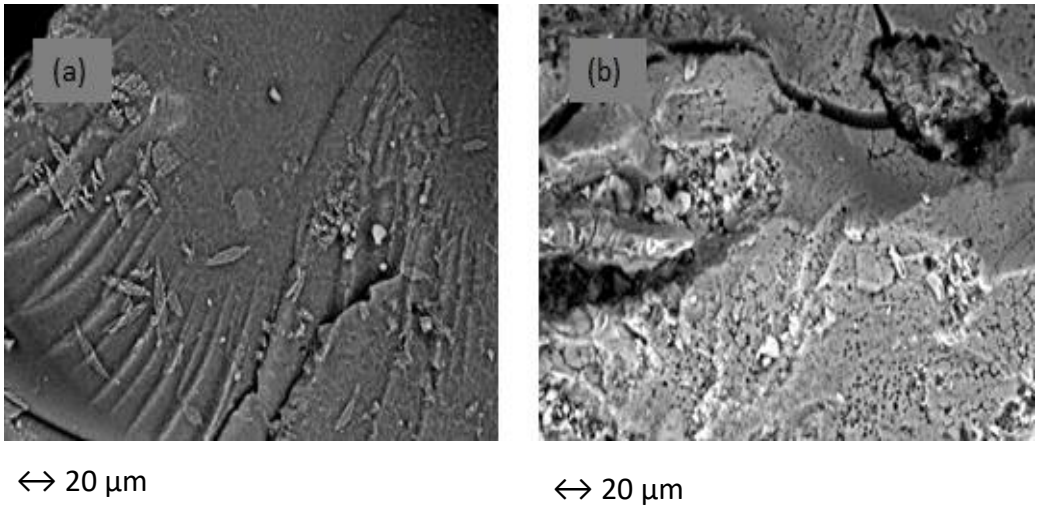

Fig.5.21: SEM micrographs of *Cladophora sp* alga immobilized in silica gel (a) before and (b) after mercury biosorption (Magnification: X300)

5.9.2.2 EDX elemental analysis of the pristine and modified forms of Cladophora sp alga before and after metal biosorption

EDX spectroscopy was used to investigate the effects of mercury biosorption on the elemental composition of the test biosorbents and verify that metal ions had bound to their surface. The results are presented in Tables 5.13, 5.14 and 5.15. Table 5.13 gives a summary of the elemental composition of pristine *Cladophora sp* alga before and after mercury biosorption. According to the findings in Table 5.13, mercury biosorption altered the elemental composition of the pristine alga. The most significant change in the elemental composition of the alga after biosorption was the presence of Hg (2.33%) which was previously absent in the control alga. This observation provided further verification that indeed mercury had bound to the

surface of the alga. The EDX data also revealed that the percent compositions of the alkali metals in the pristine alga dropped from their original values to undetectable levels after metal biosorption. This suggested that the ions of these metals exchanges with mercury during biosorption. However, the change in the percent elemental composition of mercury was not equivalent to the sum of the changes in percent compositions of the metal ions released into the solution. This implied that ion exchange was not the only mechanism contributing to the overall biosorption process. The changes in the compositions of S, O, N and P observed during biosorption also implied that they also contributed to the overall process

Table 5.11: EDX Elemental composition of pristine *Cladophora sp* alga before and after mercury biosorption (pH 5, agitation time 20 minutes, initial metal concentration 1 mg L^{-1}, biosorbent dosage 10 g L^{-1}, temperature 25˚C)

Element	Composition (%)	
	Before biosorption	After biosorption
C	51.81	46.70
O	31.40	29.71
N	9.80	14.62
P	0.69	1.03
S	2.17	3.78
Cl	1.88	1.86
K	0.35	undetected
Ca	1.06	undetected
Mg	0.74	undetected
Hg	undetected	2.33

These elements are components of the amine, carboxyl, sulfonate and phosphate functional groups which are known to be responsible for the binding of metals by algae (Abdi and Kazemi, 2015; Prakasham et al., 1999; Mehta et al., 2002). It is

possible that mercury interacts with these functional groups on the surface of the biosorbents during metal binding and alters their configuration which in turn affects the interaction of the atoms with the electron beam used for analysis. These results agree in part to those obtained for FTIR analysis which showed the participation of the amine and carboxyl functional groups in the biosorption mechanism. The findings also offer additional information on the contribution of the phosphate groups which was not apparent in the FTIR spectra analysis.

Equations 5.1, 5.2 and 5.3 give possible interactions of mercury with the amine, carboxyl, sulfonate and hydroxyl functional groups respectively

$$R - NH_2 + Hg^{2+} \rightarrow R - NH_2Hg \quad (5.1)$$

$$R - COOH + Hg^{2+} \rightarrow R - COO - Hg \quad (5.2)$$

$$R - SO_3 + Hg^{2+} \rightarrow R - SO_2Hg \quad (5.3)$$

where R represents other molecular components of the functional groups in the algal-based biosorbents.

Ahmady-Asbchin et al., (2012) also reported the use of EDX spectroscopy for the evaluation of the elemental composition of *Sargassum angustifolium* alga before and after Cu(II) biosorption. The authors deduced that the most obvious change resulting from metal binding was the appearance of a 10% elemental composition for Cu(II) which was absent in the native alga. Aside from that, high values of compositional change were observed for Ca and Mg due to their participation in the ion exchange mechanism. Still, the change reported for Mg was lower for this alga compared to that observed for *Cladophora sp* alga. High compositional changes were also observed for N and S showing that the amine and sulfonate functional groups contributed significantly to the mechanism for biosorption of Cu(II) by *Sargassum angustifolium*. The variation in the results obtained in the aforementioned studies are explicable to the different chemical compositions of the algal biosorbents studied and the varying metal-biosorbent interactions during biosorption.

Similarly, Table 5.14 gives a summary of the major elemental components of *Cladophora sp* alga immobilized in alginate beads before and after mercury

binding. According to these findings, the major elemental components of the alga immobilized in alginate beads are C (44.80%) and O (38.61%). This is explicable by the abundance of carboxyl groups in the alginate component of the biosorbent. As in the case of the pristine alga, the percent elemental composition of the alga immobilized in alginate beads also changed after exposure to mercury. Firstly, the elemental composition of the biosorbent after biosorption shows the presence of Hg (3.30%) which was previously absent. This gave a clear indication that mercury had been biosorbed onto the surface of the alga immobilized in alginate beads. In addition, as observed with the pristine alga, the proportion of Al, Ca, K, Mg and Na dropped to very low levels after biosorption thus suggesting that ion exchange was a contributory mechanism to the overall process.

Table 5.12: EDX elemental composition of *Cladophora sp* alga immobilized in alginate beads before and after mercury biosorption

Element	Composition (%)	
	Before biosorption	After biosorption
C	44.80	38.61
O	47.73	40.72
Na	0.81	0.30
Al	0.41	undetected
S	0.23	0.51
K	0.31	undetected
Ca	6.22	3.10
Mg	0.33	undetected
Cl	0.00	0.21
Hg	undetected	3.30

Large changes in the compositions of C and O were also observed thus implying that mercury biosorption altered the configuration of the carboxyl groups in the biosorbent. This affected their interactions with the electron beam used during

analysis. The interactions of the functional groups are also most likely to occur via the pathway shown in equation 1. This observation is congruent with the FTIR analysis results which demonstrated shifts and diminution in intensities of the peaks corresponding to the carboxyl group after biosorption. The EDX results obtained were unable to show the participation of the amine groups in the biosorption process.

Wang et al., (2016b) synthesized biosorbents for biosorption of Cu and Pb from aqueous solutions by immobilizing *Laminaria digitata* in alginate beads. Analysis of the resultant biosorbents using EDX spectroscopy revealed their complexity. The major components of the biosorbents were C and O corresponding to the abundant carboxyl groups in the alginate polymeric support. High proportions of light metals such as Na, K and Ca were also observed. The presence of N and S in the biosorbents was also attributed to the presence of amine and sulfonate functional groups. As expected, metal binding changed the composition of the biosorbent. First, the appearance of a new peak due to Cu provided proof of metal biosorption. The diminution of the peaks due to Al, Na, K and Ca also revealed their participation in the ion exchange mechanism. The EDX spectra also showed the major contribution of S in the biosorption process. Nonetheless, the results differed from those obtained for the biosorption of *Cladophora sp* immobilized in alginate beads in that they did not provide proof for the involvement of the carboxyl group in metal biosorption. The dissimilarity between the findings reported by Wang et al., (2016) and those found in the current study show that the mechanism for biosorption of metals by algal-based biosorbents is complex and varies between algal-metal biosorption systems.

The elemental composition of *Cladophora sp* immobilized in silica gel before and after mercury biosorption was also investigated and the results are summarized in Table 5.13. The findings illustrated that the major elemental components of the biosorbent were S and O from the SiO_2 polymeric support. However, as in the case of the other two biosorbents, the elemental composition of the alga immobilized in silica gel also changed after mercury biosorption. The major change in the composition was the occurrence of (2.82%) mercury after biosorption which was not present in the control biosorbent. As expected, the elemental compositions of

Al and K also dropped after mercury biosorption due to the metals exchanging with the mercury in solution.

Table 5.13: EDX elemental composition of *Cladophora sp* alga immobilized in silica gel before and after mercury biosorption

Element	Composition (%)	
	Before biosorption	After biosorption
C	9.70	8.21
O	55.42	50.60
Si	34.13	24.11
P	0.82	0.31
K	4.61	2.60
Al	1.62	0.41
Hg	undetected	2.82

The elemental compositions of C, O and Si also changed suggesting the participation of Si in the biosorption mechanism and alteration of the configuration of the carboxyl groups due to mercury binding. Though, these results agreed with those obtained for the FTIR analysis technique, they did not give any indication of the participation of the amine and sulfonate functional groups in the biosorption mechanism.

Buhani et al., (2011) also prepared a hybrid biosorbent by immobilizing *Nannochloropsis sp* in silica gel utilized it for metal biosorption. EDX analysis of the biosorbent revealed that it was comprised of 11.46% Si, 28.81% O, 46.17% C and 13.56% N. This showed that the biosorbent had higher composition of C than *Cladophora sp* alga immobilized in silica gel. The percent composition of N in *Nannochloropsis sp* immobilized in silica gel was also reported as 13.56% N. On the other hand, in the present study, EDX analysis did not reveal the % composition of N in *Cladophora sp* alga immobilized in silica gel. Furthermore, Buhani et al.,

(2011) did not provide any information regarding the elemental analysis of *Nannochloropsis sp* immobilized in silica gel after metal biosorption. The observed disparities in the EDX results confirm that the elemental composition and the contribution of functional groups in algal-based biosorbents varies according to the polymer support used, algal species and target metal.

5.9.3 Determination of metal content of pristine *Cladophora sp* alga

To get further information of the mechanism for the biosorption of mercury onto *Cladophora sp* alga, the total metal concentration of the alga before and after metal binding was also determined. The results are summarized in Table 5.14. These findings demonstrated pristine *Cladophora sp* had a wide variety of metal components ranging from alkali, alkaline earth to transition metals. The principal constituents of the digested alga were Al, Mg, Ca, Na and other light metals. The high concentrations of Mg and Ca were linked to the abundance of chlorophyll and other cell wall structures within the algal cells (Apiratikul and Pavasant, 2008). Like the water from which it was harvested, the alga also contained high levels of Fe and trace amounts of other transition metals like As, U, Hg, Mn, Pb and Zn. The concentration of Hg in the alga was substantially low in comparison to the amounts taken up during biosorption. It was also observed that binding of mercury onto the algal surface altered its metal composition i.e. the total concentrations of all the metals except mercury declined during the process. This trend was more apparent in the light metals particularly Al, Mg, Ca, Na and K. This is mainly because these metals were most abundant in the alga and have lower ionization energies thus they could easily lose electrons and go into solution. In contrast, the concentration of mercury in the algal samples increased during biosorption. This suggested that suggested that light metals on the surface of the alga exchanged with mercury in solution during biosorption. A comparison of total metal concentration gained during biosorption with that which was lost during the process also revealed that 192. 57 mEq of mercury were gained whilst the total concentration of the other metal constituents dropped by 154.39 mEq. This signifies that ion exchange contributes 80.17% to the entire biosorption process. These results corresponded to those reported for EDX analysis of the alga which also showed that ion exchange was the predominant mechanism.

Table 5.14: Summary of results for evaluation of total metal content in pristine *Cladophora sp* alga before and after mercury biosorption

Metal	Concentration (mg L^{-1})		Change in
	Before biosorption	After biosorption	concentration (mEq)
As	0.06 ±0.01	0.02 ± 0.01	2.99
Ba	0.05 ± 0.01	0.02 ± 0.01	4.12
Be	0.06 ±0.01	0.02 ±0.01	0.36
Ca	1.07 ± 0.11	0.19 ±0.06	35.27
Cd	0.05 ±0.01	0.02 ± 0.01	3.37
Cr	0.05 ±0.01	0.02 ± 0.01	1.56
Fe	0.73 ±0.05	0.49 ± 0.04	13.40
K	0.24 ±0.01	0.08 ±0.01	6.65
Li	0.08 ±0.01	0.02 ± 0.01	0.42
Mg	1.10 ±0.16	0.17 ± 0.01	22.60
Mn	0.09 ± 0.01	0.07 ±0.01	1.10
Na	0.72 ±0.01	0.11 ± 0.08	14.02
Pb	0.06 ± 0.01	0.02±0.01	8.29
Sr	0.05± 0.01	0.02 ±0.01	2.63
Zn	0.06 ±0.01	0.03 ± 0.01	1.96
Sc	0.05 ± 0.01	0.02 ±0.01	1.35
Ti	0.09 ±0.02	0.06 ±0.01	1.44
Al	1.38 ± 0.36	0.31 ±0.01	28.87
Cs	0.05 ±0.01	0.02 ± 0.01	3.99
Hg	0.06 ± 0.01	1.02 ±0.22	192.57

They also provided further proof that other mechanisms such as surface binding, intraparticle diffusion and functional group interactions also contributed to the overall mercury binding process.

In an earlier study, Chojnacka et al., (2005) also utilized multi-metal analysis to elucidate the mechanism for biosorption of Cr^{3+}, Cd^{2+} and Cu^{2+} by *Spirulina sp*

alga. They found that metal biosorption changed the total metal concentration of the alga. The authors also observed that the total change in metal content due to the loss of light metal ions was only 27-29% of the change due to metal biosorption. They suggested ion exchange was still the dominant mechanism; but, in this instance, the participation of protons far exceeded that of the light metals (Chojnacka et al., 2005). The variability in the results obtained in different studies can be attributed to the dissimilar chemical compositions of the algal species and the conditions under which it was grown prior to biosorption.

5.9.4 Chemical modification of functional groups

The functional groups on the surface of pristine *Cladophora sp* alga were modified to uncover the mechanism for mercury biosorption and the results are illustrated in subsections 5.10.4.1 -5.10.4.4 below.

5.9.4.1 Esterification of carboxyl groups

Fig. 5.22 gives an illustration of the results obtained for the comparison of the biosorption capabilities of the pristine alga with that of alga whose carboxyl groups had been blocked by esterification.

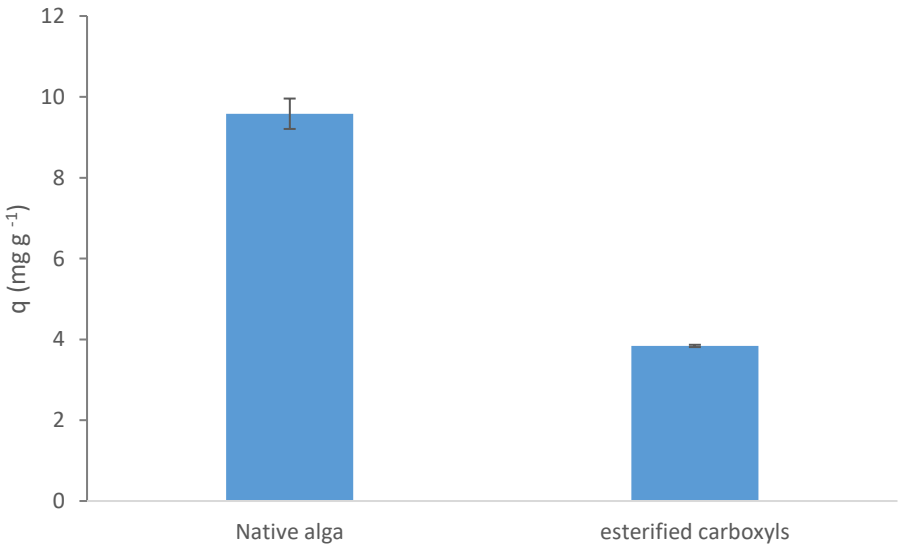

Fig. 5.22: Biosorption capacities of native and esterified *Cladophora sp* alga (pH 5, agitation time 20 minutes, initial metal concentration 1 mg L^{-1}, biosorbent dosage 10 g L^{-1}, temperature 25˚C)

As shown in the figure, esterification of the carboxyl groups led to the biosorption capacity of the alga dropping by 59.96% i.e. from 9.582 to 3.837 mg g^{-1}. This indicated that carboxyl groups play a significant role in the mechanism for the biosorption of mercury by pristine *Cladophora sp* alga. These results are in agreement with those reported for the FTIR analysis of pristine *Cladophora sp* alga before and after mercury analysis. The notable decline in the intensity of the peaks due to the carboxyl group after mercury biosorption also signified that the carboxyl groups contributed to a large extent to the overall process.

The findings of this study were also compared to those reported by Fang et al., (2011) for the biosorption of copper and cadmium using *Spirulina platensis* alga. They deduced that blocking of the carboxyl groups on non-viable biomass of the alga via esterification reduced the biosorption capacity of the biosorbent to drop by at least 45%. Fourest and Volesky, (1996) also evaluated the contribution of the carboxyl groups to the mechanism for biosorption of metals by dried *Sargassum fluitans* biomass using a shared batch equilibrium methods. Their results also revealed that esterification of the carboxyl groups negatively impacted the biosorption capacity of the alga. The maximum adsorption capacity for Cd dropped from 1.06 to 0.23 mmol g^{-1} thus signifying a depreciation of 78.30%. Though similar trends were observed in different research works, the contribution of carboxyl groups varied between studies. This is mainly because of dissimilarities in the properties of the target metals and their affinities for other functional groups on the algal biosorbents used.

5.9.4.2 Esterification of the sulfonic acid groups

The sulfonate groups on the surface of pristine *Cladophora sp* alga were also blocked by esterification to verify their role in mercury biosorption and the results are shown in Fig. 5.23. The adsorption capacity of the *Cladophora sp* alga dropped from 9.582 to 1.941 mg g^{-1} as a consequence of the esterification of the sulfonate groups. This indicated that the sulfonate groups also played a significant role in the biosorption of mercury by the alga. In fact, their modification led to a greater decline in adsorption capacity (79.74%) compared to that observed for the blockage of the carboxyl groups (59.96%). This trend can be attributed to the higher affinity of mercury for sulfur-containing compounds such as the sulfonate group (Mishra et

al., 2016). Bhatnagar et al., (2012) also investigated the mechanism for the biosorption of Ni(II) using *Pelvetia canaliculata*. They blocked the sulfonate functional groups on the surface of alga to discern their contribution to the biosorption mechanism. Their results revealed that the blocking the sulfonate groups led to complete diminution of Ni (II) biosorption by the alga. This indicated that biosorption of Ni(II) by *Pelvetia canaliculata* depended solely on the sulfonate functional groups.

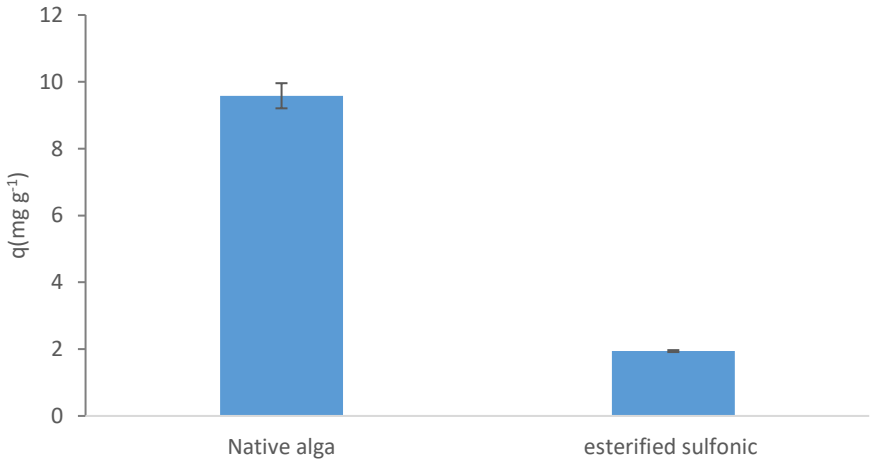

Fig. 5.23: Biosorption capabilities of native *Cladophora sp* alga and *Cladophora* alga with esterified sulfonate groups (pH 5, agitation time (20 minutes), initial metal concentration (1 mg L^{-1}), biosorbent dosage (10 g L^{-1}, temperature (25˚C))

In their study, Raize et al., (2004) also evaluated the mechanism for the biosorption of Cd, Pb and Ni using *Sargassum vulgaris* alga. Their results revealed that the metal uptake of the unmodified alga were 1.05, 0.95 and 1.2 mmol g^{-1} for Cd, Pb and Ni respectively. Esterification of the sulfonate groups on the alga caused the biosorption capacities of Cd, Pb and Ni to drop by 25, 55 and 75%, respectively. This indicated that sulfonate groups also played a significant role in the biosorption of metals (particularly Ni) by *Sargassum vulgaris*.

Hence, from the results of the current study and the above-mentioned research works, it can be deduced that the contribution of sulfonate groups to the overall

metal biosorption mechanism is dependent upon the algal species used and chemical properties of the target metal.

5.9.4.3 Acetylation of the amine and hydroxyl groups

The biosorption performance of the pristine alga was compared with that of the alga with acetylated amine and hydroxyl groups. Fig. 5.24 gives an illustration of the results obtained.

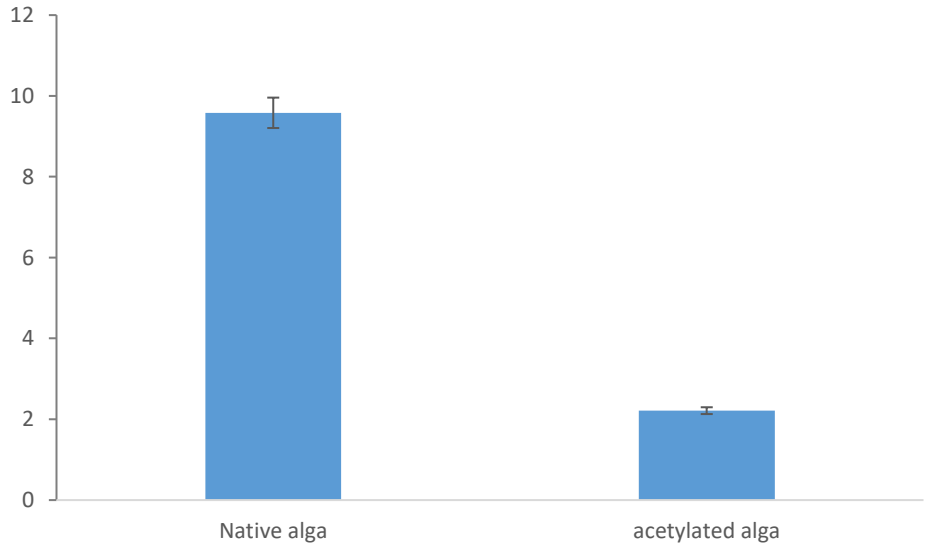

Fig. 5.24: Biosorption capabilities of pristine and acetylated *Cladophora sp* alga (pH 5, agitation time (10 minutes), initial metal concentration (1 mg L^{-1}), biosorbent dosage (10 g L^{-1}), temperature (25˚C))

The acetylation of the amine and hydroxyl functional groups also resulted in the reduction of the biosorption capacity of the alga. The decline observed in this instance (76.91 %) was much higher than that observed for the esterification of the carboxyl groups (59.96%). However, this value was lower than that shown for the esterification of sulfonic groups (79.74%). This implied that even though the amine and hydroxyl groups play a more significant role in the biosorption mechanism than the carboxyl groups, their contribution was lower than that of the sulfonic groups. This trend can be attributed to the fact that mercury has a higher affinity for sulfonic

groups over nitrogen-containing groups and carboxyl groups (Apiratikul and Pavasant, 2008; Mishra et al., 2016). Hence, the depreciation in the biosorption capacity as a result of modification of functional groups followed the order sulfonate < amine < carboxyl groups.

These observations also confirmed the results obtained for the FTIR analysis of the alga before and after mercury biosorption. The FTIR spectra revealed that the peaks due to the sulfonate and amine groups were more affected by mercury binding than those corresponding to the carboxyl groups. This signified the greater involvement of the sulfonate, hydroxyl and amine groups in the biosorption process.

Bai and Abraham, (2001) also utilized chemical modification to identify the major functional groups contributing to the mechanism for the biosorption of Cr(VI) by *Rhizopus nigricans*. The authors found that acetylation of the amine and hydroxyl groups on the algal surface caused the biosorption capacity to decline by 25%. On the other hand, Doyle et al., (1980) reported that the acetylation of amine groups on the surface of *Bacillus subtilis* enhanced it metal uptake capacity. The dissimilarities in the results reported in different research works can be explicable by variations in the nature of the microbial biosorbent used, metal species and chemical composition of the solution (Gardea-Torresdey et al., 1990).

5.9.4.4 Potentiometric titrations

Potentiometric titrations were performed to gain further insight on the acidic sites and functional groups on the surface of *Cladophora sp* alga and the results are shown in Figs. 5.25 and 5.26.

Fig. 5.25 gives an illustration of the titration curve obtained for the neutralization of the acid sites on the alga using 0.1 M NaOH. The results in Fig. 5.25 demonstrate that the initial pH of the suspension containing the pristine alga was 2.9 and increased slowly with addition of NaOH until a plateau was reached at pH 11.26. This signified the depletion of all the acidic groups on the alga surface. The titration curve also had several inflection points corresponding to the different pK_a values of the various acidic group components of the alga. Since, it was challenging to extract all these values from the titration curve, a first derivative plot of the titration data was drawn and used to accurately locate the points.

On the other hand, Fig 5.26 gives an illustration of the first derivative curve obtained. It is apparent from this figure that the titration curve 5 inflection points corresponding to pK_a values of 3.45, 5.31, 7.55, 8.81 and 9.82, respectively. These pK_a values were assigned to the carboxyl, imidazole, amine, sulfhydryl and hydroxyl groups respectively (Kirova et al., 2012; Ramrakhiani et al., 2013; Yalcin et al., 2012).

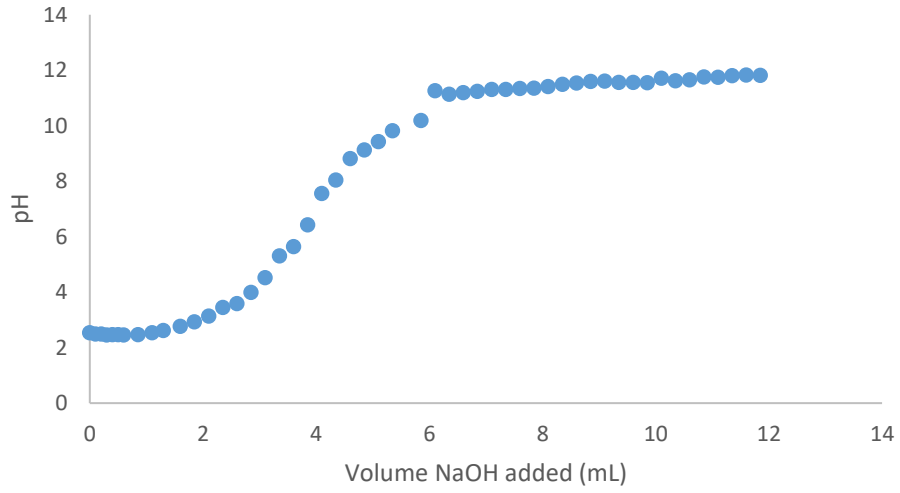

Fig. 5.25: Titration curve for the neutralization of acidic sites on pristine *Cladophora sp* alga using 0.1 M NaOH

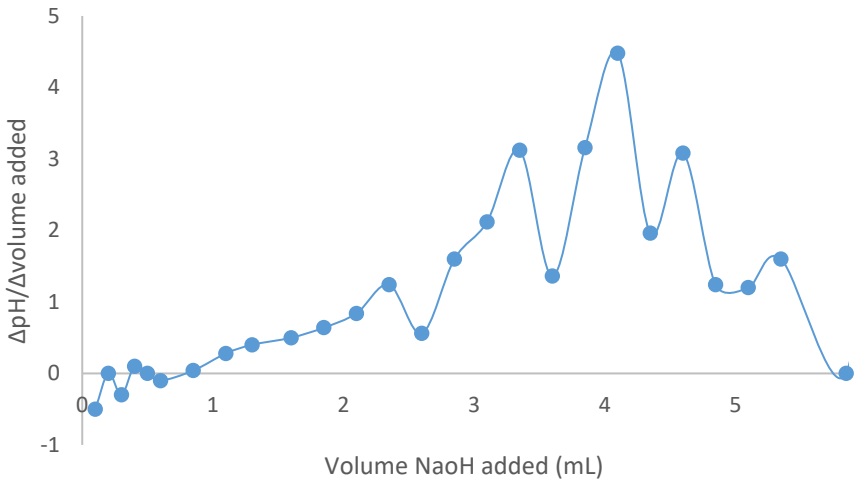

Fig. 5.26: First derivation plot of the titration data for pristine *Cladophora sp* alga using 0.1 M NaOH

Hence, the potentiometric titration provided additional information on the presence of the imidazole functional group which was not identified using FTIR analysis. The densities of the strong and weak acidic groups were estimated as 0.124 mmol g^{-1} and 0.324 mmol g^{-1} respectively. Similarly, the concentration of strong basic sites was 0.0600 mmol g^{-1} while that of the weak basic sites were 0.1840 mmol g^{-1}.

Though, the results show that the concentration of the carboxyl group is higher, chemical modification tests revealed that blocking the amine and sulfonyl groups had the highest impact on the biosorption capacity of the alga. This is mainly due to mercury's high affinity for nitrogen and sulfur containing groups (Apiratikul and Pavasant). This showed that these functional groups are most likely to be involved in the binding of mercury to the algal surface.

Yalcin et al., (2012) also used potentiometric titrations to characterize the acidic sites on the surface of *Cystoseira barbata* alga. They used the inflection points on the titration curve obtained to identify the functional groups on the algal biosorbent as the carboxyl, amine and hydroxyl groups. The authors also reported that the densities of the strong and weak acid groups as 0.9 and 2.26 mmol g^{-1} respectively. Romero-Gonzalez et al., (2000) also investigated the mechanism for biosorption of Cd by de-alginated waste seaweed. Potentiometric titration of the alga revealed that

the carboxyl and amine groups on the algal surface were responsible for metal binding (Romero-Gonzalez et al., 2000).

5.10 Theoretical treatment of batch biosorption data

The data obtained from the batch biosorption experiments was modelled against kinetic, adsorption isotherm and thermodynamic models. The results are discussed in detail in subsections 5.10.1, 5.10.2 and 5.10.3 respectively.

5.10.1 Kinetic modeling

The kinetic data for the biosorption of mercury using pristine and modified forms of *Cladophora sp* alga was modelled against the pseudo-first order, pseudo-second order and Webber- Morris models. The findings for the pseudo-first order model are presented as linear plots in Fig. 5.27.

As per the results, the pseudo-first order model plot for the pristine alga had the least linearity, the value for the correlation ratio (R^2) was 0.2311. On the contrary, the R^2 values for the alga immobilized in alginate and silica gel were 0.7029 and 0.9317. This showed that the data for the silica gel showed the best fit for the pseudo-first order model.

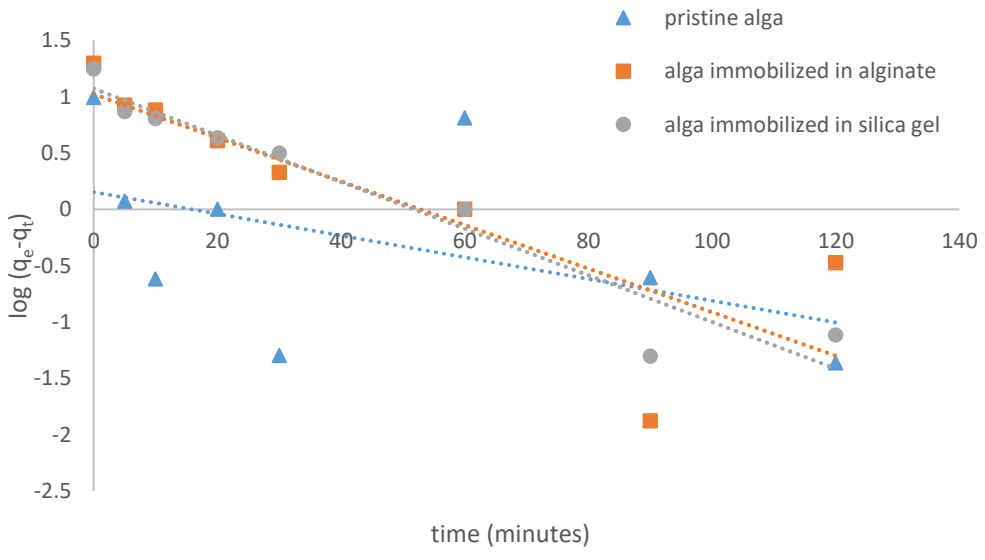

Fig. 5.27: Pseudo-first order model plots for biosorption of mercury using pristine and modified forms of *Cladophora sp* alga

Similarly, the linear plots for the pseudo-second order model for all biosorbents studied are displayed in Fig. 5.28. In this case, the R^2 values for the pristine alga, alga immobilized in alginate beads and alga immobilized in silica gel were 0.9998, 0.9973 and 0.9965, respectively.

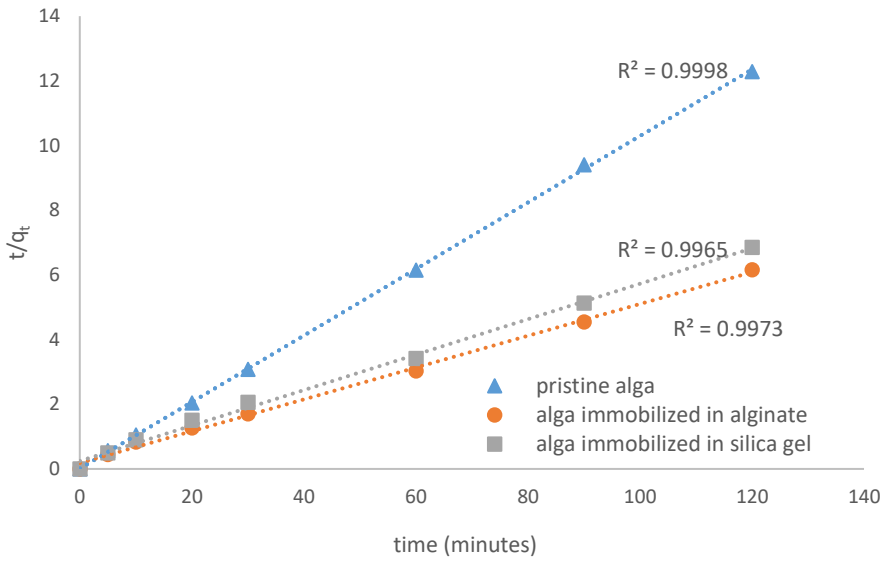

Fig. 5.28: Pseudo-second order plots for the biosorption of mercury using pristine and modified forms of *Cladophora sp* alga

Hence, for all biosorbents studied, the R^2 values for the pseudo-second order model were closer to unity than those of the pseudo-first order model. Therefore, the kinetics for the biosorption of mercury using pristine and modified forms of *Cladophora sp* alga were best described by the pseudo-second order kinetic model and chemisorption was the rate limiting mechanism (Kumar et al., 2016; Tuzen et al., 2009).

Table 5.15 also gives a summary of the pseudo-first and pseudo-second order kinetic and performance parameter for all the biosorbents. From the table, it was revealed that the values of the calculated adsorption capacities ($q_{e,\ calc}$) determined using the pseudo-second order model were closer to the experimental values (q_{exp}) than those obtained using the pseudo-first order model. This trend was observed for all the biosorbents studied. This provided further proof that the kinetics for the biosorption of mercury using pristine and modified forms of *Cladophora sp* alga

were best described by Ho's pseudo-second order model. In addition, for both kinetic models, the magnitudes of the rate constants followed the order pristine alga > alga immobilized in silica gel > alga immobilized in alginate beads. This suggested that the rate of biosorption using pristine *Cladophora sp* alga was faster than when the modified biosorbents were utilized. This is mainly because the modified biosorbents experience higher diffusion and mass transfer resistance (Abu Al-Rub et al., 2004).

Even so, the modified biosorbents compensate for this limit by having a greater number of active sites due to the functional group contributions of the polymeric supports which substantially enhanced the biosorbents' adsorption capability (Bayramoglu et al., 2006; Suharso et al., 2010).

Table: 5.15: Performance and kinetic parameters for pseudo-first and pseudo-second order kinetic models using pristine and modified *Cladophora sp* alga biosorbents (Temperature 25˚C, pH 5, biosorbent dosage 10 g L^{-1}, initial metal concentration 2 mg L^{-1})

Biosorbent	q_{exp}	Pseudo-first order		Pseudo-second order	
		$q_{e,calc}$	k_1	$q_{e,\ calc}$	k_2
Pristine alga	17.79	1.167	0.02631	19.73	1.068
Alga immobilized in alginate beads	19.84	11.79	0.02372	20.33	0.0132
Alga immobilized in silica gel	17.60	10.54	0.02465	18.25	0.0122

The kinetic data was also modelled against the Webber-Morris intraparticle diffusion model and the results are shown in Fig. 5. 29.

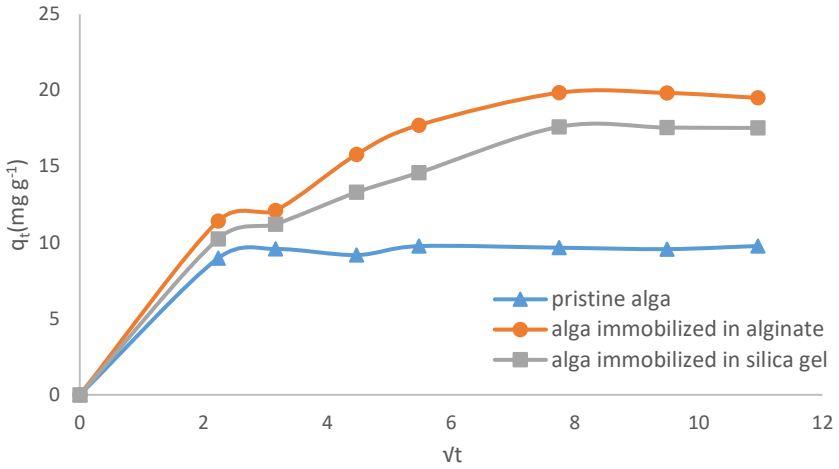

Fig. 5.29: Webber-Morris plots for the biosorption of mercury using pristine and modified forms of *Cladophora sp* alga

It is apparent from this figure that for all three biosorbents, the plot of q_t versus √t was linear for only the initial stages of the biosorption process. Therefore, it can be deduced that mercury binding using pristine and modified forms of *Cladophora sp* alga was limited by diffusion only at the start of the process. This is explicable by the fact that during the initial stages, diffusion plays a key role in the conveyance of mercuric ions towards the biosorbent surfaces (Apiratikul and Pavasant, 2008). Hence, eqn. 4.8 was only applied to the initial stages of the biosorption process and the results for all the biosorbents are summarized in Table 5.16.

Table. 5.16: Webber-Morris parameters for biosorption of Hg^{2+} using pristine and modified forms of *Cladophora sp* alga

Biosorbent	R^2	k_1
Pristine *Cladophora sp* alga	0.9469	3.210
Cladophora sp alga immobilized in alginate beads	0.9378	3.151
Cladophora sp alga immobilized in silica gel	0.8828	2.116

As illustrated in Table 5.16, the R^2 values for the Webber-Morris model were 0.9469, 0.9378 and 0.8828 for the pristine alga, alga immobilized in alginate beads and alga immobilized in silica gel, respectively. This signified that the biosorption of mercury onto the test biosorbents was governed by intraparticle diffusion at the beginning of the process. Nevertheless, as more time elapsed, other mechanisms began to take precedence. In addition, the values of the intraparticle diffusion constant (k_p) showed that the rate of diffusion was faster for the biosorption system using pristine *Cladophora sp* alga than the modified biosorbents. This was to be expected because in the latter, the alga is completely engulfed in polymer support thus increasing the diffusion and mass transfer limits (Abu Al-Rub et al., 2004). However, this effect became less significant for longer time periods.

The kinetic modelling results obtained in this study were compared with those reported in other research works. Mashitah et al., (2008) studied the biosorption of Cd by *Pycnoporus sanguineus* immobilized in agar and used kinetic modelling to assess the kinetics of the biosorption process at different temperatures (303, 308 and 313 K). Unlike in the case of the biosorption systems utilized in the current study, R^2 values for the pseudo-first order model at the different temperatures were closer to 1 than those obtained using the pseudo-second order at the same temperatures. This showed that for *Pycnoporus sanguineus* immobilized in agar, the rate limiting mechanism was physisorption. The kinetic data also fitted the intraparticle diffusion model with high R^2 values.

Tsekova et al., (2010) also immobilized *Aspergillus nigger* alga in PVA hydrogels and utilized the free and immobilized forms of the alga to remove Cd and Cu from aqueous solutions. They also modelled the experimental kinetic data and found that the plots of t/q against t were linear for both metals thus showing that chemisorption was a significant mechanism in the biosorption process. A linear plot of q_t versus $\sqrt{t}$ also revealed that intraparticle diffusion also partook in the biosorption process. The rate constants for both models were also higher for Cu than Cd.

5.10.2 Adsorption isotherm modeling

The equilibrium data for the biosorption of mercury using pristine and modified forms of *Cladophora sp* was modelled against the Freundlich, Langmuir and Dubinin-Radushkevich isotherms and the results are described in subsections *5.10.2.1*, *5.10.2.2* and *5.10.2.3*.

5.10.2.1 Modeling of the equilibrium batch data using the Freundlich and Langmuir isotherms

The plots for the Freundlich isotherm model for the biosorption of mercury by pristine *Cladophora sp* alga, *Cladophora sp* alga immobilized in alginate beads and *Cladophora sp* alga immobilized in silica gel are portrayed in Figs. 5.30, 5.31 and 5.32, respectively.

It was inferred from these plots that the R^2 values of the Freundlich isotherm were 0.8374, 0.9194 and 0.9088 for the pristine alga, alga immobilized in alginate beads and *Cladophora sp a*lga immobilized in silica gel, respectively. This showed that the Freundlich isotherm fitted the experimental kinetic data for biosorption using pristine and modified forms of *Cladophora sp* alga to a reasonable degree.

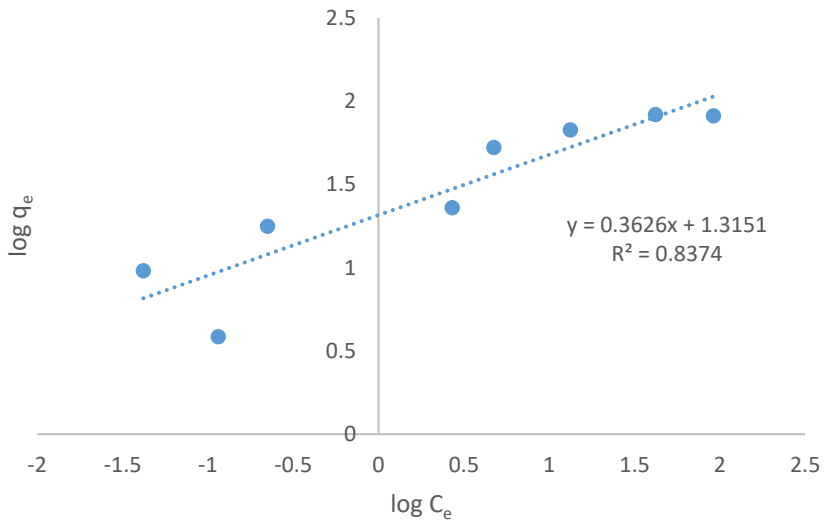

Fig. 5.30: Freundlich isotherm plot for mercury biosorption onto pristine *Cladophora sp* alga

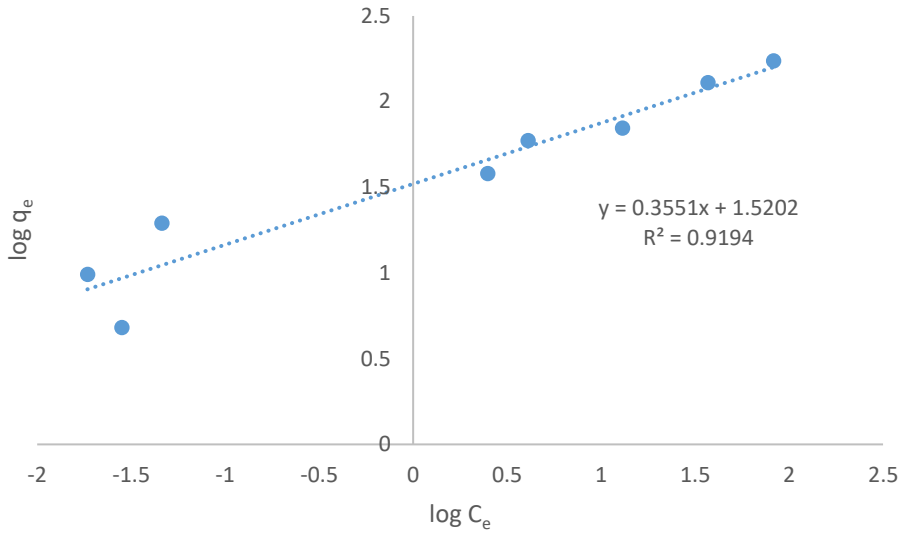

Fig. 5.31: Freundlich isotherm plot for mercury biosorption onto *Cladophora sp* alga immobilized in alginate beads

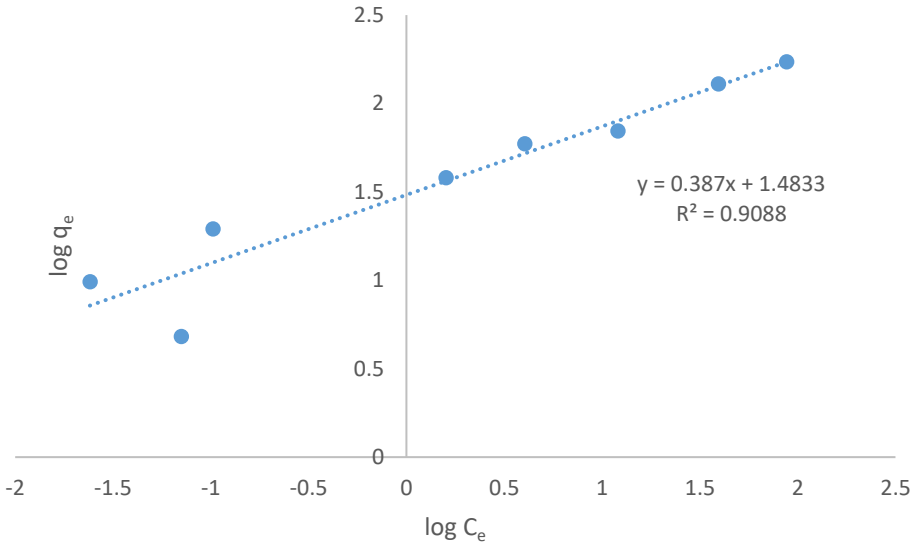

Fig. 5.32: Freundlich isotherm plot for mercury biosorption onto *Cladophora sp* alga immobilized in silica gel

Similarly, the Langmuir isotherm model plots for the pristine alga, alga immobilized in alginate beads and alga immobilized in silica gel are illustrated in

Figs. 5.33, 5.34 and 5.35, respectively. As per these results, the R^2 values for the Langmuir isotherm using the pristine alga, alga immobilized in alginate beads and alga immobilized in silica gel were 0.9949, 0.9425 and 0.9926 respectively. This showed that even though the equilibrium data for biosorption using all three biosorbents fitted both isotherms reasonably well, it was best described by the Langmuir isotherm. Therefore, biosorption onto both pristine and modified forms of *Cladophora sp* alga occurred on a homogenous layer with active sites of equivalent energies. The equations for the linear plots of the Langmuir and Freundlich isotherms were also utilized for the determination of the constants used for description of the biosorption process and the results are summarized in Table 5.17.

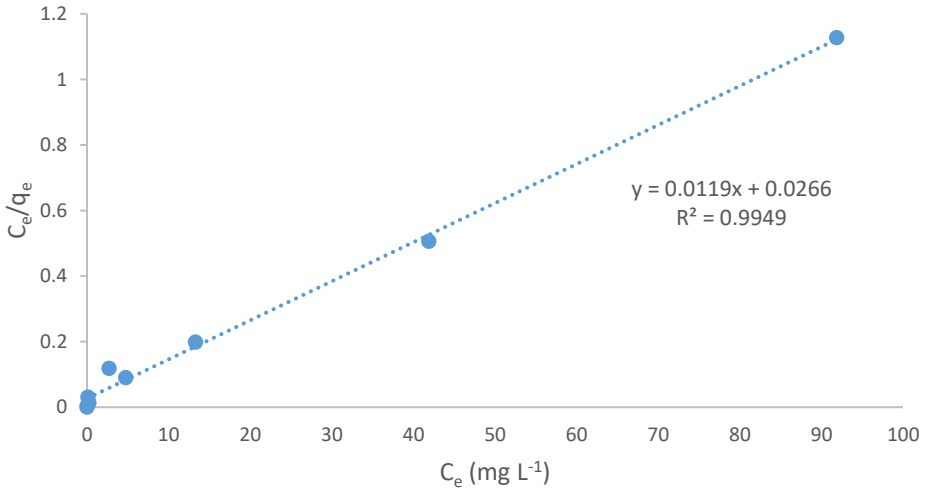

Fig.5.33: Langmuir isotherm plot for Hg^{2+} biosorption using pristine *Cladophora sp a*lga

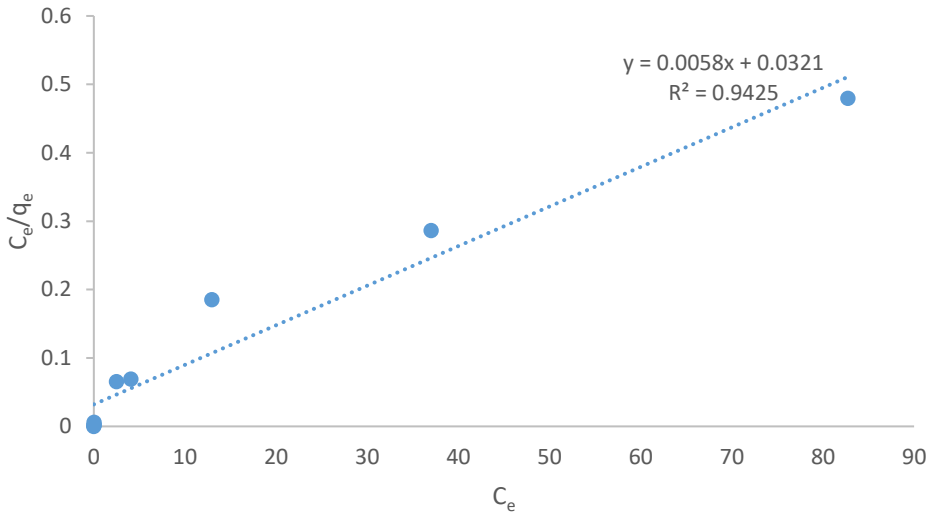

Fig.5.34: Langmuir isotherm plot for Hg^{2+} biosorption using *Cladophora sp a*lga immobilized in alginate beads

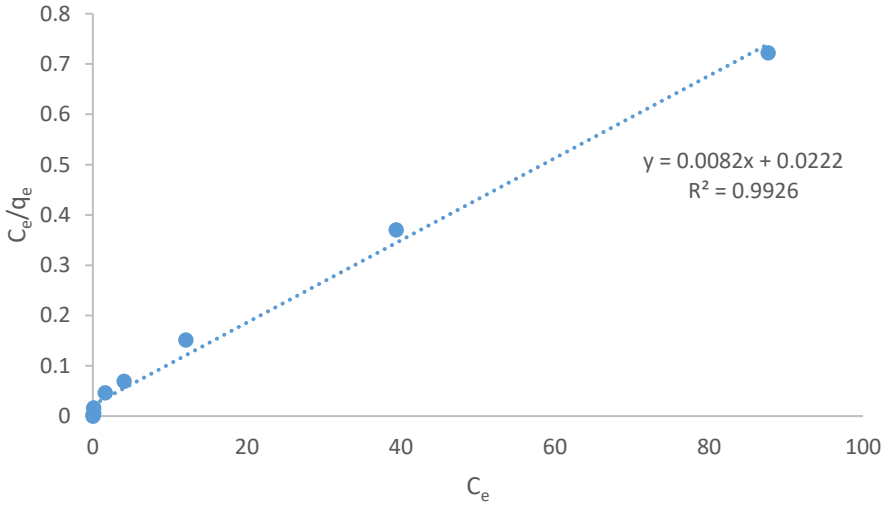

Fig. 5.35: Langmuir plot for Hg^{2+} biosorption using *Cladophora sp a*lga immobilized in silica gel

The findings demonstrated that the values of the calculated adsorption capacities ($q_{e,\ calc}$) using the Langmuir isotherm were nearer to the experimental values (q_e) than those for the Freundlich isotherm. This further verified that the equilibrium data was best described by the Langmuir isotherm.

Table 5.17: Freundlich and Langmuir isotherm model constants for mercury biosorption using pristine and modified forms of *Cladophora sp* alga

Biosorbent	q_e	Freundlich		Langmuir	
		K_F	1/n	q_m	b
Pristine *Cladophora sp*	82.93	20.66	0.3870	84.33	0.3474
Cladophora sp immobilized in alginate beads	183.4	33.13	0.3551	172.4	0.4807
Cladophora sp immobilized in silica gel	121.3	28.40	0.3626	121.9	0.3694

In addition, the values for affinity constant (b) calculated from the Langmuir isotherm also revealed that the affinities of the test biosorbents followed the order pristine alga < alga immobilized in silica gel < alga immobilized in alginate beads. It was also observed that for all the biosorbents studied, the values of 1/n calculated using the Freundlich isotherm were in the range 0 <1/n < 1 indicative of favorable adsorption. The degree of favorability of the biosorption processes also followed the above order. These observations are in line with the observation made regarding the biosorption capacities of the biosorbents which also followed the order pristine alga < alga immobilized in silica gel < alga immobilized in alginate beads.

The values for R_L were also calculated and found to be 0.02798, 0.02038 and 0.02636 for the pristine alga, alga immobilized in alginate beads and alga immobilized in silica gel respectively. This showed that the adsorption processes using all three biosorbents were favorable. However, favorability followed the order alga immobilized in alginate beads < alga immobilized in silica gel < pristine alga.

5.10.2.2 Modeling of the equilibrium batch biosorption data versus the Dubinin-Radushkevich isotherm

The equilibrium data for Hg^{2+} biosorption onto pristine *Cladophora sp*, *Cladophora sp immobilized in alginate beads* and *Cladophora sp* immobilized in silica gel was also modelled against the Dubinin-Radushkevich isotherm. Table 5.18 gives a summary of the results obtained.

According to the findings, the experimental data fitted well with the Dubinin-Radushkevich isotherm with R^2 values of 0.9634, 0.9133 and 0.9034 for the pristine alga, alga immobilized in alginate beads and alga immobilized in silica gel respectively. The values of the sorption energy (E_s) for all the sorbents studied were in the range 8-16 kJ mol^{-1} implying that the mechanism for biosorption was predominantly ion exchange (Dada et al., 2012; Tuzen et al., 2009). These results correlated with those reported for the determination of metal content and EDX analysis which showed the predominance of the ion exchange mechanism.

Table 5.18: Dubinin-Radushkevich isotherm parameters for the biosorption of Hg^{2+} using pristine and modified forms of *Cladophora sp* alga (temperature 25˚C, pH 5, bisorbent dosage 10 g L^{-1})

Biosorbent	R^2	X_m	E_s (kJ mol^{-1})
Pristine *Cladophora sp* alga	0.9634	80.23	11.07
Cladophora sp immobilized in alginate beads	0.9133	158.73	9.406
Cladophora sp immobilized in silica gel	0.9034	106.45	9.69

Dada et al., (2012) also modelled the biosorption of Zn^{2+} onto rice husk adsorbent against the Langmuir, Freundlich, Temkin and Dubinin–Radushkevich isotherms. They deduced that the R^2 values for the Langmuir, Freundlich and Temkin

isotherms were 0.99, 0.89 and 0.62 respectively thus signifying that biosorption occurred on a homogeneous layer. The equilibrium data also fitted the Dubinin-Radushkevich isotherm; but, the value of E_s for the biosorption process was 0.707 kJ mol^{-1}. This showed that the physisorption was dominant mechanism.

Zan et al., (2012) also immobilized *Saccharomyces cerevisiae* biomass in alginate beads and utilized for biosorption of Cd(II) and Cu(II) from aqueous solutions. Adsorption isotherm modelling revealed that the R^2 values for the Freundlich isotherm were 0.913 and 0.787 for Cd and Cu, respectively. The R^2 values for the same metals using the Langmuir isotherm were 0.981 and 0.973, respectively thus demonstrating that biosorption occurred on a homogeneous layer. However, the authors did not model the equilibrium data against the Dubinin-Radushkevich isotherm to get information on the biosorption mechanism. The variations in the adsorption isotherm results between studies is explicable by the use of differing biosorbents and the chemistry of the target metal in solution.

5.10.3 Thermodynamic modelling

The results for the thermodynamic modelling of the data for the biosorption of mercury using pristine and modified *Cladophora sp* alga are shown in Tables 5.19 and 5.22 below. Table 5.19 illustrates the ΔG° values for the processes using the test biosorbents at different temperature values. The findings in Table 5.21 revealed that the ΔG° values for the biosorption processes using all three test biosorbents became less negative when the temperature was increased from 16 -40˚C (298-313 K). This indicated that for all the biosorbents tested, the spontaneity of the biosorption process decreases at high temperature thus signifying the exothermic nature of the process. Moreover, at all the temperatures studied, the ΔG° values calculated for the alga immobilized in alginate beads were highest while those of the pristine alga were lowest. However, the ΔG° values computed for the alga immobilized in silica gel were intermediary between the two. This showed that the spontaneity of the biosorption process using the test biosorbents followed the order pristine alga < alga immobilized in silica gel < alga immobilized in alginate beads. The order is aligned with that established for the affinities of the biosorbents for mercury ions using the Langmuir isotherm.

Table 5.19: ΔG° values for the biosorption of Hg^{2+} using pristine and modified forms of *Cladophora sp* alga

Biosorbent	ΔG° (kJ mol^{-1})			
	289 K	298 K	303 K	313 K
Pristine *Cladophora sp* alga	-4.297	-3.095	-2.556	-0.979
Cladophora sp alga immobilized in alginate	-10.541	-4.851	-3.642	-0.863
Cladophora sp alga immobilized in silica gel	-9.897	-4.802	-2.903	-0.567

The enthalpies and entropies for the biosorption processes using pristine and modified *Cladophora sp* alga were also calculated and the findings are illustrated in Table 5.20.

Table 5.20: Thermodynamic parameters for the biosorption of Hg^{2+} by pristine and modified *Cladophora sp* alga (10 g L^{-1} biosorbent dosage, pH 5, 1 mg L^{-1} Hg^{2+})

Biosorbent	R^2	ΔH (kJ mol^{-1})	ΔS (kJ mol^{-1})
Pristine *Cladophora sp* alga	0.9905	-67.25	0.2049
Cladophora sp alga immobilized in alginate beads	0.9026	-86.96	0.2635
Cladophora sp alga immobilized in silica gel	0.9838	-73.60	0.2214

The ΔH values calculated for the biosorption processes using all three test biosorbents were negative indicative of their exothermic nature. The ΔH value for the alga immobilized in alginate beads was more negative than those of the other two biosorbents. This provided further proof that the biosorption process using the alga immobilized in alginate beads was more favorable. The negative values of entropy obtained also signified that for all biosorbents studied, the randomness at

the solid-liquid interface decreased during biosorption (Pahlavanzadeh et al., 2010; Tuzen et al., 2009).

Pahlavanzadeh et al., (2010) also evaluated the thermodynamic behavior of the process for the biosorption of Ni(II) from aqueous solution by four different brown algae (*Cystoseira indica*, *Nizmuddinia zanardini*, *Sargassum glaucescens* and *Padina australis).* They deduced that for all the biosorbents studied, the ΔG values were negative suggesting that the biosorption process was spontaneous. However, unlike in the case of the pristine and modified forms of *Cladophora sp* alga, the spontaneity of the biosorption process increased when the temperature increased showing the endothermic nature of the process. In addition, the absolute ΔH values determined for *C. indica* (7.78 kJ mol^{-1}), *N. zanardini* (11.42 kJ mol^{-1}), *S. glaucescens* (11.82 kJ mol^{-1}) and *P. australis* (6.40 kJ mol^{-1}) were lower than those obtained for the biosorbents based on *Cladophora sp* alga. The positive values of ΔH also showed that the biosorption processes using all the biosorbents were endothermic.

5.11 Continuous flow studies

Continuous flow studies were conducted using *Cladophora sp* alga immobilized in alginate beads in a packed bed configuration to assess the industrial applicability of the metal biosorption system. The effect of varying significant operational parameters was evaluated and the results are given in sections 5.11.1-5.11.4 below. The experimental data was also modelled against four kinetic models and the results are discussed in section 5.11.5.

5.11.1 Effect of bed height

The effect of bed height on the performance of the fixed bed column packed with *Cladophora sp* alga immobilized in alginate beads was investigated and Fig 5.36 gives an illustration of the breakthrough curves obtained at the different bed heights studied. The results show that the performance and breakthrough behavior of the column under study was dependent on the bed height. At the lowest value of bed height (3 cm), the column reached breakthrough in 42.5 minutes after treating only 85 mL of mercury solution.

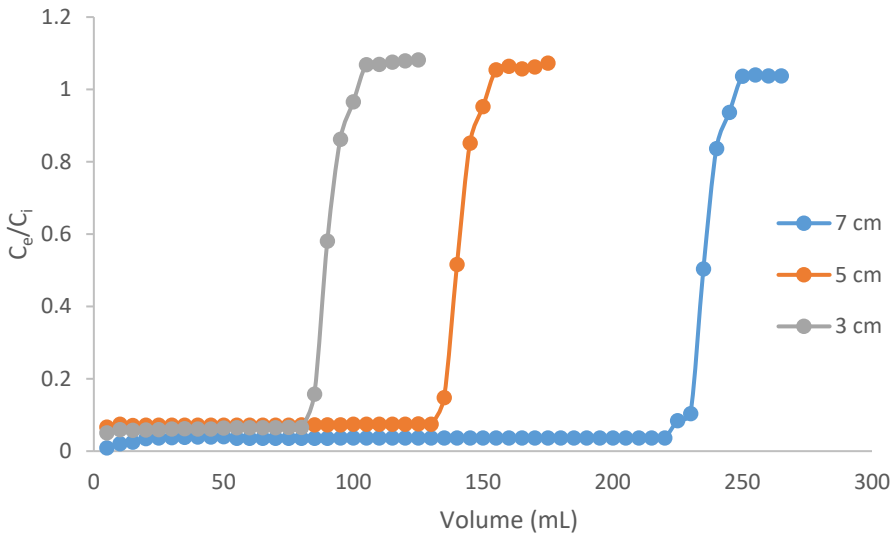

Fig. 5.36: Effect of bed height on the performance of column packed with *Cladophora sp* alga immobilized in alginate beads (solution pH 5, inlet metal concentration 2 mg L^{-1}, flow rate 2 mL min^{-1}, temperature 25˚C)

Similarly, exhaustion of the column occurred in 52.5 minutes after treatment of only 105 mL of metal solution. A summary of the performance parameters of the column at the different bed heights is also given in Table 5.23.

Table 5.21: Summary of performance parameters for column packed with *Cladophora sp* alga immobilized in alginate beads at different bed heights (solution pH 5, inlet metal concentration 2 mg L^{-1}, flow rate 2 mL min^{-1}, temperature 25˚C)

Bed height (cm)	Performance parameters				
	t_b (minutes)	t_e (minutes)	q_{total} (mg)	r (%)	q (mg g^{-1})
3	42.5	52.5	0.471	67.7	5.25
5	67.5	77.5	0.826	68.7	6.94
7	115	125	1.14	71.7	8.15

The values of $q_{total,}$ r% and q attained at this bed height were 0.471 mg, 67.7% and 5.25 mg g^{-1} respectively. Increasing the bed height of the column to 7 cm improved the performance of the column significantly. The values of t_b and t_e increased to 115 and 125 minutes respectively. In the same manner, the values of $q_{total,}$ r% and q also increased to 1.14 mg, 71.7% and 8.15 mg g^{-1}, respectively.

The observed trend is attributable to the fact that columns with longer bed heights are packed with larger amounts of biosorbent and therefore have more binding sites available for biosorption. Consequently, they are able to treat large volumes of metal solution before reaching breakthrough and saturation points (Mohamad et al., 2010; Singh et al., 2012). On the contrary, columns with shorter bed heights are less efficient and achieve breakthrough and saturation rapidly. They also have lower values of $q_{total,}$ r% and q because they contain smaller quantities of biosorbent with fewer biosorption sites. Based on these observations, 7 cm was set as the optimum bed height for the retrieval of mercury using the column packed with *Cladophora sp* immobilized in alginate beads.

A comparison of the results obtained in this research work with those reported in other studies revealed variations due to the use of different biosorbents, metal adsorbates, methodologies and experimental parameters. For instance, Mishra et al. (2016) reported the biosorption of Cr(VI) and Ni (II) using a column packed with dried modified *Hydrilla verticillata*. Their findings demonstrated that increasing the bed height of the column from 15 to 25 cm resulted in the breakthrough time of the column increasing from 50 to 100 minutes (Mishra et al., 2016). Hence, they considered 15 cm as the optimum bed height for removal of Cr(VI) and Ni (II) using modified *Hydrilla verticillata* under continuous flow mode.

Kumar et al., (2011) also utilized a hybrid biosorbent comprised of *Trichoderma viride* biomass immobilized in alginate beads for the removal of Cr (VI), Ni (II) and Zn (II) from aqueous solutions using a packed bed column configuration. The authors investigated the effect of bed height on the performance of the column using 3 values i.e. 10, 15 and 20 cm. They deduced that increasing the bed height from 10 -20 cm increased the breakthrough time for Cr (VI) from 276 to 630 minutes while the biosorption capacity increased from 5.44 to 6.30 mg g^{-1}. The breakthrough

time for biosorption of Ni (II) also increased from 274 to 610 minutes while the adsorption capacity rose from 5.52 to 6.10 mg g^{-1}. In the same way, the breakthrough time for Zn(II) increased from 66 to 228 minutes and the biosorption capacity increased from 1.32 to 2.28 mg g^{-1}.

5.11.2 Effect of flow rate

The effect of flow rate on the ability of the column packed with *Cladophora sp* immobilized in alginate beads in retrieving mercury from aqueous solutions was also investigated. The breakthrough curves for the performance of the biosorption column at different flow rates are presented in Fig. 5.37.

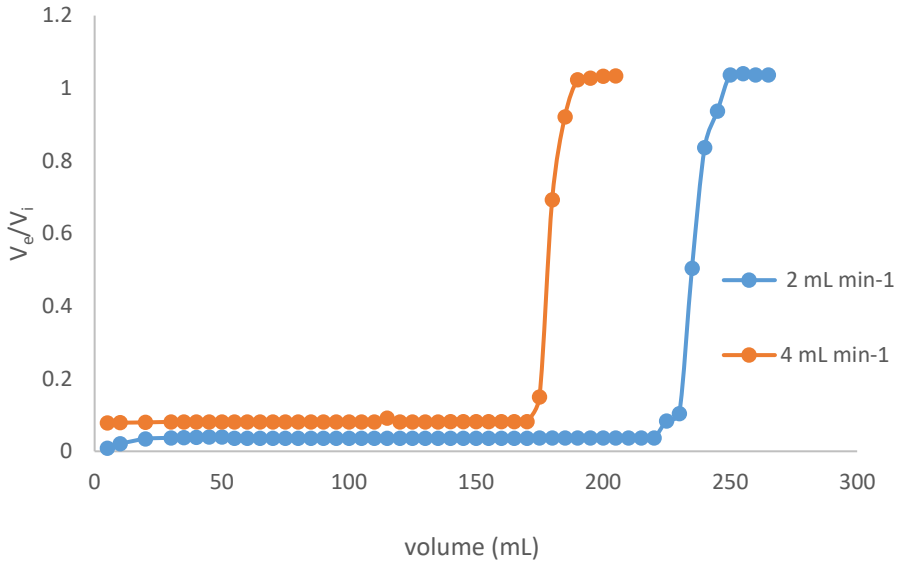

Fig. 5.37: Effect of flow rate on the performance of the column packed with *Cladophora sp* alga immobilized in alginate beads (solution pH 5, bed height 7 cm, inlet metal concentration 2 mg L^{-1}, temperature 25˚C)

Table 5.22 also provides a summary of the performance parameters of the column determined at different flow rates. The findings demonstrated that when the mercury solution was pumped into the biosorption solution at a slow rate (2 mL min^{-1}), breakthrough was attained in 115 minutes while column saturation reached in 125 minutes. The values of $q_{total,}$ r% and q at this flow rate were 1.26 mg, 72.3%

and 8.29 mg g^{-1}, respectively. Increasing the flow rate to 4 mL min^{-1} resulted in the breakthrough and exhaustion times dropping to 43.8 minutes and 47.5 minutes, respectively. The values of q_{total}, r% and q also depreciated to 0.666 mg, 63.1% and 5.59 mg g^{-1} respectively. This is mainly because of the short residence time of the metal ions in the column at high flow rates. The metal ions are rapidly flushed through the column without allowing sufficient interaction with the biosorbent (Lodeiro et al., 2007; Naddafi et al., 2007). On the contrary, slower flow rates allow adequate time for the metal ions to interact and bind to biosorbent sites. Therefore, 2 mL min^{-1} was selected as the optimum flow rate for optimal removal of mercury under the studied conditions.

Table 5.22: Summary of performance parameters for column packed with *Cladophora sp* alga immobilized in alginate beads at different flow rates (solution pH 5, bed height 7 cm, inlet metal concentration 2 mg L^{-1}, temperature 25˚C)

Flow rate ($mL\ min^{-1}$)	Performance parameters				
	t_b (minutes)	t_e (minutes)	q_{total} (mg)	r (%)	q (mg)
2	115	125	1.26	72.3	8.29
4	43.8	47.5	0.666	63.1	5.59

Long et al., (2014) also investigated the effect of flow rate on the biosorption of Pb(II) using modified *Agaricus bisporus* in a fixed bed column. Their findings revealed that increasing the flow rate from 1 to 5 mL min^{-1} decreased the value of t_b from 977.9 to 145.0 minutes. The value of q also dropped from 66.7 to 44.5 mg g^{-1} while r% depreciated from 91.5% to 78.4%. Riazi et al., (2016) also assessed the capability of Ca-pretreated *Cystoseira indica* in removing Th(IV) from aqueous solution using fixed bed continuous flow operation. Analysis of the breakthrough curves obtained revealed that increasing the flow rate from 1 to 4 mL min^{-1} reduced t_b from 1450 to 71.2 minutes. The value of t_e also dropped from 4357.6 to 1384.1 minutes while the removal efficiency of the column depreciated from 62.92 to 42.27%. Similarly, the adsorption capacity dropped from 261.3 to 229.3 mg g^{-1}.

5.11.3 Effect of influent metal concentration

The influence of inlet metal concentration on the efficiency of the column packed with *Cladophora sp* alga was also studied and the breakthrough curves are illustrated in Fig. 5. 38 and Table 5.23.

These results show that increasing influent metal concentration from 1 to 5 mg L^{-1} negatively impacted the breakthrough and exhaustion times of the column. The breakthrough time decreased from 197.5 to 72.5 minutes whilst the exhaustion time dropped from 207.0 to 87.5 minutes. On the contrary, Increasing the metal concentration had the opposite effect on q_{total} and q i.e. the values increased to 1.91 mg and 12.10 mg g^{-1} respectively. This column behavior was explicable by the fact that at higher metal concentrations, there's a higher concentration gradient between the biosorbent surface and the metal solution which serves as a driving force for mass transfer to the biosorbent. The overall resistance to film and intraparticle diffusion increases with upsurges in inlet metal concentration (Chowdhury et al., 2013; Kleinubing et al., 2011).

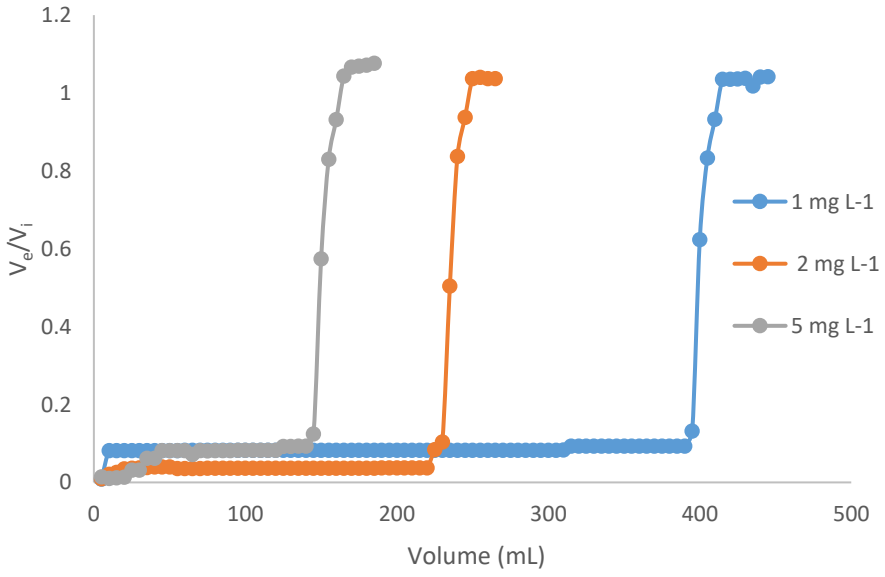

Fig. 5.38: Effect of inlet metal concentration on the performance of the column packed with *Cladophora sp* alga immobilized in alginate beads (solution pH 5, bed height 7 cm, flow rate 2 mL min^{-1}, temperature 25˚C)

Table 5.23 also gives a summary of the performance parameters for the different metal concentrations studied.

Table 5.23: Summary of performance parameters for column packed with *Cladophora sp* alga immobilized in alginate beads at different inlet metal concentrations (solution pH 5, bed height 7 cm, flow rate 2 mL min^{-1}, temperature 25˚C)

Metal concentration ($mg\ L^{-1}$)	Performance parameters				
	t_b (minutes)	t_e (minutes)	q_{total} (mg)	r (%)	q ($mg\ g^{-1}$)
1	197.5	207.5	1.06	69.5	6.67
2	115.0	125.0	1.34	71.1	8.44
5	72.5	82.5	1.91	68.5	12.11

In the case of the r%, there was an initial increase when the concentration is increased to 2 mg L^{-1}. However, further increases in concentration up to 5 mg L^{-1} resulted in a slight decrease in r% due to the rapid occupation of the binding sites on the biosorbent. On the other hand, at lower metal concentrations, the concentration gradient and resultant driving force are not sufficient for overcoming mass transfer and external diffusion resistances (Chowdhury et al., 2013; Kleinubing et al., 2011). Consequently, lower values of q_{total}, r% and q are observed in these instances (Chowdhury et al., 2013).

Bulgariu and Bulgariu, (2016) mixed waste algal biomass with Purolite A-100 anionic exchanger and utilized the resultant biosorbent for the uptake of Cd (II) from aqueous solutions using a fixed bed column configuration. Their evaluation of the effect of inlet metal concentration on the performance of the column revealed that changes in metal concentration affected the values of t_b, q and r%. Increasing the metal concentration from 35 to 55 mg L^{-1} dropped t_b from 43.75 to 9.37 minutes.

However, the same increase in concentration caused the value of q to increase from 35.93 to 51.83 mg g^{-1} while r% declined from 63.41 to 50.09%.

Jain et al., (2013) also investigated the effect of influent metal concentration on the biosorption of Cd(II) onto sunflower biomass (*Helianthus annus)* entrapped in alginate beads using a packed bed column. They deduced that increasing the inlet metal concentration from 10 to 20 mg L^{-1} caused the breakthrough time to decrease from 165 to 68 hours. The exhaustion time of the column also dropped from 220 to 110 hours under the same conditions. However, unlike in the case of the system using the *Cladophora sp* alga immobilized in alginate beads, increasing the metal concentration resulted in q depreciating from 23.4 to 19.4 mg g^{-1}. The variations in the trends and values of the performance parameters of the biosorption columns used in the different studies can be attributed to the utilization of different biosorbents, target metals and experimental conditions. For instance, the inlet metal concentrations used in the present study were much lower than those used in the other studies.

5.11.4 Evaluation of the selectivity of the biosorption column

The selectivity of the biosorption column packed with *Cladophora sp* alga immobilized in alginate beads was evaluated by using the same column set-up to treat multi-metal solutions. The breakthrough curves for the treatment of the unitary and multi-elemental solutions are depicted in Fig. 5.39. Table 5.24 also gives a comparison of the performance parameters of the biosorption column acquired during the treatment of the multi-metal solution with those for the single component one.

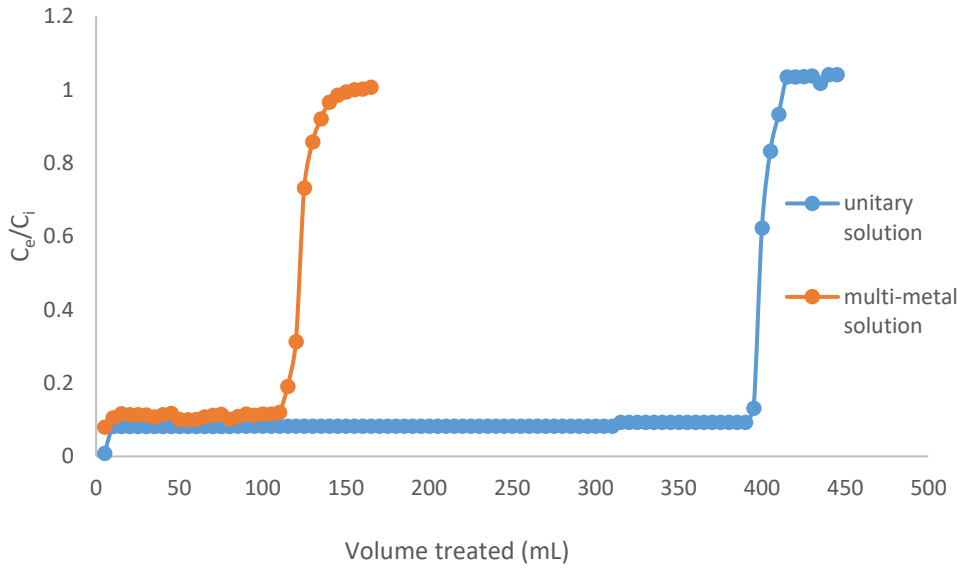

Fig. 5.39: Breakthrough curves for the biosorption of mercury from unitary and multi-elemental solutions using a column packed with *Cladophora sp* alga immobilized in alginate beads (pH 5, bed height 7 cm, flow rate 2 mL min^{-1}, inlet metal concentration 2 mg L^{-1}, temperature 25˚C)

It is clear from these results that the presence of other cations affects the performance of the biosorption column in retrieving mercury from aqueous solutions. When the biosorption column was utilized for treatment of the unitary solution, the values of t_b and t_e were 197.5 and 210.0 minutes respectively. The introduction of other components into the solution led to t_b and t_e dropping to 55.0 and 70.0 minutes respectively.

The values of q_{total}, r% and q also depreciated from 1.37 mg, 73.7% and 8.62 mg g^{-1}, respectively in the unitary solution to 0.799 mg, 69.4% and 5.04 mg g^{-1}, respectively in the multi-metal solution. This observation is attributed to the fact that in multi-metal solutions there are more metal ions which compete for the finite number of binding sites (Kleinubing et al., 2011). Therefore, the column will reach breakthrough and saturation rapidly. Moreover, because of the competition for the binding sites, less mercury will be biosorbed. Hence, the drop in the values of q_{total}, r% and q in the multi-metal solution.

Table 5.24: Performance parameters for the treatment of unitary and multi-metal solutions using *Cladophora sp* alga immobilized in alginate beads in a packed column (pH 5, temperature 25˚C, bed height 7 cm, flow rate 2 mL min^{-1})

Performance parameter	Unitary solution	Multi-metal solution
t_b (minutes)	197.5	55.0
t_e (minutes)	205	70.0
q_{total} (mg)	1.37	0.80
r (%)	73.7	69.4
q (mg g^{-1})	8.62	5.04

Kleinubing et al., (2012) also evaluated the selectivity of *Sargassum filipendula* in removing Cu(II) from aqueous solutions in a continuous flow system. Their results showed that the adsorption capacity of Cu (II) using this system in unitary solutions was 0.87 mmol g^{-1}. The introduction of an equimolar amount of Ni(II) dropped the biosorption capacity by 12% to 0.75 mmol g^{-1}. Bakir et al., (2009) also investigated the competitive biosorption of Sb, Ni and Al in a fixed column packed with *Polysiphonia larosa* alga. They discovered that the removal efficiencies of the metals from unitary solutions were 90%, 90%, 74% and 63% for Ni, Zn, Al and Sb respectively. When the same column setup was used to treat a solution comprised all 4 metals, the removal efficiencies reduced to 28, 17, 24 and 16% for the same metals. Though the aforementioned studies demonstrate the same antagonistic behavior that was observed for the system using *Cladophora sp* immobilized in alginate beads, the degree or magnitude of the competitive effect differed between research works. This was mainly because different studies entailed the use of varying algal biosorbents under dissimilar experimental conditions. The solutions used were also comprised of metal adsorbates with differing speciation, ionization stated and chemical properties.

5.11.5 Theoretical modeling of the breakthrough behavior of the column packed with *Cladophora sp* alga immobilized in alginate beads

The column biosorption data was modelled against the BDST, Adams-Bohart, Thomas and Yoon-Nelson models to predict the maximum adsorption capacity and other significant parameters required for scaling up the system. Sections 5.11.5.1 - 5.11.5.4 provide detailed descriptions of the results obtained.

5.11.5.1 BDST model

The results for the BDST model are illustrated in Fig. 5.40 and they show that the R^2 value for the BDST plot was 0.9778 which is close to 1.

This indicated that the experimental data fitted the BDST model well.

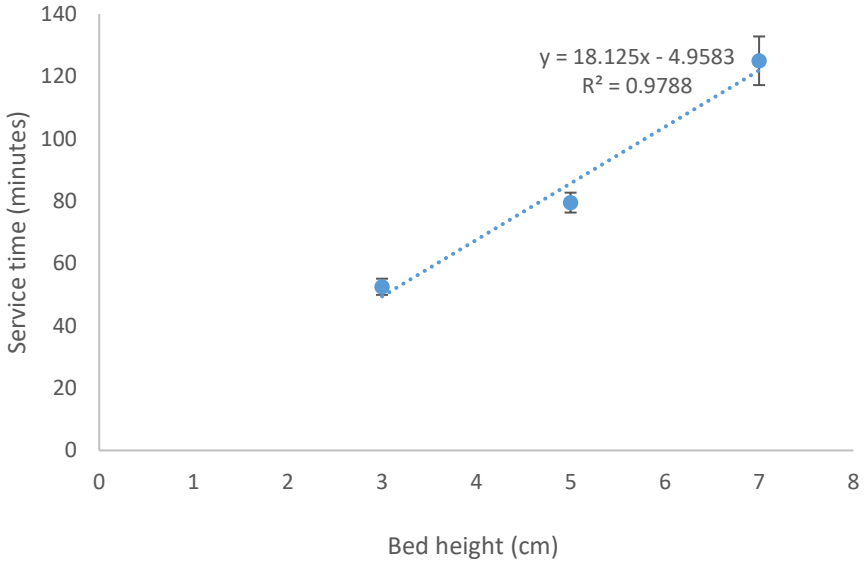

Fig. 5.40: BDST model plot for biosorption column packed with *Cladophora sp* immobilized in alginate (pH 5, temperature 25˚C, flow rate 2 mL min^{-1}, inlet metal concentration 2 mg L^{-1})

The adsorption capacity of the biosorbent was also calculated as 18.13 mg g^{-1} using this model which was not too different from the experimental value. The rate of the

biosorption process using the BDST model was 4.958 mg^{-1} min^{-1}. Muhamad et al. (2010) also used the BDST model to predict the breakthrough curves for the biosorption of Cd (II) using *Triticum sativum*. They obtained a linear relationship between bed height and service time with an R^2 value of 0.9791. The adsorption capacity of *Triticum sativum* using this model was 21.8 mg g^{-1} while the rate constant was 10.5 mg g-^{1}. Rajamohan and Sivaprakash, (2008), studied the biosorption of Cd(II) ions from aqueous solutions using *Sargassum tenerrimum* in a fixed bed column. Albeit, they found that the BDST model described the experimental data well, the adsorption capacity and rate constant were also reported as 3819 mg g^{-1} and 2.118 mg min^{-1} respectively.The adsorption capacities and rate constants calculated using the BDST model differed between studies due to the use of dissimilar algal species, target metals and experimental conditions.

5.11.5.2 Adams-Bohart model

The results for the Adams-Bohart model are displayed in Table 5.25. High values of R^2 were obtained for all the experimental conditions studied thus indicating that the Adams-Bohart model was suitable for the description of the breakthrough behavior of the column at the start of the experiment.

Table 5.25: Adam – Bohart parameters for a column packed with *Cladophora sp* alga immobilized in alginate beads at different bed heights, flow rates and inlet metal concentrations

Parameter	Bed height (cm)			Flow rate (mL min^{-1})		Metal concentration (mg L^{-1})		
	3	5	7	2	4	1	2	5
R^2	0.953	0.919	0.902	0.979	0.989	0.851	0.901	0.992
K_{AB}	0.021	0.096	0.172	0.103	0.271	0.461	0.174	0.052
N_0	2.73	3.04	4.99	4.69	2.55	5.58	4.99	4.88

The values of K_{AB} and N_0 determined using this model were also dependent on the experimental conditions. Increasing the bed height of the column resulted in increases in both K_{AB} and N_0. Similarly, increasing the flow rate of metal solution through the column increased the value of K_{AB}; but, the value of N_0 decreased. On the contrary, increases in the inlet metal concentration had a negative impact on both K_{AB} and N_0. This implied that the kinetics of the biosorption system were dominated by external mass transfer at the beginning of the experiments.

Baral et al., (2009) also applied the Adams-Bohart model for the description of the breakthrough curve for retrieval of Cr(VI) from aqueous solutions using *Salvinia cucullata* in a fixed bed column. The authors found that the R^2 values for the plot of ln (C_t/C_o) versus t were close to unity for all the values of flow rate, bed height, and initial metal concentration studied. As in the case of the *Cladophora sp* immobilized in alginate beads, increasing the metal inlet concentration caused both K_{AB} and N_0 to decrease. On the contrary, increasing the flow rate resulted in increments in both K_{AB} and N_0. Increasing the bed height also favored the increase in K_{AB} while N_0 depreciated. This trend was opposite to that observed in the current study wherein increasing bed height increased both K_{AB} and N_0. This mismatch in the trends for the changes of K_{AB} and N_0 with respect to the experimental parameters can be explained by the use of different algal species, properties of metal biosorbed and experimental conditions.

5.11.5.3 Thomas Model

The results obtained for modeling the experimental breakthrough data against the Thomas model are illustrated in Table 5.26. It is evident from the R^2 values obtained for the Thomas model were all close to 1 thus signifying that the model is suitable for the description of the experimental data. The results also showed that increasing the bed height of the column increased the values of K_{TH} and q_0 while increasing the flow rate negatively affected both K_{TH} and q_0.

Table 5.26: Summary of the Thomas model parameters for a column packed with *Cladophora sp* alga immobilized in alginate beads at different bed heights, flow rates, and inlet metal concentrations

Parameter	Bed height (cm)			Flow rate (mL min^{-1})		Metal concentration (mg L^{-1})		
	3	5	7	2	4	1	2	5
R^2	0.949	0.927	0.953	0.932	0.918	0.951	0.925	0.963
K_{TH}	0.144	0.251	0.293	0.259	0.203	0.266	0.244	0.217
q_0	13.8	40.5	57.5	59.4	41.3	39.9	57.4	76.3

Increasing the influent metal concentration increased the value of q_0 while K_{TH} depreciated. The values of q_0 computed using the Thomas were slightly inflated compared to those obtained experimentally. Regardless, the well fit of the experimental data to this model implied that external mass transfer and internal diffusion were not the rate limiting mechanisms (Baral et al., 2009; Ghasemi et al., 2011).

Qaiser et al., (2009) also studied the uptake of Pb(II) from aqueous solutions using *Ficus religiosa* immobilized in polysulfone beads using a packed bed configuration. The column data fitted the Thomas model and the values of K_{TH} and q_0 determined were dependent on the flow rate. Increasing the flow rate from 5-20 mL min^{-1} caused q_0 to decrease while the value of K_{TH} increased. Unlike in the case of the *Cladophora sp* system used in the current study, the values of q_0 calculated using this model were congruent to those found experimentally. Nonetheless, decreasing the flow rate to low values resulted in deviations between the two sets of values were observed. Ghasemi et al., (2011) also found that the Thomas model was suitable for the description of the breakthrough behavior of a column packed Ca-treated *Cystoseira indica* alga used for the biosorption of U(VI).Contrary to the results reported in the current study, they found that increasing the flow rate increased the value of K_{TH} while q_0 decreased. Increasing the bed height had the opposite effect in that it enhanced q_0 and caused K_{TH} to decrease. They also revealed that the calculated values of q_0 were higher than the experimental ones.

Vijayaraghavan et al., (2005) studied the biosorption of Cu, Co, and Ni in a fixed bed column. They also predicted the breakthrough of the column using the Thomas model. Their findings revealed that increasing the flow rate increased K_{TH} for all the metals studied. However, different metals showed different responses in q_0 when the flow rate was increased. For Cu, increasing flow rate enhanced C_0; but, in the case of Co and Ni, increasing flow rate reduced the value of q_0. These inconsistencies in the trends for the changes in q_0 and K_{TH} between different metals and algal-metal biosorption systems is proof that the biosorption behavior of algae in fixed bed columns is correlated to the algal species and chemical properties of the metals studied.

5.11.5.4 Yoon-Nelson model

The column data was also modeled against the Yoon-Nelson and the results are illustrated in Table 5.27.

Table 5.27: Summary of the Yoon-Nelson model parameters for a column packed with *Cladophora sp* alga immobilized in alginate beads at different bed heights, flow rates, and inlet metal concentrations

Parameter	Bed height (cm)			Flow rate (mL min^{-1})		Metal concentration (mg L^{-1})		
	3	5	7	2	4	1	2	5
R^2	0.965	0.978	0.951	0.966	0.937	0.964	0.961	0.929
K_{YN}	0.362	0.343	0.322	0.331	0.352	0.371	0.325	0.313
τ	17.2	24.9	38.8	38.9	32.5	74.86	38.9	25.3

According to the results, , the R^2 values at the various experimental conditions were very close to one thus implying that the model was well-suited for description of the column data. It was also observed that the values of K_{YN} and τ were affected by changes in the column operation parameters. Increasing the bed height resulted in an increase in the value of τ while K_{YN} declined. On the other hand, increasing the

flow rate led to an increase in K_{YN} while τ decreased. Increasing the influent metal concentrations also caused both K_{YN} and τ decreased. This trend also corresponded to that observed in the experimental column data thus showing that the Yoon-Nelson method was best-suited for the modeling of the biosorption column data.

Baral et al., (2009) also utilized the Yoon-Nelson method to predict the breakthrough behavior for biosorption of Cr(VI) onto *Salvinia cucullata* packed in a fixed bed column. Their results revealed that increases in flow rate yielded increases in the value of K_{YN} whereas τ decreased. On the converse, increasing the initial metal concentration caused both K_{YN} and τ to drop. This trend was only observed up to 200 mg L^{-1}, further increases in inlet metal concentration caused the value of K_{YN} to rise while τ continued to decline. Similarly, increasing the bed height to 8 cm caused K_{YN} to drop whereas τ increased.

Vijayaraghavan and Prabu, (2006) also examined the potential of *Sargassum wightii* biomass in Cu(II) removal from aqueous solutions using a packed bed column configuration. They modeled the experimental column data against the Yoon-Nelson model and found that the operational parameters affected the values of K_{YN} and τ. Increasing the bed height of the column from 15 -25 cm dropped K_{YN} by 16.4% while τ increased by 43.8%. Conversely, increasing the flow rate from 5 -20 mL min^{-1} caused the value of K_{YN} to increase by 184% whereas τ dropped by 75.2%. Increasing the inlet metal concentration also increased the value of K_{YN} whilst τ declined.

5.11.6 Comparison of the column studies results with those obtained in the batch studies

The results obtained for the biosorption capacity of *Cladophora sp* immobilized in alginate beads using the continuous flow mode at different inlet metal concentrations were compared with those for the batch scale experiments. Table 5.28 gives a summary of the results obtained using the two different operation modes. The results illustrate that increasing the initial metal concentration enhanced the adsorption capacity of the biosorbent for both batch scale and column studies. This was due to the higher concentration gradients which rapidly drove the metal ions to the binding sites on the biosorbent surface (Kleinubing et al., 2011). It was

also observed that for all three concentrations investigated, the adsorption capacities of *Cladophora sp* alga immobilized in alginate beads obtained using batch equilibrium studies far exceeded those determined using packed column system.

Table 5.28: Comparison of the performance of the batch and the continuous flow mode for the biosorption of mercury using *Cladophora sp* alga immobilized in alginate beads (pH 5, temperature 25˚C)

Metal concentration (mg L^{-1})	Adsorption capacity (mg g^{-1})	
	Batch studies	Column studies
1	9.81	6.67
2	19.54	8.45
5	38.09	12.15

This trend was attributed to the fact that batch scale studies entailed the continuous agitation of reaction vessels which promoted thorough mixing of the reaction mixtures. Hence, enhanced interaction between the metal ions and metal binding sites on the biosorbent surface occurred thus leading to higher metal biosorption (Ghasemi et al., 2011). On the converse, packed bed column studies did not provide sufficient contact time between the metal ions and the algal-based biosorbent for the attainment of equilibrium. Hence, their adsorption capacities tend to be slightly lower than those reported for batch scale studies (Gokhale et al., 2009). Nonetheless, column studies are still essential because they permit the treatment of large volumes of solution in a short time span and are easier to scale up for industrial applications (Pahlavanzadeh et al., 2010).

Ghasemi et al., (2011) also performed batch scale and continuous flow biosorption studies to evaluate the biosorption capacity of *Cystoseira indica* alga in sequestering U(VI) from aqueous solutions. The authors revealed that biosorption using batch equilibrium studies yielded an adsorption capacity of 454.4 mg g^{-1}. On the other hand, using the same biosorbent under continuous flow operation mode

dropped the adsorption capacity to 315.4 mg g^{-1}. On the other hand, Muhamad et al., (2010) observed contradictory behavior for the biosorption of Cd onto *Triticum sativum* biomass using batch scale and continuous flow studies. They found that the adsorption capacity of the biosorbent during batch biosorption studies was 15.7 mg g^{-1} while that observed for the packed bed column studies was 16.9 mg g^{-1}. The variation between the trend observed in the current study and those reported in the literature could be due to the differences in the algal species used and their interactions with the metals of interest.

5.11.7 Comparison of the performance of the biosorption column packed with *Cladophora sp* alga immobilized in alginate beads with other fixed-bed biosorption systems

To gain further perspective on the efficiency of the fixed bed column packed with *Cladophora sp* alga immobilized in alginate beads, its adsorption capacity was compared with those of other fixed bed biosorption systems reported in the literature. A summary of the results obtained are displayed in Table 5.29.

Table 5.29: Comparison of the performance of *Cladophora sp* alga immobilized in alginate in a packed column with those of other biosorbents using the same mode

Biosorbent	q (mg g^{-1})	Reference
Cladophora sp immobilized in alginate	12.21 (Hg)	This work
Spirulina platensis immobilized in alginate	1.4 (Zn)	Konig-Peter et al., (2014)
Aspergillus nigger	1.08 (Cd)	Kapoor &Viraraghavan, (2005)
Chaetomorpha linum	0.1288 (Zn)	Ajjabi & Chouba, (2009)
Spyridia filamentosa	0.1782 (Pb)	Kowanga et al., (2015)
Hydrilla verticillata	89.32 (Cr)	Mishra et al., (2012)

According to these results, the adsorption capacity of the biosorption column used in the present study was either higher than or comparable to those of other biosorbents reported in the literature. The adsorption capacity of the biosorption column packed with *Cladophora sp* alga immobilized in alginate beads was also much lower than that of the modified *Hydrilla verticillata* biomass. These disparities are due to the different experimental conditions used and variety of biosorbents and target metals studied.

5.12 Design of biotraps and their application for the treatment of environmental samples

The results for the design of biotraps and their subsequent application to environmental samples are described in section 5.13.1 and 5.13.2 respectively.

5.12.1 Development of biotraps based on *Cladophora sp* alga immobilized in alginate beads

Fig. 5. 41 gives an illustration of the biotraps constructed using *Cladophora sp* alga immobilized in alginate beads.

This figure shows that the built biotraps were compact with the biosorbent tightly held in a ‘teabag-like formation’ with a nylon string attached for easy removal of the device from bulk solution after completion of the biosorption process. The biotraps were also more robust and easier to handle then the loose biosorbents. Hence, they would be more convenient for application to ‘real’ environmental samples.

Fig. 5.41: Teabag-like biotrap constructed using *Cladophora sp* alga immobilized in alginate beads

5.12.2 Application of the biotraps for treatment for environmental samples

The industrial applicability of the biotraps was evaluated by treatment of environmental samples and the results are illustrated in Tables 5.30 and 5.31. Table 5.32 gives the hydrochemical properties of the AMD samples formed by dissolution of acidic environmental crusts while Table 5.33 illustrates the total metal concentrations in the samples before and after treatment using the tea-bag biotraps.

These findings in Table 5.30 revealed that the AMD samples were acidic with pH values ranging from 3.02 to 3.16. The EC and TDS values also very high indicating the samples contained elevated amounts of metal solutes. This corroborated with the results obtained for metal content of the samples (Table 5.33) which revealed relatively high concentrations of Hg, Cd, Co, Cu, Fe, Ni and Pb. In addition, the data in Table 5.31 also demonstrated that the constructed biotraps were effective in removing mercury from the environmental water. The adsorption capacity and removal efficiency were 6.081 mg g^{-1} and 67.81% respectively.

Table: 5.30: Hydrochemical properties of AMD samples used

Parameter	Sample 1	Sample 2	Sample 3
Temperature (˚C)	21.8	21.9	21.9
pH	3.16	3.04	3.02
EC (μS cm^{-1})	760	765	785
TDS (μg L^{-1})	362	380	382
Redox potential (mV)	366	375	383

These values show a slight decline from those obtained when the biosorbent was used for biosorption from synthetic solutions. This could be attributed to the matrix effects which were higher in the environmental samples. The values of K_D shown in table 5.33 also revealed that the biosorbents retained their selectivity for mercury over divalent metals even when they were converted to biotraps. Also, as in the batch equilibrium studies conducted using *Cladophora sp* immobilized in alginate beads, the biosorption capacities of the biotraps for the metals in the environmental water followed the order Hg>Pb>Cu> Ni, Fe> Co> Cd.

Table 5.31: Summary of results for application of biotraps for treatment of environmental water samples

Metal	C_0 (mg L^{-1})	C_e (mg L^{-1})	q (mg g^{-1})	r (%)	K_D
Hg	1.052	0.444	6.081	67.81	1.371
Cd	1.252	1.056	1.956	15.62	0.185
Co	0.976	0.702	2.743	28.10	0.391
Cu	0.861	0.478	3.843	44.63	0.806
Fe	0.975	0.659	3.161	32.41	0.479
Ni	1.063	0.705	3.577	35.65	0.507
Pb	0.778	0.385	3.932	49.48	1.322

Campaner et al., (2014) also evaluated the geochemical properties of AMD samples collected from a coal mine in Southern Brazil. Even though, the authors did not measure the TDS and EC of the samples, they found that the pH ranged from 3.2 - 4.5.The redox potentials also fell between 445 and 628 mV showing that the samples were oxidizing. Metal analysis also showed that the samples contained very high levels of As, Al, Cd, Co, Cr, Cu, Mn, Ni, Zn and Pb pollutants. In fact, the levels of Fe, Mn and Zn exceeded those stipulated by Brazilian regulations. Notwithstanding, treatment via chemical neutralization by a mixture of CaO and MgO led to the concentrations of metals depreciating to values within environmentally accepted limits. The removal efficiencies of the treatment method ranged from 0.08% for Al to 67.5% for Mn. The differences between the characteristics of the samples studied by Campaner et al., (2014) and those used in the present study can be explained by variations in geographical location. The disparities in metal removal efficiencies are also due the use of different treatment methods and properties of the AMD samples.

CHAPTER 6: CONCLUSIONS AND RECOMMENDATIONS

This chapter gives a brief overview of the conclusions made from the findings of the study. Recommendations on future work that could be done on the research topic were also made.

6.1 General conclusions

Based on the observations made in this study, it can be concluded that pristine and modified forms of *Cladophora sp* alga are effective biosorbents for the sequestration of mercury from aqueous solutions. Their performances depended on experimental conditions such as pH, initial metal concentration and dosage, temperature and agitation time. The biosorption capacities of the modified biosorbents (particularly the alga immobilized in alginate beads) far exceeded that of the pristine alga. All the biosorbents could be reused up to 3 successive cycles after regeneration using 0.1 M HCl and their biosorption capabilities of the biosorbents were also negatively impacted by the presence of competing ions in solution. However, the modified algal biosorbents were more selective for mercury than the pristine alga.

Kinetic modelling of the biosorption processes also revealed that for all the biosorbents studied, chemisorption was the rate limiting step and intraparticle diffusion was significant only at the start of the biosorption process. Similarly, adsorption isotherm modelling also proved that biosorption of mercury on all the three biosorbents occurred on a homogenous layer and ion exchange was the predominant mechanism. Thermodynamic modelling also demonstrated that the biosorption processes using all the three biosorbents were exothermic.

Continuous flow studies showed that *Cladophora sp* immobilized in alginate beads could be effectively used to biosorb mercury from aqueous solutions using a packed bed configuration. The performance of the column was also affected by experimental conditions i.e. bed height, flow rate and influent metal concentration. The experimental column data was best described by the BDST, Thomas and Yoon

Nelson models. Biotraps based on the alga immobilized in alginate beads were also constructed and they effectively removed mercury from environmental waters.

Therefore, in general, it can be concluded that the results of the study demonstrated that the modified biosorbents (especially *Cladophora sp* immobilized in alginate beads) had potential for utilization in the development of technologies for enhancing mercury removal acid-impacted effluents flowing through wetland systems.

6.2 Recommendations

Based on the findings of the study, the following recommendations are made on how the efficiency of the biosorption systems and method used can be enhanced. First, the production of the alga immobilized in alginate beads step can be automated to save time. Preconcentration of MeHg in the algal samples during the speciation analysis can also be performed using on-line techniques like HPLC –ICP MS to enhance the sensitivity of the method. Further insight on the biosorption mechanism using pristine *Cladophora sp* alga can also be gained by conducting proteomic studies to investigate the role of metallothioneins such as phytochelatins and glutathione in the biosorption process. The effect of mercury sequestration on the photosynthetic pigment of the alga can also be evaluated. Prediction of the breakthrough behavior of the biosorption column packed with *Cladophora sp* alga in large scale operations can also be augmented using statistical models such as artificial neural networks and factorial design experiments. The applicability of the biotraps in wetlands can also be evaluated by upsizing and upscaling them followed by deployment in real wetland conditions so as to study the effects of seasonality and other wetland conditions.

REFERENCES

Abbas, S.H., Ismail, I.M., Mostafa, T.M. and Sulaymon, A.H. (2014) Biosorption of heavy metals: a review. *Journal of Chemical Science and Technology*, vol. 3, no. 4, pp.74-102.

Abdel-Aty, A.M., Ammar, N.S., Ghafar, H.H.A. and Ali, R.K. (2013) Biosorption of cadmium and lead from aqueous solution by fresh water alga *Anabaena sphaerica* biomass. *Journal of Advanced Research*, vol. 4, no. 4, pp.367-374.

Abdel-Raouf, M.S. and Abdul-Raheim, A.R.M. (2017) Removal of heavy metals from industrial waste water by biomass-based materials: a review. *Journal of Pollution Effects and Control*, vol. 5, pp.180-193.

Abdi, O. and Kazemi, M. (2015) A review study of biosorption of heavy metals and comparison between different biosorbents. *Journal of Materials and Environmental Science*, vol. 6, no. 5, pp.1386-1399.

Agrawal, S.B., Agrawal, M., Lee, E.H., Kramer, G.F. and Pillai, P. (1992) Changes in polyamine and glutathione contents of a green alga, *Chlorogonium Elongatum* (Dang) France exposed to mercury, *Environmental and Experimental Botany*, vol. 32, no. 2, pp. 145-151.

Ahmady-Asbchin, S., Andres, Y., Gérente, C. and Le Cloirec, P. (2008) Biosorption of Cu (II) from aqueous solution by *Fucus serratus*: Surface characterization and sorption mechanisms. *Bioresource Technology*, vol. 99, no. 14, pp.6150-6155.

Ahmady-Asbchin, S. and Azhdehakoshpour, A. (2012) Biosorption of Cu (II) and Ni (II) ions from aqueous solution by marine brown algae *Sargassum angustifolium*. *Journal of Biodiversity and Environmental Sciences*, vol. 6, no. 18, pp.271-279.

Akcil, A. and Koldas, S., (2006). Acid Mine Drainage (AMD): causes, treatment and case studies. *Journal of Cleaner Production*, vol. 14, no. 12-13, pp.1139-1145.

Aksu, Z., (2001) Equilibrium and kinetic modeling of cadmium (II) biosorption by *Chlorella vulgaris* in a batch system: effect of temperature. *Separation and Purification Technology*, vol. 21, no. 3, pp.285-294.

Al-Homaidan, A.A., Al-Houri, H.J., Al-Hazzani, A.A., Elgaaly, G. and Moubayed, N.M. (2014). Biosorption of copper ions from aqueous solutions by *Spirulina platensis* biomass. *Arabian Journal of Chemistry*, vol. 7, no. 1, pp.57-62.

Al Rmalli, S.W., Dahmani, A.A., Abuein, M.M. and Gleza, A.A. (2008). Biosorption of mercury from aqueous solutions by powdered leaves of castor tree (*Ricinus communis L.*). *Journal of Hazardous Materials*, vol. 152, no. 3, pp.955-959.

Al-Rub, F.A., El-Naas, M.H., Benyahia, F. and Ashour, I. (2004). Biosorption of nickel on blank alginate beads, free and immobilized algal cells, *Process Biochemistry*, vol. 39, no. 11, pp.1767-1773.

Al-Qodah, Z., Al-Shannag, M., Amro, A., Bob, M., Bani-Melhem, K. and Alkasrawi, M. (2017). Impact of surface modification of green algal biomass by phosphorylation on the removal of copper (II) ions from water. *Turkish Journal of Chemistry*, vol. 41, no.2, pp.190-208.

Amin, F., Talpur, F.N., Balouch, A., Chandio, Z.A., Surhio, M.A. and Afridi, H.I. (2016). Biosorption of mercury (II) from aqueous solution by fungal biomass *Pleurotus eryngii*: isotherm, kinetic, and thermodynamic studies. *Environmental Progress & Sustainable Energy*, vol. 35, no. 5, pp.1274-1282.

Amde, M., Yin, Y., Zhang, D. and Liu, J. (2016) Methods and recent advances in speciation analysis of mercury chemical species in environmental samples: a review. *Chemical Speciation & Bioavailability*, vol. 28, no. 1-4, pp.51-65.

Anirudhan, T.S. and Sreekumari, S.S. (2011) Adsorptive removal of heavy metal ions from industrial effluents using activated carbon derived from waste coconut buttons. *Journal of Environmental Sciences*, vol. 23, no. 12, pp.1989-1998.

Apiratikul, R. and Pavasant, P. (2008) Batch and column studies of biosorption of heavy metals by *Caulerpa lentillifera*. *Bioresource technology*, vol. 99, no. 8, pp.2766-2777.

Aravindhan, R., Fathima, N.N., Rao, J.R. and Nair, B.U. (2007) Equilibrium and thermodynamic studies on the removal of basic black dye using calcium alginate beads. *Colloids and Surfaces A: Physicochemical and Engineering Aspects*, vol. 299, no. 1-3, pp.232-238.

Babel, S. and Kurniawan, T.A. (2003) Low-cost adsorbents for heavy metals uptake from contaminated water: a review. *Journal of Hazardous Materials*, vol. 97, no. 1-3, pp.219-243.

Babu, P.N., Binnal, P. and Kumar, D.J. (2015) Biosorption of Zn+ 2 on non-living biomass of *Spirulina platensis* immobilized on polyurethane foam cubes&58; Column studies. *Journal of Biochemical Technology*, vol. 6, no. 1, pp.852-859.

Bağda, E., Tuzen, M. and Sarı, A. (2017) Equilibrium, thermodynamic and kinetic investigations for biosorption of uranium with green algae (*Cladophora hutchinsiae*). *Journal of Environmental Radioactivity*, vol. 175, pp.7-14.

Bai, R.S. and Abraham, T.E. (2002) Studies on enhancement of Cr (VI) biosorption by chemically modified biomass of *Rhizopus nigricans*. *Water Research*, vol. 36, no. 5, pp.1224-1236.

Bakir, A., McLoughlin, P., Tofail, S.A. and Fitzgerald, E. (2009) Competitive Sorption of Antimony with Zinc, Nickel, and Aluminum in a Seaweed Based Fixed-bed Sorption Column. *CLEAN–Soil, Air, Water*, vol.37, no. 9, pp.712-719.

Ballan-Dufrançais, C., Marcaillou, C. and Amiard-Triquet, C. (1991) Response of the phytoplanctonic alga *Tetraselmis suecica* to copper and silver exposure: vesicular metal bioaccumulation and lack of starch bodies. *Biology of the Cell*, 72, no. 1-2, pp.103-112.

Baral, S.S., Das, N., Ramulu, T.S., Sahoo, S.K., Das, S.N. and Chaudhury, G.R. (2009) Removal of Cr (VI) by thermally activated weed *Salvinia cucullata* in a

fixed-bed column. *Journal of Hazardous Materials*, vol. 161, no. 2-3, pp.1427-1435.

Barsanti, L. and Gualtieri, P. (2006) *Algae: Anatomy, Biochemistry, and Biotechnology*. CRC press, Boca Raton, Florida, USA.

Bayramoğlu, G., Tuzun, I., Celik, G., Yilmaz, M. and Arica, M.Y. (2006) Biosorption of mercury (II), cadmium (II) and lead (II) ions from aqueous system by microalgae *Chlamydomonas reinhardtii* immobilized in alginate beads. *International Journal of Mineral Processing*, vol. 81, no. 1, pp.35-43.

Bayramoğlu, G. and Arıca, M.Y. (2009) Construction of a hybrid biosorbent using *Scenedesmus quadricauda* and Ca-alginate for biosorption of Cu (II), Zn (II) and Ni (II): kinetics and equilibrium studies. *Bioresource Technology*, vol. 100, no. 1, pp.186-193.

Beining, B.A. and Otte, M.L. (1997) Retention of metals and longevity of a wetland receiving mine leachate. In: *Proceedings of the 14th National Meeting of American Society for Surface Mining and Reclamation*. Austin, Texas pp. 43-46.

Benavente, M., Moreno, L. and Martinez, J. (2011) Sorption of heavy metals from gold mining wastewater using chitosan. *Journal of the Taiwan Institute of Chemical Engineers*, vol. 42, no. 6, pp.976-988.

Bermúdez, Y.G., Rico, I.L.R., Bermúdez, O.G. and Guibal, E. (2011) Nickel biosorption using *Gracilaria caudata and Sargassum muticum*. *Chemical Engineering Journal*, vol. 166, no. 1, pp.122-131.

Bhatnagar, A., Vilar, V.J., Ferreira, C., Botelho, C.M. and Boaventura, R.A. (2012) Optimization of nickel biosorption by chemically modified brown macroalgae (*Pelvetia canaliculata*). *Chemical Engineering Journal*, vol. 193, pp. 256-266. Blue, L.Y., Van Aelstyn,

Blue, L.Y., Van Aelstyn, M.A. and Atwood, D.A (2008) Low-level mercury removal from groundwater using a chelating ligand. *Water Research*, vol. 42, pp. 2025– 2028

Bonanno, G. (2013) Comparative performance of trace element bioaccumulation and biomonitoring in the plant species *Typha domingensis*, *Phragmites australis* and *Arundo donax*. *Ecotoxicology and Environmental Safety*, vol. 97, pp.124-130.

Braaten, H, F, V., de Wit, H. A., Fjeld, E. and Rognerod, S. (2014) Environmental factors influencing mercury speciation in Subarctic boreal lakes. *Science of the Total Environment*, vol. 476-477, pp.336-345

Branfireun, B.A., Roulet, N.T., Kelly, C. and Rudd, J.W. (1999) In situ sulfate stimulation of mercury methylation in a boreal peatland: Toward a link between acid rain and methylmercury contamination in remote environments. *Global Biogeochemical Cycles*, vol. 13, no. 3, pp.743-750.

Bravo, A.G., Le Faucheur, S., Monperrus, M., Amouroux, D. and Slaveykova, V.I. (2014) Species-specific isotope tracers to study the accumulation and biotransformation of mixtures of inorganic and methyl mercury by the microalga *Chlamydomonas reinhardtii*, *Environmental Pollution*, vol. 192, pp.212-215.

Bulgariu, D. and Bulgariu, L. (2012) Equilibrium and kinetics studies of heavy metal ions biosorption on green algae waste biomass. *Bioresource Technology*, vol. 103, no. 1, pp.489-493.

Bulgariu, D. and Bulgariu, L. (2016) Potential use of alkaline treated algae waste biomass as sustainable biosorbent for clean recovery of cadmium (II) from aqueous media: batch and column studies. *Journal of Cleaner Production*, vol. 112, pp.4525-4533.

Bulut, Y. and Tez, Z. (2007) Removal of heavy metals from aqueous solution by sawdust adsorption. *Journal of Environmental Sciences*, vol. 19, no. 2, pp.160-166.

Butler, M. Haskew, A.E. and Young, M.M. (1980) Copper tolerance in the green alga, *Chlorella vulgaris*. *Plant, Cell & Environment*, vol. 3, no. 2, pp.119-126.

Calderón, J., Gonçalves, S., Cordeiro, F. and de la Calle, B. (2013) *Determination of Methylmercury in Seafood by Direct Mercury Analysis: Standard Operating Procedure*. European Commission Joint Research Center, Report JRC 80259 EN, pp.1-12.

Campaner, V.P., Luiz-Silva, W. and Machado, W. (2014). Geochemistry of acid mine drainage from a coal mining area and processes controlling metal attenuation in stream waters, southern Brazil. *Anais da Academia Brasileira de Ciências*, vol. 86, no. 2, pp.539-554.

Carrilho, E.N.V., Nóbrega, J.A. and Gilbert, T.R. (2003) The use of silica-immobilized brown alga (*Pilayella littoralis*) for metal preconcentration and determination by inductively coupled plasma optical emission spectrometry. *Talanta*, vol. 60, no. 6, pp.1131-1140.

Carro, L., Barriada, J.L., Herrero, R. and de Vicente, M.E.S. (2011) Adsorptive behavior of mercury on algal biomass: Competition with divalent cations and organic compounds. *Journal of Hazardous Materials*, vol. 192, no.1, pp.284-291.

Carro, L., Barriada, J.L., Herrero, R. and de Vicente, M.E.S. (2013) Surface modifications of *Sargassum muticum* algal biomass for mercury removal: A physicochemical study in batch and continuous flow conditions. *Chemical Engineering Journal*, vol. 229, pp.378-387.

Cazón, J.P., Viera, M., Donati, E. and Guibal, E. (2013) Zinc and cadmium removal by biosorption on *Undaria pinnatifida* in batch and continuous processes. *Journal of Environmental Management*, vol. 129, pp.423-434.

Chander, S. and Zhou, R. (1992) Effect of organic additives on acid generation from pyrite waste. In : *Emerging Process Technologies for a Cleaner Environment*, eds., S. Chander, PE Richardson and H. El-Shall, Society of Mining, Metallurgy and Exploration, Inc, pp.131-139.

Chen, Y. Li, Y. Cai, M. Belzile, N. and Dhang, Z. (2006a) Prevention of oxidation of iron sulfides minerals by polyethylene amines, *Minerals Engineering*, vol. 19, pp. 19-27

Chen, T.Y. Kao, C. M. Yeh, T.Y Chein, H.Y. and Chao, A.C. (2006b) Application of a constructed wetland for industrial wastewater treatment: a pilot-scale study, *Chemosphere*, vol. 64, no. 3, pp. 497-502.

Chen, J.P., and Yang, L. (2006) Study of a heavy metal biosorption onto raw and chemically modified *Sargassum sp*. via spectroscopic and modeling analysis. *Langmuir*, vol. 22, no. 21, pp.8906-8914.

Chen, C., Wen, D. and Wang, J. (2014) Cellular surface characteristics of *Saccharomyces cerevisiae* before and after Ag (I) biosorption. *Bioresource Technology*, vol. 156, pp.380-383.

Chen, G.Q. Li, J.S. Chen, B. Wen, C. Yang, Q. Alsaedi, A. and Hayat, T. (2016) An overview of mercury emissions by global fuel combustion: the impact of international trade. *Renewable and Sustainable Energy Reviews*, vol. 65, pp.345-355.

Chojnacka, K., Chojnacki, A., and Gorecka, H. (2005) Biosorption of Cr^{3+}, Cd^{2+} and Cu^{2+} ions by blue-green algae *Spirulina sp*.: kinetics, equilibrium and the mechanism of the process. *Chemosphere*, vol. 59, no. 1, pp.75-84.

Chojnacki, A., Chojnacka, K., Hoffmann, J., and Gorecki, H. (2004) The application of natural zeolites for mercury removal: from laboratory tests to industrial scale. *Minerals Engineering*, vol. 17, no. 7-8, pp.933-937.

Chowdhury, Z.Z., Zain, S.M., Rashid, A.K., Rafique, R.F. and Khalid, K. (2013) Breakthrough curve analysis for column dynamics sorption of Mn (II) ions from wastewater by using *Mangostana garcinia* peel-based granular-activated carbon. *Journal of Chemistry*, vol. 2013, pp. 1-8.

Crhribi, A. and Chlendi, M. (2011) Modeling of fixed bed adsorption: application to the adsorption of an organic dye. *Asian Journal of Textile*, vol. 1, no. 4, pp.61-171.

Cobbett, C. and Goldsbrough, P. (2002) Phytochelatins and metallothioneins: roles in heavy metal detoxification and homeostasis. *Annual Review of Plant Biology*, vol. 53, no. 1, pp.159-182.

Covelli, S., Faganeli, J., Horvat, M. and Brambati, A. (1999) Porewater distribution and benthic flux measurements of mercury and methylmercury in the Gulf of

Trieste (Northern Adriatic Sea), *Estuarine, Coastal and Shelf Science*, vol. 48, no. 4, pp.415-428.

Cravotta, C.A. (2003) Size and performance of anoxic limestone drains to neutralize acidic mine drainage, *Journal of Environmental Quality*, vol. 32, no. 4, pp. 1277-1289.

Creswell, J.E., Shafer, M.M., Babiarz, C.L., Tan, S.Z., Musinsky, A.L., Schott, T.H., Roden, E.E. and Armstrong, D.E. (2017) Biogeochemical controls on mercury methylation in the Allequash Creek wetland. *Environmental Science and Pollution Research*, vol. 24, no. 18, pp.15325-15339.

Crhribi, A. and Chlendi, M. (2011) Modeling of fixed bed adsorption: application to the adsorption of an organic dye. *Asian Journal of Textile*, no. 1, pp.161-171.

Cyr, P.J., Suri, R.P. and Helmig, E.D. (2002) A pilot scale evaluation of removal of mercury from pharmaceutical wastewater using granular activated carbon. *Water Research*, vol. 36, no. 19, pp.4725-4734.

Dada, A.O., Olalekan, A.P., Olatunya, A.M. and Dada, O. (2012) Langmuir, Freundlich, Temkin and Dubinin–Radushkevich isotherms studies of equilibrium sorption of Zn2+ unto phosphoric acid modified rice husk. *International Organization of Scientific Research Journal of Applied Chemistry*, vol. 3, no. 1, pp.38-45.

Daemi, H. and Barikani, M. (2012) Synthesis and characterization of calcium alginate nanoparticles, sodium homopolymannuronate salt and its calcium nanoparticles, *Scientia Iranica*. vol. 19, no. 6, pp.2023-2028.

Das, S.K, Das, A.R. and Guha, A.K. (2007) A study on the biosorption mechanism of mercury on *Aspergillus versicolor* biomass, *Environmental Science and Technology*, vol. 41, pp. 8281-8287

Dash, H.R. and Das, S. (2012) Bioremediation of mercury and the importance of bacterial mer genes. *International Biodeterioration & Biodegradation*, vol. 75, pp.207-213.

De, M., Azargohar, R., Dalai, A.K. and Shewchuk, S.R. (2013) Mercury removal by bio-char based modified activated carbons. *Fuel*, vol.103, pp.570-578.

Dean, A.P., Lynch, S., Rowland, P., Toft, B.D., Pittman, J.K. and White, K.N. (2013) Natural wetlands are efficient at providing long-term metal remediation of freshwater systems polluted by acid mine drainage. *Environmental Science & Technology*, vol. 47, no. 21, pp.12029-12036.

De-Bashan, L.E. and Bashan, Y. (2010) Immobilized microalgae for removing pollutants: review of practical aspects. *Bioresource Technology*, vol. 101, no. 6, pp.1611-1627.

De Klerk, L.P., De Klerk, A.R. and Wepener, V. (2013) An assessment of mercury contamination and the relationship between environmental variables and mercury concentrations in a seasonal wetland. *Water, Air, & Soil Pollution*, vol. 224, no. 5, p.1547.

Demirbas, A., (2008) Heavy metal adsorption onto agro-based waste materials: a review. *Journal of Hazardous Materials*, vol. 157, no. (2-3), pp.220-229.

Di Natale, F., Erto, A., Lancia, A. and Musmarra, D. (2011) Mercury adsorption on granular activated carbon in aqueous solutions containing nitrates and chlorides. *Journal of Hazardous Materials*, vol. 192, no. 3, pp.1842-1850.

Dönmez, G.Ç., Aksu, Z., Öztürk, A. and Kutsal, T. (1999) A comparative study on heavy metal biosorption characteristics of some algae. *Process Biochemistry*, vol. 34, no. 9, pp. 885-892.

Doshi, H., Ray, A. and Kothari, I.L. (2007) Bioremediation potential of live and dead Spirulina: spectroscopic, kinetics and SEM studies. *Biotechnology and Bioengineering*, vol. 96, no. 6, pp.1051-1063.

Driscoll, C.T., Mason, R.P., Chan, H.M., Jacob, D.J. and Pirrone, N. (2013) Mercury as a global pollutant: sources, pathways, and effects. *Environmental Science & Technology*, vol. 47, no. 10, pp.4967-4983.

Dufault, R. LeBlanc, B. Schnoll, R. Cornett, C. Schweitzer, L. Wallinga, D. Hightower, J. Patrick, L. and Lukiw, W.J. (2009) Mercury from chlor-alkali plants:

measured concentrations in food product sugar, *Environmental Health*, vol. 8, no. 1, pp. 2-6.

Durand, J.F. (2012) The impact of gold mining on the Witwatersrand on the rivers and karst system of Gauteng and North West Province, South Africa. *Journal of African Earth Sciences,* vol. 68, pp.24-43.

Ebinghaus, R. Turner, R.R. de Lacerda, L.D. Vasiliev, O. and Salomons, W. eds., (1999) *Mercury Contaminated Sites: Characterization, Risk assessment and Remediation*, Springer Science & Business Media, Berlin, Germany

Eckley, C, S. and Hintelmann, H., (2006) Determination of mercury methylation potentials in the water column of lakes across Canada, *Science of the Total Environment,* vol. 368, pp. 111-125

Egiebor, N.O. and Oni, B., (2007) Acid rock drainage formation and treatment: a review. *Asia-Pacific Journal of Chemical Engineering,* vol. 2, no. 1, pp.47-62.

El Hassouni, H., Abdellaoui, D., El Hani, S. and Bengueddour, R. (2014) Biosorption of cadmium (II) and copper (II) from aqueous solution using red alga (*Osmundea pinnatifida*) biomass. *Journal of Materials and Environmental Science*, vol. 5, pp.967-974.

El-Sikaily, A., El Nemr, A. and Khaled, A. (2011) Copper sorption onto dried red alga Pterocladia capillacea and its activated carbon. *Chemical Engineering Journal*, vol. 168, no. 2, pp.707-714.

Esmaeili, A., Saremnia, B. and Kalantari, M. (2015) Removal of mercury (II) from aqueous solutions by biosorption on the biomass of *Sargassum glaucescens* and *Gracilaria corticata*. *Arabian Journal of Chemistry*, vol. 8, no. 4, pp.506-511.

Equeenuddin, S.M., Tripathy, S., Sahoo, P.K. and Panigrahi, M.K. (2010) Hydrogeochemical characteristics of acid mine drainage and water pollution at Makum Coalfield, India. *Journal of Geochemical Exploration*, vol. 105, no. 3, pp.75-82.

Etale, A., Tutu, H., and Drake, D.C. (2016) Application of maghemite nanoparticles as sorbents for the removal of Cu (II), Mn (II) and U (VI) ions from aqueous

solution in acid mine drainage conditions. *Applied Water Science*, vol. 6, no. 2, pp.187-197.

Fardmousavi, O. and Faghihian, H. (2014) Thiol-functionalized hierarchical zeolite nanocomposite for adsorption of Hg^{2+} from aqueous solutions. *Comptes Rendus Chimie*, vol. 17, no. 12, pp.1203-1211.

Fang, L., Zhou, C., Cai, P., Chen, W., Rong, X., Dai, K., Liang, W., Gu, J.D. and Huang, Q. (2011) Binding characteristics of copper and cadmium by cyanobacterium *Spirulina platensis*. *Journal of Hazardous Materials*, vol. 190, no. 1-3, pp.810-815.

Faulwetter, J.L., Gagnon, V., Sundberg, C., Chazarenc, F., Burr, M.D., Brisson, J., Camper, A.K. and Stein, O.R. (2009) Microbial processes influencing performance of treatment wetlands: a review. *Ecological Engineering*, vol. 35, no. 6, pp.987-1004.

Feather, C.E. and Koen, G.M. (1975) Mineralogy of the Witwatersrand reefs. *Minerals Science and Engineering*, vol. 7, pp. 189-224

Feng, D., Aldrich, C. and Tan, H. (2000) Treatment of acid mine water by use of heavy metal precipitation and ion exchange. *Minerals Engineering*, vol. 13, no. 6, pp.623-642.

Ferraz, A.I., Tavares, T. and Teixeira, J.A. (2004) Cr (III) removal and recovery from *Saccharomyces cerevisiae*, *Chemical Engineering Journal*, vol. 105, no. 1-2, pp.11-20.

Figueira, M.M., Volesky, B. and Mathieu, H.J. (1999) Instrumental analysis study of iron species biosorption by *Sargassum* biomass. *Environmental Science & Technology*, vol. 33, no. 11, pp.1840-1846.

Figueira, P., Lopes, C.B., Daniel-da-Silva, A.L., Pereira, E., Duarte, A.C. and Trindade, T. (2011) Removal of mercury (II) by dithiocarbamate surface functionalized magnetite particles: application to synthetic and natural spiked waters. *Water Research*, vol. 45, no. 1, pp.5773-5784.

Filote, C., Ungureanu, G., Boaventura, R., Santos, S., Volf, I. and Botelho, C. (2017) Green macroalgae from the Romanian coast of Black Sea: Physico-chemical characterization and future perspectives on their use as metal anions biosorbents. *Process Safety and Environmental Protection*, vol. 108, pp.34-43.

Fomina, M. and Gadd, G.M. (2014) Biosorption: current perspectives on concept, definition and application. *Bioresource Technology*, vol. 160, pp.3-14.

Fourest, E. and Volesky, B. (1995) Contribution of sulfonate groups and alginate to heavy metal biosorption by the dry biomass of *Sargassum fluitans*. *Environmental Science & Technology*, vol. 30, no. 1, pp.277-282.

Frohne, T., Rinklebe, J., Langer, U., Laing, G.D., Mothes, S. and Wennrich, R. (2012) Biogeochemical factors affecting mercury methylation rate in two contaminated floodplain soils. *Biogeosciences*, vol. 9, no. 1, pp.493-507.

Fu, F. and Wang, Q. (2011) Removal of heavy metal ions from wastewaters: a review. *Journal of Environmental Management*, vol. 92, no. 3, pp.407-418.

Gaikwad, R.W. and Gupta, D.V. (2008) Review on removal of heavy metals from acid mine drainage. *Applied Ecology and Environmental Research*, vol. 6, no. 3, pp.81-98.

Garland, R., (2011) Acid mine drainage-the chemistry: environmental science. *Quest*, vol. 7, no. 2, pp.50-52.

Gazea, B. Adam, K. and Kontopoulos, A. (1996) A review of passive systems for the treatment of acid mine drainage. *Minerals Engineering*, vol. 9, no. 1, pp.23-42.

Ghasemi, M., Keshtkar, A.R., Dabbag, R. and Jabber, S.S. (2011) Biosorption of uranium in a continuous flow packed bed column using *Cystoseira indica* biomass: Breakthrough curve studies and modeling. *Journal of Hazardous Materials*, vol. 189, pp. 141-149

Ghodbane, I. and Hamdaoui, O. (2008). Removal of mercury (II) from aqueous media using eucalyptus bark: kinetic and equilibrium studies. *Journal of Hazardous Materials*, vol. 160, no. 2-3, pp.301-309.

Ghoneim, M.M., El-Desoky, H.S., El-Moselhy, K.M., Amer, A., El-Naga, E.H.A., Mohamedein, L.I. and Al-Prol, A.E. (2014) Removal of cadmium from aqueous solution using marine green algae, *Ulva lactuca*. *The Egyptian Journal of Aquatic Research*, vol. 40, no. 3, pp.235-242.

Gibert, O. Rötting, T. Cortina, J.L. de Pablo, J. Ayora, C. Carrera, J. and Bolzicco, J. (2011) In-situ remediation of acid mine drainage using a permeable reactive barrier in Aznalcollar (SW Spain). *Journal of Hazardous Materials*, vol. 191, no. 1-3, pp.287-295.

Gin, K.Y.H., Tang, Y.Z. and Aziz, M.A. (2002) Derivation and application of a new model for heavy metal biosorption by algae. *Water Research*, vol. 36, no. 5, pp.1313-1323.

Gokhale, S.V., Jyoti, K.K. and Lele, S.S. (2009) Modeling of chromium (VI) biosorption by immobilized *Spirulina platensis* in packed column. Journal of Hazardous Materials, vol. 170, no. 2-3, pp.735-743.

Gomes, M.V.T., de Souza, R.R., Teles, V.S. and Mendes, É.A. (2014) Phytoremediation of water contaminated with mercury using *Typha domingensis* in constructed wetland. *Chemosphere*, vol. 103, pp.228-233.

Gönen, F. and Aksu, Z. (2003) A comparative adsorption/biosorption of phenol to granular activated carbon and immobilized activated sludge in a continuous packed bed reactor. *Chemical Engineering Communications*, vol. 190, no. 5-8, pp.763-778.

González, P.G. and Pliego-Cuervo, Y.B. (2014) Adsorption of Cd (II), Hg (II) and Zn (II) from aqueous solution using mesoporous activated carbon produced from *Bambusa vulgaris striata*. *Chemical Engineering Research and Design*, vol. 92, no.11, pp.2715-2724.

Gray, N.F. (1997) Environmental impact and remediation of acid mine drainage: a management problem. *Environmental Geology*, vol. 30, no. 1-2, pp.62-71.

Green-Ruiz, C. (2006) Mercury (II) removal from aqueous solutions by nonviable *Bacillus sp.* from a tropical estuary. *Bioresource Technology*, vol. 97, no. 15, pp.1907-1911.

Guler, U.A. and Sarioglu, M. (2013) Single and binary biosorption of Cu (II), Ni (II) and methylene blue by raw and pretreated *Spirogyra sp*.: equilibrium and kinetic modeling. *Journal of Environmental Chemical Engineering*, vol. 1, no. 3, pp.369-377.

Gupta, R., Ahuja, P., Khan, S., Saxena, R.K. and Mohapatra, H. (2000) Microbial biosorbents: meeting challenges of heavy metal pollution in aqueous solutions. *Current Science*, pp.967-973.

Gupta, V.K., Shrivastava, A.K. and Jain, N. (2001) Biosorption of chromium (VI) from aqueous solutions by green algae *Spirogyra* species. *Water Research*, vol. 35, no. 17, pp.4079-4085.

Gupta, V.K., Rastogi, A., Saini, V.K. and Jain, N. (2006) Biosorption of copper (II) from aqueous solutions by *Spirogyra* species, *Journal of Colloid and Interface Science*, vol. 296, no. 1, pp.59-63.

Gupta, V.K. and Rastogi, A. (2008) Biosorption of lead (II) from aqueous solutions by non-living algal biomass *Oedogonium sp*. and *Nostoc sp*.—a comparative study. *Colloids and Surfaces B: Biointerfaces*, vol. 64, no. 2, pp.170-178.

Gustin, M.S., Chavan, P.V., Dennett, K.E., Donaldson, S., Marchand, E. and Fernanadez, G. (2006) Use of constructed wetlands with four different experimental designs to assess the potential for methyl and total Hg outputs. *Applied Geochemistry*, vol. 21, no. 11, pp.2023-2035.

Hackbarth, F.V., Girardi, F., de Souza, S.M.G.U., de Souza, A.A.U., Boaventura, R.A. and Vilar, V.J. (2014) Marine macroalgae *Pelvetia canaliculata* (*Phaeophyceae*) as a natural cation exchanger for cadmium and lead ions separation in aqueous solutions. *Chemical Engineering Journal*, vol. 242, pp.294-305.

Hadi, P., To, M.H., Hui, C.W., Lin, C.S.K. and McKay, G. (2015) Aqueous mercury adsorption by activated carbons. *Water Research*, vol.73, pp.37-55.

Hafeznezami, S. Kim, J.L. and Redman, J. (2012) Evaluating removal efficiency of heavy metals in constructed wetlands. *Journal of Environmental Engineering*, vol. 138, no. 4, pp.475-482.

Hall, B.D., Aiken, G.R., Krabbenhoft, D.P., Marvin-DiPasquale, M. and Swarzenski, C.M. (2008) Wetlands as principal zones of methylmercury production in southern Louisiana and the Gulf of Mexico region. *Environmental Pollution*, vol. 154, no. 1, pp.124-134.

Han, D.S., Orillano, M., Khodary, A., Duan, Y., Batchelor, B. and Abdel-Wahab, A. (2014) Reactive iron sulfide (FeS)-supported ultrafiltration for removal of mercury (Hg (II)) from water. *Water Research*, vol. 53, pp.310-321.

Harris, R., Murray, M.W., Saltman, T., Mason, R., Krabbenhoft, D.P. and Reash, R. eds. (2007) *Ecosystem Responses to Mercury Contamination: Indicators of Change.* CRC Press. Webster, NY, USA

Haydar, S., Ahmad, M.F. and Hussain, G. (2016) Evaluation of new biosorbents prepared from immobilized biomass of *Candida sp*. for the removal of nickel ions. *Desalination and Water Treatment*, vol. 57, no. 12, pp.5601-5613.

He, J. and Chen, J.P. (2014) A comprehensive review on biosorption of heavy metals by algal biomass: materials, performances, chemistry, and modeling simulation tools. *Bioresource Technology*, vol. 160, pp.67-78.

Hegazy, A.K., Abdel-Ghani, N.T. and El-Chaghaby, G.A. (2011) Phytoremediation of industrial wastewater potentiality by *Typha domingensis*. *International Journal of Environmental Science & Technology*, vol. 8, no. 3, pp.639-648.

Herrero, R., Lodeiro, P., Rey-Castro, C., Vilariño, T. and De Vicente, M.E.S. (2005) Removal of inorganic mercury from aqueous solutions by biomass of the marine macroalga *Cystoseira baccata*. *Water Research*, vol. 39, no. 14, pp.3199-3210.

Hoggarth, C.G., Hall, B.D. and Mitchell, C.P. (2015) Mercury methylation in high and low-sulfate impacted wetland ponds within the prairie pothole region of North America. *Environmental Pollution*, vol. 205, pp.269-277.

Huang, S. and Lin, G. (2015) Biosorption of Hg (II) and Cu (II) by biomass of dried *Sargassum fusiforme* in aquatic solution. *Journal of Environmental Health Science and Engineering*, vol. 13, no. 1, p.21.

Huang, S., Ma, C., Liao, Y., Min, C., Du, P. and Jiang, Y. (2016) Removal of mercury(II) from aqueous solutions by adsorption on poly1-amino-5-chloroanthraquinone nanofibrils. *Journal of Nanomaterials*, vol. 2016, p.53-64.

Hudson, R.J. Gherini, S.A. Watras, C.J. and Porcella, D.B. (1994) Modeling the biogeochemical cycle of mercury in lakes: The mercury cycling model (MCM) and its application to the MTL study lakes, *Mercury pollution: integration and synthesis*, pp.473-523.

Hutchison, A.R. and Atwood, D.A. (2003) Mercury pollution and remediation: the chemist's response to a global crisis. *Journal of Chemical Crystallography*, vol. 33, no. 8, pp.631-645.

Islam, S., Bhuiyan, M.R. and Islam, M.N. (2017) Chitin and chitosan: structure, properties and applications in biomedical engineering. *Journal of Polymers and the Environment*, vol. 25, no. 3, pp.854-866.

Jain, M., Garg, V.K. and Kadirvelu, K. (2013) Cadmium (II) sorption and desorption in a fixed bed column using sunflower waste carbon calcium–alginate beads. *Bioresource Technology*, vol. 129, pp.242-248.

Jeffers, T.H., Ferguson, C.R. and Bennett, P.G. (1991) *Biosorption of Metal Contaminants using Immobilized Biomass: A Laboratory Study*. US Department of the Interior, Bureau of Mines.

Jeon, C.S., Baek, K., Park, J.K., Oh, Y.K. and Lee, S.D. (2009) Adsorption characteristics of As (V) on iron-coated zeolite. *Journal of Hazardous Materials*, vol. 163, no. 2-3, pp.804-808.

Ji, L., Xie, S., Feng, J., Li, Y. and Chen, L. (2012) Heavy metal uptake capacities by the common freshwater green alga *Cladophora fracta*. *Journal of Applied Phycology*, vol. 24, no. 4, pp.979-983.

Jiang, C.L., Wang, X.H. and Parekh, B.K. (2000) Effect of sodium oleate on inhibiting pyrite oxidation. *International Journal of Mineral Processing*, vol. 58, no. 1-4, pp.305-318.

Johnson, M., Shivkumar, S. and Berlowitz-Tarrant, L. (1996) Structure and properties of filamentous green algae. *Materials Science and Engineering: B*, vol. 38, no. 1-2, pp.103-108.

Johnson, D.B. and Hallberg, K.B. (2005) Acid mine drainage remediation options: a review. *Science of the Total Environment*, vol. 338, no. 1-2, pp.3-14.

Kacar, Y., Arpa, Ç., Tan, S., Denizli, A., Genç, Ö. and Arıca, M.Y. (2002) Biosorption of Hg (II) and Cd (II) from aqueous solutions: comparison of biosorptive capacity of alginate and immobilized live and heat inactivated *Phanerochaete chrysosporium*. *Process Biochemistry*, vol. 37, no. 6, pp.601-610.

Kadlec, R.H. and Knight, R.L. (1996) *Treatment Wetlands*, CRC, Baca Raton, FL.

Kalin, M., Fyson, A. and Wheeler, W.N. (2006) The chemistry of conventional and alternative treatment systems for the neutralization of acid mine drainage. *Science of the Total Environment*, vol. 366, no. 2-3, pp.395-408.

Kang, C.U., Jeon, B.H., Park, S.S., Kang, J.S., Kim, K.H., Kim, D.K., Choi, U.K. and Kim, S.J. (2016) Inhibition of pyrite oxidation by surface coating: a long-term field study. *Environmental Geochemistry and Health*, vol. 38, no. 5, pp.1137-1146.

Kapoor, A. and Viraraghavan, T. (1998) Removal of heavy metals from aqueous solutions using immobilized fungal biomass in continuous mode. *Water Research*, vol. 32, no. 6, pp.1968-1977.

Karthikeyan, S., Balasubramanian, R. and Iyer, C.S.P. (2007) Evaluation of the marine algae Ulva fasciata and Sargassum sp. for the biosorption of Cu (II) from aqueous solutions. *Bioresource Technology*, vol. 98, no. 2, pp.452-455.

Kefeni, K.K., Msagati, T.A. and Mamba, B.B. (2017) Acid mine drainage: prevention, treatment options, and resource recovery: a review. *Journal of Cleaner Production*, vol. 151, pp.475-493.

Khan, S. Ahmad, I. Shah, M.T. Rehman, S. and Khaliq, A. (2009) Use of constructed wetland for the removal of heavy metals from industrial wastewater. *Journal of Environmental Management*, vol. 90, no. 11, pp.3451-3457.

Khoramabadi, S. G., Jafari, A., and Jamshidi, H. J. (2008) Biosorption of mercury (II) from aqueous solutions by *Zygnema fanicum* algae. *Journal of Applied Sciences*, vol. 8, pp.2168-2172.

Khoramzadeh, E., Nasernejad, B. and Halladj, R. (2013) Mercury biosorption from aqueous solutions by sugarcane bagasse. *Journal of the Taiwan Institute of Chemical Engineers*, vol. 44, no. 2, pp.266-269.

King, J.K., Harmon, S.M., Fu, T.T. and Gladden, J.B. (2002) Mercury removal, methylmercury formation, and sulfate-reducing bacteria profiles in wetland mesocosms. *Chemosphere*, vol. 46, no. 6, pp.859-870.

Kirova, G., Velkova, Z. and Gochev, V. (2012) Copper (II) removal by heat-inactivated *Streptomyces fradiae* biomass: Surface chemistry characterization of the biosorbent. *Journal of Bioscience and Biotechnology*, pp.77-82.

Kleinmann, R.L., and Erickson, P.M. (1982) Control of acid mine drainage using anionic surfactants. In: *International Mine Water Association Proceedings*, pp. 51-64.

Kleinübing, S.J., Da Silva, E.A., Da Silva, M.G.C. and Guibal, E., (2011) Equilibrium of Cu (II) and Ni (II) biosorption by marine alga *Sargassum filipendula* in a dynamic system: competitiveness and selectivity. *Bioresource Technology*, vol. 102, no. 7, pp.4610-4617.

Kolbash, R.L. and Romanoski, R.L. (1989) Windsor coal company wetland: an overview. In: *Constructed Wetlands for Wastewater Treatment: Municipal, Industrial and Agricultural*. Lewis Publishers, Chelsea Michigan. 1989. pp. 788-792,

Kong, S., Kamga, E.T., Fossog, V. and Nanseu-Njiki, C.P. (2016) Removal of mercury(II) from aqueous solution by modified *Triplochyton scleroxylon* sawdust. *Journal of Chemical and Pharmaceutical Research*, vol. 8, no. 5, pp. 342-353

Kosolapov, D.B. Kuschk, P. Vainshtein, M.B. Vatsourina, A.V. Wiessner, A. Kästner, M. and Müller, R.A. (2004) Microbial processes of heavy metal removal

from carbon-deficient effluents in constructed wetlands. *Engineering in Life Sciences*, vol. 4, no. 5, pp.403-411.

Krabbenhoft, D.P. and Rickert, D.A. (1995) Mercury contamination of aquatic ecosystems (No. 216-95), *US Geological Survey*.

Kratochvil, D. and Volesky, B., (1998) Advances in the biosorption of heavy metals. *Trends in Biotechnology*, vol. 16, no. 7, pp.291-300.

Kumar, R., Bhatia, D., Singh, R., Rani, S. and Bishnoi, N.R., (2011) Sorption of heavy metals from electroplating effluent using immobilized biomass *Trichoderma viride* in a continuous packed-bed column. *International Journal of Biodeterioration & Biodegradation*, vol. 65, no. 8, pp.1133-1139.

Kumar, K.S., Dahms, H.U., Won, E.J., Lee, J.S. and Shin, K.H. (2015) Microalgae –a promising tool for heavy metal remediation. *Ecotoxicology and Environmental Safety*, vol. 113, pp.329-352.

Kumar, D., Pandey, L.K. and Gaur, J.P. (2016) Metal sorption by algal biomass: From batch to continuous system. *Algal Research*, vol. 18, pp.95-109.

Kumari, S., Udayabhanu, G. and Prasad, B. (2010) Studies on environmental impact of acid mine drainage generation and its treatment: an appraisal. *Indian Journal of Environmental Protection*, vol. 30, no. 11, pp.953-967.

Kuncoro, E.P. and Fahmi, M.Z. (2013) Removal of Hg and Pb in aqueous solution using coal fly ash adsorbent. *Procedia Earth and Planetary Science*, vol. 6, pp.377-382.

Kurniawan, T.A., Chan, G.Y., Lo, W.H. and Babel, S. (2006) Comparisons of low-cost adsorbents for treating wastewaters laden with heavy metals. *Science of the Total Environment*, vol. 366, no. 2-3, pp.409-426.

Kuyucak, N. (2002) Acid mine drainage prevention and control options. *CIM Bulletin*, pp.96-102.

La Bella, N. and Hilliker, A. (2003) Mercury in the Environment. *The Traprock*, vol. 2, pp. 33-36.

Lau, P.S., Lee, H.Y., Tsang, C.C.K., Tam, N.F.Y. and Wong, Y.S. (1999) Effect of metal interference, pH and temperature on Cu and Ni biosorption by *Chlorella vulgaris* and *Chlorella miniata*. *Environmental Technology*, vol. 20, no. 9, pp.953-961.

Lee, Y.C. and Chang, S.P. (2011) The biosorption of heavy metals from aqueous solution by *Spirogyra* and *Cladophora* filamentous macroalgae. Bioresource technology, vol. 102, no. 9, pp.5297-5304.

Lehnherr, I. (2013) Methylmercury biogeochemistry: a review with special reference to Arctic aquatic ecosystems. *Environmental Reviews*, vol. 22, no.3, pp.229-243.

Leick, S., Henning, S., Degen, P., Suter, D. and Rehage, H. (2010) Deformation of liquid-filled calcium alginate capsules in a spinning drop apparatus. *Physical Chemistry Chemical Physics*, vol. 12, no. 12, pp.2950-2958.

Lesmana, S.O., Febriana, N., Soetaredjo, F.E., Sunarso, J. and Ismadji, S. (2009) Studies on potential applications of biomass for the separation of heavy metals from water and wastewater. *Biochemical Engineering Journal*, vol. 44, no. 1, pp.19-41.

Li, N., Bai, R. and Liu, C. (2005) Enhanced and selective adsorption of mercury ions on chitosan beads grafted with polyacrylamide via surface-initiated atom transfer radical polymerization. *Langmuir*, vol. 21, no. 25, pp.11780-11787.

Li, L., Hu, N., Ding, D., Xin, X., Wang, Y., Xue, J., Zhang, H. and Tan, Y. (2015) Adsorption and recovery of U (VI) from low concentration uranium solution by amidoxime modified *Aspergillus niger*. *RSC Advances*, vol. 5, no. 81, pp.65827-65839.

Lin, C.J. and Pehkonen, S.O., (1999) The chemistry of atmospheric mercury: a review. *Atmospheric Environment*, vol. 33, no. 13, pp.2067-2079.

Liu, B., Schaider, L.A., Mason, R.P., Shine, J.P., Rabalais, N.N. and Senn, D.B., (2015). Controls on methylmercury accumulation in northern Gulf of Mexico sediments. Estuarine, *Coastal and Shelf Science*, vol. 159, pp.50-59.

Lizama, K. Fletcher, T.D. and Sun, G. (2011) Removal processes for arsenic in constructed wetlands. *Chemosphere*, vol. 84, no. 8, pp.1032-1043.

Lodeiro, P., Herrero, R. and de Vicente, M.S. (2006) The use of protonated *Sargassum muticum* as biosorbent for cadmium removal in a fixed-bed column. Journal of Hazardous Materials, vol. 137, no. 1, pp.244-253.

Lopes, S., Bueno, L., Aguiar, J. F.D. and Finkler, C. (2017) Preparation and characterization of alginate and gelatin microcapsules containing *Lactobacillus rhamnosus*. *Annals of the Brazilian Academy of Sciences*, vol. 89, no. 3, pp. 1601-161.

Long, Y., Lei, D., Ni, J., Ren, Z., Chen, C. and Xu, H. (2014) Packed bed column studies on lead (II) removal from industrial wastewater by modified *Agaricus bisporus*. *Bioresource Technology*, vol. 152, pp.457-463.

van Loon, G.W., Duffy, S.J. (2005) Environmental Chemistry A Global Perspective, Oxford University Press Inc. New York

Lusilao-Makiese, J.G., Cukrowska, E.M., Tessier, E., Amouroux, D. and Weiersbye, I. (2013) The impact of post gold mining on mercury pollution in the West Rand region, Gauteng, South Africa. *Journal of Geochemical Exploration*, vol. 134, pp.111-119.

Mahanadi, C., Mupa, M. and Jackson, G.E. (2015) Competitive adsorptive removal of Pb, Cu and Cd from water using water Pennywort fixed on alginate, *Journal of Bioremediation and Biodegradation*, Vol. 6, no. 4, pp. 1-7

Maine, M.A. Sune, N. Hadad, H., Sánchez, G. and Bonetto, C. (2009) Influence of vegetation on the removal of heavy metals and nutrients in a constructed wetland. *Journal of Environmental Management*, vol. 90, no. 1, pp.355-363.

Malassa, H., Al-Qutob, M., Al-Khatib, M. and Al-Rimawi, F. (2013) Determination of different trace heavy metals in ground water of South West Bank/Palestine by ICP/MS. *Journal of Environmental Protection*, vol. 4, no. 8, pp.818.

Mallick, N. (2002) Biotechnological potential of immobilized algae for wastewater N, P and metal removal: a review. *Biometals*, vol. 15, no. 4, pp.377-390.

Manohar, D.M., Krishnan, K.A. and Anirudhan, T.S. (2002) Removal of mercury (II) from aqueous solutions and chlor-alkali industry wastewater using 2-mercaptobenzimidazole-clay. *Water Research*, vol. 36, no. 6, pp.1609-1619.

Mapolelo, M. and Torto, N. (2004) Trace enrichment of metal ions in aquatic environments by *Saccharomyces cerevisiae*. *Talanta*, vol. 64, no. 1, pp.39-47.

Martínez-Juárez, V.M., Cárdenas-González, J.F., Torre-Bouscoulet, M.E. and Acosta-Rodríguez, I. (2012) Biosorption of mercury (II) from aqueous solutions onto fungal biomass. *Bioinorganic Chemistry and Applications*, vol. 2012, pp. 1-5.

Mashitah, M.D., Azila, Y.Y. and Bhatia, S. (2008) Biosorption of cadmium (II) ions by immobilized cells of *Pycnoporus sanguineus* from aqueous solution, *Bioresource Technology*, vol. 99, no. 11, pp. 4742-4748.

Mason, R.P. Fitzgerald, W.F. and Morel, F.M. (1994) The biogeochemical cycling of elemental mercury: anthropogenic influences, *Geochimica et Cosmochimica Acta*, vol. 58, no. 15, pp.3191-3198.

Mashitah, M.D., Azila, Y.Y. and Bhatia, S. (2008) Biosorption of cadmium (II) ions by immobilized cells of *Pycnoporus sanguineus* from aqueous solution, *Bioresource Technology*, vol. 99, no. 11, pp. 4742-4748.

Mata, Y.N., Blazquez, M.L., Ballester, A., Gonzalez, F. and Munoz, J.A. (2008) Characterization of the biosorption of cadmium, lead and copper with the brown alga *Fucus vesiculosus*. *Journal of Hazardous Materials*, vol. 158, no. (2-3), pp.316-323.

Mata, Y.N., Blázquez, M.L., Ballester, A., González, F. and Munoz, J.A. (2009) Biosorption of cadmium, lead and copper with calcium alginate xerogels and immobilized *Fucus vesiculosus*, *Journal of Hazardous Materials*, vol. 163, no. 2-3, pp.555-562.

Matagi, S.V., Swai, D. and Mugabe, R. (1998) A review of heavy metal removal mechanisms in wetlands. *African Journal of Hydrobiology and Fisheries*, vol. 8, pp. 23-35

Mays, P.A., and Edwards, G.S. (2001) Comparison of heavy metal accumulation in a natural wetland and constructed wetlands receiving acid mine drainage, *Ecological Engineering*, vol. 16, no. 4, pp.487-500.

Mazyck, D.W. (2009) Aqueous Phase Mercury Removal: Strategies for a Secure Future Water Supply. National Institute for Standards and Instrumentation, Technology Innovation Program, U.S. Department of Commerce

Maznah, W.W., Al-Fawwaz, A.T. and Surif, M. (2012) Biosorption of copper and zinc by immobilized and free algal biomass, and the effects of metal biosorption on the growth and cellular structure of *Chlorella sp*. and *Chlamydomonas sp*. isolated from rivers in Penang, Malaysia, *Journal of Environmental Sciences*, vol. 24, no. 8, pp. 1386-1393.

Mbonimpa, M., Bouda, M., Demers, I., Benzaazoua, M., Bois, D. and Gagnon, M. (2015) Preliminary geotechnical assessment of the potential use of mixtures of soil and acid mine drainage neutralization sludge as materials for the moisture retention layer of covers with capillary barrier effects. *Canadian Geotechnical Journal*, vol. 53, no. 5, pp.828-838.

McCarthy, T.S. (2011) The impact of acid mine drainage in South Africa. *South African Journal of Science*, vol. 107, no. 5-6, pp.01-07.

Meena, A.K., Mishra, G.K., Kumar, S., Rajagopal, C. and Nagar, P.N. (2004) Low-cost adsorbents for the removal of mercury (II) from aqueous solution-a comparative Study. *Defense Science Journal*, vol. 54, no. 4, p.537-548.

Metin, A.Ü. and Alver, E. (2016) Fibrous polymer-grafted chitosan/clay composite beads as a carrier for immobilization of papain and its usability for mercury elimination. *Bioprocess and Biosystems Engineering*, vol. 39, no. 7, pp.1137-1149.

Michalak, I. and Chojnacka, K. (2010) Interactions of metal cations with anionic groups on the cell wall of the macroalga *Vaucheria sp*. *Engineering in Life Sciences*, vol. 10, no. 3, pp.209-217.

Michalak, I., Chojnacka, K., and Witek-Krowiak, A. (2013) State of the art for the biosorption process—a review. *Applied Biochemistry and Biotechnology*, vol. 170, no.6, pp.1389-1416.

Miretzky, P. and Cirelli, A.F. (2009) Hg (II) removal from water by chitosan and chitosan derivatives: a review. *Journal of Hazardous Materials*, vol. 167, no. 1-3, pp.10-23.

Mishra, A., Tripathi, B.D., and Rai, A.K. (2016) Packed-bed column biosorption of chromium (VI) and nickel (II) onto Fenton modified *Hydrilla verticillata* dried biomass. *Ecotoxicology and Environmental Safety*, vol. 132, pp.420-428.

Mohan, D. and Singh, K.P. (2002) Single-and multi-component adsorption of cadmium and zinc using activated carbon derived from bagasse—an agricultural waste. *Water Research*, vol. 36, no. 9, pp.2304-2318.

Montazer-Rahmati, M.M., Rabbani, P., Abdolali, A. and Keshtkar, A.R. (2011) Kinetics and equilibrium studies on biosorption of cadmium, lead, and nickel ions from aqueous solutions by intact and chemically modified brown algae. *Journal of Hazardous Materials*, vol. 185, no. 1, pp.401-407.

Monteiro, C.M., Castro, P.M. and Malcata, F.X. (2012) Metal uptake by microalgae: underlying mechanisms and practical applications. *Biotechnology Progress*, vol. 28, no. 2, pp.299-311.

Moreno-Garrido, I. (2008) Microalgae immobilization: current techniques and uses. *Bioresource Technology*, vol. 99, no. 10, pp.3949-3964.

Motsi, T., Rowson, N.A., and Simmons, M.J.H. (2009) Adsorption of heavy metals from acid mine drainage by natural zeolite. *International Journal of Mineral Processing*, vol. 92, no. 1-2, pp.42-48.

Muhamad, H., Doan, H., and Lohi, A. (2010) Batch and continuous fixed-bed column biosorption of Cd^{2+} and Cu^{2+}. *Chemical Engineering Journal*, vol. 158, no. 3, pp.369-377.

Muhammad, S.N., Kusin, F.M., Zahar, M.S.M., Halimoon, N. and Yusuf, F.M., (2015) Passive treatment of acid mine drainage using mixed substrates: batch experiments. *Procedia Environmental Sciences*, vol. 30, pp.157-161.

Mulopo, J. (2015) Continuous pilot scale assessment of the alkaline barium calcium desalination process for acid mine drainage treatment. *Journal of Environmental Chemical Engineering*, vol. 3, no. 2, pp.1295-1302.

Mureseanu, M., Cioatera, N., Trandafir, I., Georgescu, I., Fajula, F. and Galarneau, A. (2011) Selective Cu^{2+} adsorption and recovery from contaminated water using mesoporous hybrid silica bio-adsorbents. *Microporous and Mesoporous Materials*, vol. 146, no. 1-3, pp.141-150.

Mungur, A.S. Shutes, R.B.E. Revitt, D.M. and House, M.A. (1997) An assessment of metal removal by a laboratory scale wetland, *Water Science and Technology*, vol. 35, no. 5, pp.125-133.

Munthe, J., Wängberg, I., Pirrone, N., Iverfeldt, Å., Ferrara, R., Ebinghaus, R., Feng, X., Gårdfeldt, K., Keeler, G., Lanzillotta, E. and Lindberg, S.E. (2001) Intercomparison of methods for sampling and analysis of atmospheric mercury species. *Atmospheric Environment*, vol. 35, no. 17, pp.3007-3017.

Naicker, K., Cukrowska, E. and McCarthy, T.S. (2003) Acid mine drainage arising from gold mining activity in Johannesburg, South Africa and environs. *Environmental Pollution*, vol. 122, no. 1, pp.29-40.

Naja, G. and Volesky, B. (2008) Optimization of a biosorption column performance. *Environmental Science & Technology*, vol. 42, no. 15, pp.5622-5629.

Namasivayam, C. and Kadirvelu, K. (1999) Uptake of mercury (II) from wastewater by activated carbon from an unwanted agricultural solid by-product: coirpith. *Carbon*, vol. 37, no. 1, pp.79-84.

Nanseu-Njiki, C.P., Tchamango, S.R., Ngom, P.C., Darchen, A. and Ngameni, E. (2009) Mercury (II) removal from water by electrocoagulation using aluminum and iron electrodes. *Journal of Hazardous Materials*, vol. 168, no. 2-3, pp.1430-1436.

Neculita, C.M. Zagury, G.J. and Bussière, B. (2007) Passive treatment of acid mine drainage in bioreactors using sulfate-reducing bacteria, *Journal of Environmental Quality*, vol. 36, no. 1, pp. 1-16.

Nicolardi, V., Cai, G., Parrotta, L., Puglia, M., Bianchi, L., Bini, L. and Gaggi, C. (2012) The adaptive response of lichens to mercury exposure involves changes in the photosynthetic machinery. *Environmental Pollution*, vol. 160, pp.1-10.

Noller, B.N. Woods, P.H. and Ross, B.J. (1994) Case studies of wetland filtration of mine waste water in constructed and naturally occurring systems in Northern Australia, *Water Science and Technology*, vol. 29, no. 4, pp.257-265.

Nyquist, J. and Greger, M. (2009) A field study of constructed wetlands for preventing and treating acid mine drainage. *Ecological Engineering*, vol. 35, no. 5, pp.630-642.

Ogoyi, D.O., Mwita, C.J., Nguu, E.K., and Shiundu, P.M. (2011) Determination of heavy metal content in water, sediment and microalgae from Lake Victoria, East Africa. *The Open Environmental Engineering Journal*, vol. 4, pp.156-161

Oguz, E. and Ersoy, M. (2014) Biosorption of cobalt (II) with sunflower biomass from aqueous solutions in a fixed bed column and neural networks modelling. *Ecotoxicology and Environmental Safety*, vol. 99, pp.54-60.

Okoronkwo, N.E., Igwe, J.C., and Okoronkwo, I.J. (2007) Environmental impacts of mercury and its detoxification from aqueous solutions. *African Journal of Biotechnology*, vol. 6, no. 4, pp. 335-340

Oyetibo, G.O., Ishola, S.T., Ikeda-Ohtsubo, W., Miyauchi, K., Ilori, M.O. and Endo, G. (2015) Mercury bioremoval by *Yarrowia* strains isolated from sediments of mercury-polluted estuarine water. *Applied Microbiology and Biotechnology*, vol. 99, no. 8, pp.3651-3657

Öztürk, M., Özözen, G., Minareci, O. and Minareci, E. (2009) Determination of heavy metals in fish, water and sediments of Avsar Dam Lake in Turkey. *Iranian Journal of Environmental Health, Science and Engineering*, vol. 6, no. 2, pp.73-80.

Pacyna, J.M., Munthe, J., Larjava, K. and Pacyna, E.G. (2005) Mercury emissions from anthropogenic sources: estimates and measurements for Europe. In: Dynamics *of Mercury Pollution on Regional and Global Scales*, Springer, Boston, MA, pp. 51-64.

Pacyna, E.G., Pacyna, J.M., Steenhuisen, F. and Wilson, S. (2006) Global anthropogenic mercury emission inventory for 2000. *Atmospheric Environment*, vol. 40, no. 22, pp.4048-4063.

Pacyna, E.G. Pacyna, J.M. Sundseth, K., Munthe, J. Kindbom, K. Wilson, S. Steenhuisen, F. and Maxson, P. (2010) Global emission of mercury to the atmosphere from anthropogenic sources in 2005 and projections to 2020. *Atmospheric Environment*, vol. 44, no. 20, pp.2487-2499.

Pacyna, J.M., Travnikov, O., De Simone, F., Hedgecock, I.M., Sundseth, K., Pacyna, E.G., Steenhuisen, F., Pirrone, N., Munthe, J. and Kindbom, K. (2016) Current and future levels of mercury atmospheric pollution on a global scale. *Atmospheric Chemistry and Physics*, vol. 16, no. 19, p.12495-12511.

Pahlavanzadeh, H., Keshtkar, A.R., Safdari, J. and Abadi, Z. (2010) Biosorption of nickel (II) from aqueous solution by brown algae: Equilibrium, dynamic and thermodynamic studies. *Journal of Hazardous Materials*, vol. 175, no. 1-3, pp.304-310.

Park, D., Yun, Y.S. and Park, J.M. (2010) The past, present, and future trends of biosorption. *Biotechnology and Bioprocess Engineering*, vol. 15, no. 1, pp.86-102.

Patel, N., Lalwani, D., Gollmer, S., Injeti, E., Sari, Y. and Nesamony, J. (2016) Development and evaluation of a calcium alginate based oral ceftriaxone sodium formulation. *Progress in Biomaterials*, vol. 5, no. 2, pp.117-133.

Pawlik-Skowrońska, B. (2001) Phytochelatin production in freshwater algae *Stigeoclonium* in response to heavy metals contained in mining water; effects of some environmental factors. *Aquatic Toxicology*, vol. 52, no. 3-4, pp.241-249.

Peniche-Covas, C., Alvarez, L.W. and Argüelles-Monal, W. (1992) The adsorption of mercuric ions by chitosan. *Journal of Applied Polymer Science*, vol. 46, no. 7, pp.1147-1150.

Perales-Vela, H.V., Pena-Castro, J.M. and Canizares-Villanueva, R.O. (2006) Heavy metal detoxification in eukaryotic microalgae. *Chemosphere*, vol. 64, no. 1, pp.1-10.

Petrovič, A. and Simonič, M., (2016) Removal of heavy metal ions from drinking water by alginate-immobilized *Chlorella sorokiniana*. *International Journal of Environmental Science and Technology*, vol. 13, no.7, pp.1761-1780.

Pirrone, N., Cinnirella, S., Feng, X., Finkelman, R.B., Friedli, H.R., Leaner, J., Mason, R., Mukherjee, A.B., Stracher, G.B., Streets, D.G. and Telmer, K. (2010) Global mercury emissions to the atmosphere from anthropogenic and natural sources. *Atmospheric Chemistry and Physics*, vol. 10, no. 13, pp.5951-5964.

Plaza, J., Viera, M., Donati, E. and Guibal, E. (2011) Biosorption of mercury by *Macrocystis pyrifera* and *Undaria pinnatifida*: Influence of zinc, cadmium and nickel. *Journal of Environmental Sciences*, vol. 23, no. 11, pp.1778-1786.

Pozo-Antonio, S., Puente-Luna, I., Lagüela-López, S. and Veiga-Ríos, M. (2014) Techniques to correct and prevent acid mine drainage: A review. *Dyna*, vol. 81, no. 186, pp.73-80.

Pradhan, S. and Rai, L.C. (2001) Copper removal by immobilized *Microcystis aeruginosa* in continuous flow columns at different bed heights: study of the adsorption/desorption cycle. *World Journal of Microbiology and Biotechnology*, vol. 17, no. 9, pp.829-832.

Prakasham, R.S., Merrie, J.S., Sheela, R., Saswathi, N. and Ramakrishna, S.V. (1999) Biosorption of chromium VI by free and immobilized *Rhizopus arrhizus*. *Environmental Pollution*, vol. 104, no. 3, pp.421-427.

Prasad, B.B., Banerjee, S. and Lakshmi, D., (2006) An ALGASORB column for the quantitative sorption of arsenic (III) from water samples. *Water Quality Research Journal of Canada*, vol. 41, no. 2, pp.190-197.

Prasher, S.O., Beaugeard, M., Hawari, J., Bera, P., Patel, R.M. and Kim, S.H. (2004) Biosorption of heavy metals by red algae (*Palmaria palmata*). *Environmental Technology*, vol. 25, no. 10, pp.1097-1106.

Preetha, B. and Viruthagiri, T. (2007) Batch and continuous biosorption of chromium (VI) by *Rhizopus arrhizus*. *Separation and Purification Technology*, vol. 57, no. 1, pp.126-133.

Priyadarshani, I., Sahu, D. and Rath, B. (2011) Microalgal bioremediation: Current practices and perspectives. *Journal of Biochemical Technology*, vol. 3, no. 3, pp. 299-304

Qaiser, S., Saleemi, A.R. and Umar, M. (2009) Biosorption of lead from aqueous solution by Ficus religiosa leaves: batch and column study. *Journal of Hazardous Materials*, vol. 166, no. 2-3, pp.998-1005.

Qasaimeh, A., Al Sharie, H. and Masoud, T. (2015) A review on constructed wetlands components and heavy metal removal from wastewater. *Journal of Environmental Protection*, vol. 6, no. 7, pp. 710 -718.

Qiusheng, Z., Xiaoyan, L., Jin, Q., Jing, W. and Xuegang, L. (2015) Porous zirconium alginate beads adsorbent for fluoride adsorption from aqueous solutions. *Royal Society of Chemistry Advances*, vol. 5, no. 3, pp.2100-2112.

Rafaj, P., Bertok, I., Cofala, J. and Schoepp, W. (2013) Scenarios of global mercury emissions from anthropogenic sources. *Atmospheric Environment*, vol. 79, pp.472-479.

Rahman, M. and Sathasivam, K.V. (2015) Heavy metal adsorption onto *Kappaphycus sp*. from aqueous solutions: The use of error functions for validation of isotherm and kinetics models. *BioMed Research International*, vol. 2015, pp. 1-13.

Rajamohan, N. and Sivaprakash, B. (2008) Biosorption of heavy metal using brown seaweed in a regenerable continuous column. *Asia-Pacific Journal of Chemical Engineering*, vol. 3, no. 5, pp.572-578.

Raize, O., Argaman, Y. and Yannai, S. (2004) Mechanisms of biosorption of different heavy metals by brown marine macroalgae. *Biotechnology and Bioengineering*, vol. 87, no. 4, pp.451-458.

Rajfur, M. (2013) Algae-Heavy Metals Biosorbent. *Ecological Chemistry and Engineering*, vol. 20, no. 1, pp.23-40.

Ramavandi, B., Rahbar, A. and Sahebi, S. (2016) Effective removal of Hg^{2+} from aqueous solutions and seawater by *Malva sylvestris*. *Desalination and Water Treatment*, vol. 57, no. 50, pp.23814-23826.

Ramrakhiani, L., Majumder, R., and Khowala, S. (2011) Removal of hexavalent chromium by heat-inactivated fungal biomass of *Termitomyces clypeatus*: Surface characterization and mechanism of biosorption. *Chemical Engineering Journal*, vol. 171, no. 3, pp.1060-1068.

Rao, L.N., and Prabhakar, G. (2011) Removal of heavy metals by the biosorption-an overall review. *Journal of Engineering Research and Studies*, vol. 2, no. 4, pp.17-22.

Rezaee, A., Ramavandi, B., and Ganati, F. (2006) Equilibrium and spectroscopic studies on biosorption of mercury by algae biomass. *Pakistan Journal of Biological Sciences*, vol. 9, no. 4, pp.777-782.

Riazi, M., Keshtkar, A.R. and Moosavian, M.A. (2016) Biosorption of Th (IV) in a fixed-bed column by Ca-pretreated Cystoseira indica. *Journal of Environmental Chemical Engineering*, vol. 4, no. 2, pp.1890-1898.

Riefler, R.G., Krohn, J., Stuart, B. and Socotch, C. (2008) Role of sulfur-reducing bacteria in a wetland system treating acid mine drainage. *Science of the Total Environment*, vol. 394, no. 2-3, pp.222-229.

Rizzuti, A.M., Ellis, F.L., Cosme, L.W. and Cohen, A.D. (2015) Biosorption of mercury from aqueous solutions using highly characterized peats. *Mires & Peat*, vol. 16, pp. 1-7.

Rocha, L.S., Lopes, C.B., Henriques, B., Tavares, D.S., Borges, J.A., Duarte, A.C. and Pereira, E. (2014) Competitive effects on mercury removal by an agricultural

waste: application to synthetic and natural spiked waters. *Environmental Technology*, vol. 35, no. 6, pp.661-673.

Rocher, V., Siaugue, J.M., Cabuil, V. and Bee, A. (2008) Removal of organic dyes by magnetic alginate beads. *Water Research*, vol. 42, no. 4-5, pp.1290-1298.

Romera, E., González, F., Ballester, A., Blázquez, M.L. and Munoz, J.A. (2007) Comparative study of biosorption of heavy metals using different types of algae. *Bioresource Technology*, vol. 98, no. 17, pp.3344-3353.

Romero-González, M.E., Williams, C.J., and Gardiner, P.H. (2001) Study of the mechanisms of cadmium biosorption by dealginated seaweed waste, *Environmental Science & Technology*, vol. 35, no. 14, pp.3025-3030.

Sag, Y. and Kutsal, T. (2001) Recent trends in the biosorption of heavy metals: a review. *Biotechnology and Bioprocess Engineering*, vol. 6, no. 6, pp.376-385.

Samuel, J., Pulimi, M., Paul, M.L., Maurya, A., Chandrasekaran, N. and Mukherjee, A. (2013) Batch and continuous flow studies of adsorptive removal of Cr (VI) by adapted bacterial consortia immobilized in alginate beads. *Bioresource Technology*, vol. 128, pp.423-430.

Santa Cruz, L., Garralón, A., Escribano, A., Gómez, P., Turrero, M.J., Peña, J., Robredo, L., Buil, B. and Sánchez, L. (2013) Chemical characteristics of acid mine drainage from an As-W mineralized zone in western Spain. *Procedia Earth and Planetary Science*, vol. 7, pp.284-287.

Sarı, A. and Tuzen, M. (2008) Biosorption of Pb (II) and Cd (II) from aqueous solution using green alga (*Ulva lactuca*) biomass. *Journal of Hazardous Materials*, vol. 152, no. 1, pp.302-308.

Sciban, M., Klasnja, M. and Skrbic, B. (2006) Modified hardwood sawdust as an adsorbent of heavy metal ions from water. *Wood Science and Technology*, vol. 40, no. 3, p.217-227.

Schiffer, D.M. (1989) Water-quality variability in a central Florida wetland receiving highway runoff. *Water: Laws and Management*. American Water Resources Association, Bethesda, Maryland, pp. 7 A1-7 A11.

Schroeder, W.H. and Munthe, J. (1998) Atmospheric mercury—an overview, *Atmospheric Environment*, vol. 32, no. 5, pp.809-822.

Schumann, R., Häubner, N., Klausch, S. and Karsten, U. (2005) Chlorophyll extraction methods for the quantification of green microalgae colonizing building facades. *International Biodeterioration & Biodegradation*, vol. 55, no. 3, pp.213-222.

Selin, N.E. (2009) Global biogeochemical cycling of mercury: a review. *Annual Review of Environment and Resources*, vol. 34. pp. 43-63

Shabudeen, S.P.S., Daniel, S. and Indhumathi, P. (2013) Utilizing the pods of *Delonix regia* activated carbon for the removal of mercury (II) by adsorption technique. *International Journal of Research in Chemistry and Environment*, vol. 3, pp.60-65.

Shamshuddin, J., Muhrizal, S., Fauziah, I. and Van Ranst, E. (2004) A laboratory study of pyrite oxidation in acid sulfate soils. *Communications in Soil Science and Plant Analysis*, vol. 35, no. 1-2, pp.117-129.

Shanab, S., Essa, A. and Shalaby, E. (2012) Bioremoval capacity of three heavy metals by some microalgae species (Egyptian Isolates). *Plant Signaling & Behavior*, vol. 7, no. 3, pp.392-399.

Shao, H., Liu, X., Zhou, Z., Zhao, B., Chen, Z. and Xu, M. (2016) Elemental mercury removal using a novel KI modified bentonite supported by starch sorbent. *Chemical Engineering Journal*, vol. 291, pp.306-316.

Sheikha, D., Ashour, I. and Al-Rub, F.A. (2008) Biosorption of zinc on immobilized green algae: Equilibrium and dynamics studies. *The Journal of Engineering Research*, vol. 5, no. 1, pp.20-29.

Sheng, P.X., Ting, Y.P., Chen, J.P. and Hong, L. (2004) Sorption of lead, copper, cadmium, zinc, and nickel by marine algal biomass: characterization of biosorptive capacity and investigation of mechanisms. *Journal of Colloid and Interface Science*, vol. 275, no. 1, pp.131-141.

Sheng, P.X., Ting, Y.P. and Chen, J.P. (2007) Biosorption of heavy metal ions (Pb, Cu, and Cd) from aqueous solutions by the marine alga *Sargassum sp*. in single-and multiple-metal systems. *Industrial & Engineering Chemistry Research*, vol. 46, no. 8, pp.2438-2444.

Sheoran, A.S. and Sheoran, V. (2006) Heavy metal removal mechanism of acid mine drainage in wetlands: a critical review, *Minerals Engineering*, vol. 19, no. 2, pp. 105-116.

Siddiquee, S., Rovina, K., Azad, S.A., Naher, L., Suryani, S. and Chaikaew, P. (2015) Heavy metal contaminants removal from wastewater using the potential filamentous fungi biomass: a review. *Journal of Microbial and Biochemical Technology*, vol. 7, pp.384-393.

da Silva, V.M.D., Silva, L.A., Andrade, J.B.D., Veloso, M.C. and Santos, G.V. (2008) Determination of moisture content and water activity in algae and fish by thermoanalytical techniques. *Quimica Nova*, vol. 31, no. 4, pp.901-905.

Simate, G.S. and Ndlovu, S. (2014) Acid mine drainage: Challenges and opportunities. *Journal of Environmental Chemical Engineering*, vol. 2, no. 3, pp.1785-1803.

Singh, A., Mehta, S.K. and Gaur, J.P. (2007) Removal of heavy metals from aqueous solution by common freshwater filamentous algae. *World Journal of Microbiology and Biotechnology*, vol. 23, no. 8, p.1115.

Singh, A., Kumar, D., and Gaur, J.P. (2012) Continuous metal removal from solution and industrial effluents using *Spirogyra* biomass-packed column reactor, *Water Research*, vol. 46, no. 3, pp.779-788.

Singh, S.K., Dixit, K. and Sundaram, S. (2014) Effect of acidic and basic pretreatment of wild algal biomass on Cr (VI) biosorption. IOSR *Journal of Environmental Science Toxicology and Food Technology*, vol. 8, pp.38-41.

Sinha, A., Pant, K.K. and Khare, S.K. (2012) Studies on mercury bioremediation by alginate immobilized mercury tolerant *Bacillus cereus* cells. *International Biodeterioration & Biodegradation*, vol. 71, pp.1-8.

Skjånes, K., Knutsen, G., Källqvist, T., and Lindblad, P. (2008) H_2 production from marine and freshwater species of green algae during sulfur deprivation and considerations for bioreactor design. *International Journal of Hydrogen Energy*, vol. 33, no. 2, pp.511-521.

Skousen, J. (1997) Overview of passive systems for treating acid mine drainage. *Green Lands*, vol. 27, no. 4, pp.34-43.

Skousen, J., Zipper, C.E., Rose, A., Ziemkiewicz, P.F., Nairn, R., McDonald, L.M. and Kleinmann, R.L. (2017) Review of passive systems for acid mine drainage treatment. *Mine Water and the Environment*, vol. 36, no. 1, pp.133-153.

Smith, K. (1997). Constructed wetlands for treating acid mine drainage. *University of Minnesota Student Online Journal*, vol. 2, no. 7, pp. 1-7

Sobolewski, A. (1999). A review of processes responsible for metal removal in wetlands treating contaminated mine drainage, *International Journal of Phytoremediation*, vol. 1, no. 1, pp. 19-51.

Song, D., Park, S.J., Kang, H.W., Park, S.B. and Han, J.I. (2013). Recovery of lithium (I), strontium (II), and lanthanum (III) using Ca-alginate beads. *Journal of Chemical & Engineering Data*, vol. 58, no. 9, pp.2455-2464.

Sud, D., Mahajan, G. and Kaur, M.P. (2008) Agricultural waste material as a potential adsorbent for sequestering heavy metal ions from aqueous solutions–A review. *Bioresource Technology*, vol. 99, no. 14, pp.6017-6027.

Suharso, B., Buhani, A. and Sumadi, B. (2010) Immobilization of *S. duplicatum* supported silica gel matrix and its application on adsorption-desorption of Cu (II), Cd (II) and Pb (II) ions. *Desalination*, vol. 263, no. 1-3, pp.64-69.

Sulaymon, A.H., Ebrahim, S.E., Abdullah, S.M. and Al-Musawi, T.J. (2010) Removal of lead, cadmium, and mercury ions using biosorption. *Desalination and Water Treatment*, vol. 24, no. 1-3, pp.344-352.

Sundseth, K., Pacyna, J.M., Pacyna, E.G., Pirrone, N. and Thorne, R.J. (2017) Global sources and pathways of mercury in the context of human health.

International Journal of Environmental Research and Public Health, vol. 14, no. 1, pp.105-119.

Svecova, L., Spanelova, M., Kubal, M. and Guibal, E. (2006) Cadmium, lead and mercury biosorption on waste fungal biomass issued from fermentation industry. I. Equilibrium studies. *Separation and Purification Technology*, vol. 52, no. 1, pp.142-153.

Swain, E.B., Engstrom, D.R., Brigham, M.E., Henning, T.A. and Brezonik, P.L. (1992) Increasing rates of atmospheric mercury deposition in midcontinental North America. *Science*, vol. 257, no. 5071, pp.784-787.

Sweetly, J. (2014) Macroalgae as a Potentially Low-Cost Biosorbent for Heavy Metal Removal A Review. *International Journal of Pharmaceutical & Biological Archive*, vol. 5, no. 2. pp. 17-26

Tabaraki, R., Nateghi, A. and Ahmady-Asbchin, S. (2014) Biosorption of lead (II) ions on *Sargassum ilicifolium*: Application of response surface methodology. *International Biodeterioration & Biodegradation*, vol. 93, pp.145-152.

Tamilselvan, N., Hemachandran, J., Thirumalai, T., Sharma, C.V., Kannabiran, K. and David, E. (2013) Biosorption of heavy metals from aqueous solution by *Gracilaria corticata varcartecala* and *Grateloupia lithophila*. *Journal of Coastal Life Medicine*, vol. 1, no. 2, pp.102-107.

Thien, D.T., An, N.T. and Hoa, N.T. (2015) Preparation of Fully Deacetylated Chitosan for Adsorption of Hg (II) Ion from Aqueous Solution. *Chemical Sciences Journal*, vol. 6, no. 2, pp.1-8.

Tovar, T. C., Ortiz, V. Á. and Garcés J, L.E. (2015) Kinetics of adsorption in mercury removal using cassava (*Manihot esculent*a) and lemon (*Citrus limonium*) wastes modified with citric acid. *Ingeniería y Universidad*, vol. 19, no. 2, pp.283-298.

Tran, H, N., You, S., Houssein-Bandegharaei. and Chao, H. (2017) Mistakes and inconsistencies regarding adsorption of contaminants from aqueous solutions : A critical review. *Water Research*, vol.120, pp.88-116

Trgo, M., Medvidović, N.V. and Perić, J. (2011) Application of mathematical empirical models to the dynamic removal of lead on natural zeolite clinoptilolite in a fixed bed column. *Indian Journal of Chemical Technology*, vol. 18, pp. 123-131

Tsekova, K., Todorova, D., Dencheva, V., and Ganeva, S. (2010) Biosorption of copper (II) and cadmium (II) from aqueous solutions by free and immobilized biomass of *Aspergillus niger*, *Bioresource technology*, vol. 101, no. 6, pp.1727-1731.

Tshumah-Mutingwende, R.R.M.S. (2014) Assessment of Algae as Mercury Bioindicators in Acid Mine Drainage waters and Their Potential for Phytoremediation (Masters Dissertation).

Tutu, H., McCarthy, T.S., and Cukrowska, E. (2008) The chemical characteristics of acid mine drainage with particular reference to sources, distribution and remediation: The Witwatersrand Basin, South Africa as a case study. *Applied Geochemistry*, vol. 23, no. 12, pp.3666-3684.

Tuzen, M., Sarı, A., Mendil, D., Uluozlu, O.D., Soylak, M. and Dogan, M. (2009) Characterization of biosorption process of As (III) on green algae *Ulothrix cylindricum*. *Journal of Hazardous Materials*, vol. 165, no. 1-3, pp.566-572.

Tüzün, I., Bayramoğlu, G., Yalçın, E., Başaran, G., Celik, G. and Arıca, M.Y. (2005) Equilibrium and kinetic studies on biosorption of Hg (II), Cd (II) and Pb (II) ions onto microalgae *Chlamydomonas reinhardtii*, *Journal of Environmental Management*, vol. 77, no. 2, pp.85-92.

Ullrich, S.M., Tanton, T.W. and Abdrashitova, S.A. (2001) Mercury in the aquatic environment: a review of factors affecting methylation. *Critical Reviews in Environmental Science and Technology*, vol. 31, no. 3, pp.241-293.

Valente, T., Rivera, M.J., Almeida, S.F.P., Delgado, C., Gomes, P., Grande, J.A., de la Torre, M.L. and Santisteban, M. (2016) Characterization of water reservoirs affected by acid mine drainage: geochemical, mineralogical, and biological (diatoms) properties of the water. *Environmental Science and Pollution Research*, vol. 23, no. 7, pp.6002-6011.

Veglio, F. and Beolchini, F. (1997) Removal of metals by biosorption: a review. *Hydrometallurgy*, vol. 44, no. 3, pp.301-316.

Verhoeven, J.T. and Meuleman, A.F. (1999) Wetlands for wastewater treatment: opportunities and limitations, *Ecological Engineering*, vol. 12, no. 1-2, pp.5-12.

Verma, V.K. and Tripathi, I.N. (2014) Kinetic study on the removal of mercury by fly ash, *Global Nest Journal*, vol. 16, no. 2, pp. 385-392.

Verma, A., Kumar, S. and Kumar, S. (2016) Biosorption of lead ions from the aqueous solution by Sargassum filipendula: Equilibrium and kinetic studies. *Journal of Environmental Chemical Engineering*, vol. 4, no.4, pp.4587-4599.

Vijayaraghavan, K., Jegan, J., Palanivelu, K. and Velan, M. (2005) Biosorption of copper, cobalt, and nickel by marine green alga *Ulva reticulata* in a packed column. *Chemosphere*, vol. 60, no. 3, pp.419-426.

Vijayaraghavan, K. and Prabu, D. (2006) Potential of *Sargassum wightii* biomass for copper (II) removal from aqueous solutions: Application of different mathematical models to batch and continuous biosorption data. *Journal of Hazardous Materials*, vol. 137, no. 1, pp.558-564.

Vijayaraghavan, K. and Balasubramanian, R. (2015) Is biosorption suitable for decontamination of metal-bearing wastewaters? A critical review on the state-of-the-art of biosorption processes and future directions. *Journal of Environmental Management*, vol. 160, pp.283-296.

Vinodhini, V. and Das, N. (2010) Packed bed column studies on Cr (VI) removal from tannery wastewater by neem sawdust. *Desalination*, vol. 264, no. 1-2, pp.9-14.

Von Canstein, H., Li, Y., Timmis, K.N., Deckwer, W.D. and Wagner-Döbler, I. (1999) Removal of Mercury from Chloralkali Electrolysis Wastewater by a Mercury-Resistant *Pseudomonas putida* Strain. *Applied and Environmental Microbiology*, vol. 65, no.12, pp.5279-5284.

Vymazal, J. (2010) Constructed wetlands for wastewater treatment: five decades of experience. *Environmental Science & Technology*, vol. 45, no. 1, pp.61-69.

Walters, C.R., Somerset, V.S., Leaner, J.J. and Nel, J.M. (2011) A review of mercury pollution in South Africa: Current status. *Journal of Environmental Science and Health, Part A*, vol. 46, no. 10, pp.1129-1137.

Wang, Q., Kim, D., Dionysiou, D.D., Sorial, G.A. and Timberlake, D. (2004). Sources and remediation for mercury contamination in aquatic systems—a literature review. *Environmental Pollution*, vol. 131, no.2, pp.323-336.

Wang, J., Deng, B., Wang, X. and Zheng, J. (2009) Adsorption of aqueous Hg (II) by sulfur-impregnated activated carbon. *Environmental Engineering Science*, vol. 26, no. 12, pp.1693-1699.

Wang, J., Feng, X., Anderson, C.W., Xing, Y. and Shang, L. (2012) Remediation of mercury-contaminated sites–a review. *Journal of Hazardous Materials*, vol. 221, pp.1-18.

Wang, F., Wang, S., Meng, Y., Zhang, L., Wu, Q. and Hao, J. (2016a) Mechanisms and roles of fly ash compositions on the adsorption and oxidation of mercury in flue gas from coal combustion. *Fuel*, vol. 163, pp.232-239.

Wang, S., Vincent, T., Faur, C. and Guibal, E. (2016b) Alginate and algal-based beads for the sorption of metal cations: Cu (II) and Pb (II), *International Journal of Molecular Sciences*, vol. 17, no. 9, pp.1453.

White, R.A., Freeman, C. and Kang, H. (2011) Plant-derived phenolic compounds impair the remediation of acid mine drainage using treatment wetlands. *Ecological Engineering*, vol. 37, no. 2, pp.172-175.

Whitehead, P.G., and Prior, H. (2006) Bioremediation of acid mine drainage: an introduction to the Wheal Jane wetlands project, *Science of the Total Environment*, vol. 338, no. 1-2, pp.15-21.

Windham-Myers, L., Fleck, J.A., Ackerman, J.T., Marvin-DiPasquale, M., Stricker, C.A., Heim, W.A., Bachand, P.A., Eagles-Smith, C.A., Gill, G., Stephenson, M. and Alpers, C.N. (2014) Mercury cycling in agricultural and managed wetlands: A synthesis of methylmercury production, hydrologic export, and bioaccumulation

from an integrated field study. *Science of the Total Environment*, vol. 484, pp.221-231.

Xu, W., Wang, H., Zhu, T., Kuang, J. and Jing, P. (2013) Mercury removal from coal combustion flue gas by modified fly ash. *Journal of Environmental Sciences*, vol. 25, no. 2, pp.393-398.

Yalçın, S., Sezer, S. and Apak, R. (2012) Characterization and lead (II), cadmium (II), nickel (II) biosorption of dried marine brown macro algae *Cystoseira barbata*. *Environmental Science and Pollution Research*, vol. 19, no. 8, pp.3118-3125.

Yardim, M.F., Budinova, T., Ekinci, E., Petrov, N., Razvigorova, M. and Minkova, V. (2003) Removal of mercury (II) from aqueous solution by activated carbon obtained from furfural. *Chemosphere*, vol. 52, no. 5, pp.835-841.

Yeh, T.Y. (2008) Removal of metals in constructed wetlands. *Practice Periodical of Hazardous, Toxic, and Radioactive Waste Management*, vol. 12, no. 2, pp. 96-101.

Yu, Q., Matheickal, J.T., Yin, P. and Kaewsarn, P. (1999) Heavy metal uptake capacities of common marine macro algal biomass. *Water Research*, vol. 33, no. 6, pp.1534-1537.

Zabihi, M., Asl, A.H. and Ahmadpour, A.H.M.A.D. (2010) Studies on adsorption of mercury from aqueous solution on activated carbons prepared from walnut shell. *Journal of Hazardous Materials*, vol. 174, no. 1-3, pp.251-256.

Zaib, M., Athar, M.M., Saeed, A., Farooq, U., Salman, M. and Makshoof, M.N. (2016) Equilibrium, kinetic and thermodynamic biosorption studies of Hg (II) on red algal biomass of *Porphyridium cruentum*. *Green Chemistry Letters and Reviews*, vol. 9, no. 4, pp.179-189.

Zeraatkar, A.K., Ahmadzadeh, H., Talebi, A.F., Moheimani, N.R. and McHenry, M.P. (2016) Potential use of algae for heavy metal bioremediation, a critical review. *Journal of Environmental Management*, vol. 181, pp.817-831.

Zeroual, Y., Moutaouakkil, A., Dzairi, F.Z., Talbi, M., Chung, P.U., Lee, K. and Blaghen, M. (2003) Biosorption of mercury from aqueous solution by *Ulva lactuca* biomass. *Bioresource Technology*, vol. 90, no. 3, pp.349-351.

Zhang, F.S., Nriagu, J.O. and Itoh, H. (2005) Mercury removal from water using activated carbons derived from organic sewage sludge. *Water research*, vol. 39, no. 2-3, pp.389-395.

Zhang, X.Y., Wang, Q.C., Zhang, S.Q., Sun, X.J. and Zhang, Z.S. (2009) Stabilization/solidification (S/S) of mercury-contaminated hazardous wastes using thiol-functionalized zeolite and Portland cement. *Journal of Hazardous Materials*, vol. 168, no. 2-3, pp.1575-1580.

Zhang, M. and Wang, H. (2014) Organic wastes as carbon sources to promote sulfate reducing bacterial activity for biological remediation of acid mine drainage. *Minerals Engineering*, vol. 69, pp.81-90.

Zhang, D.Q. Jinadasa, K.B.S.N. Gersberg, R.M. Liu, Y. Ng, W.J. and Tan, S.K. (2014) Application of constructed wetlands for wastewater treatment in developing countries–a review of recent developments (2000–2013). *Journal of Environmental Management*, vol. 141, pp.116-131.

Zhi, W. and Ji, G. (2012) Constructed wetlands, 1991–2011: A review of research development, current trends, and future directions. *Science of the Total Environment*, vol. 441, pp.19-27.

Zhu, J., Yang, J. and Deng, B. (2009) Enhanced mercury ion adsorption by amine-modified activated carbon. *Journal of Hazardous Materials*, vol. 166, no. 2-3, pp.866-872.

Ziemkiewicz P.F, Skousen J. G, Brant D.L, Sterner P.L and Lovett R.J. (1997) Acid mine drainage treatment with armored limestone in open limestone channel, *Journal of Environmental Quality*, vol. 26, no. 4, pp.1017-24.

Ziemkiewicz, P.F. Skousen, J.G. and Simmons, J. (2003) Long-term performance of passive acid mine drainage treatment systems. *Mine Water and the Environment*, vol. 22, no. 3, pp.118-129.

Zillioux, E.J. Porcella, D.B. and Benoit, J.M. (1993) Mercury cycling and effects in freshwater wetland ecosystems. *Environmental Toxicology and Chemistry*, vol. 12, no. 12, pp.2245-2264.

APPENDIX

Appendix A

Table 1A: Raw data for the effect of pH on the biosorption of mercury by pristine and modified forms of *Cladophora sp* alga (Temperature 25˚C, initial metal concentration 10 mg L^{-1}, agitation time 120 minutes, biosorbent dosage 10 g L^{-1})

pH	Pristine alga		Alga immobilized in alginate beads		Alga immobilized in silica gel	
	q (mg g^{-1})	Standard deviation	q (mg g^{-1})	Standard deviation	q (mg g^{-1})	Standard deviation
3	49.49	0.3161	54.19	1.048	52.19	0.2363
5	52.88	0.2203	69.24	0.3885	62.80	0.2858
6.5	37.15	1.020	47.81	0.5406	41.69	0.1815
8.5	35.41	0.4401	44.34	0.3256	39.30	0.2155

Table 2A: Raw data for the effect of contact time on the biosorption of mercury by pristine and modified forms of *Cladophora sp* alga (Temperature 25˚C, initial metal concentration 1 mg L^{-1}, pH 5, biosorbent dosage 10 g L^{-1})

Contact time (minutes)	Pristine alga		Alga immobilized in alginate beads		Alga immobilized in silica gel	
	q (mg g^{-1})	Standard deviation	q (mg g^{-1})	Standard deviation	q (mg g^{-1})	Standard deviation
0	0	0	0	0	0	0
5	5.136	0.1023	7.9334	0.01424	7.083	0.02094
10	6.561	0.1199	8.939	0.08751	8.389	0.06352
20	7.343	0.05771	9.539	0.06350	9.087	0.04797
30	7.243	0.1889	10.09	0.02821	9.736	0.02801
60	7.226	0.006839	10.84	0.02233	9.833	0.007549
90	7.217	0.02062	10.72	0.04692	9.812	0.04082
120	7.238	0.01076	10.69	0.01105	9.6968	0.03850

Table 3A: Raw data for the effect of initial metal concentration on the biosorption of mercury by pristine and modified forms of *Cladophora sp* alga (Temperature 25˚C, pH 5, biosorbent dosage 10 g L^{-1})

Metal concentration ($mg\ L^{-1}$)	Pristine alga		Alga immobilized in alginate beads		Alga immobilized in silica gel	
	q ($mg\ g^{-1}$)	Standard Deviation	q ($mg\ g^{-1}$)	Standard Deviation	q ($mg\ g^{-1}$)	Standard Deviation
0	0	0	0	0	0	0
0.5	3.832	0.02738	4.809	0.09424	4.291	0.1142
1	9.540	0.3786	9.812	0.2127	9.756	0.03850
2	17.79	0.1265	19.54	0.1878	19.94	0.07379
5	22.90	0.2951	38.09	0.02821	34.06	0.1253
10	52.65	0.2358	69.33	0.1484	62.70	0.3960
20	67.02	0.1504	76.79	0.1144	85.21	1.571
50	82.81	0.4293	129.1	0.2126	107.1	1.013
100	81.56	0.1728	172.5	0.07620	121.3	0.3524

Table 4A: Raw data for the effect of biosorbent dosage on the biosorption of mercury by pristine and modified forms of *Cladophora sp* alga (Temperature 25˚C, initial metal concentration1 mg L^{-1}, pH 5)

Biosorbent dosage ($mg\ L^{-1}$)	Pristine alga		Alga immobilized in alginate beads		Alga immobilized in silica gel	
	q ($mg\ g^{-1}$)	Standard Deviation	q ($mg\ g^{-1}$)	Standard Deviation	q ($mg\ g^{-1}$)	Standard Deviation
0	0	0	0	0	0	0
5	3.763	0.1026	6.815	0.02358	5.643	0.07951
10	9.781	0.07077	17.91	0.3109	13.85	0.1301
20	5.839	0.04795	12.68	0.1664	9.182	0.03407
40	4.135	0.05048	10.71	0.06180	6.634	0.04629
50	2.171	0.03923	9.582	0.02151	5.614	0.01609

Table 5A: Raw data for the effect temperature on the biosorption of mercury by pristine and modified forms of *Cladophora sp* alga

Temperature (˚C)	Pristine alga		Alga immobilized in alginate beads		Alga immobilized in silica gel	
	q (mg g^{-1})	Standard Deviation	q (mg g^{-1})	Standard Deviation	q (mg g^{-1})	Standard Deviation
16	37.42	0.4045	43.87	0.3351	39.47	0.3661
25	25.85	0.2183	41.42	0.4255	37.37	0.3889
30	21.62	0.2730	29.28	0.2857	25.44	0.2451
40	12.71	0.1973	16.13	0.1058	17.43	0.3837